

**DEVELOPMENT OF A PROCESS FOR THE PREPARATION OF  
LINALOOL FROM *CIS*-2-PINANOL**

**Subash Ramnarain Buddoo**

Thesis submitted in fulfilment of the requirements for the degree

**DOCTOR TECHNOLOGIAE**

In the faculty of Applied Science at the  
NELSON MANDELA METROPOLITAN UNIVERSITY

June 2008

Promoter : Prof. B. Zeelie

Co-promoter : Dr. J. Dudas

## ACKNOWLEDGEMENTS

The author wishes to express his sincere appreciation to:

- My promoters, Prof. B. Zeelie and Dr. J. Dudas for their assistance, guidance and encouragement to conclude this project;
- The Department of Science and Technology for funding the project under the Support Programme for Industrial Innovation (SPII);
- The THRIP fund for providing funds for the purchase of equipment required for the laboratory experimental investigations;
- Teubes Pty. Ltd. for financial support, provision of starting material (CST and  $\alpha$ -pinene) and for permission to use this material for a thesis;
- S. Farnworth for the management of the CST project;
- N. Siyakatshana for his assistance with the reaction kinetics and computer modelling of the process;
- B. Cowan for assistance with the GC-MS analysis; and
- My wife (Shelina), son (Kavish) and daughter (Sarisha) for their encouragement, patience and tolerance.

## SUMMARY

Linalool is a key intermediate for the production of important fragrance chemicals such as geraniol, nerol, geranial, and neral. Linalool can be produced via a two-step process from  $\alpha$ -pinene which is a major component of crude sulphated turpentine (CST) a foul-smelling, volatile waste product of the pulp and paper industry. The key step in this process is the pyrolysis step which involves the isomerisation of *cis*-2-pinanol to linalool and requires high temperatures (600-650°C) and is not very selective due to the decomposition of the product itself under these conditions. A client of the CSIR, Teubes Pty. Ltd., is a manufacturer of flavour and fragrance compounds for the local and international fragrance market and expressed an interest in producing linalool since the company would then gain access to other valuable fragrance chemicals via relatively simple processes. Earlier work conducted by AECl, R & D did not meet with much success since the selectivity to linalool was very poor and the process could hardly be deemed as scalable.

The main objective of this project was therefore to develop a process for the selective isomerisation of *cis*-2-pinanol to linalool with minimum by-product formation and using process equipment that could be scaled to full-scale production. Since *cis*-2-pinanol could not be purchased in sufficient quantities for process development, a process had to be developed for the bench-scale preparation of kilogram quantities of *cis*-2-pinanol from  $\alpha$ -pinene obtained from the client. Although this synthesis formed a minor part of this investigation, several process improvements and innovations were introduced to produce high quality *cis*-2-pinanol, in very good yields at kilogram scale.

A major part of this investigation was the design and set up of a pyrolysis rig capable of operating at elevated temperatures (400 - 750°C) for the evaluation of various process parameters. Various vaporizer, reactor, and condensation systems were evaluated for their ability to cope with the demanding conditions on a consistent basis. The initial part of the investigation was a screening exercise to evaluate various process parameters as well as solvents, materials of construction, catalysts, etc. A comprehensive statistical design was also conducted to determine the critical process parameters and the model obtained was used to predict the optimum conditions

required for the preparation of in-specification product on a consistent basis. These conditions were used in the preparation of a 1kg sample which was required by the client for market evaluation purposes.

The use of a novel microreactor system was also evaluated for the pinanol pyrolysis reaction. To our knowledge, this is the first time that a microreactor has been successfully used for this type of reaction in the Fragrance industry and a patent application is being filed by the CSIR. The kinetics of the reaction in both the tubular reactor system and the microreactor system was investigated. Computer modelling studies on both the systems were also conducted.

The raw material cost to produce a kilogram of linalool is \$1.40. There is a significant margin of 60.8% between the raw material cost of linalool and the current selling price (\$3.57/kg). This clearly indicates that the project is potentially feasible from an economic point of view and we can now proceed with confidence to the next stage which is the engineering design, building and commissioning of the large scale pyrolysis rig. The rest of the process steps will be conducted on existing equipment currently present at the CSIR's large scale facility (Imbiza in Isando, Gauteng).

## **KEYWORDS**

Linalool, crude sulphated turpentine (CST), Paper and pulp industry,  $\alpha$ -pinene, *cis*-pinane, pinane-2-hydroperoxide, *cis*-2-pinanol, tubular reactor, pyrolysis, isomerisation, vaporizer, condensation system, microreactor, computer modelling

## CONTENTS

1	Introduction.....	8
1.1	Historical Background .....	8
1.2	History of Linalool.....	10
1.3	Problem statement.....	11
1.4	The Global Fragrance Industry .....	11
1.5	The Fragrance Industry in South Africa .....	16
1.6	Aroma Chemicals from Turpentine .....	18
1.6.1	Turpentine .....	18
1.6.2	Aroma Chemicals.....	20
1.6.3	Feedstock Analysis .....	21
1.7	Commercial Production of Terpenoids – General Considerations .....	24
1.7.1	Safety .....	25
1.7.2	Environment.....	26
1.7.3	Purity.....	29
1.7.4	Reproducibility .....	31
1.7.5	Capacity .....	31
1.7.6	Cost .....	32
1.7.7	Sustainability.....	34
1.8	Chemistry .....	35
1.8.1	Definitions and Classification.....	35
1.8.2	The Isoprene Rule .....	37
1.8.3	Nomenclature .....	39
1.8.4	Acyclic Monoterpenoids .....	42
1.8.5	Bicyclic Monoterpenoids .....	58
1.9	Commercial Production of Terpenoids including Linalool .....	77
1.9.1	Fragrance Ingredients derived from Terpenoids.....	77
1.9.2	Interconversion of the Five Key Terpenoids .....	79
1.9.3	Commercial Aspects .....	81
1.9.4	Linalool Production/Synthesis .....	82
1.10	Zeolites as Catalysts.....	97
1.11	Microreactors .....	98
1.12	Equipment Considerations .....	100
1.12.1	Introduction.....	100
1.12.2	Overall Equipment .....	101
1.12.3	Generation of Feed Streams.....	102
1.12.4	Product Condensation and Sampling.....	106
1.13	Technology: Production of Terpene aroma chemicals .....	107
1.13.1	South African Market Analysis .....	107
1.13.2	Conclusion .....	111
1.14	Feasibility of the Production of Terpene Aroma Chemicals .....	111
1.14.1	Affordable Capital .....	111
1.14.2	Single Year Costing Model.....	113
1.14.3	Capital Cost.....	114
1.14.4	Conclusion .....	116
1.15	Research Hypothesis .....	117
1.16	Specific Research Objectives.....	117
2	Experimental .....	119
2.1	Materials .....	119

2.1.1	Reagents for synthesis.....	119
2.1.2	Reagents for analysis .....	120
2.2	Equipment .....	121
2.3	Design of pinanol pyrolysis rig.....	121
2.4	Procedures involving equipment evaluation.....	124
2.4.1	Various designs of vaporizer systems.....	124
2.4.2	Various designs of condenser systems.....	130
2.5	Synthesis procedures.....	134
2.5.1	cis-2-Pinanol preparation .....	134
2.5.2	Pinanol pyrolysis – Tubular reactor (AECI R&D) .....	136
2.5.3	Pinanol pyrolysis – Screening experiments .....	137
2.5.4	Determination of important reaction variables .....	143
2.5.5	Investigation of linalool decomposition.....	143
2.5.6	Preparation of 1kg market sample and robustness test .....	144
2.5.7	Use of microreactor system for pyrolysis .....	144
2.6	Analytical procedures .....	145
2.6.1	Gas Chromatography .....	145
3	Results and Discussion .....	147
3.1	Equipment .....	147
3.1.1	Evaluation of vaporizer systems .....	147
3.1.2	Evaluation of condenser systems .....	153
3.2	cis-2-Pinanol preparation .....	156
3.2.1	Preparation of cis-Pinane .....	158
3.2.2	Preparation of pinane-2-hydroperoxide and reduction to cis-2-pinanol 160	
3.2.3	Purification of cis-2-pinanol .....	164
3.3	Pinanol pyrolysis – Initial investigation .....	165
3.4	Pinanol pyrolysis – Screening experiments .....	168
3.4.1	n-Butanol base case.....	168
3.4.2	Effect of solvent.....	170
3.4.3	Effect of pinanol concentration using ethanol as diluent.....	173
3.4.4	Vacuum pyrolysis .....	175
3.4.5	Effect of inert packing .....	176
3.4.6	Effect of various reactor materials.....	179
3.4.7	Effect of zeolites .....	182
3.4.8	Effect of pyridine .....	183
3.4.9	Effect of ammonia.....	185
3.5	Determination of important reaction variables .....	190
3.5.1	Analysis of conversion response.....	191
3.5.2	Analysis of selectivity response.....	199
3.5.3	Model Optimization .....	202
3.6	Investigation of linalool decomposition.....	204
3.7	Preparation of market sample/Robustness test .....	207
3.8	Use of microreactor system for pinanol pyrolysis .....	209
3.9	Reaction kinetics and mathematical modelling of the pyrolysis reaction in tubular and microreactor systems .....	212
3.9.1	Theoretical .....	212
3.9.2	Kinetics .....	213
3.9.3	Mathematical modelling .....	214
3.9.4	CFD Modelling .....	216

3.9.5	Results and Discussion .....	217
3.10	Scale-up Issues.....	232
3.10.1	Process Block and Flow Diagrams .....	232
3.10.2	Large scale reactor design.....	236
3.10.3	Raw material costing.....	237
3.11	General Discussion .....	240
4	Conclusions.....	247

## CHAPTER 1

### Introduction

#### 1.1 Historical Background

Perfumes have been intimately associated with man's history. There is evidence that they have been used since antiquity in religious ceremonies and in the treatment of sickness. They not only have pleasing odours but numerous aroma chemicals possess useful bacteriostatic and antiseptic properties. Moreover, the rarity and high cost of aromatic resins, spices and perfumes have made them useful as currencies and as gifts exchanged between rulers. Yet there is no information regarding the invention of the first process for elaborating perfumes that is common to all of the major basic technical advances that are at the origin of our civilization.

The history of perfumery is generally identified first with the history of natural perfumes. The introduction of synthetic products in this domain is extremely recent and did not occur until the end of the nineteenth century. For the ancient civilizations, perfumes were synonymous with crude aromatic raw materials. These were important objects of barter, being both rare and precious in small quantities. Perfumes were also added to the mystique of religious ceremonies. In China, the first reports of the use of perfumes in this way go back more than a thousand years. The same can be said for India. In these countries, statues of the gods were required to be anointed with perfumed water and perfumes are still used widely in religious ceremonies to this very day. Similar rites were found in the religious customs of ancient Egypt. It is here that we see the art of perfumery finally progressing from the use of crude natural objects to become a relatively sophisticated element in the art of healing. The civilization of the Nile has passed on to us, through the stone of its monuments, a complete iconography of the processes used for preparing oils, balsams, and fermented liqueurs<sup>1</sup>.

Not until the studies of Wallach, carried out between 1880 and 1914, was there any real understanding of the composition of essential oils<sup>2</sup>. During this time he wrote



180 treatises which were assembled into a single book entitled "Terpene und Camphor". Even at that time, he was able to draw more or less exact conclusions regarding their biogenic interrelationships. As early as 1887, he realized that these compounds "must be constructed from isoprene units." Thirty years later, Robinson (Nobel prize in chemistry in 1947) was able to perfect Wallach's isoprene rule by indicating that the joining of these units must take place in a head to tail fashion<sup>3</sup>. The work of Wallach is of such importance that he was honoured in 1910 with the Nobel Prize in chemistry "in recognition of the impetus he gave to the development of organic chemistry and the chemical industry by his pioneering work in the domain of alicyclic substances."

Since this early era, the number of synthetic fragrance materials has increased to the extent that today's perfumer has several thousand synthetic products to choose from. Moreover, every day the search goes on for original perfumery notes which will enrich even more this "palette" among the many new substances generated by chemists in the research laboratories of French, Swiss, German, Dutch, English, American, and Japanese fragrance manufacturers<sup>4</sup>.

Thus far, most of the syntheses have been very simple ones with only one or two steps and starting generally from cheap and abundant raw materials. For this reason they obviously have great industrial interest, but this does not detract in any way from the challenge of the search which exists at two levels<sup>5</sup>.

The first level concerns syntheses which can be qualified as academic in that they employ the most sophisticated synthetic methods and often involve a very large number of steps. In short, no economic considerations can be said to be taken into account in this case for which only the final objective counts. If such syntheses were to be commercialized they would lead to prices exceeding even those of the natural products.

The second level of the challenge concerns the industrial synthesis of terpenoids. It was only in 1955 that the first total industrial synthesis of linalool at a cost price below that of natural linalool was made in Grasse. Syntheses such as these, which are often called "acetylenic syntheses", also give access to aliphatic, mono-, di-, and

sesquiterpenoids and they permit the total synthesis of vitamins A, E, and K as well as numerous carotenoids<sup>5</sup>.

Processes which use natural substances as relays are considered to be only “half-syntheses”. In this investigation the raw material is obtained as waste from an industrial process, i.e. crude sulphated turpentine, which is nonetheless derived naturally from trees in the form of wood pulp.

## **1.2 History of Linalool<sup>6,7</sup>**

Linalool and its esters are distributed in a vast number of essential oils from trace up to major amounts. Its early production was accomplished in 1875 by isolation from Cayenne Bois de Rose oil from French Guiana. A Frenchman by the name of Licare was so involved with the oil’s production that linalool was initially called Licareol. Subsequent production shifted to Brazil (Bois de Rose oil) and Mexico (Linaloe oil) and then from Ho-leaf and Ho-wood oil (Taiwan, China and Japan). Availability of natural linalool has remained fairly constant since 1925. The volume of supply of natural product, however, has been dwarfed by the supply of synthetic product. The demand for linalool cannot be met by the production of natural oils.

Growing world demand for aroma chemicals just after the Second World War led to intense research programs to synthesize products and discover new substitutes for others. Coincidentally with that activity, the chemical developments in synthetic vitamin production made by BASF and Hoffman-La Roche provided raw material product streams which allowed the production of synthetic linalool and its derivatives (discussed in more detail in § **1.7.4 Linalool Synthesis**).

Initially, pure synthetic linalool met with great resistance by perfumers. It lacked the fine, intricate shading of organoleptic impression that the natural products displayed due to the presence of trace amounts of impurities. Moreover, the synthetic linalool contained impurities that shaded the impression in a new way. In most case, these impurities are not a direct result of the primary feedstock used to begin the production, but arise from the co-generation of by-products in the steps just prior to the creation of the linalool. As the impurities are present in small amounts and are of

similar boiling points, their removal is prohibited by economics, if not technology. Nevertheless, the availability and price eventually won out and synthetic linalool became the dominant product.

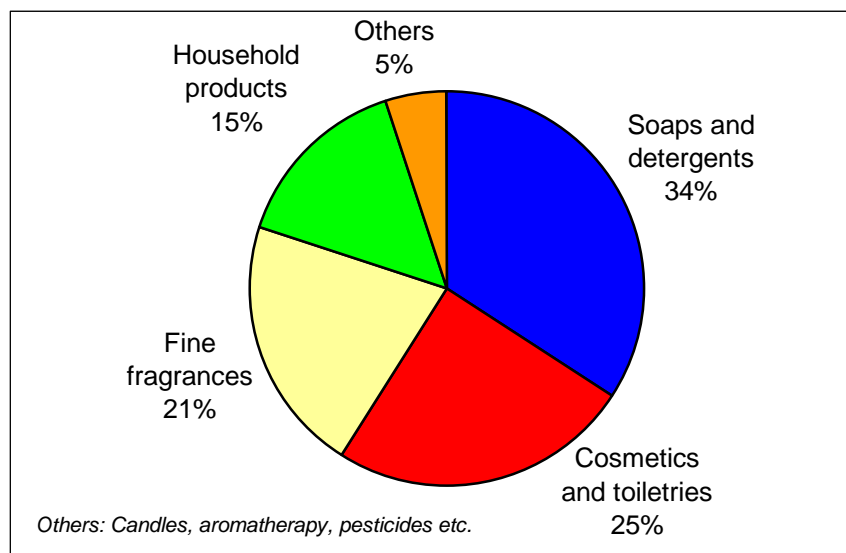
### 1.3 Problem statement

Linalool is a key intermediate for the production of important fragrance chemicals such as geraniol, nerol, geranial, and neral. Linalool can be produced via a two-step process from  $\alpha$ -pinene which is a major component of crude sulphated turpentine (CST) which is a foul-smelling, volatile waste product of the pulp and paper industry. The key step in this process is the pyrolysis step which involves the isomerisation of *cis*-2-pinanol to linalool and requires high temperatures (600-650°C) and is not very selective due to the decomposition of the product itself under these conditions. A client of the CSIR, Teubes Pty. Ltd., is a manufacturer of flavour and fragrance compounds for the local and international fragrance market and is interested in producing linalool since they would then gain access to other valuable fragrance chemicals via relatively simple processes. Earlier work conducted by AECl, R & DD did not meet with much success since the selectivities to linalool were very poor and the process could hardly be deemed as scalable.

### 1.4 The Global Fragrance Industry<sup>8</sup>

Fragrance formulations are widely used globally for enhancing, among others, cosmetics, detergents and pharmaceutical products. Compounded fragrances are thus complex blends designed to impart an attractive aroma to consumer products such as perfumes, toiletries, household cleaners, etc. The formulations may contain aroma chemicals as well as essential oils and natural extracts. The formulation will also contain solvents, diluents and carriers.

**Figure 1.1** outlines the breakdown of the use of fragrance compositions in the end-markets<sup>9</sup>.



**Figure 1.1: Fragrances End-Use Market**

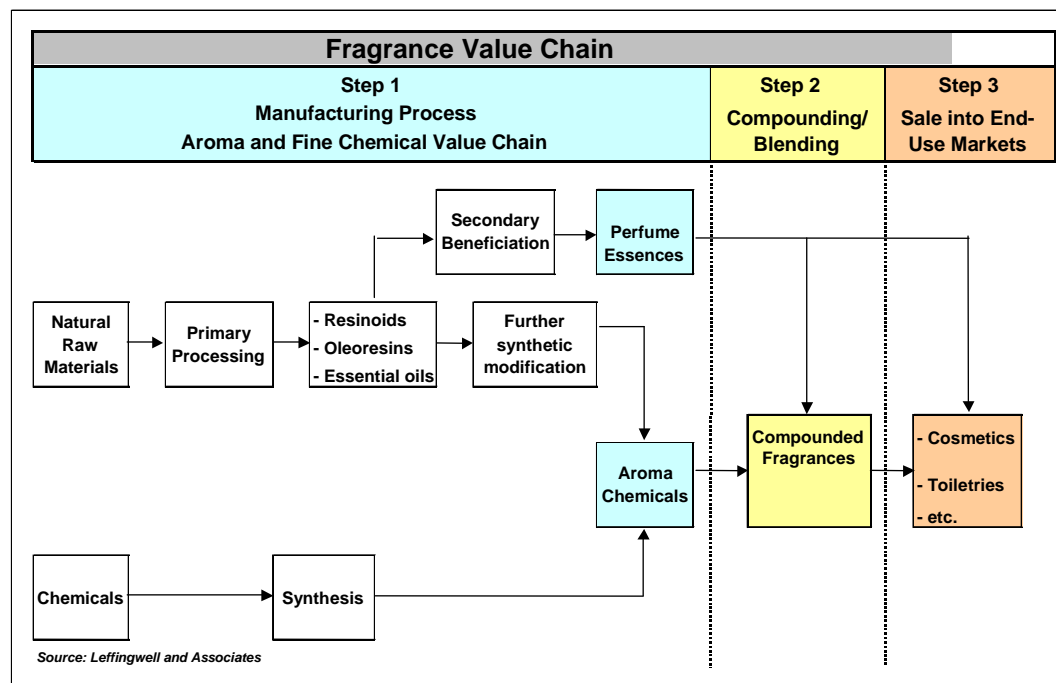
In the fragrance end-use market, over 50% is used in two applications i.e. soaps/detergents and cosmetics/toiletries. These end-use markets are characteristically first-world markets. This is supported by the global consumption usages for flavour and fragrances, which show that the USA accounts for 31% of the market, with Western Europe representing about 29% of the world market and Japan 12%<sup>8</sup>. The rest of the market lies in developing countries with high growth rates, or growth potential, as use of the consumer products in these particular major end-use markets increase. The South African market in 1999 was worth a total of \$ 107.3 million<sup>9</sup>.

In 2002, the worldwide fragrance business, including sales of compounded fragrance products, aroma chemicals as well as essential oils and natural extracts, was valued at an estimated \$ 5.3 billion. The industry is segmented broadly into three areas:

1. Isolation of synthetic and natural aroma chemicals or essential oils/natural products. (Aroma Chemicals are single, chemically defined substances which act on the senses of smell and taste; and essential oils are naturally occurring, volatile products obtained from various parts of plants.)
2. Compounding of these products into formulations tailored to meet specific customer requirements

3. The sale and use of these formulations in the production of personal care and pharmaceutical active ingredients, food and beverage markets, etc.

The fragrance value chain is represented in **Figure 1.2**<sup>10</sup>.



**Figure 1.2: Fragrance Industry Value Chain**

**Table 1.1** illustrates the relative values of the various components of this value chain. It is worth noting that over 75 % of the industry's value lies in the composition of the flavours and fragrances.

**Table 1.1: Value of the Flavour and Fragrance Industry 2002**

	% of the Value Chain	\$ Billion
Aroma Chemicals	12%	1.8
Essential Oils and Natural Extracts	12%	1.8
Flavour Compositions	41%	6.2
Fragrance Compositions	35%	5.3
<b>TOTAL</b>	<b>100%</b>	<b>15.1</b>

A recent survey by the market research company, Freedonia Group<sup>11</sup>, forecasted growth in global demand for flavours and fragrances of 5.4% per annum, with the industry to reach \$18.4 billion in 2004. Market growth was predicted to be primarily due to strong growth in the developing regions of Latin America and Asia (excluding Japan). Countries such as China, Brazil, India, Mexico, Vietnam and Chile particularly are experiencing dramatic growth in their food-processing and consumer-product industries. It was also predicted that the growth in developed markets will in contrast be slow. The developed countries market growth is characterised by trends, which favour less flavour and fragrance-intensive consumer goods, consolidation in end-user industries, strong pressure on price reductions, and market maturity. It was also anticipated that the growth in the essential oil and natural extract market will exceed that in the synthetic aroma chemical market.

Large international Flavour and Fragrance houses specialise in the compounding of flavour and fragrance products. A number of these houses also produce selected aroma chemicals for captive use. In addition, some also manufacture personal care active ingredients from captive and purchased aroma chemicals. Generally, success in the formulation and compounding business is dependant on the ability to offer a basket of products, and an ability to respond quickly to ever-changing trends in consumer preference. Most major participants in the Flavour and Fragrance industry operate internationally and maintain a presence in virtually all markets of the globe. The major motivation for this is that the leading Flavour and Fragrance houses are following key end users such as food processors and detergent producers to these regions. China, Brazil, and Mexico have as a result seen a strong growth in production.

Over recent years there has been a large amount of rationalisation and consolidation within the industry and this process is likely to continue. It has been estimated that there are over 1,000 companies active in this industry worldwide, but 12 international flavour and fragrance companies hold over 65% of the market share. One major reason for this is that of the cost of owning an adequate infrastructure, which includes the cost of toxicological testing, research and development, quality control, and efficient manufacturing and marketing, is so high that only the largest of companies

can afford it. The costs associated with these activities also explain the reason for the high value associated with this segment of the market.

**Table 1.2** lists the top 12 companies in 2002<sup>12</sup>. It is noticeable that the top 6 participants have sales of over \$ 800 million. The next tier has sales in the region of \$ 200 to 400 million. Below this level, the industry is highly fragmented with a host of much smaller players. A recent report from SRI International<sup>13</sup> notes that there is a “virtual absence of medium-sized participants” with sales in the region of \$ 75 to \$ 100 million.

**Table 1.2: Estimated Sales Volume Flavour and Fragrance Companies 2002**

Company	Country	\$ million	Market Share
Givaudan	Switzerland	1,933	12.8%
IFF	USA	1,809	12.0%
Firminech	Switzerland	1,373	9.1%
Symrise	Germany	1,300	8.6%
Quest International	UK	1,153	7.6%
Takasago	Japan	850	5.6%
Sensient Technologies	USA	423	2.8%
T.Hasagawa	Japan	381	2.5%
Mane SA	France	270	1.8%
Danisco	Denmark	263	1.75
Degussa Flavours	Germany	234	1.5%
Robertet	France	218	1.4%
<b>TOTAL TOP 12 COMPANIES</b>		<b>10,206</b>	<b>68%</b>
Others		4,894	32%
<b>TOTAL</b>		<b>15,100</b>	<b>100%</b>

There are a number of reasons for this consolidation. A major reason has been the pressure on prices. As outlined above, the major market is the USA followed by Europe and Japan. In the USA the advent and power of the supermarket chains has placed pressure on consumer product manufacturers to drop costs in order to be given “shelf space”. This has led to consolidation amongst consumer product manufacturers. These manufacturers in turn have pressurized the Flavour and Fragrance houses (which once commanded huge margins) to reduce prices. The

Flavour and Fragrance industry is thus reacting to the concentration of its customer base. In addition, end-users have found it too costly to deal with too many Flavour and Fragrance houses, and accordingly only deal with the largest few. If the Flavour and Fragrance house is not strong in all markets it cannot keep the custom of a larger customer such as a Unilever or Procter and Gamble. Thus growth in turnover by the Flavour and Fragrance houses has come primarily from acquisitions with the company profiting from economies of scale.

A further reason for the consolidation has arisen from the drive of major chemical companies to stick to core business of high volume manufacturing. As a result, many of them have sold their Flavour and Fragrance divisions to previous competitors. A recent example is Bayer, which used to own Haarmann and Reimer, which was merged with Dragoco to form Symrise in 2002. In 2000, Roche spun off Givaudan. The only chemical company still with a Flavour and Fragrance house is ICI with Quest International.

The smaller and medium sized companies active in the Flavour and Fragrance industry have survived by concentrating on their specialist knowledge within a niche market and offering services and products that the industry giants don't offer. An example of this is Treatt plc, based in the United Kingdom. This company acts as a one-stop shop for the Flavour and Fragrance industry in Europe, but not in the US. Fine chemical companies are increasingly forging partnerships with Flavour and Fragrance customers through joint projects and special services, and are becoming indispensable partners of the Flavour and Fragrance industry. Rhodia is an example of this trend, producing natural vanillin under license from Givaudan who could not justify operating the process on its requirements alone. Fine chemical companies can develop new compounds at a smaller scale or offer process improvements to customers losing patent protection.

## **1.5 The Fragrance Industry in South Africa**<sup>8,13,14</sup>

The market for fragrances in South Africa and Sub-Saharan Africa in 1999 and 2004 is shown in **Table 1.3** below:



**Table 1.3: Market for Fragrance in Sub-Saharan Africa (\$M): 2001-2004<sup>8</sup>**

<b>Fragrance</b>	2001	2002	2003	2004
<b>Soaps/Detergents</b>	24.6	27.7	28.6	36.5
<b>Cosmetics/Toiletries</b>	12.0	14.7	13.0	17.2
<b>Household cleaners</b>	8.3	9.2	5.9	7.4
<b>Fine Fragrances</b>	2.5	2.7	1.1	1.3
<b>Others</b>	3.2	3.4	3.7	4.1
<b>Total</b>	50.6	57.8	52.3	66.5
<b>Growth rate</b>		2.7%		4.9%

In South Africa, the current emergence of the black middle class is having a positive impact on the consumption levels of flavour and fragrance containing compounds.

Within the fragrance sector, the largest use is in soaps and detergents. Within this sector, washing soap is predominant in the less affluent regions where the use of washing machines is at nominal levels. Many cosmetics and toiletries multinationals have located production facilities in South Africa as a production base for the Sub-Saharan region.

The total South African market in 2004 was predicted to be \$ 133 million. At an exchange rate of R 7/US\$ this is equivalent to R 877 million. This figure for the value of the South African Flavour and Fragrance market in 2004 has been confirmed by industry sources. The regional South and Sub-Saharan African market in 2004 was expected to be in the order of \$ 279 million or R1,887 million. Growth in the region in the fragrance market is anticipated to continue to be strong at approximately 4%.

Any increase in aroma chemical and essential oil production in South Africa would increase the potential of participating more in the regional Flavour and Fragrance market.

## 1.6 Aroma Chemicals from Turpentine<sup>15,16</sup>

### 1.6.1 Turpentine

Turpentine is the volatile oil obtained from pine trees by three manufacturing processes, namely gum turpentine, sulphate turpentine, and wood turpentine. Turpentine obtained by distillation from the oleoresin collected via the tapping of living trees of the genus *Pinus* (whether natural stands or plantations) is known as gum turpentine. This distinguishes it from turpentine recovered as a by-product from chemical pulping of pines and which is referred to as sulphate turpentine. Wood turpentine is obtained from aged pine stumps. This latter product is no longer of any commercial significance<sup>17</sup>.

Turpentine purchased by the chemical industry as a source of isolates for conversion to pine oil and fragrance and flavour compounds is assessed on the basis of its composition. Crude sulphate turpentine is a complex mixture of C<sub>10</sub> monoterpene hydrocarbons composed mostly of alpha pinene (60 – 65%), beta pinene (25 – 35%) and other monocyclic terpenes such as limonene and a small amount of anethole. Beta pinene is more versatile chemically, although alpha pinene is usually more abundant.

The composition of turpentine varies considerably according to the species of pine from which it is harvested and this greatly influences its value and end use. A total pinene content of 90 % or greater would be regarded as good, becoming excellent as the beta-pinene contribution increases above 30-40 %. Portuguese, American and Brazilian turpentines are all high in pinenes. Anything much less than 70-80 % pinene would be of limited value for derivative manufacture, at least if the turpentine were offered for sale on the international market. The presence of certain compounds in the turpentine lowers its value; the most common of these is 3-carene, which may comprise 50% or more of Indian turpentine. This product finds little use other than as a solvent.

It has been estimated that the total world production of turpentine is around 335,000 tons, of which around 100,000 tons is believed to be gum turpentine, most of the remainder being sulphate turpentine. Of the 335,000 tons, approximately 100,000 tons are used as starting material for the production of aroma chemicals. The USA

and the People's Republic of China are the world's largest producers and consumers of turpentine. The Southeast region of the USA is the largest crude sulphated turpentine producing area of the world. Most American requirements are met by domestic sulphate turpentine production but gum turpentine is also imported for fractionation and conversion into derivatives. Chinese requirements are met by internal production of gum turpentine.

The biggest single turpentine derivative is synthetic pine oil, which is used in disinfectants, cleaning agents and other products with a "pine" odour. There are also some specialized uses, for example in the pharmaceutical industry. Most turpentine nowadays, however, is used as a source of chemical isolates, which are then converted into a wide range of products. The alpha and beta pinene constituents of turpentine are the starting materials for the synthesis of a wide range of fragrances, flavours, vitamins and polyterpene products and form the basis of a substantial and growing chemical industry. Derivatives such as isobornyl acetate, camphor, citral, linalool, citronellal, menthol and many others are used either in their own right, or for the elaboration of other fragrance and flavour compounds. Many of the odours and flavours in use today, which are associated with naturally occurring oils, may well be derived from turpentine.

Turpentine is traded in much higher volumes than other essential oils and is often imported direct from source by the end-user or fractionator. Prices are subject to negotiation although they are very dependent on the quality and composition of the turpentine: the greater the proportion of beta-pinene compared to alpha-pinene, the higher its value.

The price of turpentine is linked to the pulp and paper market. When the industry, is weak, production of crude sulphated turpentine suffers. From 1997 through 1999, the paper and pulp industry performed poorly, leading to a shortage of crude sulphated turpentine. In 1998, prices had peaked at US\$ 1.75/gallon. As demand fell off and inventories rose, the price collapsed to US\$ 0.5/gallon in 2000. Prices have stayed in this region, even though the production of turpentine in the US has decreased. Globally, the overall market for turpentine has declined. Other markets include commodity products such as polyterpene resins and dipentene.

The market for crude sulphated turpentine in 2003 was oversupplied and demand low. In addition, a new source of competition is gum turpentine, supplied from China. This type of turpentine does not contain sulphur, which makes synthesis easier since sulphurous compounds do not need to be removed.

### 1.6.2 Aroma Chemicals

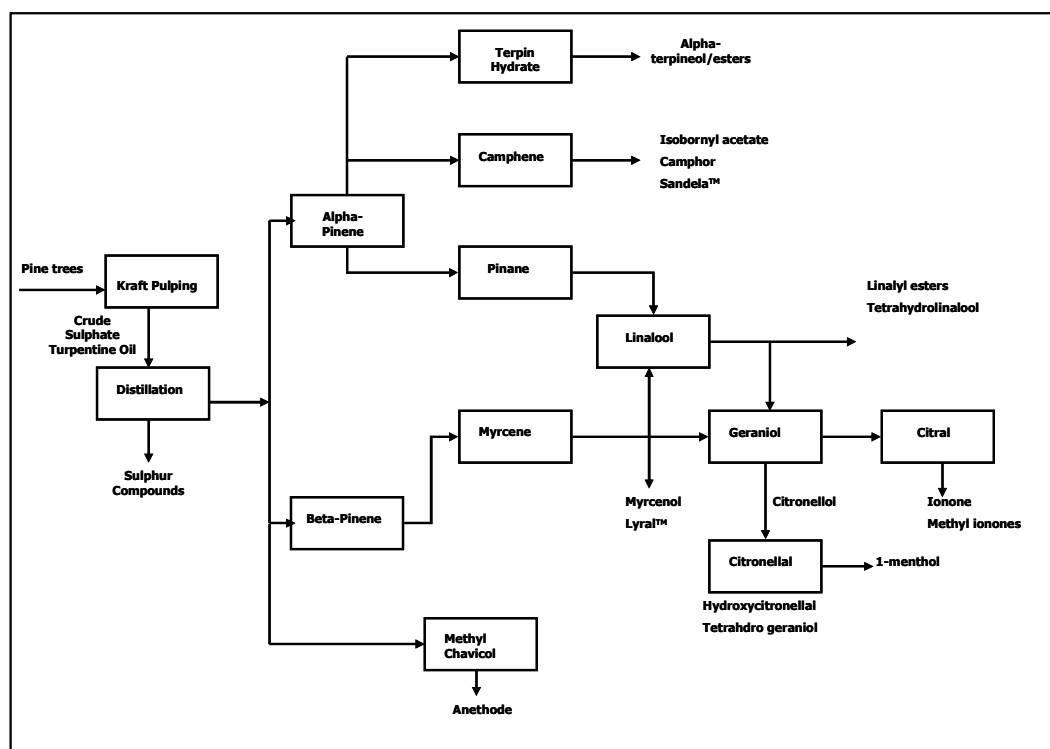
The sulphate turpentine method produces turpentine and tall oil as by-products of the sulphate pulping of pine, commonly known as the Kraft pulping process. In this process, wood chips (chiefly pine) are cooked in an alkaline liquor to produce pulp. During the cook the turpentine contained in the oleoresin of the pine chips is volatilised and then condensed. The condensate contains crude sulphate turpentine, which has a dark colour and foul odour from the constituent sulphur compounds. During further synthesis, the sulphur compounds are removed from the crude sulphated turpentine. The Kraft pulping of pine trees produces roughly 204 kg of chemical by-products and 5 tonnes of cellulose pulp from 10 tonnes of wood chips.

Components of the crude sulphated turpentine, such as alpha and beta pinene are distilled and used to produce a variety of flavour and fragrance materials as shown in **Figure 1.3**, below. While terpenoids are components of essential oils and oleoresins of plants, most terpenoids consumed in the Flavour and Fragrance industry are however produced via synthetic methods.

The cost of pinenes, ex crude sulphated turpentine, significantly affects the price of the terpenoid aroma chemicals. For example, geraniol, which is typically stable, declined when the price of crude sulphated turpentine fell in 1999 and 2000. Price volatility and supply uncertainty limit the competitiveness of natural terpenoids, as users often switch between natural and synthetic materials, depending on the relative cost and availability of the compounds. For example, when heavy rains in the main growing regions of *Litsea Cubeba* substantially escalated the price of natural citral and its lemongrass oil feedstock in the late 1990's, some users of citral switched to synthetic alternatives. Natural types are however sometimes preferred for higher value applications such as for fine fragrances. For example, natural geraniol produced

from fractionating palmarosa oil is preferred in these applications whereas the synthetic version is favoured in soaps and detergents.

A short review of some of the more important aroma chemicals produced from turpentine or alpha/beta-pinene are shown in **Figure 1.3**, below<sup>10</sup>.



**Figure 1.3: Conversion of Turpentine Oil to Aroma Chemicals**

### 1.6.3 Feedstock Analysis<sup>10,18</sup>

Crude sulphated turpentine is a by-product of cellulose/paper pulp obtained from pinewood using the Kraft sulphate wood pulping process. The source of crude sulphated turpentine within South Africa is therefore limited to those paper and pulp plants which use the Kraft process on softwood i.e. pine. A recent report from the Paper Manufacturers Association of South Africa published a Table of the capacities and products from the South African pulp mills.

From **Table 1.4** it can be seen that the only potential sources of crude sulphated turpentine are the Mondi Richard's Bay mill and the Sappi Ngodwana mill. Mondi is however increasingly switching to hardwood. Discussions with Mondi indicated that

it no longer produces crude sulphated turpentine. Sappi Ngodwana is the only South African mill producing any crude sulphated turpentine in significant quantities. This mill currently produces roughly 30 tons per month. The Sappi Tugela and Sappi Usutu (Swaziland) mills produce minor amounts of crude sulphated turpentine, in the region of 10 tons per month each, however these quantities are variable. The maximum amount of crude sulphated turpentine available from the Sappi plants therefore appears to be in the range of 360 – 600 tons annually.

**Table 1.4: South African pulp mill capacities 2001**

<b>Company</b>	<b>Mill</b>	<b>Products</b>	<b>2001 Capacity (1000 t/a)</b>
Mondi	Richards Bay Mill	Hardwood and softwood Kraft pulp	576
	Piet Retief Mill	Hardwood and softwood neutral sulphite semi-chemical pulp	55
	Felixton Mill	Unbleached bagasse pulp	50
	Merebank Mill	Thermomechanical pulp Groundwood pulp	171 55
Sappi	Ngodwana Mill	Hardwood and softwood Kraft pulp Groundwood pulp	410 100
	Tugela Mill	Unbleached softwood pulp Hardwood neutral sulphite semi-chemical pulp	230 120
	Stanger Mill	Bleached bagasse pulp	60
	Enstra Mill	Bleached hardwood pulp	90
	Saiccor Mill	Dissolving pulp	600
		<b>Total</b>	<b>2,517</b>

The specification of Tugela Turpentine is shown in **Table 1.5** below. This specification may change with species and other processing parameters, but gives an indication of the alpha and beta pinene content of South African turpentine.

**Table 1.5: Specification of Tugela Turpentine**

<b>Constituent</b>	<b>Percentage</b>
Alpha Pinene	51.3%
Beta Pinene	24.7%
Beta Phellandrene	17.6%
Myrcene, camphene, limonene, and alpha terpineol	6.4%
<b>TOTAL</b>	<b>100%</b>

Sappi is, however, currently reviewing its South African pulping processes. There is a strong possibility that within the next few years the Ngodwana mill may change one of its digesters to Eucalyptus (hardwood). The reason for this change would be driven by Sappi's strategy in terms of maximising its profitability by optimising the types of paper produced as well as the amount of short-fibre pulp sold internationally. Currently there is a large global demand for short-fibre pulp, on which the profitability is high. Short fibre requires Eucalyptus.

Should this change occur, it would obviously have a dramatic impact on the quantity of crude sulphated turpentine available, as only one digester will remain on softwood. This change is not a certainty, and before any decision is taken a full feasibility study including an environmental analysis would have to be performed. However, in the long-term, the possibility of a decrease in the availability of crude sulphated turpentine must be considered. The other two Sappi mills producing crude sulphated turpentine i.e. Tugela and Usutu will not change from softwood. These plants however produce crude sulphated turpentine in much smaller quantities than Ngodwana.

The sustainable volume from the Ngodwana mill is expected to be decreased by 50%. Feedstock from the Tugela and Usutu mills varies between 0 – 240 tons annually. Depending on whether 1 or 2 digesters remain on softwood, the Sappi Ngodwana capacity is expected to range between 180 – 360 tons annually. Discounting one of the Ngodwana mills therefore, leaves the sustainable amount of feedstock nationally between 180 and 420 tons crude sulphated turpentine annually. This translates into a corresponding amount of alpha and pinene of only 137- 319 tons per annum.. The future feedstock supply in South Africa can be summarised as follows (**Table 1.6**):

**Table 1.6: Future CST Feedstock Supply in South Africa**

	<b>Tons</b>
Sappi Ngodwana	180
Sappi Usutu	0 – 120
Sappi Tugela	0 – 120
<b>Total Potential Crude Sulphated Turpentine</b>	<b>180 – 420</b>

As the product is extremely environmentally unfriendly, Sappi disposes of the product as quickly as possible. This entails putting it immediately into tankers and selling it. There is currently only one customer who purchases the entire amount, including the small volumes from Usutu and Tugela. This customer is a South African trader, based in London. The crude sulphated turpentine is all shipped off-shore to this customer who pays a price linked to the crude sulphated turpentine index, which ranges from R 800 – 1400/ton depending on exchange rates. The price is paid to Sappi in Rands/ton, although internationally crude sulphated turpentine is traded in litres. Sappi performs some minor chemical analyses, mostly related to the water content, but the customer does other additional tests, and on the basis of these results determines the price.

In principle, Sappi is prepared to sell to a local South African customer, provided that this customer is prepared to commit to an immediate off-take as Sappi obviously cannot afford to have the product unsold.

### **1.7 Commercial Production of Terpenoids – General Considerations**

When designing a synthesis for large-scale commercial production, factors such as safety, environment, feedstock availability and raw material and process costs come into play. The development chemist must find a satisfactory balance between them all. In principle, every production hurdle must be overcome, but the solution will always involve a cost. This cost, whether it relates to the cost of feedstock or reagents, waste treatment and disposal, engineering, logistics and R&D, will become part of the total production cost. The role of the process development chemist is,



therefore, to find the lowest possible overall production cost. This is a difficult task and requires skills in both chemistry and economics, together with a knowledge of the fine chemicals market, available process technologies and legislation affecting chemical production.

The reason for the commercial production of chemicals is to provide a benefit to the consumer. That benefit could be a drug to cure illness, a fragrance to enhance the pleasure and benefit of using a bar of soap, an improved construction material and so on. In every case, there will be a limit to the amount that the consumer is prepared to pay for this benefit and also a limit to what society is prepared to tolerate in terms of side effects of the production process and the use of the product. Seven crucial parameters in a commercial-scale chemical process are safety, environment, purity, reproducibility, capacity, cost, and sustainability<sup>19</sup>.

### **1.7.1 Safety**

By far the most important consideration is that of safety. No company would wish to endanger either its employees or the public and any responsible company will invest considerable time, effort and money into ensuring that it does not do so.

Chemical process safety relates largely to handling of hazardous materials and to exothermic reactions. Handling of hazardous materials, which may be starting materials, reagents, catalysts, intermediates or products may present a danger to the process operators and anyone else within range of the plant in case of accidental emissions. Exothermic reactions present a danger in that if they are not controlled adequately and the heat produced removed efficiently, they can lead to escape of material from the reactor possibly with explosive violence. In the event of an explosion, fragments of the reactor body and associated plant are likely to become dangerous missiles.

Good practice dictates that a detailed analysis of the thermodynamics of the process will be carried out before scale up. The ratio between surface area and volume decreases as the size of the reactor increases. Thus, the larger the reactor, the smaller is its surface area relative to its volume and so the less able it is to dissipate heat. An exotherm which is too small to be noticeable on a laboratory scale might be sufficient

to present a serious hazard on manufacturing scale. The effects can also be magnified if, as is usually the case, the heat produced leads to an increase in the reaction rate. In turn, this increase in the reaction rate leads to an increase in the rate of release of heat, which, in turn, leads to a further increase in rate and so on. Such a situation is known as a thermal runaway.

The materials of construction of a chemical plant must be resistant to their contents over a long period of time and testing of samples of the materials in the reaction media must be carried out to ensure that corrosion does not lead to escape of reaction materials or failure of plant components. This work is usually carried out in collaboration between development chemists and chemical engineers.

Before a process can be scaled up, it is usual to carry out what is referred to as a Hazard and Operability Study, or HAZOP. In this study, all possible issues of safety will be considered and checked to see that safety precautions are adequate. This will include consideration of the possible consequences of accidental omission of one or more reagents or catalysts, accidental addition of excess of any reagent, wrong order of addition, mixing of any combination of the reagents outside the reactor (e.g. leaks on storage), incorrect profile of reaction temperature, etc.

Inspectors from governmental health and safety organisations have the power to close down any operation which is deemed to be unsafe and to fine and imprison companies and individuals who carry out, authorise the operation of, or allow unsafe practices to be carried out. Thus the law provides a strong motivation for ensuring the safety of chemical processes, in addition to the ethical and financial (loss avoidance) for doing the same.

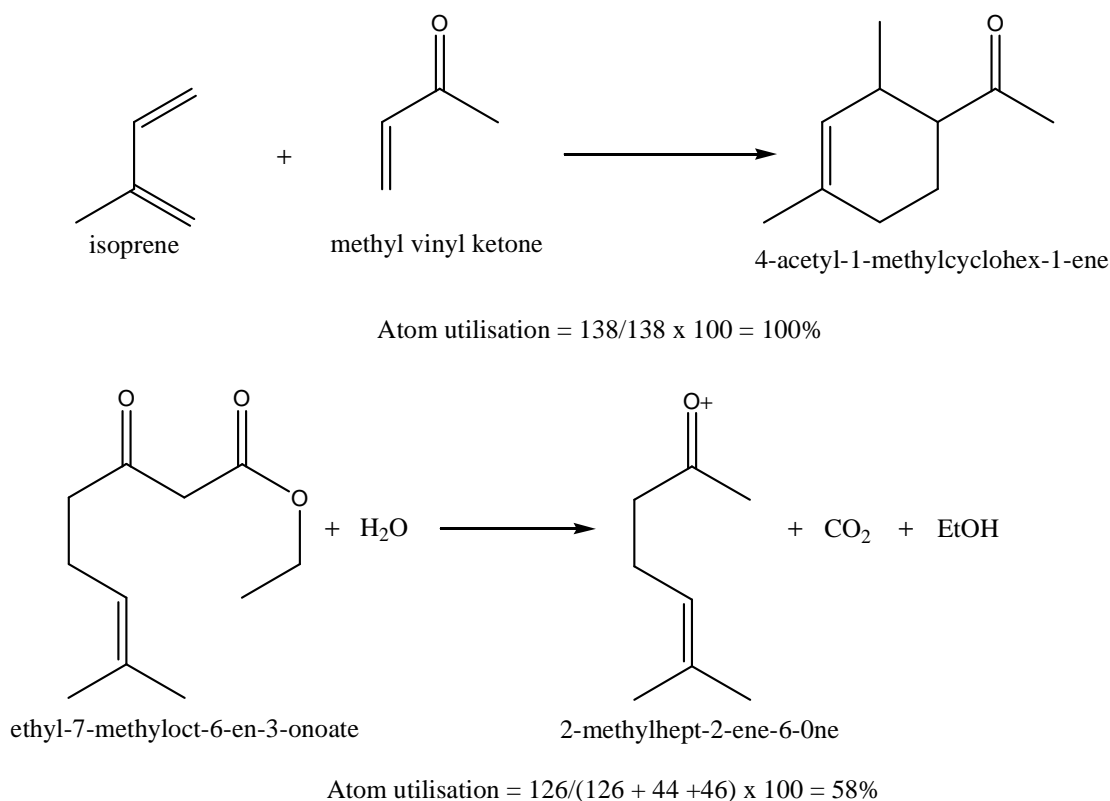
### **1.7.2 Environment**

Any of the starting materials, reagents, catalysts, products and by-products of a chemical process could possibly find their way into the environment. The chemical company must ensure that precautions are taken to ensure that there are no accidental releases into the environment. Nonetheless, it will also have contingency plans for dealing with any escape of material if such precautions should fail. All excess materials, spent catalysts, etc. and other effluent streams must either be recycled or

disposed of in an acceptable manner. Obviously, for environmental reasons, hazardous feedstocks, reagents and catalysts are best avoided. Every raw material must be transported to the production site, and they and all intermediates produced must be stored and handled safely there. Hazardous materials, therefore, present issues in terms of the capital cost of the transport systems and plants which will be necessary to enable their safe use. Everything can be handled safely but the more intrinsically dangerous it is, the higher will be the cost of safety precautions.

As far as the disposal of materials is concerned; the environmental effects of materials are handled in a similar way to product safety. The environmental fate of chemicals must satisfy certain criteria for their use to be desirable or even legal. There are strict rules concerning the types of chemical waste and the manner in which they may be disposed off. The cost of disposal is dependant on the type of waste e.g. it is more costly to dispose of toxic waste since they have to be encapsulated and buried in specific sites. It is therefore desirable, as far as possible, to utilise catalytic reactions in the process rather than stoichiometric amounts of reagents. In most cases, the catalyst can be recycled and spent catalyst can be bought back by the suppliers for metal recovery and/or regeneration.

Much work has been done in recent years around the environmental impact of chemical processes. The question is, "How do we measure the environmental impact of a process?" In the early 1990s, Professors Barry Trost and Roger Sheldon proposed methods to quantify the environmental impact of a process. Trost<sup>20</sup> proposed a factor called "atom utilisation" or "atom efficiency". Atom utilisation is defined as the molecular weight of the desired product of a reaction divided by the total of the molecular weight of all species produced in the reaction, multiplied by 100 to give a percentage figure. This concentrates on the stoichiometry of the reaction. Thus a reaction of the type  $A + B = C$  is likely to be better than one of the type  $A + B = C + D$ . For example, a Diels-Alder reaction will have a higher atom utilisation than hydrolysis and decarboxylation of a  $\beta$ -keto ester, as illustrated in **Figure 1.4**, below:



**Figure 1.4: Atom utilisation**

Here two reactions are shown, both of which produce intermediates of potential use in terpenoid synthesis. In the first, isoprene adds to methyl vinyl ketone in a Diels-Alder reaction to give 4-acetyl-1-methylcyclohex-1-ene with 100% atom utilisation. On the other hand, the hydrolysis and decarboxylation of ethyl-7-methyloct-6-en-3-onoate to give 2-methylhept-2-ene-6-one proceeds with only 58% atom efficiency.

Sheldon's E-factor<sup>21,22</sup> considers not only the starting materials and products of a reaction, but also all of the materials consumed by the process. It is defined as the ratio of desired product to the sum of all by-products as shown in **Equation 1**. An alternate way of expressing this is shown in **Equation 2**.

Thus, for example, solvent and catalyst handling losses can be included. Energy can also be included by adding the weight of fuel burnt to provide it. The energy consumption is often very difficult to measure in practice because a steam generator, for example, will be used to heat a number of reactors and also other buildings, such

as laboratories and offices, on the site. Therefore, determining exactly how much steam is consumed by any individual reactor is not straightforward. Multiplication of the E-factor by an “unfriendliness quotient”, Q, (e.g. 1 for an environmentally benign salt such as sodium sulphate and 1000 for a highly toxic heavy metal) we obtain an Environmental Quotient (EQ) as shown in **Equation 3**. The lower E and EQ are, the more environmentally benign is the process.

$$E = \text{kg waste/kg product} \quad \text{(Equation 1)}$$

$$E = (\text{total kg material used and not recycled} - \text{kg product})/\text{kg prod.} \quad \text{(Equation 2)}$$

$$EQ = E \times Q \quad \text{(Equation 3)}$$

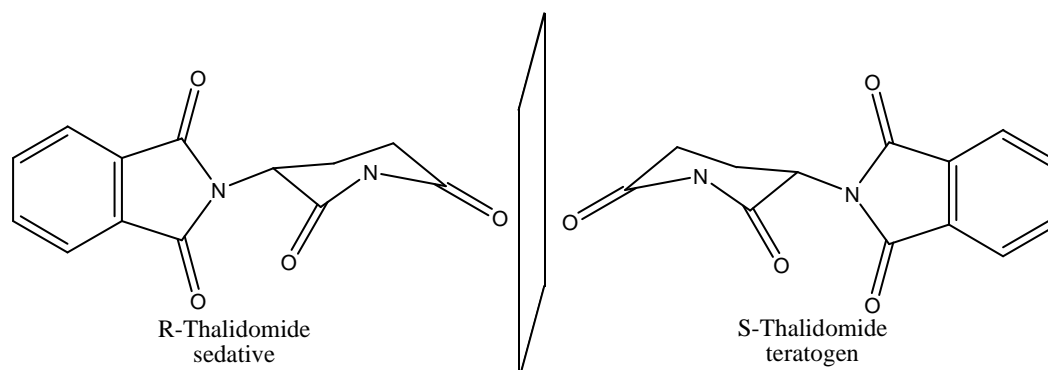
### 1.7.3 Purity

Product purity may seem an obvious factor in the development of a chemical process. However, there are a few subtleties which need to be considered. There will always be a number attached to statements of purity. For example, there may be a claim that a chemical is 99% pure or contains less than 1% of other components. The other components may have specified upper limits. For example, a product may be labelled as  $\alpha$ -pinene containing no more than 0.1%  $\beta$ -pinene. The ultimate purity limit will always depend on the ability to analyse the product. If, for the sake of argument,  $\beta$ -pinene could not be determined at concentrations below 1 part per billion (ppb) in  $\alpha$ -pinene, then the purest grade of  $\alpha$ -pinene cannot be better than “less than 1 ppb  $\beta$ -pinene”.

In many cases the nature of individual impurities may be more important than the total level of all of them. For instance, in a pharmaceutical product, the presence of 1 ppm of a potent neurotoxin is likely to be more of an issue than 1% of sodium citrate. In the fragrance industry, where the materials used are all of low toxicity, the main issue in purity terms is the presence of ingredients with very low odour thresholds since traces of such compounds can seriously affect the odour of the sample. For example, 1% of citronellol in a sample of geraniol will have less of an effect than would 1 ppm of thioterpineol as the latter would be more than enough to add a very noticeable grapefruit note to the otherwise rosy odour. In any fine chemicals industry, a sound understanding of all aspects of the product is beneficial when considering specifications of product purity.

Another important factor to be considered is the effect of starting material purity on product purity. Minor impurity components in starting materials can make their way through processes, with or without being modified structurally by the process chemistry, to appear as minor components of the product. In the case of the present study, the source of the raw material is as a waste product from the paper and pulp industry and would be expected to have numerous “impurities” in varying amounts. Therefore, there would have to be several purification steps to produce a starting material of acceptable quality.

One parameter which has become increasingly important over the last few decades is that of enantiomeric purity. This issue came into the spotlight when the drug Thalidomide was offered for sale (**Figure 1.5**).



**Figure 1.5: Thalidomide enantiomers**

The sedative properties are due solely to the R-isomer and it was not until after Thalidomide had been in use and its devastating side effects became evident that it was discovered that the S-isomer is a teratogen<sup>23</sup>. The question of enantiomeric purity is less important for the fragrance industry, partly because of the lower toxicity of fragrance ingredients and partly because chirality does not always make a significant difference to the odour of a material. Furthermore, many fragrance ingredients are manufactured from natural starting materials, such as limonene or pinene, which are enantiopure and so the products retain optical purity. With the much lower selling prices and profit margins of the fragrance industry, the economic balance between any

increased performance of a homochiral product and the increased cost of producing it, relative to that of a racemate, is more often in favour of the racemate than is the case in the pharmaceutical industry. However, even in the fragrance industry, there is a growing interest in homochiral products.

#### **1.7.4 Reproducibility**

As with purity, the requirement for reproducibility may seem obvious but on looking in more depth, one will find many instances where it is, or has been, an issue. In principle, if a production process is run in the same way every time, the outcome should always be the same. Variations arise in two ways. Firstly, variations in feedstock will give rise to variations in product. This is a particular issue when the feedstock is a natural product, such as turpentine. Variations in the weather, pests, and in genetics of any plant source are some of the factors which can produce fluctuations in the compositions of oils produced from them. The other potential cause of variability of processes lies in their sensitivity to changes in conditions. It is obviously much better to run a process which can tolerate reasonable deviations in operating parameters since one which alters course when tiny changes take place will be susceptible to factors such as accuracy of weights/volumes, temperature or pressure control and reaction times. During development, it is therefore essential to determine the robustness of a process by running it many times to ensure that a consistent output is achieved. If a process is not robust, it would be very unwise to introduce it into a plant because of the risk of loss of material or much more seriously, the risk to the safety of the operators and others in the vicinity.

#### **1.7.5 Capacity**

When a process is introduced into a plant, an estimate of sales volume would have been planned by the development chemists and chemical engineers to run the process in vessels of suitable capacity. However, by definition, such estimates are only guesses and so the forward thinking development team will have, at least at the back of their minds, a contingency plan for the eventuality that much more material is required than was anticipated. Consider, for example, a new fragrance product for which a marketing plan has been drawn up. This plan will be based on the growth of comparable materials in the past and will reflect the likely level of incorporation of the ingredient in a fragrance. It will also reflect the likelihood of fragrances

containing it winning submissions against customers' briefs. Such a plan may estimate that 1 ton of the ingredient will be needed in its first year. However, it is always possible that demand for this fragrance may be exceeded and the plant will be confronted by increased orders for this ingredient. Failure to produce it will result in serious damage to the company's relationship with the customer. So the development team, in cooperation with the plant, must be prepared for such eventualities and know how to increase production capacity rapidly if required.

## **1.7.6 Cost**

### **1.7.6.1 Raw Material Cost**

Raw materials can be the subject of negotiation with suppliers but the prices asked by suppliers will depend on the intrinsic costs of the materials and these can be estimated before any development work commences. Obviously, before carrying out any practical work, it is worthwhile calculating the raw material's contribution to a product, using a reasonable estimate of yield at every step. If the result is above the target cost of the product, then the route will never be a success. Reagent cost is also important. For example, if a base is required for a reaction, then the cost will be lower if sodium hydroxide can be used than it would if it was necessary to use *t*-butyl lithium. The, more suppliers there are for a material, the stiffer will be the competition and consequently, the lower the price. Having a large number of potential suppliers also increases the security of supply. The general rule is therefore to use starting materials and reagents which are inexpensive and which can be bought from a number of suppliers. Catalyst cost must be included in this section. Clearly, a catalyst is preferable to a stoichiometric reagent since the catalyst, in principle, can be recovered and re-used. However, handling losses and catalyst poisoning can result in a loss of active catalyst. Allowance must therefore be made in the costing for loss of a catalyst. The turnover number (TON) is normally used as a measure of catalyst efficiency and refers to the number of moles of substrate converted by one mole of catalyst before the catalyst loses its activity. A catalyst might be very expensive in terms of cost per kg from the supplier, but if it has a very high TON, then the contribution of the catalyst cost to the final price of the product will be small.



### **1.7.6.2 Overall yield of the process**

When comparing several alternative routes to a particular product, several criteria have to be considered before a particular process is selected for further investigation. One of the most important criteria is the overall yield. The yield on each stage is made up of two components, conversion and selectivity. The conversion is the moles of starting material which was consumed in the reaction divided by the moles of starting material initially used. The selectivity is the moles of the desired product divided by the moles of starting material converted. Thus, the yield of a reaction is the product of conversion and selectivity. The selectivity is the more important of the two. Low conversion is more acceptable than low selectivity since in the former case, the unreacted starting material can be recovered and recycled whereas, in the latter, the unwanted products are waste which must be disposed of.

### **1.7.6.3 Cost of waste disposal**

The formation of by-products increases the cost of the desired product by using up raw materials and reagents which otherwise could be converted to product. Waste must be disposed of in an acceptable manner and this inevitably involves cost. Similarly, the use of stoichiometric reagents generates wastes and consequent disposal costs. As an example the use of sodium borohydride for a reduction will result in the formation of sodium borate on work-up. A much better alternative would be to use catalytic hydrogenation for reduction processes when practically feasible.

### **1.7.6.4 Energy costs**

The cost of the energy used to carry out a process, must be considered in order to present a total picture. For example, there might be a choice between two reagents for a reaction and the less expensive of the two is less reactive and therefore requires a much higher temperature to effect conversion.

### **1.7.6.5 Labour and capital costs**

Every manual operation involved in a process will add labour costs to the overall cost. Charging and discharging reactors, monitoring reaction progress, monitoring batch distillations, washing regimes, and transferring the product to drums are some examples of such manual handling. Chemical plant operators are skilled people with a responsible job and so these costs will be significant. What a laboratory chemist

would regard as a one-step procedure, a chemical engineer will see as a number of unit operations. Because of the value of its products, the pharmaceutical industry might be able to stand multi-step processes with numerous unit operations per step, but most fine chemical operations, such as fragrance ingredient synthesis, cannot. One solution to this issue is to use automation wherever possible and to use continuous reactions rather than batch ones. Doing so, of course, is likely to increase the capital cost of the plant and reduce the variability of the process and so an optimum balance must be found. The use of hazardous materials or high pressures will also increase the cost of the plant. In the former case, the materials of construction and the safety precautions will add to the cost. In the latter, the vessels must be stronger, hence usually thicker walled and with additional safety features, again resulting in higher costs. The capital cost is usually depreciated over a set period, determined by the average lifetime of the type of plant in question.

### **1.7.7 Sustainability**

There are many definitions of sustainability. The most widely accepted is the one which states that “Sustainability constitutes meeting the needs of the present generation without reducing the ability of future generations to meet their needs”. All of the above factors are included since all of them must be right in order to have a sustainable process. In addition to minimising waste, as part of ensuring a sustainable operation, the industrial chemist must think about their source of feedstocks. By using particular feedstocks, will they be diminishing the ability of future generations to provide for their needs? Petrochemicals are the obvious example. The world’s reserves of crude oil are finite and their use does potentially compromise future generations. The percentage of crude oil used for chemical synthesis is very small compared to that used for energy production but, nonetheless, synthetic chemists are beginning to search for renewable feedstocks to replace oil. The fragrance industry is fortunate in that there are natural feedstocks which can be used as an alternative to petrochemicals for many of its ingredients. In the present case, the feedstock is renewable and another advantage is that an otherwise noxious waste material is being converted into higher value fragrance chemicals.

The use of halogenated solvents is considered to be environmentally unacceptable nowadays. However, when seeking alternatives, the development chemist must keep

the total picture in mind. For example, it might be possible to replace dichloromethane with liquid carbon dioxide in a given process. However, energy is required to provide the necessary pressure to liquefy carbon dioxide. This energy will probably come from burning fossil fuel and so the environmental damage from that might be greater than that caused by small losses of dichloromethane. There is also growing interest in the use of “Green processes” such as reactions in water (supercritical water), ionic liquids, solvent-free systems, and enzyme technologies.

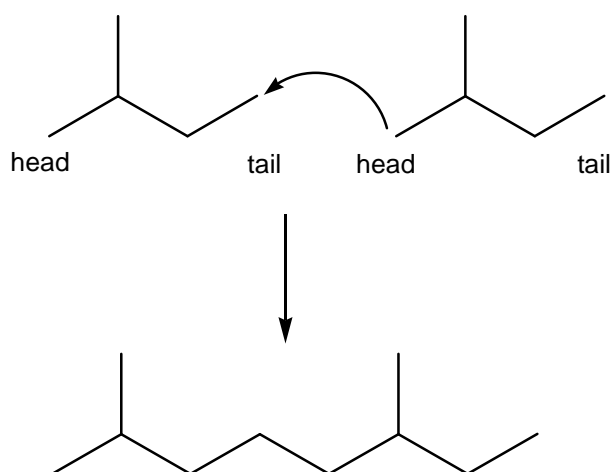
At present, there are no really good, comprehensive methods for measuring sustainability and consequently, efforts are being made to find sound and practical ways of doing so. In the meantime, the development chemist uses his experience, instinct, creativity, and lateral thinking in order to seek continual improvement in sustainability.

## 1.8 Chemistry

### 1.8.1 Definitions and Classification

Plants and animals produce an amazingly diverse range of chemicals. Most of these are based on carbon and so the chemistry of carbon came to be known as organic chemistry, i.e. the chemistry of living organisms, the chemistry of life. These chemical products can be classified into primary and secondary metabolites. Primary metabolites are those common to all species and can be subdivided into proteins, carbohydrates, lipids and nucleic acids. These four groups of materials are defined according to the chemical structures of their members. The secondary metabolites are often referred to as “natural products”. These can be sub-divided into terpenoids, alkaloids, shikimates and polyketides. The classification is based on the means by which the materials were made during biosynthetic or biogenetic pathways.

Terpenoids are defined as materials with molecular structures containing carbon backbones made up of isoprene (2-methylbuta-1,3-diene) units<sup>24</sup> (**Figure 1.6**).



**Figure 1.6: Head-to-tail fusion of isoprene units**

Isoprene contains five carbon atoms and therefore, the number of carbon atoms in any terpenoid is a multiple of five. Degradation products of terpenoids in which carbon atoms have been lost through chemical or biochemical processes may contain different numbers of carbon atoms, but their overall structure will indicate their terpenoid origin and they will still be considered as terpenoids.

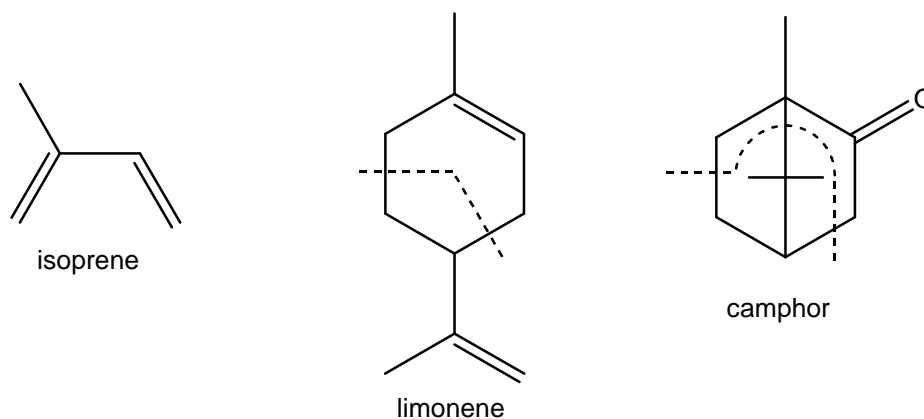
The generic name “terpene” was originally applied to the hydrocarbons found in turpentine, the suffix “ene” indicating the presence of olefinic bonds. Each of these materials contains two isoprene units, hence ten carbon atoms. Related materials containing twenty carbon atoms are named diterpenes. The relationship to isoprene was discovered later, by which time the terms monoterpene and diterpene were well established. Hence the most basic members of the family, i.e. those containing only one isoprene unit, came to be known as hemiterpenoids. **Table 1.7** shows various sub-divisions of the terpenoid family based on this classification<sup>25</sup>.

**Table 1.7: Classification of Terpenoids**

Name	Isoprene Units	Carbon Atoms
Hemiterpenoids	1	5
Monoterpenoids	2	10
Sesquiterpenoids	3	15
Diterpenoids	4	20
Sesterterpenoids	5	25
Triterpenoids	6	30
Tetraterpenoids	8	40
Carotenoids	8	40
Polyisoprenoids	>8	>40

### 1.8.2 The Isoprene Rule

The isoprene rule, proposed by Wallach in 1887, defines terpenoids as chemicals containing a carbon skeleton formed by the joining together of isoprene units<sup>2</sup>. Some 30 years later, Robinson<sup>3</sup> extended the “isoprene rule” by pointing out that in monoterpenes and such higher terpenes as were then known, the units were almost invariably linked in a head-to-tail fashion as shown for limonene and camphor<sup>26</sup> (**Figure 1.7**).



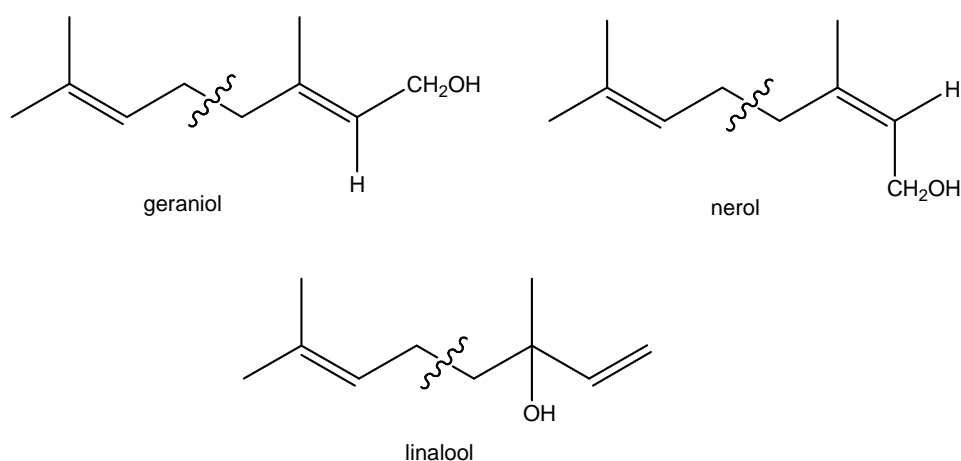
**Figure 1.7: “Isoprene Rule”**

However, many higher terpenes and a few monoterpenes were later found not to obey this amended rule, and Ruzicka and his collaborators proposed a “biogenetic isoprene rule”<sup>27-29</sup>. This generalization, which is now universally accepted, states that naturally occurring terpenoids are derived directly or by way of predictable stereospecific cyclizations, rearrangements, and dimerizations from acyclic C-10, C-15, C-20, and C-30 precursors – geraniol, farnesol, geranylgeraniol, and squalene, respectively. This rule implies a common pathway of biosynthesis for the whole family and proposals for “irregular” biogenetic routes must be treated with reservations<sup>30</sup>.

Although isoprene has been formed on pyrolytic decomposition of some monoterpenes, it is not found in plants, and many speculations were made as to the nature of the “active isoprene” of the condensing unit ranging from apiose to tiglic acid. The C-5 unit was also postulated to arise from degradation of carbohydrates, proteins, amino acids, and many other classes of plant metabolites or by elaboration of acetic acid, ethyl acetoacetate, or acetone. These early views have been well summarized<sup>31</sup>. Many C-10 compounds have been implicated as progenitors of monoterpenes, including citral, geraniol, nerol, limonene, linalool, ocimene, and others.

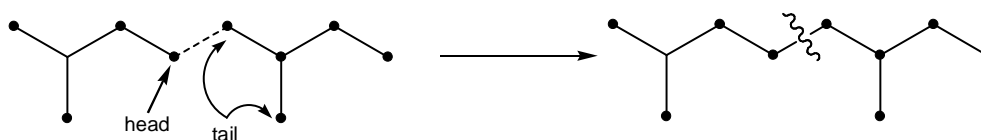
### 1.8.3 Nomenclature<sup>24,32</sup>

The terpenoids are divided into groups and sub-groups according to the pathway by which nature synthesized them and hence, by their skeletal structures since these arise directly from the biosynthesis. The first basis for classification is the number of isoprene units which make up the terpenoid, as shown in **Table 1.7**. Of particular interest to this investigation are the monoterpenoids. These contain 10 carbon atoms and can be cleaved into two isoprene units as shown in **Figure 1.8**.



**Figure 1.8: Typical monoterpenoids showing isoprene units**

The great majority of known terpene compounds result from a so-called “head-to-tail” coupling of isoprene units (**Figure 1.9**).



**Figure 1.9: Head-to-tail coupling of isoprene units**

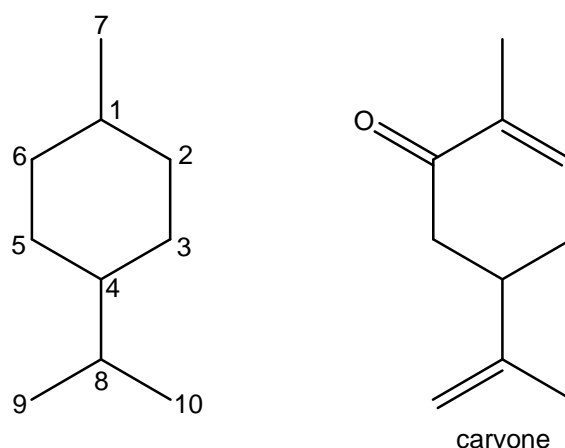
Such a structure is called “regular”, as in the case of geraniol (**Figure 1.10**) and predominates in the sesquiterpenes, diterpenes and sesterterpenes.





Families of terpenoids possessing the same skeleton are named after a principal member of that family, usually either the most common or the first to have been discovered. To name an individual terpenoid, it is customary to use the IUPAC or CAS systems of nomenclature. However, it is more convenient to use either a trivial name or a semi-systematic name derived from the terpenoid structural family to which the material in question belongs. The trivial names often relate to a natural source in which the terpenoid occurs.

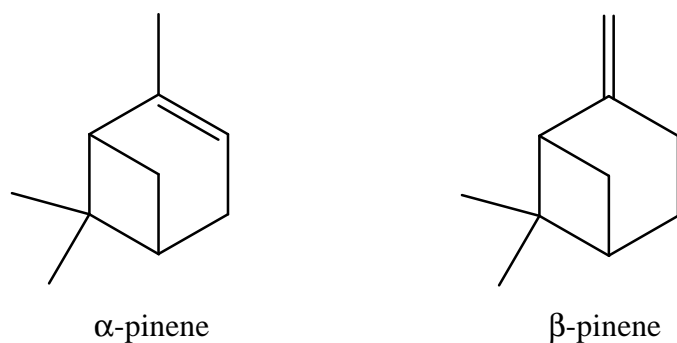
As an example of the co-existence of systematic, semi-systematic and trivial names, we could look at the monoterpenoid ketone, carvone<sup>33</sup>. Carvone occurs in both enantiomeric forms in nature, the *laevo*-form in spearmint and the *dextro*-form in caraway. The trivial name carvone is derived from the Latin name for caraway, *Carum carvi*. The basic carbon skeleton is that of 1-isopropyl-4-methylcyclohexane. This skeleton is very common in nature and is particularly important in the genus *Mentha*, which includes various types of mint, since it forms the backbone of most of the important components of mint oils. The skeleton has therefore been given the name *p*-menthane and the numbering system used for it is shown in **Figure 1.13**.



**Figure 1.13: Numbering system**

Therefore, any of the following names may be used to describe the same molecule: carvone, *p*-mentha-1,8-dien-6-one and 1-methyl-4-(1-methylethenyl)cyclohex-1-ene-6-one. To classify it, we could say it was an unsaturated ketone of the *p*-menthane family of monoterpenoids.

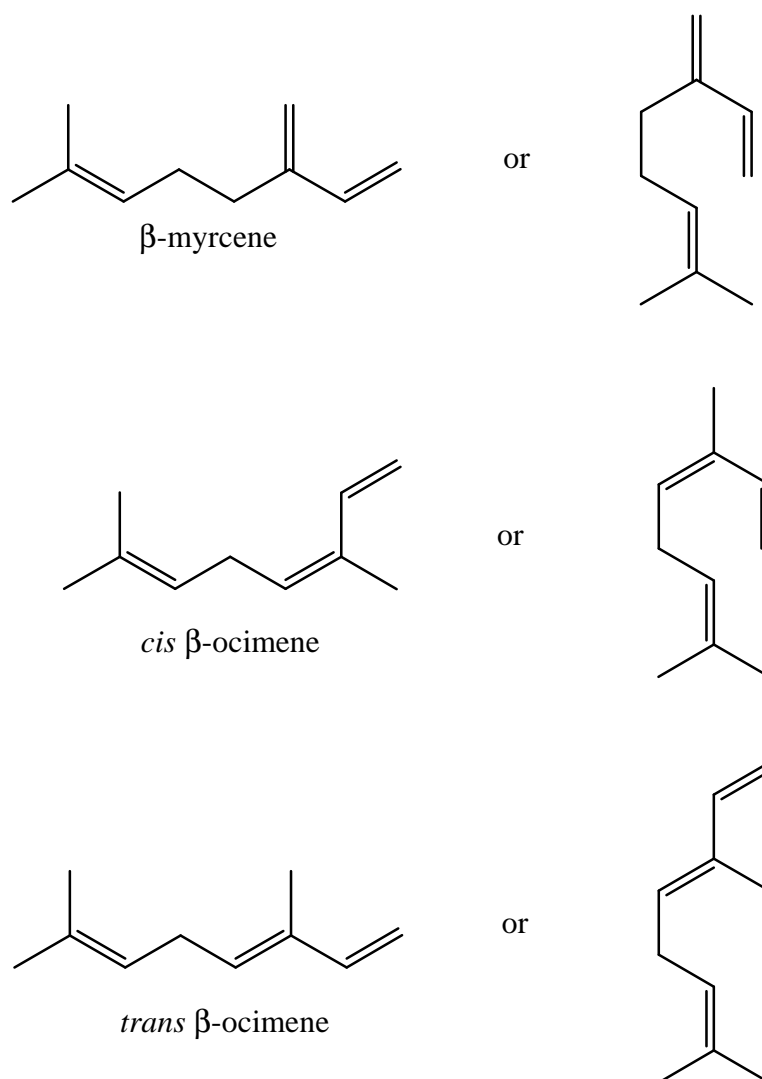
Greek letters are used in various ways to distinguish between isomeric terpenoids. They may indicate the order in which the isomers were discovered or their relative abundance in the oil. For instance,  $\alpha$ -pinene is the most significant component of turpentine, comprising almost 75% of the oil by weight. The next most significant component is  $\beta$ -pinene. These structures are shown in **Figure 1.14**.



**Figure 1.14: Use of Greek letters**

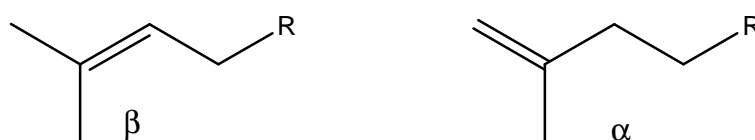
#### 1.8.4 Acyclic Monoterpenoids<sup>34</sup>

The acyclic monoterpenes, of which linalool is of particular interest, are almost all derived from 2,6-dimethyloctane. There are three principal hydrocarbons:  $\beta$ -myrcene, *cis*  $\beta$ -ocimene, and *trans*  $\beta$ -ocimene (**Figure 1.15**).



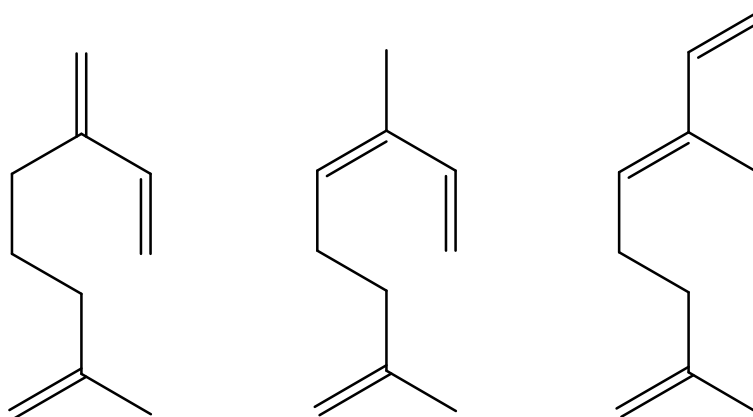
**Figure 1.15: Principal hydrocarbons**

The prefix “ $\beta$ ” indicates the isopropylidene form as opposed to the isoprene form, which is qualified as “ $\alpha$ ”. **Figure 1.16.**



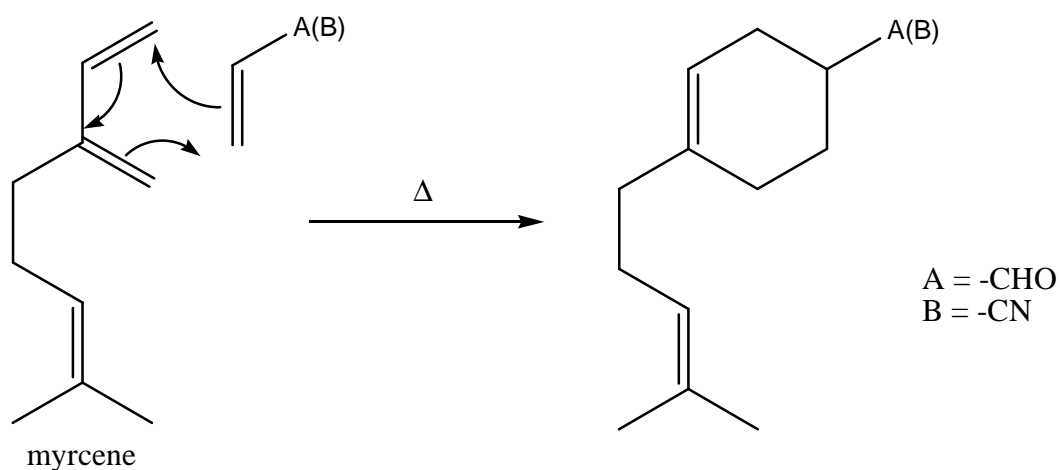
**Figure 1.16: Isopropylidene and Isoprene forms**

Some reactions give rise to the  $\alpha$ -myrcene as well as the *cis*- and *trans*-ocimenes. It is evident that the majority of natural products exist in the “ $\beta$ ”-form, isopropylidene **Figure 1.17.**



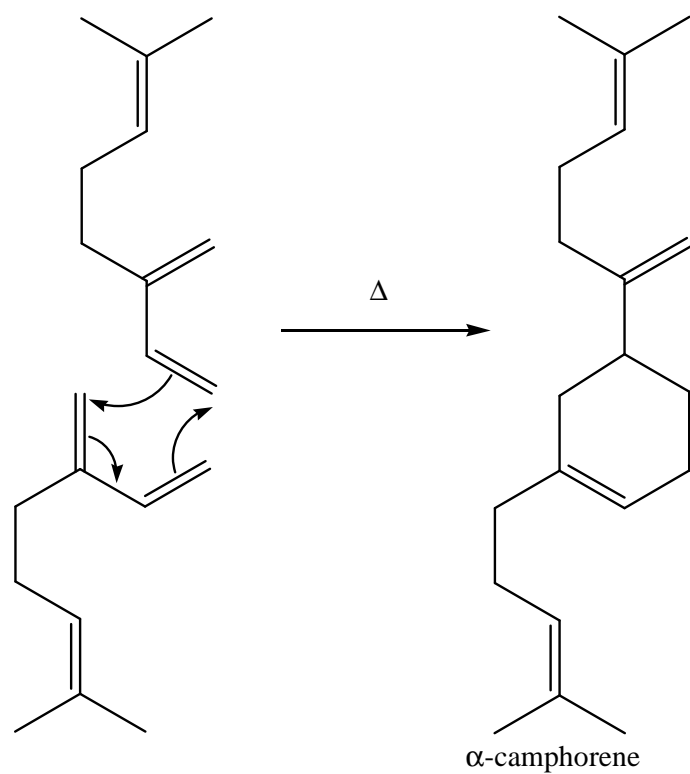
**Figure 1.17: Highly unsaturated hydrocarbons**

These highly unsaturated hydrocarbons are very sensitive to oxygen and elevated temperatures. By virtue of their conjugated diene structures, when stereochemistry permits, they will undergo Diels-Alder reactions. In this way, myrcene reacts with dienophiles such as acrolein and acrylonitrile to give adducts A and B, respectively (**Figure 1.18**)<sup>35</sup>.



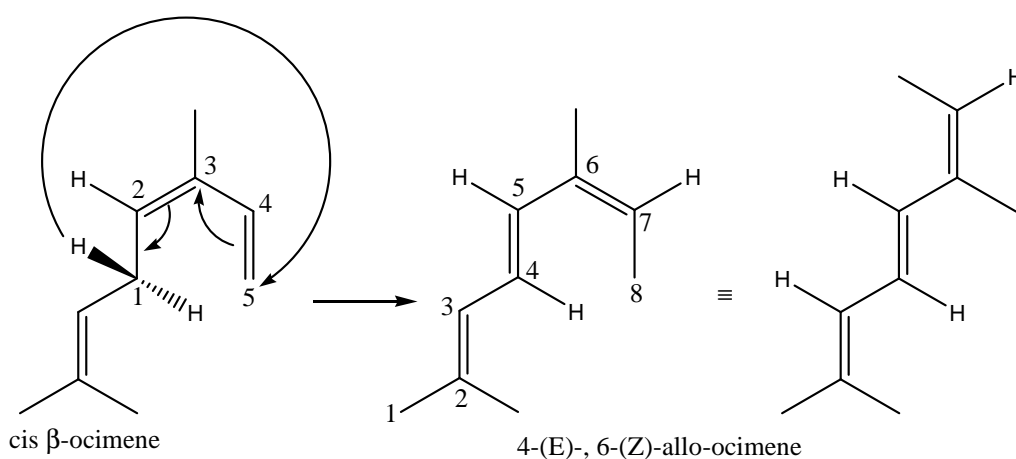
**Figure 1.18: Reactions of myrcene**

It is also possible to observe dimerization reactions. One molecule of myrcene can play the role of diene and the second molecule can act as the dienophile, thereby obtaining  $\alpha$ -camphorene (**Figure 1.19**).



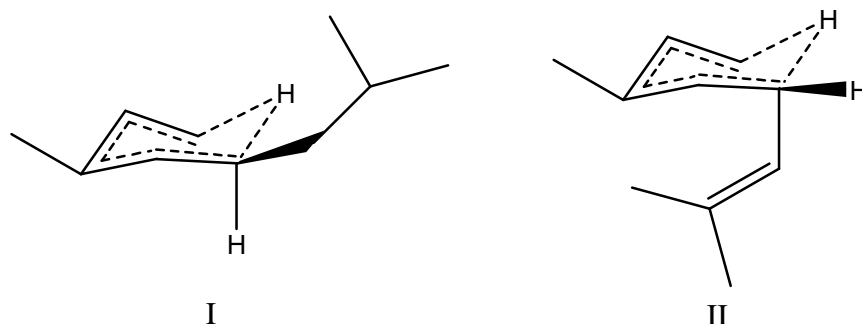
**Figure 1.19: Myrcene dimerization**

Heating *cis*  $\beta$ -ocimene to 185°C gives rise to a completely different reaction belonging to the group of sigmatropic rearrangements; in this case a thermally permitted 1,5 H-migration, according to Woodward-Hoffman rules (**Figure 1.20**)<sup>36</sup>.



**Figure 1.20: Sigmatropic rearrangement – 1,5 H-migration**

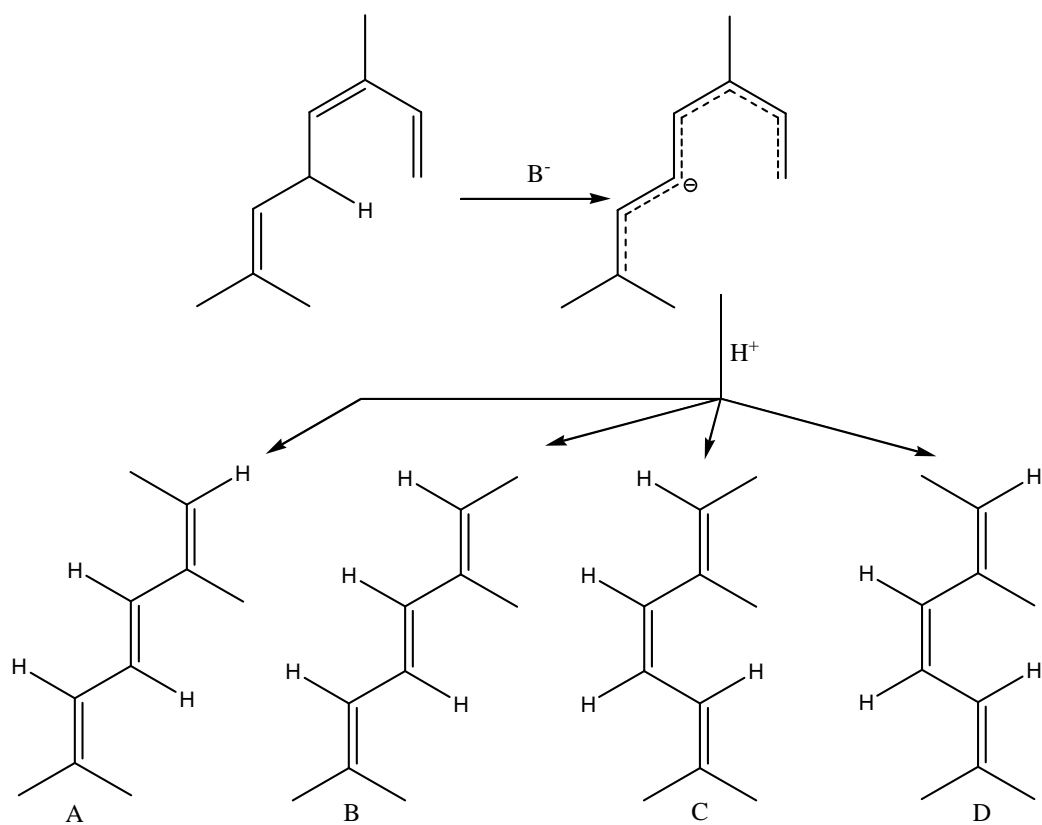
The product obtained is 4-(*E*)-, 6-(*Z*)-allo-ocimene in which the three double bonds are conjugated. The stereochemistry of the product can be explained by the structure of the two possible transition states I and II (**Figure 1.21**).



**Figure 1.21: Transition states I and II**

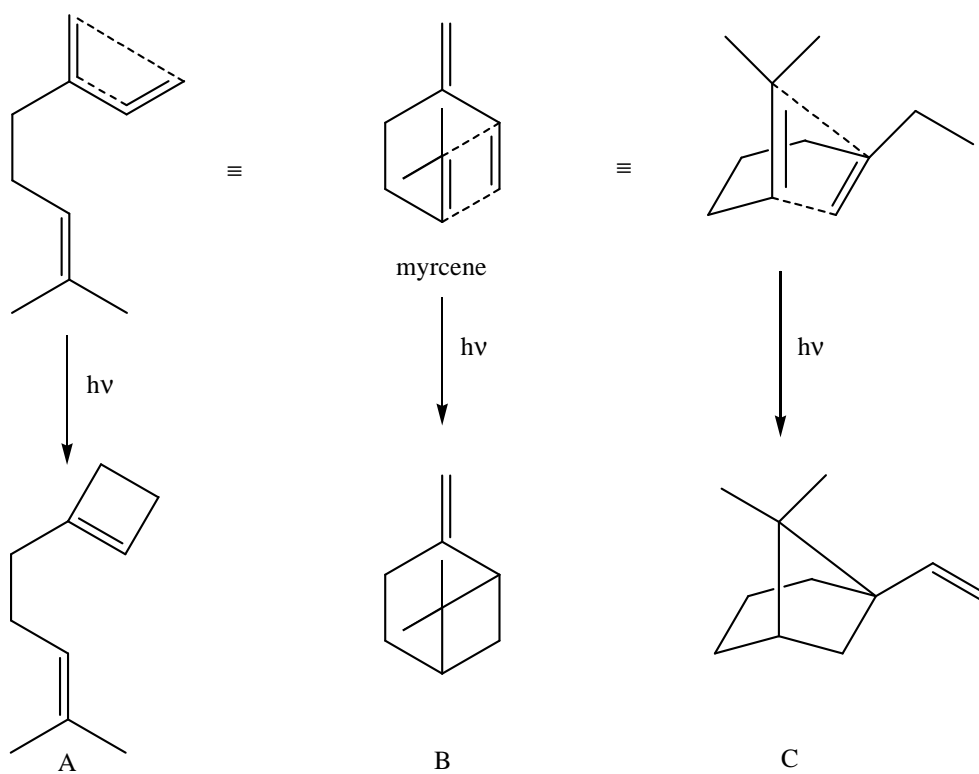
The transition state I, in which the isobutenyl group is equatorial, is less “strained” than II, in which the same group is axial. The rules which control pericyclic reactions (Woodward Hoffman, Dewar-Zimmerman) also provide an explanation of the stereospecificity of the reaction.

The  $\beta$ -ocimenes possess an activated  $-\text{CH}_2-$  group since they are intercalated between two double bonds (allylic H). Under the action of bases, it forms a delocalized anion which when reprotonated gives a mixture of four allo-ocimene isomers in which the (*E*)-4-(*Z*)-6-isomer B predominates (the isomers C and D are practically absent) (**Figure 1.22**).



**Figure 1.22: Effect of base on  $\beta$ -ocimene**

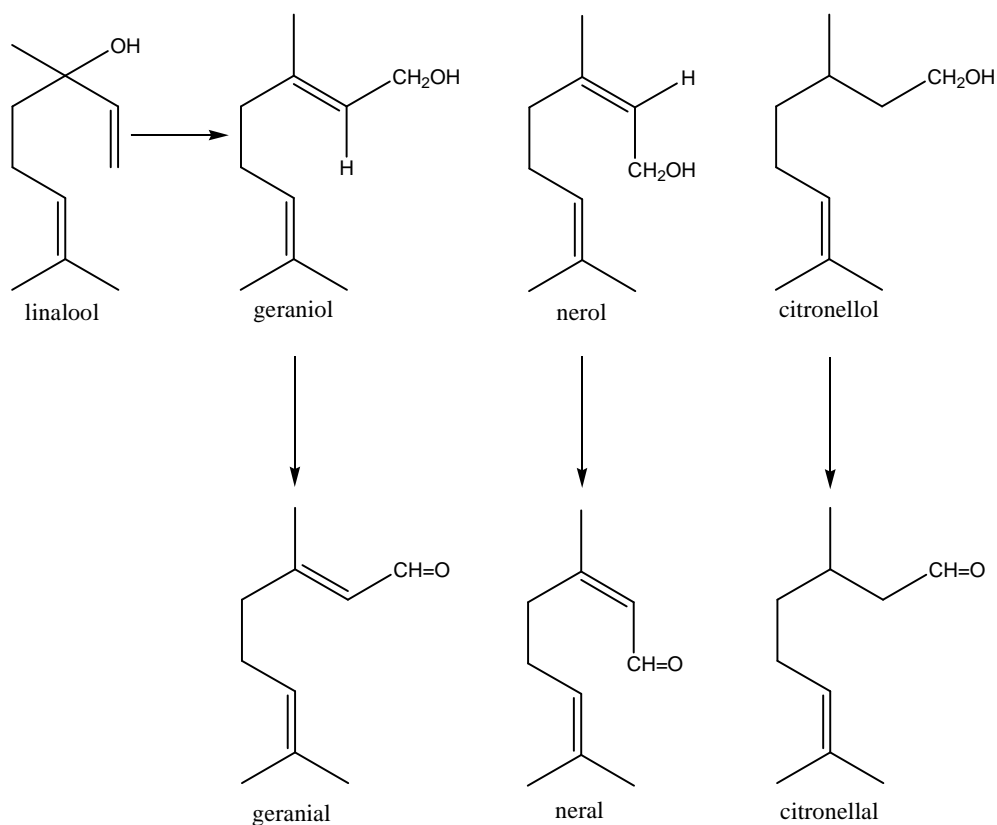
The hydrocarbons can also undergo photochemical reactions. For example, myrcene gives the three products A, B, and C. In the absence of photosensitisers, compound C, 1-vinyl-6,6-dimethylbicyclohexane constitutes the principle product (**Figure 1.23**)<sup>37</sup>.



**Figure 1.23: Photochemical reaction of  $\beta$ -myrcene**

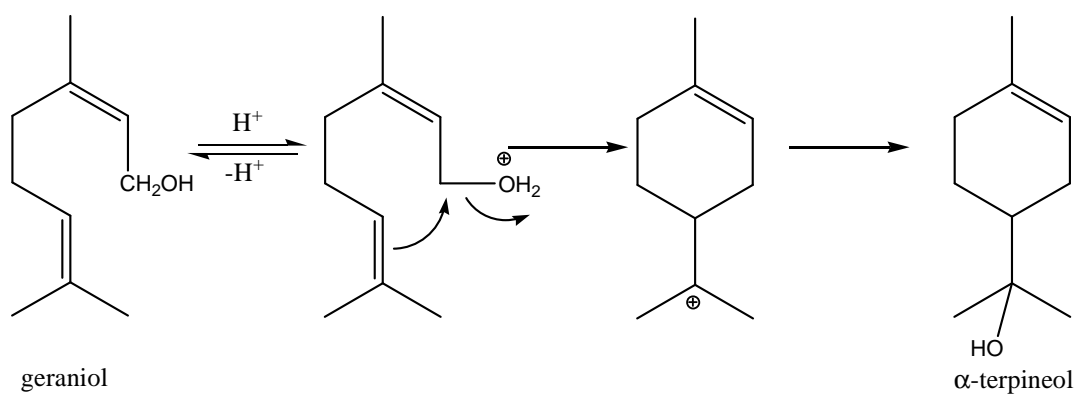
$\beta$ -Myrcene especially is of considerable importance to the perfumery industry as an intermediate for the preparation of numerous oxygenated terpenes – the principal ones being linalool, geraniol, nerol, citronellol and the corresponding aldehydes (citral and citronellal) (**Figure 1.24**)<sup>38</sup>.





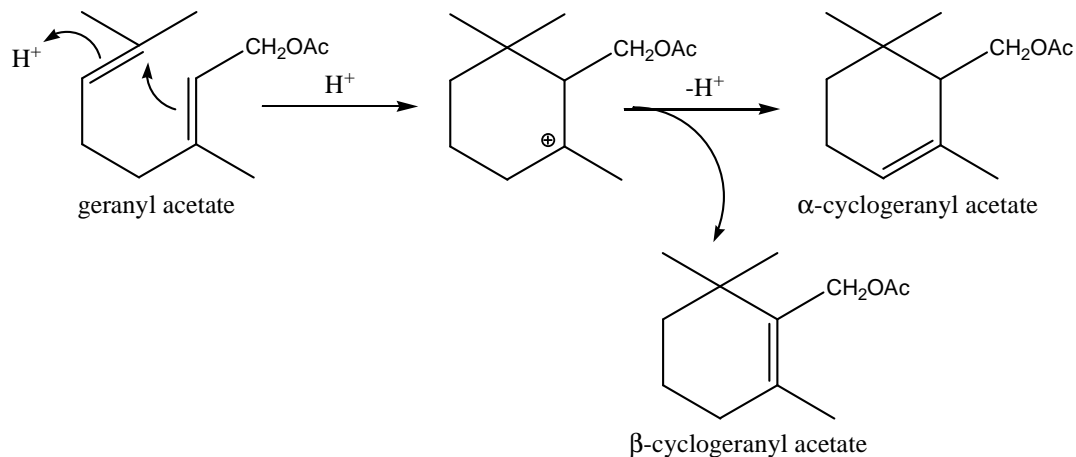
**Figure 1.24: Important derivatives of  $\beta$ -myrcene**

The three allylic alcohols rearrange in acidic media to yield an equilibrium mixture (allylic migration). Kinetic studies on this reaction show that geraniol and nerol are consumed at roughly the same rate; however, geraniol gives linalool while nerol gives  $\alpha$ -terpineol at a rate which is 18 times faster than for geraniol (more favourable stereochemistry of the double bond) (**Figure 1.25**).



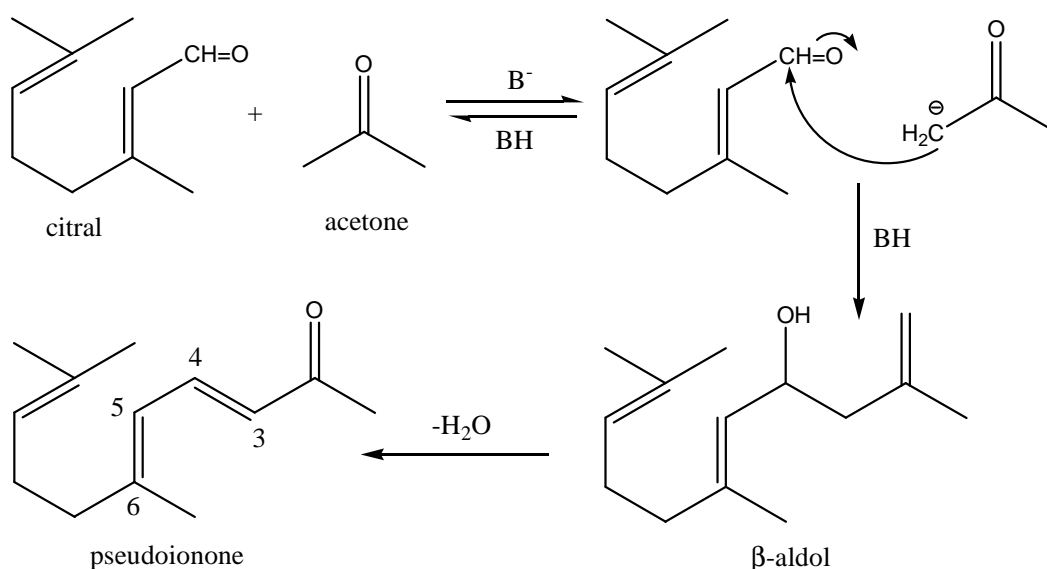
**Figure 1.25: Rearrangement of geraniol to  $\alpha$ -terpineol**

When the alcohol functional group of geraniol is blocked (for example by acetylation), it is possible to carry out a cyclisation in acidic media to obtain a mixture of  $\alpha$ - and  $\beta$ -cyclogeranyl acetates (**Figure 1.26**).



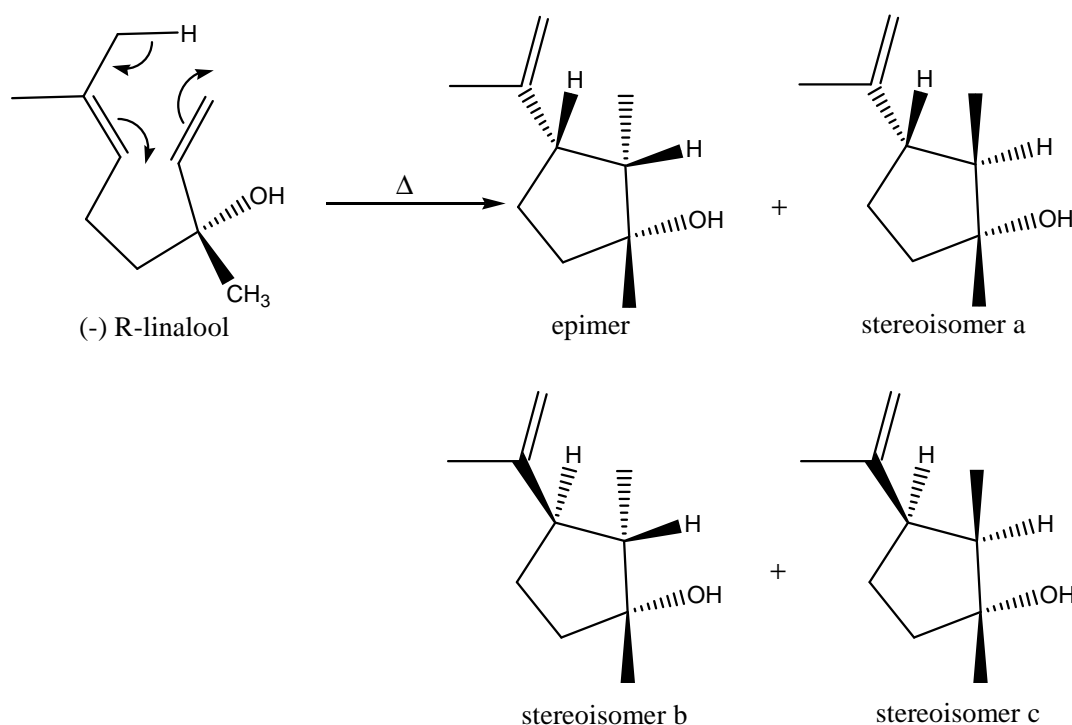
**Figure 1.26: Cyclisation of geranyl acetate**

This type of acid catalysed cyclisation is very important because of its ability to provide a number of derivatives such as ionones and the methylionones, which are of great importance to the perfumery industry. In this way, citral (geranial + neral) is first condensed with acetone or methylethylketone in basic media. Aldolisation followed by crotonisation gives pseudoionones or pseudomethylionones depending on the ketone used (**Figure 1.27**)<sup>39</sup>.





In this way, from a compound having only one asymmetrical carbon, a product containing three is obtained. This permits the possible existence of  $2^3=8$  optical isomers of which four will be dextro-rotatory and four will be levo-rotatory. However, as is frequently the case in concerted reactions, asymmetrical induction occurs. In this way, if optically pure linalool is used, the main product is the epimer which is favoured over its stereoisomers a, b, and c (**Figure 1.30**).



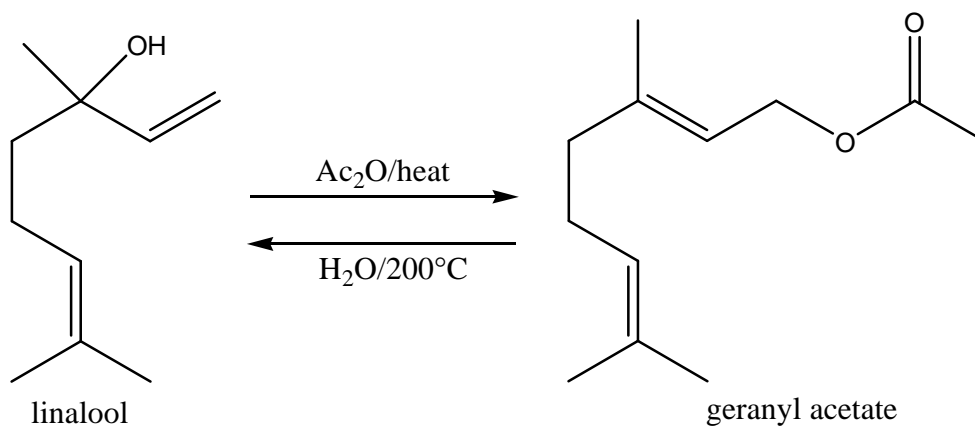
**Figure 1.30: Asymmetrical induction of linalool**

#### 1.8.4.1 Chemistry of Linalool<sup>24,42</sup>

Linalool is a widely occurring fragrant chemical. The richest source is Ho leaf oil which can contain over 95% linalool. Rosewood contains 80-85% and freesia about 80% linalool. It also occurs at levels around 50% in lavender and in herbs such as coriander and basil. Citrus leaves and flowers also contain significant amounts of linalool. However, it takes its name from the oil of linaloe wood, where it accounts for about 30% of the total oil content<sup>43,44</sup>.

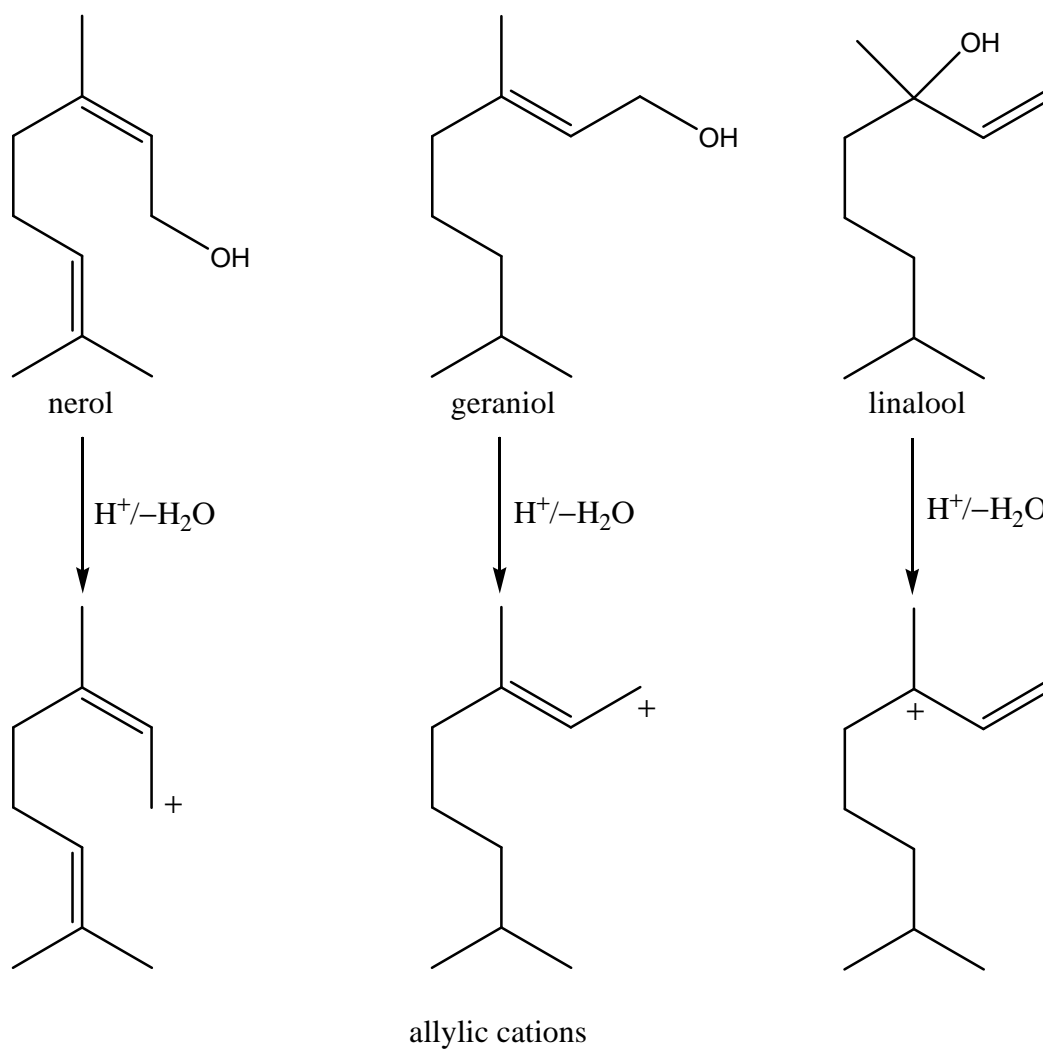
Linalyl acetate also occurs in many essential oils, significant levels being present in lavender, clary sage and the leaf oil of bitter orange. Early attempts to prepare linalyl

acetate by esterification of linalool using acetic anhydride gave an unexpected result. The acetate ester obtained was not that of linalool but that of geraniol. Conversely, when geranyl acetate was treated with steam at 200 °C under pressure, the hydrolysis product was not geraniol but linalool (**Figure 1.31**).

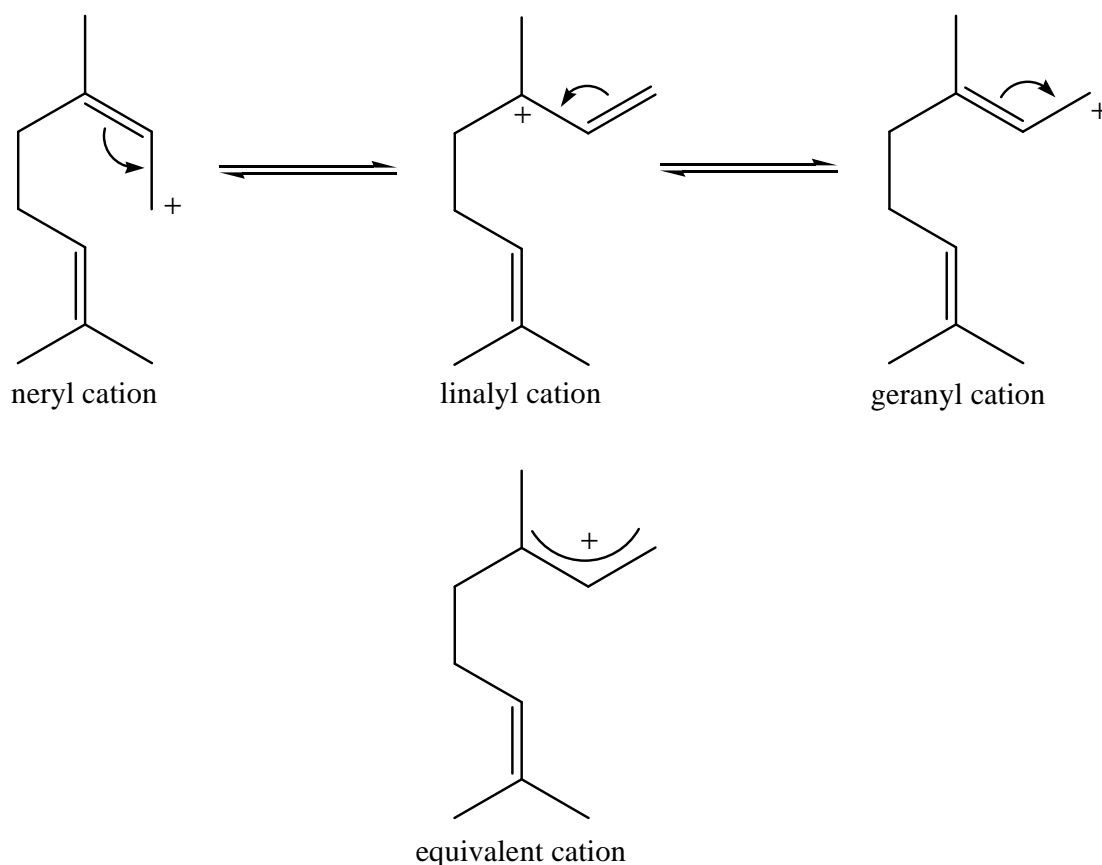


**Figure 1.31: Linalool esterification**

An explanation for these observations is presented in **Figures 1.32 and 1.33**.



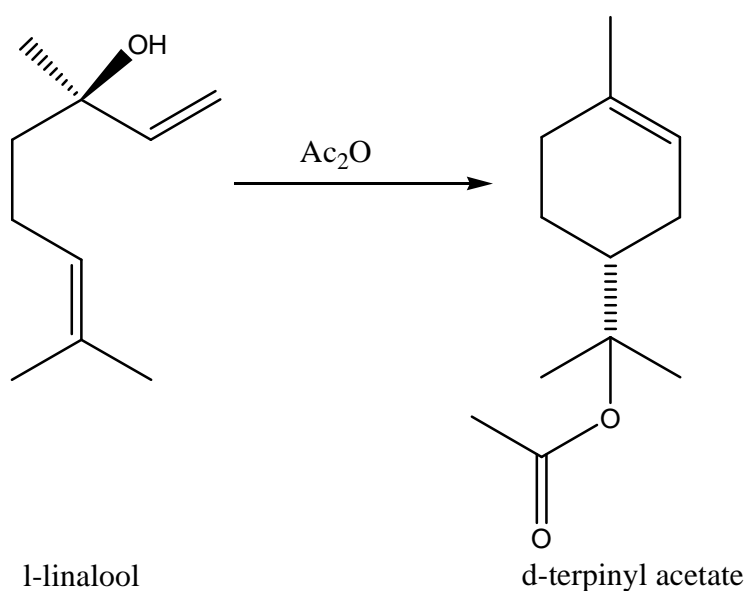
**Figure 1.32: Protonation of alcohols**



**Figure 1.33: Generation of isomeric allylic cation**

In **Figure 1.32** protonation of the alcohol functions of nerol, geraniol and linalool lead to the corresponding allylic cations. The  $\pi$ -electrons (**Figure 1.33**) of the double bond of an allylic cation can move towards the carbon atom bearing the positive charge. This generates an isomeric allylic cation, with the positive charge on the opposite end of the 3-atom system. In free allylic cations, this exchange is so rapid that the two isomers are indistinguishable. In fact, in molecular orbital theory, the system is considered to consist of a single set of orbitals which stretches across all three atoms. Since there is single bond character in each of the bonds, rotation is possible and the three cations, viz. geranyl, neryl and linalyl, become equivalent. Therefore, in reactions such as at in **Figure 1.31**, once the carbon-oxygen bond of the starting material has been broken, the incoming nucleophile can add to either the same carbon atom which carried the original substituent, or to the one at the opposite end of the allylic system. The exact course of the reaction will be determined by the reagents and the reaction conditions.

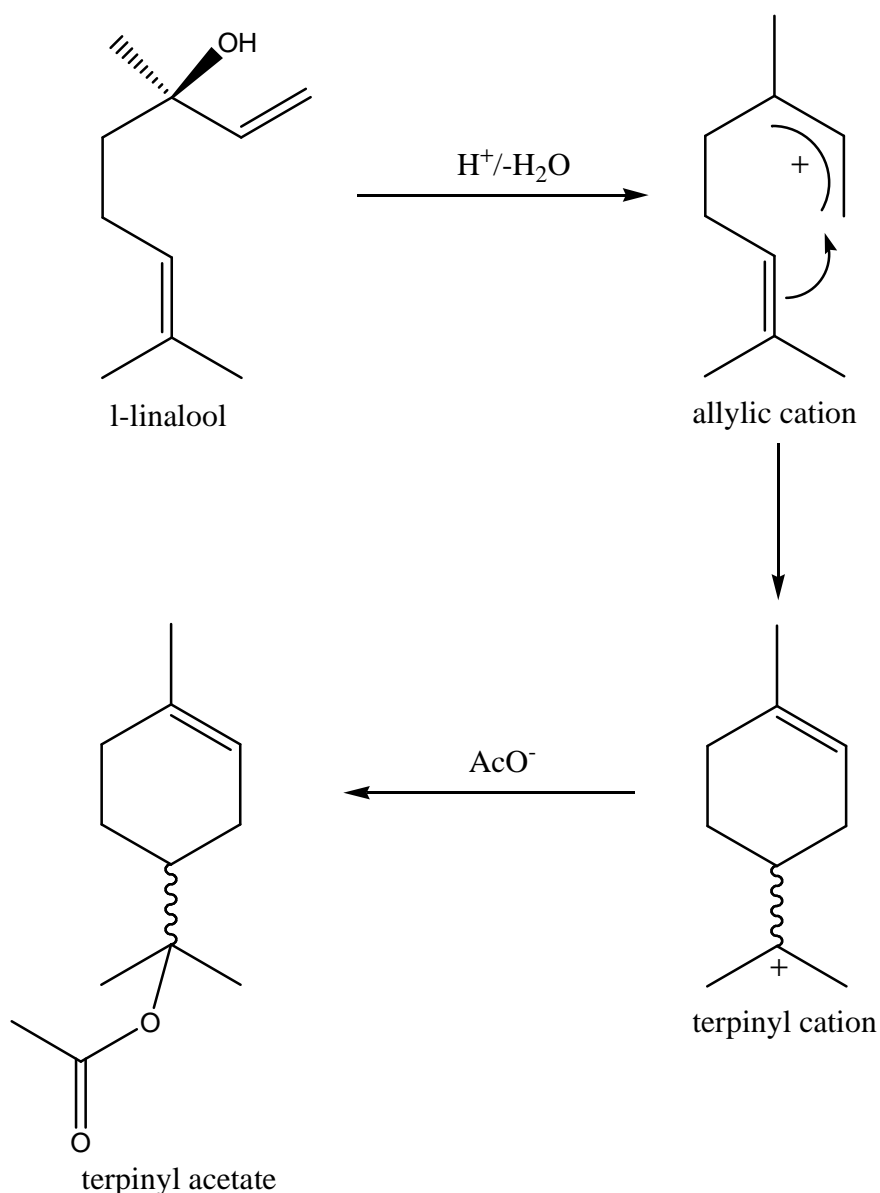
From the preceding discussion, a total scrambling of regiochemistry and stereochemistry in such carbocation reactions may be expected. However, when *l*-linalool is treated with acetic anhydride, *d*-terpinyl acetate is obtained, as shown in **Figure 1.34**<sup>45</sup>.



**Figure 1.34: Reaction of *l*-linalool with acetic anhydride**

A simple loss of water from linalool to give a carbocation followed by cyclisation and trapping of the newly formed carbocation by acetate, is expected to give a racemic product as shown in **Figure 1.35**.



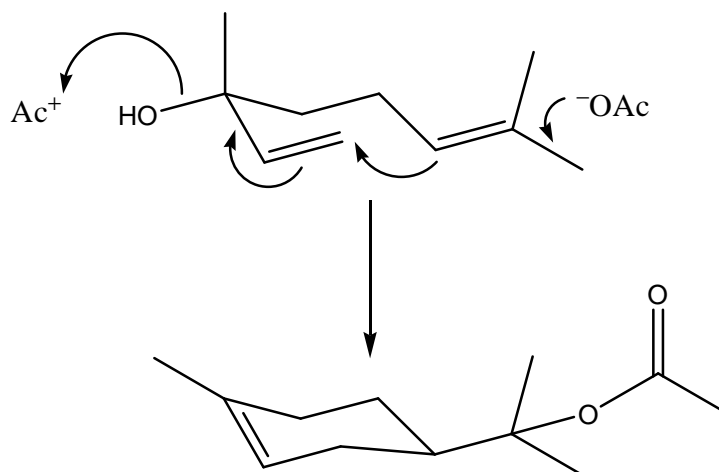


**Figure 1.35: Expected reaction of linalool with acetic anhydride**

Loss of water from the protonated linalool would give the allylic cation. If this were a free species as shown in **Figure 1.35**, cyclisation by reaction with the double bond could occur equally from either face to give a 50:50 mixture of stereoisomers in the terpinyl cation to produce racemic terpinyl acetate.

Since the actual product had retains the enantiomeric purity of the starting material, the mechanism must involve some factor which constrains the reactive centres throughout the course of the reaction. This is known as the *trans-anti-periplanar* rule. This rule states that the bonds being formed or destroyed during a reaction, prefer to

exist in a geometry which places them in the same plane as each other, or in a *trans*- or *anti*- relationship to each other. This arrangement allows for maximum interaction of the orbitals involved in the reaction. The working of the *trans-anti*-periplanar rule in the above reaction is shown in **Figure 1.36**.



**Figure 1.36: Working of *trans-anti*-periplanar rule in Prelog's reaction**

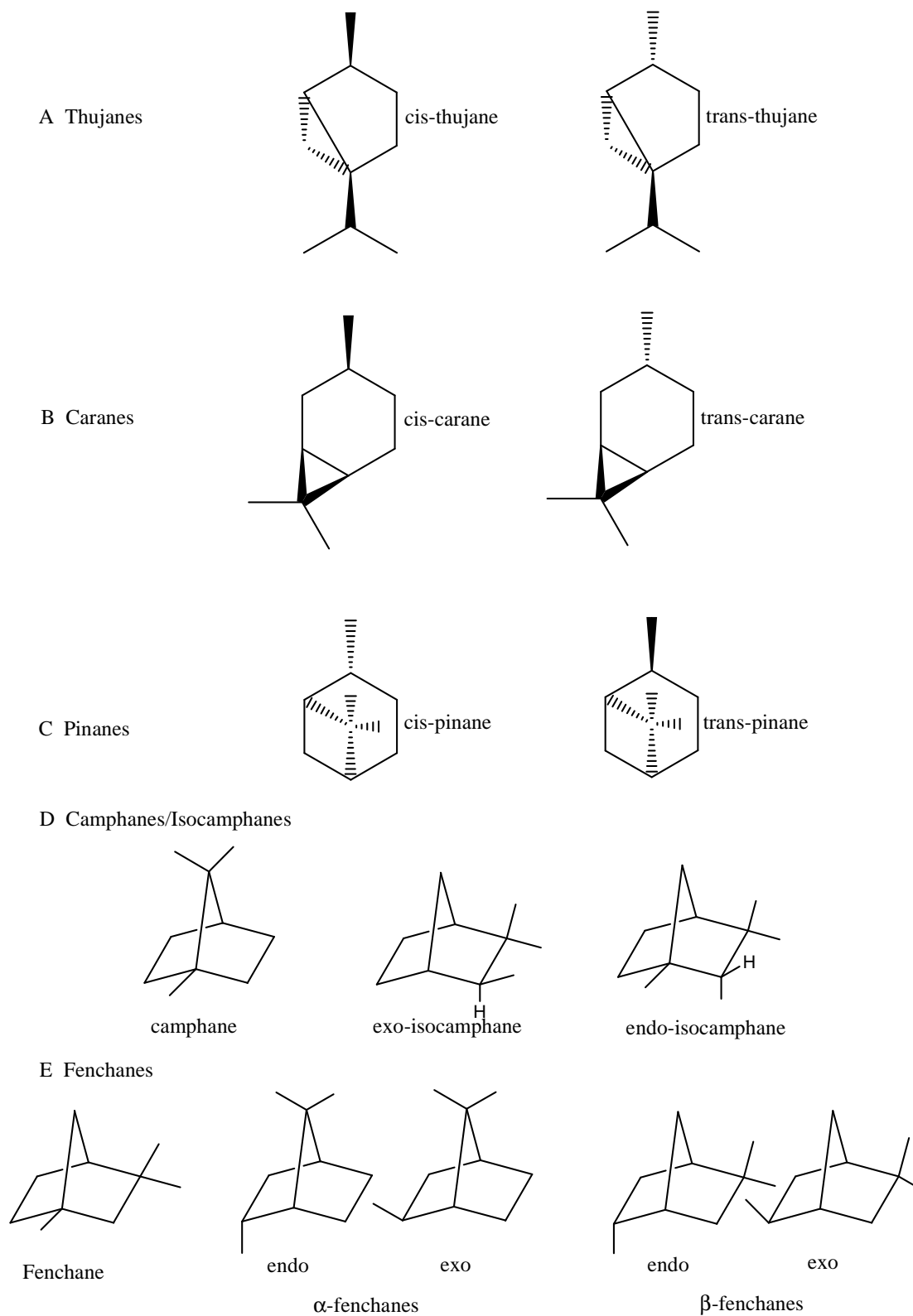
As can be seen from **Figure 1.36**, all bonds are lined up *trans*- to each other in a single plane. The stereochemistry of the carbon carrying the alcohol group in the starting material therefore determines the stereochemistry of the asymmetric ring carbon atom in the product. Since the starting material is homochiral, the product will also be homochiral. The reaction is essentially synchronous with all bonds being formed or broken simultaneously.

### 1.8.5 Bicyclic Monoterpenoids<sup>33</sup>

The bicyclic monoterpenoids are of particular interest in this project since most of the chemical intermediates are bicyclic compounds and an understanding of the chemistry will provide an insight into the mechanisms involved in the individual process steps.

There are five principal types of bicyclic monoterpenic compounds (**Figure 1.37**):

- A. Thujanes
- B. Caranes
- C. Pinanes
- D. Camphenes – isocamphenes
- E. Fenchanes



**Figure 1.37: Principal bicyclic monoterpenoids**

These compounds are all formed from geranyl pyrophosphate in nature. The initial cyclisation reaction gives the *p*-menthane skeleton and then a second ring is formed to give a bicyclic compound. In the case of the caranes and thujanes, the second ring is a three membered one, whereas in the pinanes it is four membered. In the other compound there is a five membered ring fused across the cyclohexane ring to give the [2.2.1]-bicycloheptyl system, often referred to as the norbornyl ring system.

### 1.8.5.1 Carbocation Chemistry<sup>5,46</sup>

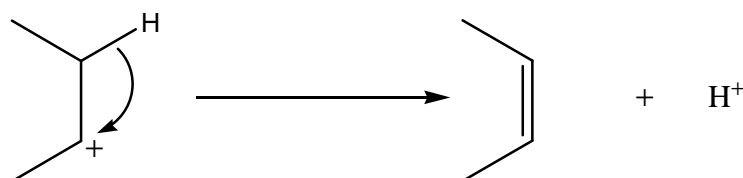
In studying the chemistry of carbocations the things which need to be considered are the reactions which they undergo, the forces which drive these reactions and the factors which induce selectivity into them. There are four basic types of reactions which carbocations can undergo and there are three forces which drive them. Two factors control the chemo- and regioselectivity of additions to double bonds and the other major factor in determining selectivity is the *trans-anti*-periplanar (TAP) rule. This is summarised in **Table 1.8**.

**Table 1.8: The 4-3-2-1 Rule**

<b>4 Types of reaction</b>	<b>Elimination</b> <b>Solvolysis</b> <b>H-Shift</b> <b>C-Shift</b>
<b>3 Driving forces</b>	<b>Cation stability</b> <b>Ring strain</b> <b>Steric strain</b>
<b>2 Selectivity factors</b>	<b>Electron density</b> <b>Polarisability</b>
<b>1 Other factor</b>	<b><i>Trans-anti</i>-periplanar rule</b>

### 1.8.5.1.1 Reaction Type 1 – Elimination

A common reaction of carbocations is to eliminate an adjacent proton to give an olefin as shown in **Figure 1.38**.

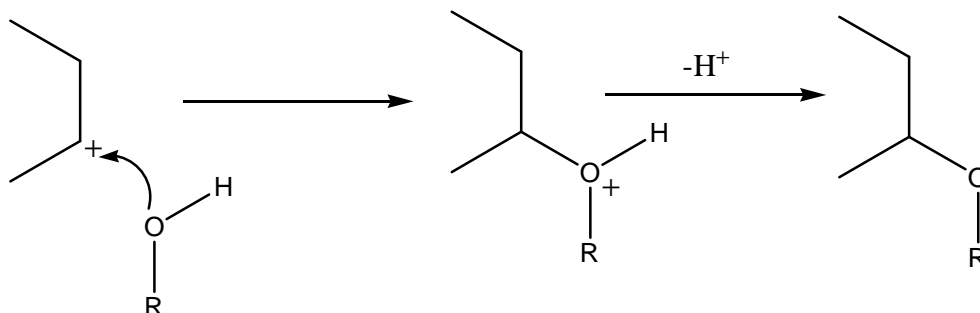


**Figure 1.38: Deprotonation of carbocation**

If the cation was initially formed by heterolysis of a bond between a carbon atom and a group X, then the overall process constitutes an elimination of HX. For example, if a chloride ion was to be lost initially by cleavage of the carbon-chlorine bond, and the resultant carbocation were to eliminate a proton, the overall process would constitute an elimination of hydrogen chloride. The carbocation which loses the proton is not necessarily the one which was formed by cleavage of the carbon-chlorine bond. The initial carbocation can undergo rearrangement before a proton is lost.

### 1.8.5.1.2 Reaction Type 2 – Solvolysis

Another common reaction of carbocations is to form a new bond with an anion or nucleophile as shown in **Figure 1.39**.

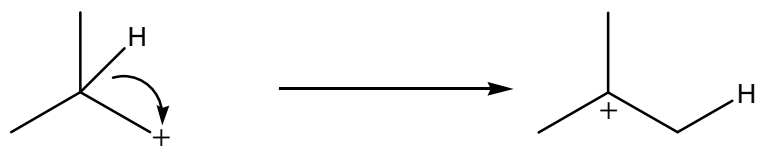


**Figure 1.39: Solvolysis of carbocation**

A pair of electrons from the nucleophile is used to form a bond with the positively charged carbon atom. If the nucleophile is an anion, then the addition product will be neutral. If the nucleophile is electrically neutral, then a new cation will be formed as shown in **Figure 1.39**. Loss of a proton from this species, results in the formation of a neutral product. Strictly speaking, the term solvolysis is restricted to those cases where the nucleophile is a solvent molecule. For simplicity, the term is used to cover nucleophilic substitution and nucleophilic addition reactions.

### 1.8.5.1.3 Reaction Type 3 – H-shift

It is possible for a hydrogen atom to move from one carbon atom to being bonded to an adjacent one which is carrying a positive charge. This is referred to as a 1,2-hydrogen shift and is shown in **Figure 1.40**.

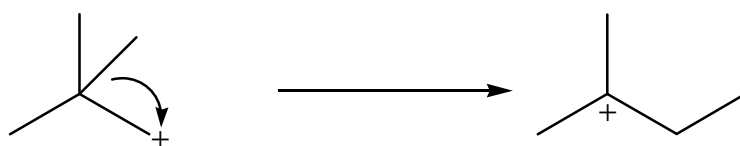


**Figure 1.40: H-Shift of carbocation**

As the hydrogen atom moves from one carbon to another, the positive charge moves in the opposite direction to form a new carbocation. The hydrogen can move to a more remote carbon atom and so other shifts are possible e.g. 1,3- or 1,5-shifts, but the commonest is a 1,2-shift.

### 1.8.5.1.4 Reaction Type 4 – C-shift

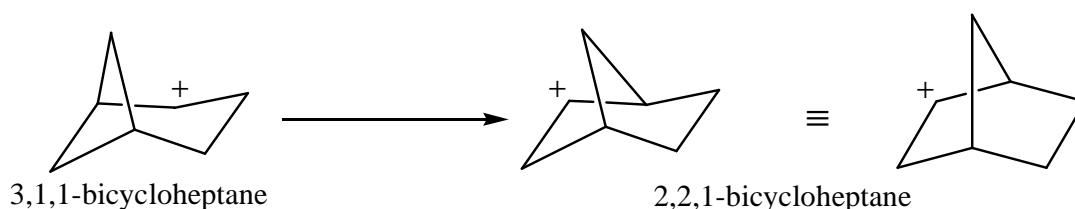
Just as a hydrogen atom can move onto a neighbouring carbon atom bearing a positive charge, so can a carbon atom. A simple 1,2-carbon shift reaction is shown in **Figure 1.41**.



**Figure 1.41: 1,2-carbon shift reaction**

In this example there is a positive charge on C1 of 2,2-dimethylpropane. One of the methyl groups on C2 moves across onto C1, taking the electrons of its bond with it and consequently, the positive charge is transferred to C2. Carbon shifts have a significant impact on the structure of the molecule. The basic skeleton has changed from that of 2,2-dimethylpropane to that of 2-methylbutane.

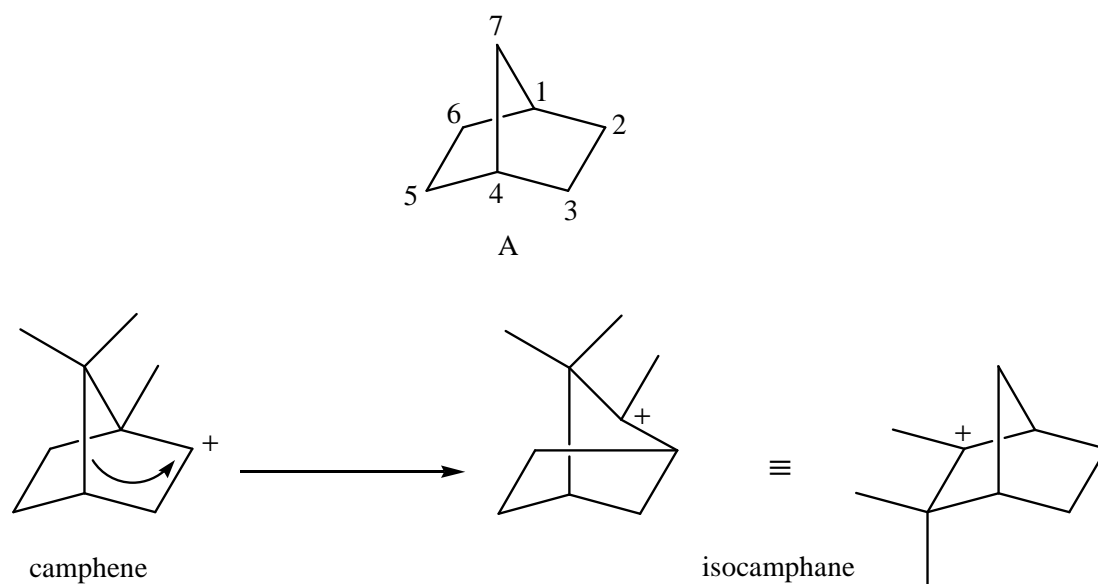
When a carbon shift occurs in a ring system, the change in skeleton can be more difficult to see. **Figure 1.42** shows an example of a simple 1,2-carbon shift which appears much more complex because it transforms a pinane ring system (3,1,1-bicycloheptane) into a bornane (2,2,1-bicycloheptane) ring system.



**Figure 1.42: 1,2 carbon shift in pinane ring system**

Reactions of the above type are generally known as the Wagner-Meerwein rearrangement reactions.

**Figure 1.43** shows a 1,2-carbon shift in a bornane which produces another bornane.

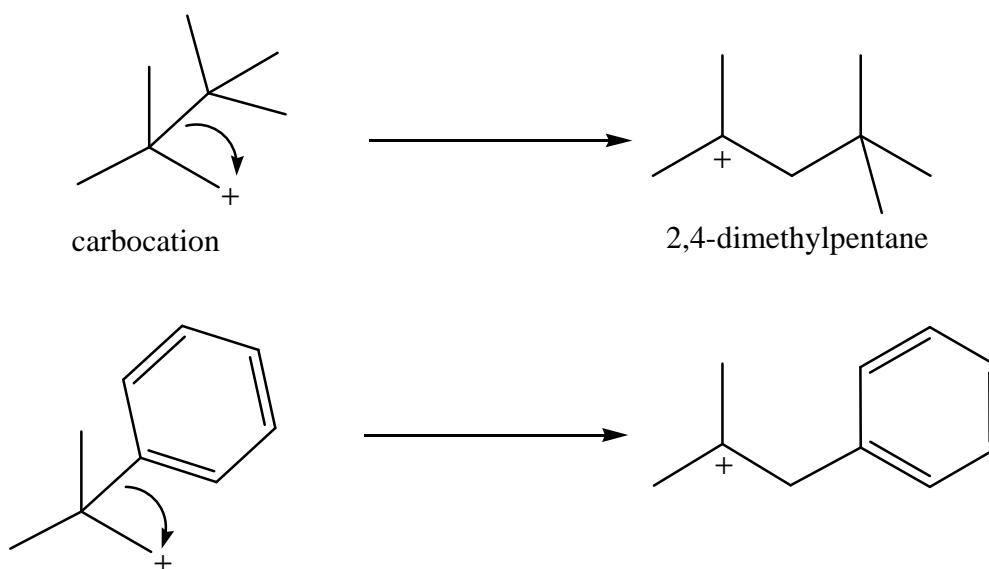


**Figure 1.43: 1,2 Carbon shift in bornane system**

For clarity, structure **A** shows the numbering system of the 2,2,1-bicycloheptyl skeleton. This ring system nomenclature is based on the bridgehead carbon atoms where the two bridgehead carbon atoms are first identified and the number of atoms in each bridge is then counted. Thus in **Figure 1.43A** there are two bridges of two carbon atoms and one of one, hence the name 2,2,1-bicycloheptane. The numbering of the individual carbon atoms starts on a bridgehead and then proceeds round the largest bridge, continues round the next largest bridge and finally the smallest bridge. Normally the reaction shown in **Figure 1.42** would be shown simply as one structure going to the next. The first impression is that all three methyl groups have changed their positions in the ring. In reality, none of the methyl groups have moved from the carbons to which they are bonded. It is another bond in the ring which has moved. Initially, C6 is bonded to C1. However, the presence of a positive charge on C2 allows a Wagner-Meerwein rearrangement to occur, with the electrons which form the bond between C1 and C6 moving towards the positive charge and thus simultaneously breaking the bond between C6 and C1 to form a new one between C6 and C2. The positive charge now resides on C1 and we have a new structure. If we follow bond connectivities around these two structures we will see that the two are identical (the whole molecule having been rotated through about 120°).

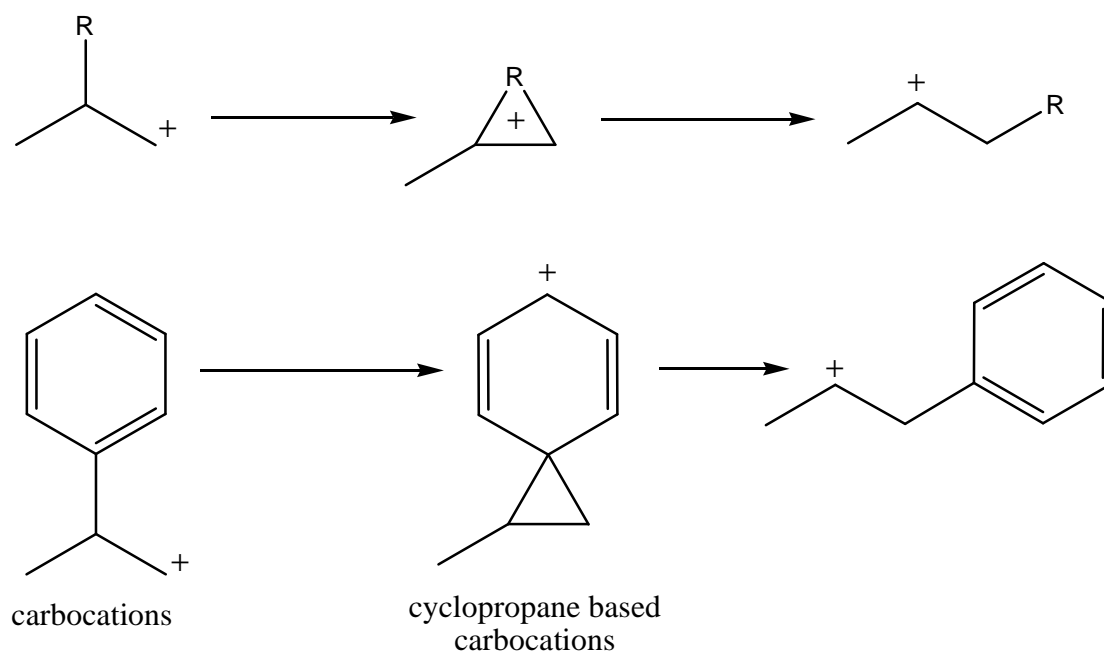


When there are two groups which can undergo a carbon shift and there are no factors to overcome the effect, there is a general rule that the more heavily substituted carbon atom will move. Thus, for example in the case of the carbocation in **Figure 1.44**, it is possible for either the tertiary butyl carbon, or one of the two methyl carbons to move across to the carbon carrying the positive charge.



**Figure 1.44: Carbon shift of more heavily substituted carbon**

The carbon carrying three other carbon atoms is the one which moves, giving the 2,4-dimethylpentane skeleton rather than the alternative 2-*t*-butylbutane which would be the product of a methyl shift. The reason for this lies in the greater ability of the more substituted atom to stabilise the transient positive charge through an inductive effect. As the carbon atom moves from one position to another, we can envisage an intermediate in the form of a cyclopropyl ring with the positive charge spread across all three component atoms as shown in **Figure 1.45**.



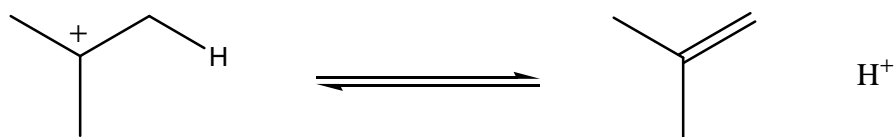
**Figure 1.45: Examples of methyl shift**

The greater the ability of the moving group, R to stabilise the charge, the more likely it will be to move. If there is a benzene ring which can move, then it will do so in preference to any alkyl groups. For example, in **Figure 1.44**, it is the phenyl group which moves to give cations because of the ability of the aromatic ring to stabilise the positive charge through delocalisation. For instance, the structure shows one canonical form with the positive charge located on the opposite end of the benzene ring. The cyclopropane based carbocations are both examples of non-classical carbocations i.e. carbocations in which the positive charge is spread across a number of atoms rather than being localised on one.

#### 1.8.5.1.5 Driving Force 1 – Cation Stability

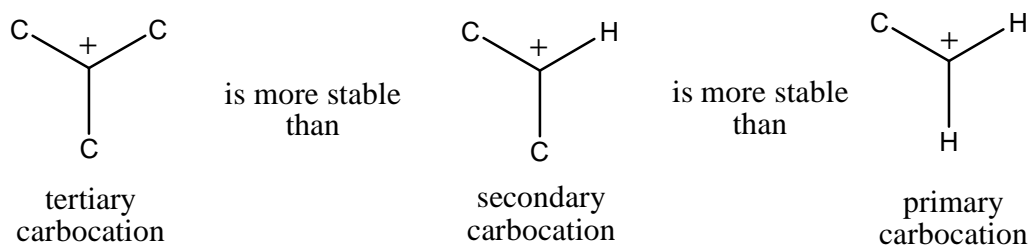
The stability of a positive charge on a carbon atom is increased if electrons can be drawn in from neighbouring atoms through an inductive effect. The more electrons there are on the neighbouring atoms, the more charge stabilisation there will be. A hydrogen atom can donate only the two electrons of the bond which holds it to the carbon atom. A carbon atom has more electrons of its own and can also draw in the electrons of the hydrogens to which it is attached through hyperconjugation. **Figure**

1.46 shows the canonical forms at either extreme of hyperconjugation, the reality being a sharing of the positive charge across the entire system.



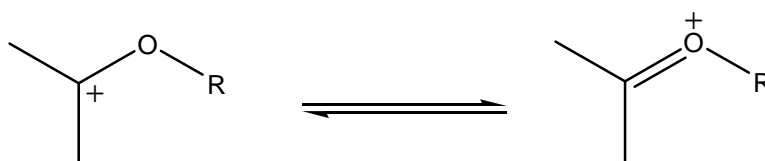
**Figure 1.46: Canonical forms at either extreme of hyperconjugation**

These factors mean that there is a marked increase in stability on going from a primary to a secondary to a tertiary cation as shown in **Figure 1.47**.



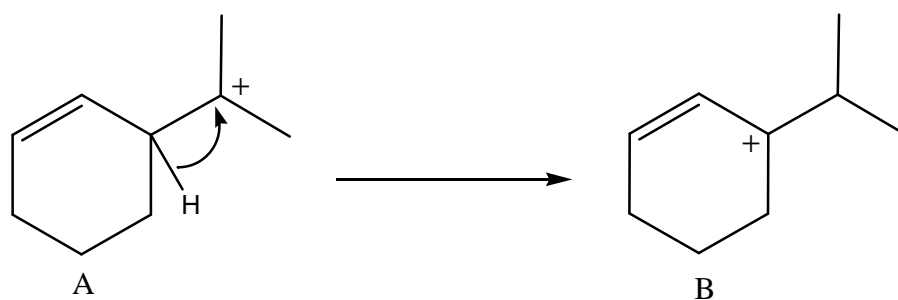
**Figure 1.47: Increasing stability**

A carbocation will be even more stable if there is a neighbouring oxygen atom which can donate electron density from its lone pairs of electrons. The canonical forms of a carbocation stabilised in this way are shown in **Figure 1.48**.



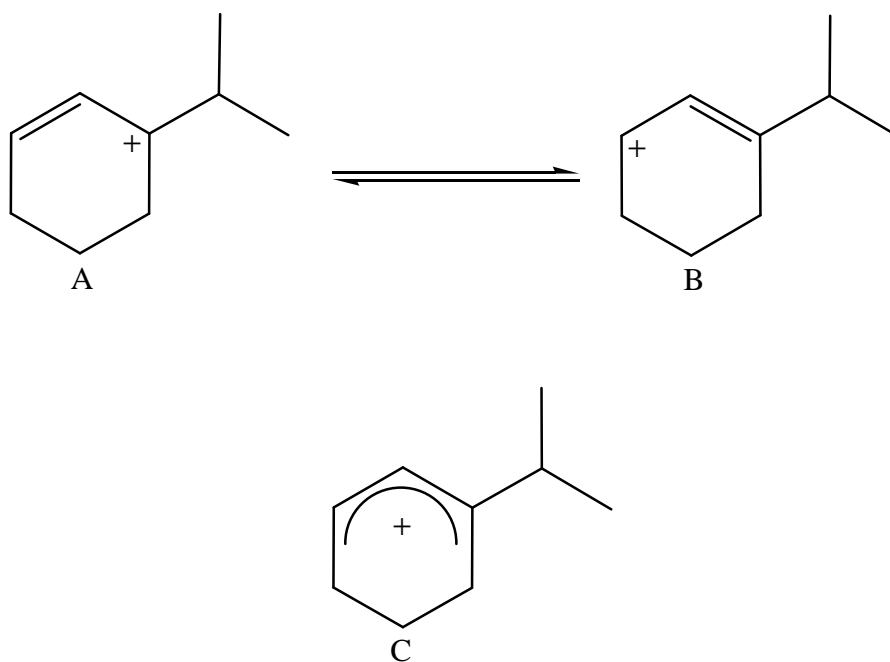
**Figure 1.48: Canonical form of stabilised carbocation**

As already mentioned, if a charge can be shared over more than one atom, then the partial charge over each is reduced which lowers the energy of the system. Thus, in **Figure 1.49**, the 1,2 H-shift from A to B, brings the positive charge into conjugation with the double bond and thus lowers the overall energy of the molecule.



**Figure 1.49: 1,2 Hydrogen -shift**

The carbocation of **Figure 1.49** can be written either as one of the two canonical forms A and B or using an electron smear, C, as shown in **Figure 1.50**.


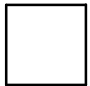
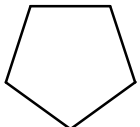
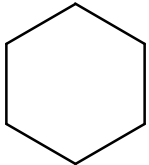
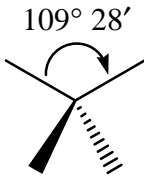


**Figure 1.50: Canonical forms of the carbocation**

The smear is closer to reality since the molecular orbitals of the molecule will be distributed across the three carbons of the allylic cation. However, it will be able to react as if the positive charge were localised at either end. For each individual reaction, the nature of the other reactive species, the reactions conditions and the nature of the product will determine which way round the system will react.

### 1.8.5.1.6 Driving Force 2 – Ring Strain

The concept of ring strain was first developed by von Baeyer in 1885. There are two components in ring strain, i.e. angle strain and steric strain. The angle between the bonds of a tetrahedral  $sp^3$  carbon atom is compared with the internal angles of regular polygons in **Figure 1.51**.

polygon	internal angle	
	$60^\circ$	
	$90^\circ$	
	$108^\circ$	
	$120^\circ$	

**Figure 1.51: Internal angles of regular polygons**

Constraining a tetrahedral carbon atom into either a cyclopropyl or cyclobutyl ring involves bending the bonding angles considerably. This is known as angle strain. The tetrahedral bond angle is similar to angles in a regular pentagon of cyclopentane and, with a little puckering of the ring, leads to a stable structure. In the case of the cyclohexane ring, the angle of the regular hexagon is larger, but the ring can still pucker to accommodate the tetrahedral angle. Not only that, but, by doing so, it allows the substituents on the ring carbon atoms to become staggered and therefore minimise the steric, or spatial, interaction between them. Cyclohexane rings can exist in various conformations but the two most favoured are what are called the chair and boat conformations. These are shown in **Figure 1.52**.

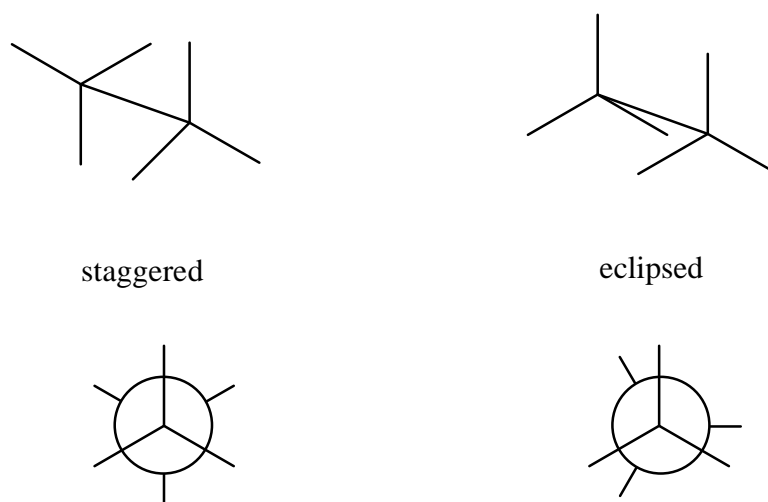


**Figure 1.52: Chair and boat conformations of cyclohexane ring**

If one looks along any of the carbon-carbon bonds in a model of the chair form one will see that all of the other bonds attached to the two carbons are staggered. The substituents are held either at right angles to, or lie in the plane of the ring. The former is referred to as axial and the latter, equatorial. In the boat configuration, the substituents are not so well staggered and, in most cases, this is a less preferred conformation. For ring sizes greater than six, there is no problem with angle strain as the rings can pucker to accommodate the tetrahedral angle. However, by doing so, rings from cyclopentane to cyclodecane are forced to bring substituents on opposite sides of the ring into close proximity across the ring centre. This leads to problems of van der Waals repulsion between them. This is known as steric strain. Larger rings, for example those with 15 or 20 carbons in them, do not have this problem as there is sufficient distance across the ring to allow substituents to point inwards. There is therefore a general principle that five- and six-membered rings are preferred to other sizes. Smaller rings will tend to spring open or enlarge in order to reduce angle strain. Rings between 8 and 12 will tend to break open, reduce in size or form new bonds across the ring in order to reduce the steric crowding.

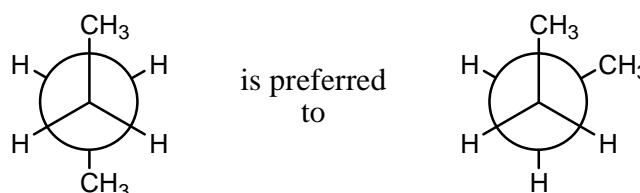
#### **1.8.5.1.7 Driving Force 3 – Steric Strain**

Steric problems can exist in open chain structures and between substituents on rings. Bringing atoms closer together when they are not bonded to each other, will lead to van der Waals repulsion. This can happen with substituents on adjacent carbon atoms or with substituents which are brought together through the geometry of the molecule. Interactions between substituents on adjacent carbon atoms may be illustrated as shown in **Figure 1.53**.



**Figure 1.53: Newman projections**

It is clear from **Figure 1.53** that the eclipsed configuration brings substituents closer together. The larger the substituents, the larger will be the repulsion and the greater the energy difference between the two configurations. In **Figure 1.54**, the Newman projections show how, in the staggered configuration, two larger substituents will prefer to be aligned opposite each other, rather than adjacent, since in the latter arrangement, there is still a considerable degree of steric interaction.

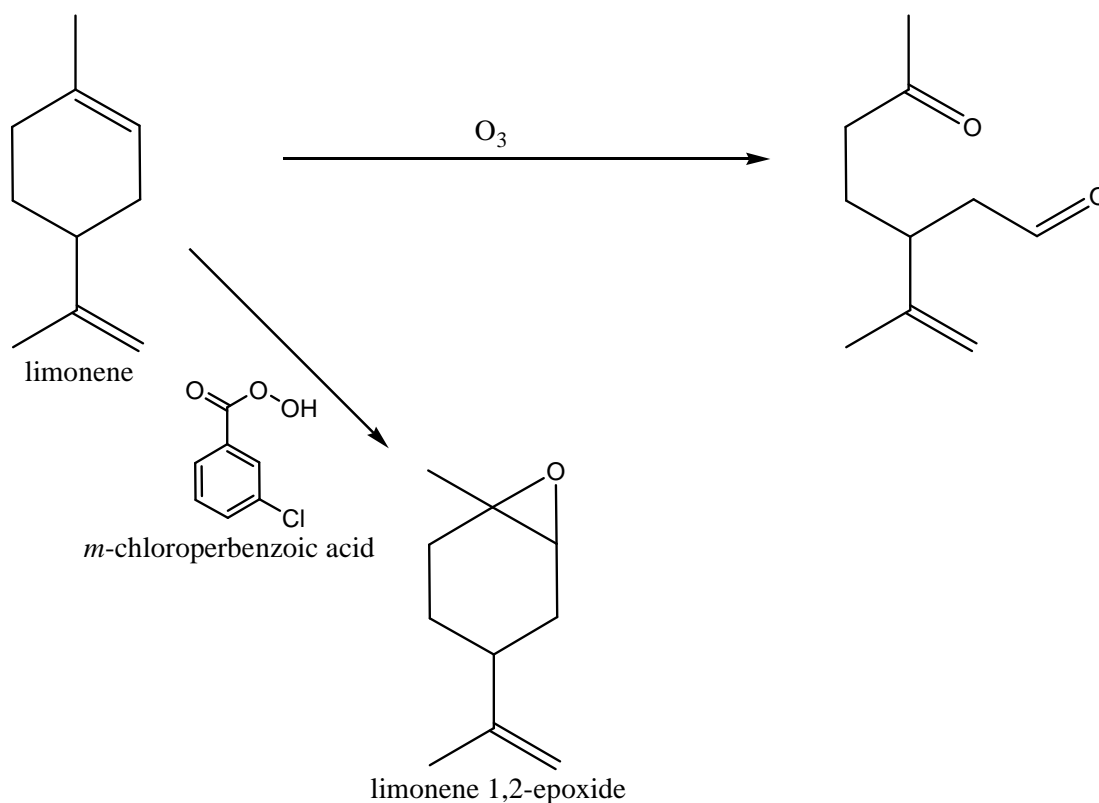


**Figure 1.54: Steric interaction**

#### 1.8.5.1.8 Selectivity Factor 1 – Electron Density

Just as different substituents are able to stabilise carbocations by releasing electrons towards them, substituents can release electrons into double bonds or draw them out of it. Electron donating groups such as alkyl groups and ethers will increase the electron density of double bonds to which they are attached. Therefore, in hydrocarbons the more heavily substituted double bonds will be more electron-rich. Thus, if there are two or more double bonds in a molecule, electron deficient reagents such as ozone or peracids will preferentially attack the more/most electron rich olefin.

Limonene (**Figure 1.55**) provides an example of this type of selectivity.



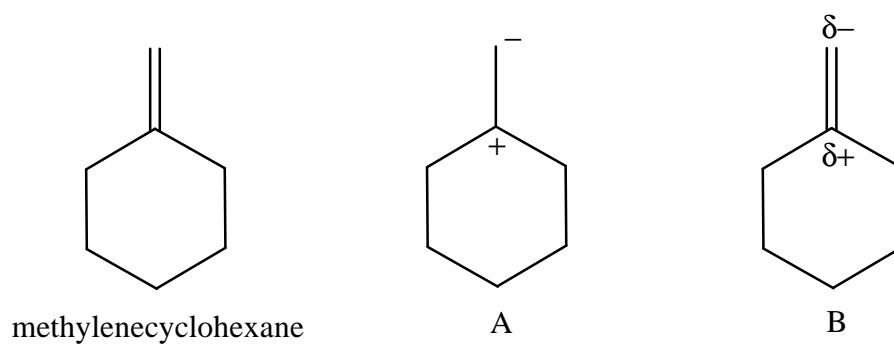
**Figure 1.55: Attack of ozone on electron-rich olefins**

The endocyclic double bond of limonene is trisubstituted and is therefore richer in electrons than the disubstituted olefin in the isopropenyl group. Ozone will therefore selectively cleave the ring double bond leaving the other untouched, provided of course, that no more than one molar equivalent of ozone is used. Similarly, one molar equivalent of *m*-chloroperbenzoic acid will selectively give only limonene 1,2-epoxide.

#### 1.8.5.1.9 Selectivity Factor 2 – Polarisability

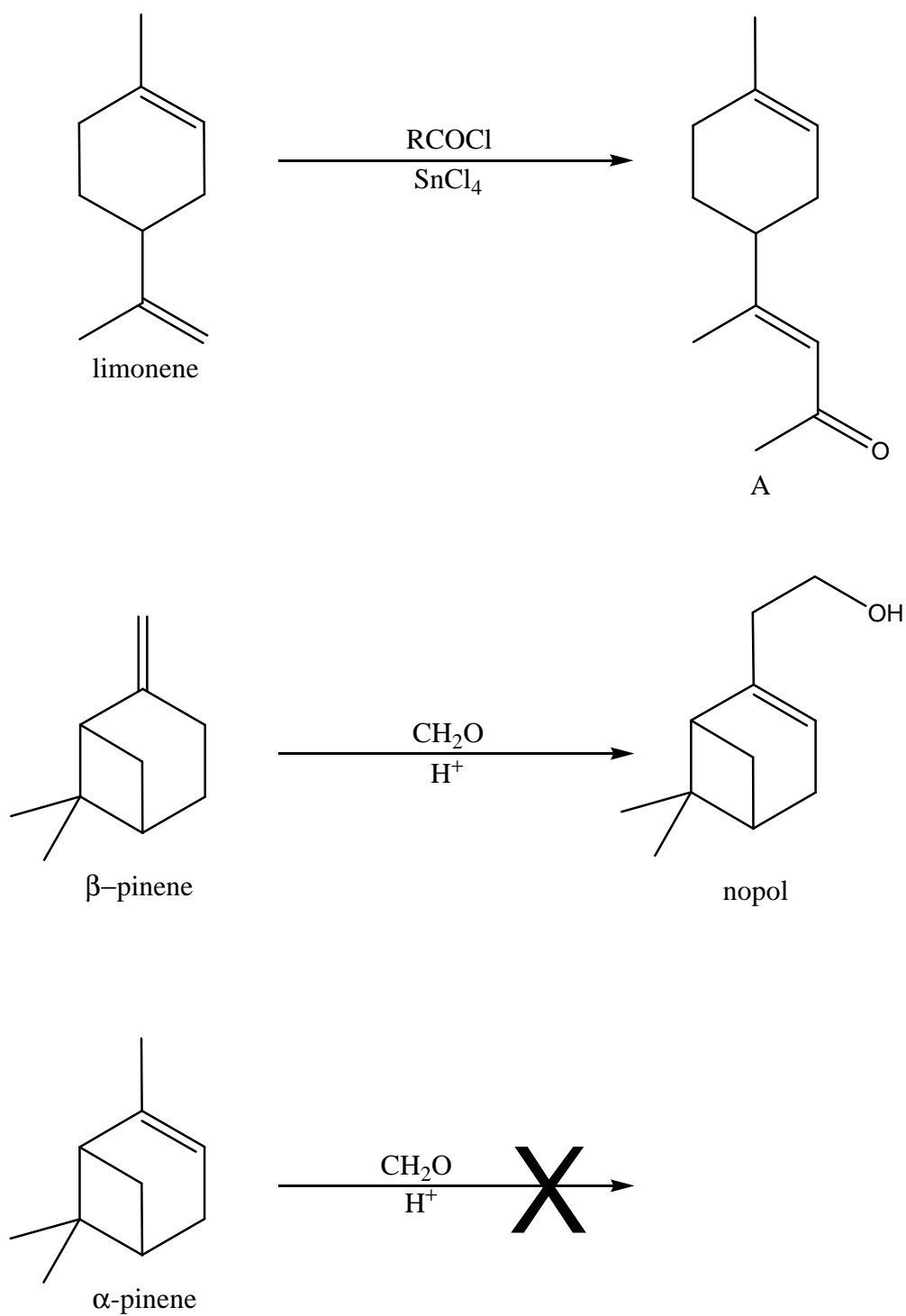
If a double bond is more heavily substituted at the one end than the other, then the  $\pi$ -electrons will be capable of being polarised so that the electron density moves towards the less substituted end leaving a partial positive charge at the more heavily substituted end as is illustrated by the extreme representations in **Figure 1.56**.





**Figure 1.56: Polarisation of methylene bond**

It must, of course, be remembered that polarisability is the capacity to be polarised rather than the actual degree of polarisation in the ground state. Reagents such as Friedel –Crafts reagents, carbon monoxide and formaldehyde, prefer a polarisable olefinic substrate. Some examples of selectivity relating to such polarisability are illustrated in **Figure 1.57**.



**Figure 1.57: Selectivity through polarisability**

The Friedel-Crafts acylation of limonene demonstrates two effects of polarisability. Firstly, the acylating species prefers the more polarisable of the two bonds in the molecule, hence there is attack only at the isopropenyl group. Secondly, the olefin

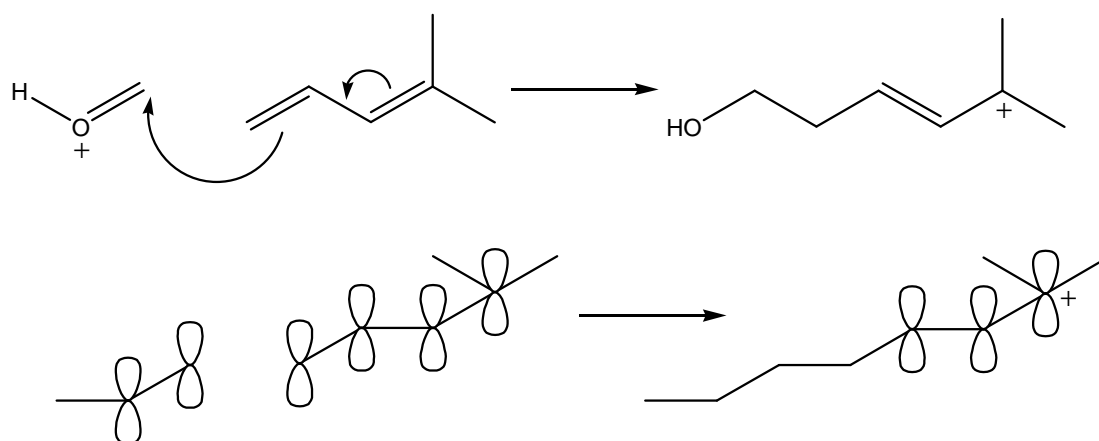
only polarises in one direction, the less substituted end, resulting in total regioselectivity and (A) as the sole product.

The second example of selectivity through polarisability is the Prins reaction of the pinenes. The double bond of  $\beta$ -pinene is more easily polarise than that of  $\alpha$ -pinene, hence only the  $\beta$ -isomer undergoes the reaction. With the Friedel-Crafts reaction of limonene, the regioselectivity is total because only the more negative end of the olefin adds to the positive carbon atom of the protonated formaldehyde. The product of the Prins reaction is known as nopol. The reaction is usually carried out in acetic acid and the resulting acetate is a useful perfumery ingredient.

#### 1.8.5.1.10 The *Trans-Anti-Periplanar* Rule

The rule states that all bonds being made or broken in a concerted reaction should preferably be coplanar and aligned in a *trans, anti* geometry relative to each other. The explanation for this lies in the molecular orbitals involved. The Prins addition of formaldehyde to 1,1-dimethylbuta-1,3-diene and the elimination of water from an alcohol are good illustrative examples of this.

The Prins reaction is shown in two different ways in **Figure 1.58**.

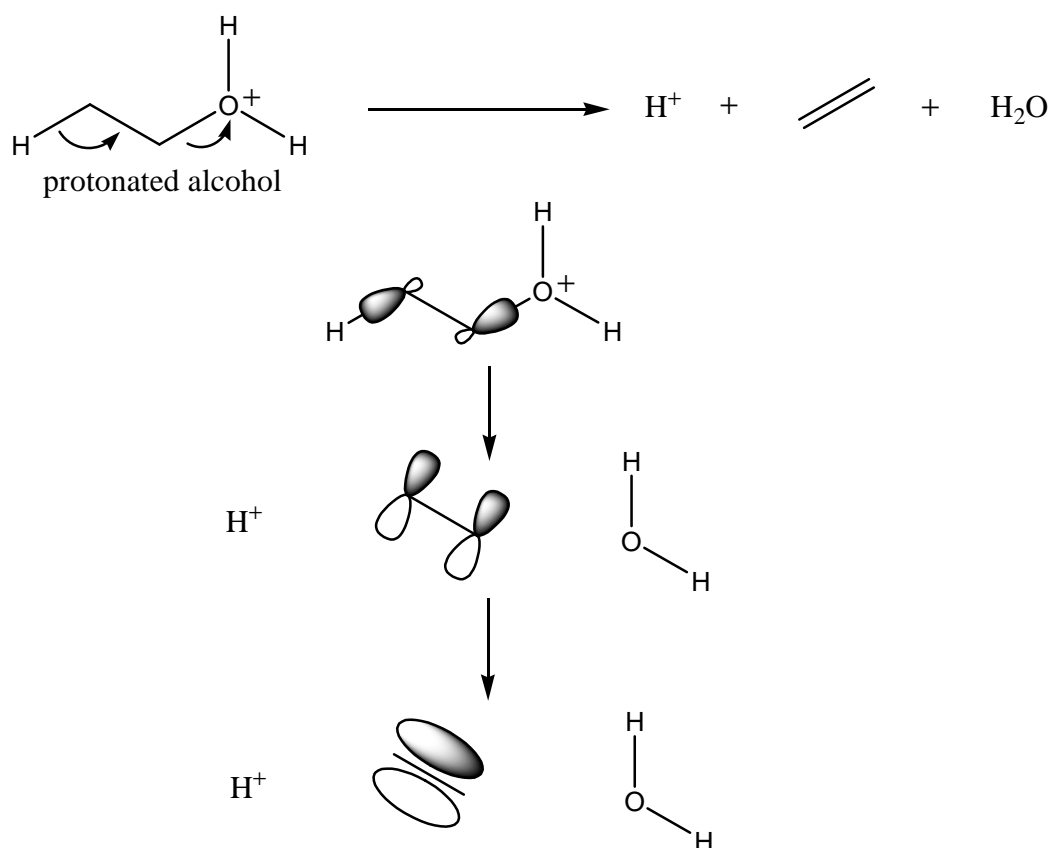


**Figure 1.58: The Prins reaction**

The top of the figure shows the traditional way of depicting the flow of electrons from the diene system to the protonated formaldehyde to give the intermediate carbocation.

The lower part of the figure shows how, aligning the p-orbitals of the three double bonds into a TAP configuration, maximum overlap is achieved between them. The electrons are therefore perfectly set up to move from the bonding pattern of the starting materials to that of the product.

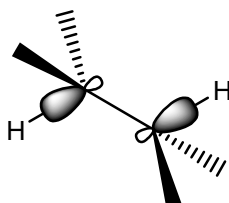
**Figure 1.59** depicts the elimination of water from a protonated alcohol to give an olefin, water and a proton.



**Figure 1.59: Elimination of water from protonated alcohol**

Again, the upper part of the figure shows the standard representation. In the lower part of the figure, we can once again see the TAP rule at work. In the starting material, only the orbitals of the breaking single bonds are shown. These are aligned TAP which gives the maximum degree of overlap between the smaller lobes at the back of each  $\sigma$ -bond with the larger lobe of the one opposite. This facilitates the formation of the new  $\pi$ -orbital, *via* the p-orbitals, between the two carbon atoms.

Earlier, it was stated that the explanation as to why the staggered conformation is more favourable than the eclipsed, lies in the steric repulsion of neighbouring atoms. There is an alternative explanation which is related to the TAP rule. **Figure 1.60** shows the  $\sigma$ -bonds between two geminal carbon atoms and one hydrogen atom attached to each.



**Figure 1.60:  $\alpha$ -Bonds between geminal carbon atoms**

The bond between the carbon atoms is shown in the staggered conformation and it can be seen how the two  $\sigma$ -bonds lie in the same plane allowing some degree of overlap between the large lobe of each one and the small lobe of the other. It is therefore possible that this stabilisation by overlap is responsible, either totally or in addition to the steric factor, for the preference for the staggered conformation. Evidence to support this theory comes from the fact that, when there is competition between the steric and electronic factors, the electronic one seems to take precedence.

## 1.9 Commercial Production of Terpenoids including Linalool

### 1.9.1 Fragrance Ingredients derived from Terpenoids<sup>47</sup>

The terpenoids form the largest group of natural odourants and so it is only to be expected that they also form the largest group of modern fragrance ingredients. Thousands of different terpenoid structures, both natural and synthetic, will be found in perfumes from fine fragrances to household cleaners. Some of the more important ones are shown in **Table 1.9**.

**Table 1.9: Some of the more important terpenoid fragrance materials<sup>47</sup>**

<b>Materials</b>	<b>Odour</b>	<b>Global usage per annum (tonnes)</b>
Menthol	Mint, coolant	5000
$\alpha$ -Terpineol and acetate	Pine	3000
Dihydromyrcenol	Citrus, floral	2500
Borneol/ <i>isoborneol</i> and acetate	Pine	2000
Carvone	Spearmint	1200
Acetylated cedarwood	Cedar	500
Amberlyn®/Ambrox®/Ambroxan®	Ambergris	10
Geraniol/Nerol and esters	Rose	6000
Citronellol and esters	Rose	6000
Linalool	Floral, wood	4000
Linalyl acetate	Fruit, floral	3000
Methyl ionones	Violet	2500
Hydroxycitronellal	Muguet	1000

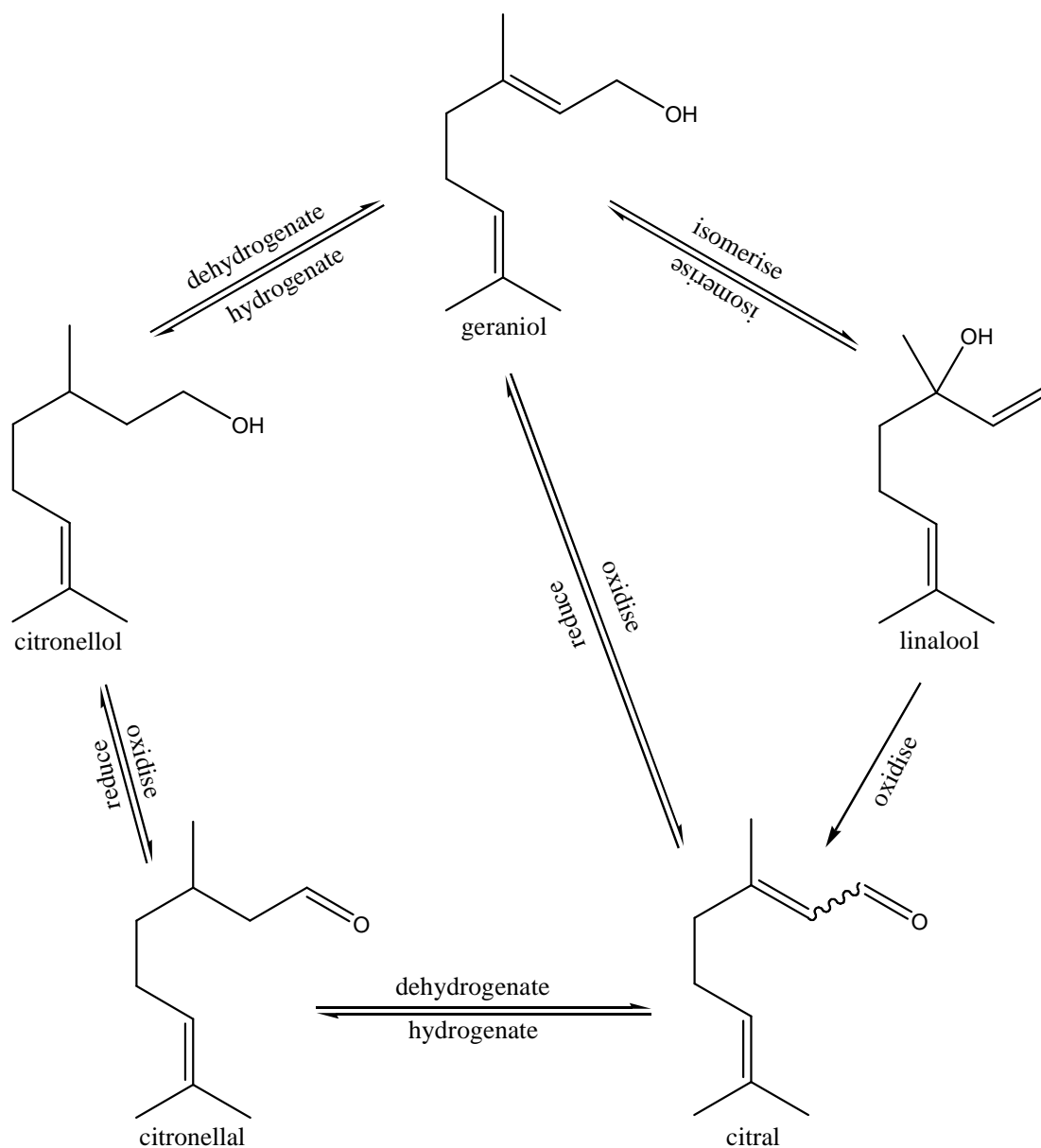
The terpene hydrocarbons generally have weak odours and are used mainly as feedstock. The higher molecular weights of the sesquiterpenoids results in their having lower vapour pressures than their monoterpenoid counterparts. Thus, sesquiterpenoids are present at a lower concentration in the air above a perfume than are monoterpenoids with the result that they must have a greater effect on the receptors of the nose in order to be detected. Hence, a lower percentage of sesquiterpenoids have useful odours than monoterpenoids. For the same reason, very few di- or higher terpenoids have odours. However, those sesqui- and higher terpenoids which do have odours are very tenacious because their lower volatility

means that they are lost more slowly from perfumes. Such materials form the basis of perfumes and serve also to fix the more volatile components.

These factors are reflected in **Table 1.9** where it can be seen that most of the higher tonnage materials are monoterpenoids. Amberlyn® is used only in relatively low volume but it commands a very high price because of the intensity and persistence of its odour. The alcohols geraniol, nerol, citronellol, and linalool are known as rose alcohols because of their presence in roses and the fact their odours are key parts of the complex rose fragrance. The ionone family are prepared from citral, which is the aldehyde corresponding to geraniol and nerol. Thus, it is clear from the Table that this group of geraniol/citral related materials is of major importance to the fragrance industry. Their importance is even greater since citral is also the key synthetic intermediate for the preparation of vitamins A, E, K<sub>1</sub> and K<sub>2</sub>. The consumption of citral for vitamins is comparable to that for fragrances.

### **1.9.2 Interconversion of the Five Key Terpenoids<sup>48</sup>**

**Figure 1.61** shows another reason for the importance of these five key terpenoids.



**Figure 1.61: Interconversion of key terpenoids**

They can be readily interconverted by isomerisation, hydrogenation and oxidation as appropriate. The ability to manufacture any one of these five terpenoids, therefore, opens up the potential to produce all of them and, hence, a wide range of other terpenes. Obviously, if one company produces geraniol/nerol initially and another linalool and both do so at the same cost per kilogram for their individual initial product, then they will not be able to compete with each other on both products. The first will have an advantage in geraniol/nerol and the second in linalool. Thus the



range of products which any terpene producer can market effectively will depend on a fine balance of its feedstock and process costs as compared to those of its competitors.

### **1.9.3 Commercial Aspects**

The major producers of rose alcohols and citral have developed these specific business lines for a variety of reasons. Companies which manufacture wood and paper products produce sulphate turpentine or similar by-products rich in pinenes. They may then produce terpenoid fragrance materials from pinenes as a way of generating income from their by-product. Pharmaceutical companies which manufacture vitamins use terpenoid intermediates and so will often diversify into the manufacture of aroma chemicals. Their basic feedstocks are likely to be of petrochemical origin. Similarly, manufacturers of synthetic rubber possess technology for the use of isoprene as a feedstock and are also likely to diversify into terpene aroma chemical manufacture. Fragrance companies will develop a position in terpenoid chemistry because of the importance of terpenoids as ingredients.

The fragrance industry lies between the petrochemical and pharmaceutical industries in terms of scale of production and cost per kilogram of product. The production scale is closer to that of the pharmaceutical industry but the prices are closer to those of the bulk chemicals industry.

The largest volume fragrance ingredients are produced in quantities of 5000-6000 tonnes per annum and some ingredients, mostly those with extremely powerful odours are required in only kilogram quantities.

The cost constraints on the industry are, ultimately, imposed by the consumer. In many products, such as soap and laundry powder, the fragrance may be a significant contributor to the overall cost of the finished goods. If the price of one product is not acceptable, the consumer will select a competitive brand. The manufacturer of these products, therefore, puts considerable pressure on the fragrance supplier to come up with the most effective fragrance at the lowest possible cost.

All these factors mean that process chemists working in the fragrance industry have to work hard and think creatively and opportunistically in order to provide materials at

an acceptable cost and without the advantages of scale that the bulk chemicals industry enjoys.

#### 1.9.4 Linalool Production/Synthesis

Fritzsche D & O (BASF) have a linalool capacity estimated to be about 500 M tons<sup>42</sup>. Initially BASF began production of vitamins using the acetylene-acetone route to methylheptenone via methylbutynol, which generates the intermediate dehydrolinalool. Dehydrolinalool is subsequently semi-hydrogenated to linalool. However, this route never completely removes all the dehydrolinalool unless the hydrogenation is incomplete and the remaining dehydrolinalool is destroyed by reversing the ethynylation process, leading to yield losses. Attempts to remove the dehydrolinalool by over-hydrogenation result in production of tetrahydrolinalool. BASF's most recent process uses methylheptenone, generated by the condensation of isobutylene, formaldehyde and acetone. The methylheptenone is then converted to linalool via a vinyl Grignard reagent, producing a clean, synthetic product, which is difficult to detect in reconstituted essential oils.

Givaudan (Hoffman-La Roche), which have its production facilities in Europe, has an estimated production capacity of 1400 M tons per annum. The technology is based on the classical acetone-acetylene route through methylbutynol via Tedeschi catalytic ethynylation. Methylbutynol is converted to methylheptenone which is then catalytically ethynylated to dehydrolinalool, which is then semi-hydrogenated to linalool. The linalool produced contains trace amount of dehydrolinalool, thus marking it as synthetic. The advantage of the Hoffman-La Roche technology is that it tolerates the feed of different types of ketone, thereby allowing the production of substituted linalools, eg. ethyl linalool.

Glidco (SCM) has an estimated capacity of 8000 M tons per annum of linalool/geraniol and is the only company to produce the material in the USA. Its process begins with  $\alpha$ -pinene obtained from turpentine. The  $\alpha$ -pinene is converted to *cis*-2-pinanol via the hydroperoxide, which is pyrolysed to linalool. Due to investment in new innovative technology and the construction of a modern plant at a time when worldwide linalool capacity was in great excess, its capacity today has made Glidco the largest producer of linalool/geraniol in the world.

Kuraray's linalool capacity is estimated at 3000 M tons per annum. However, significant capacity is used to produce isophytol and squalene as well as linalool. Kuraray has licensed the old Rhodia process which uses isoprene to generate prenyl chloride, and which is subsequently converted to methylheptenone. Catalytic ethynylation of methylheptenone in liquid ammonia then yields dehydrolinalool which is semi-hydrogenated to linalool.

These processes are discussed in more detail in the following sections.

#### **1.9.4.1 Myrcene as substrate<sup>49,50</sup>**

Of all the various products obtained from the pyrolysis of  $\beta$ -pinene, myrcene (**Figure 1.62**), has the largest industrial interest.

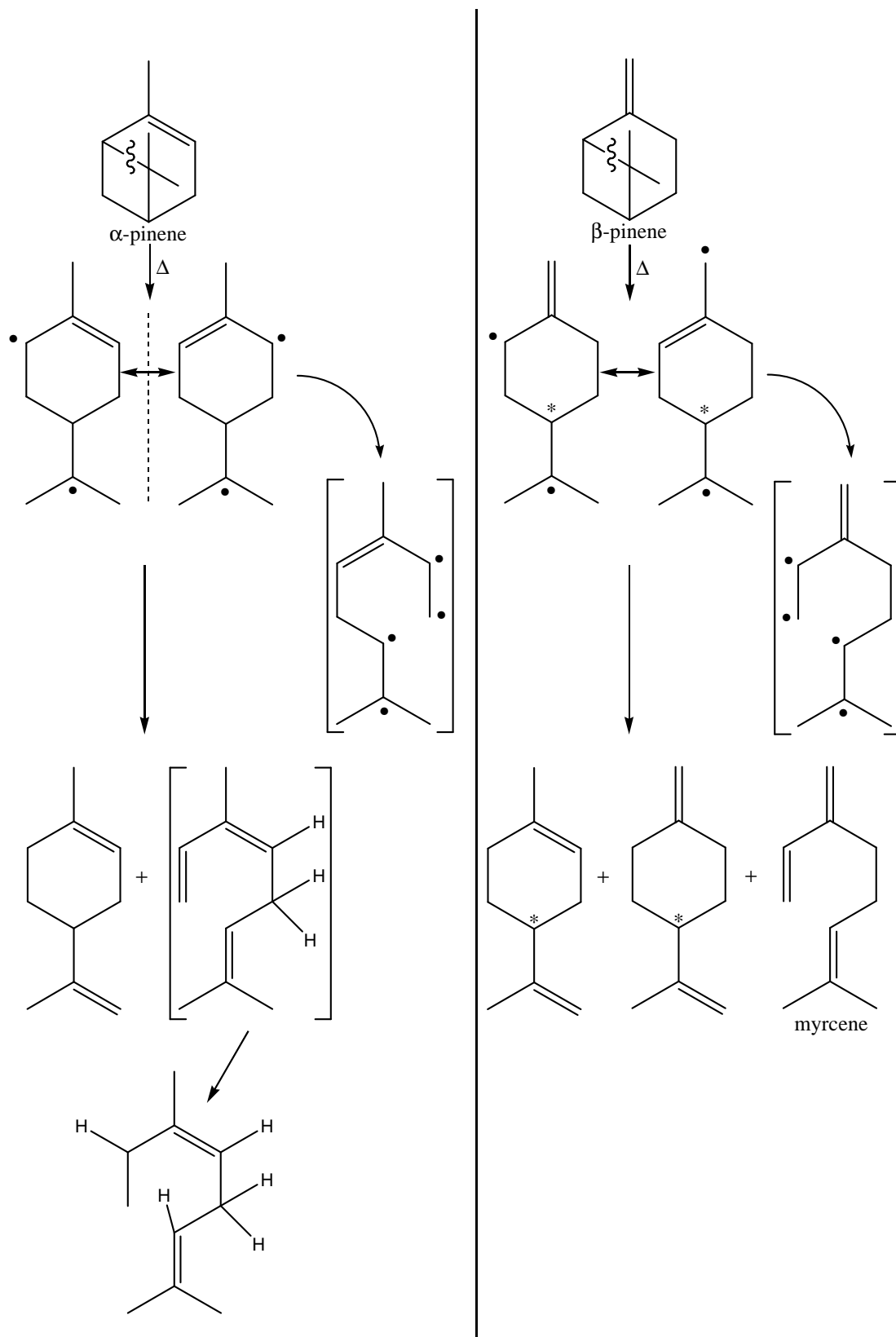
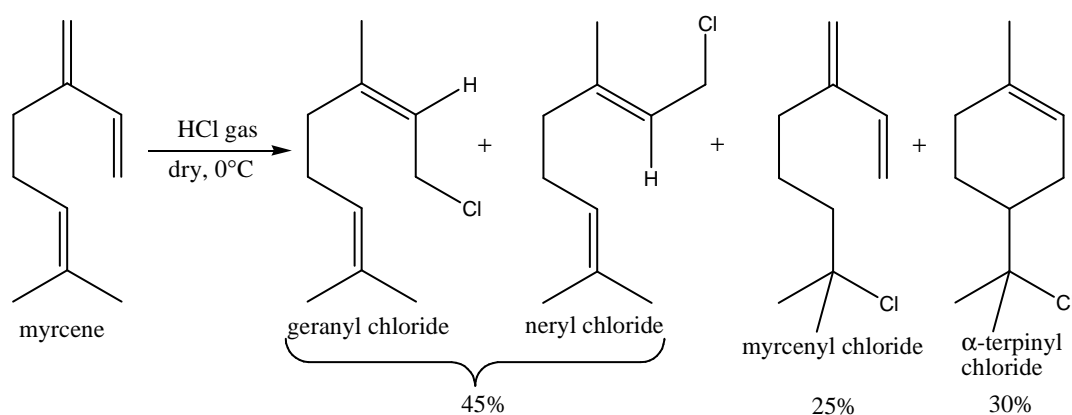


Figure 1.62: Pyrolysis products of  $\alpha$ - and  $\beta$ -pinene

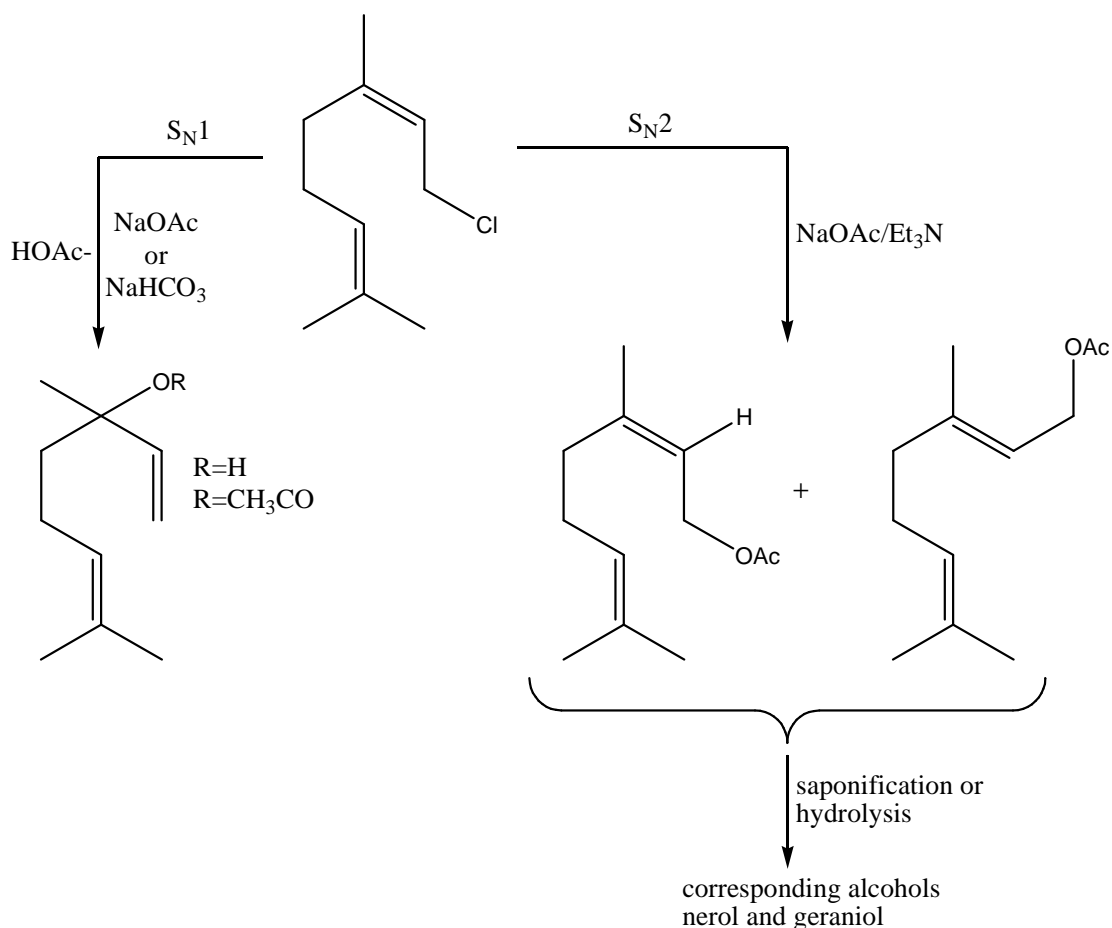
Under the action of dry or aqueous hydrochloric acid, myrcene gives a complex mixture of chlorides which can then be converted into the corresponding alcohols<sup>51</sup>. When myrcene is treated at 0°C and in the absence of catalyst with a stream of dry HCl, a mixture containing geranyl chloride, neryl chloride, myrcenyl chloride and  $\alpha$ -terpenyl chloride is obtained as shown in **Figure 1.63**.



**Figure 1.63: Action of HCl on myrcene**

The chlorides obtained can be transformed into the acetates by treatment with sodium acetate. Two distinct mechanisms may be operating in this substitution reaction.

- A monomolecular solvolytic reaction (reaction with the solvent) catalysed by cuprous chloride. The end product is either linalyl acetate or linalool, depending on whether acetic acid or water is used as solvent.
- A bimolecular  $SN_2$  reaction. In this case, the acetates of nerol and geranyl are formed exclusively (**Figure 1.64**).



**Figure 1.64: Conversion of chlorides into acetates**

It is evident that the economic viability of these processes depends on the use of highly efficient distillation equipment. This is true both for the purification of myrcene used as starting material and for the separation of alcohols and esters which are formed. Furthermore, in order to obtain these compounds and their derivatives, it is necessary to have access to pure  $\beta$ -pinene and this necessitates carrying out fractionation of turpentine oil.

#### 1.9.4.2 $\beta$ -Methylheptenone as substrate

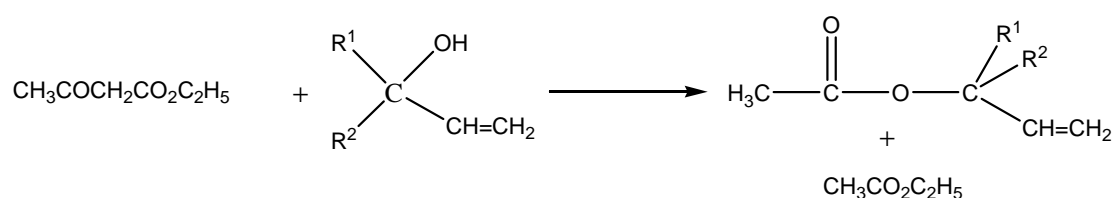
$\beta$ -Methylheptenone is a key intermediate for the production of a number of very economically important chemicals, particularly linalool, via the hydrogenation of dehydrolinalool<sup>52,53</sup>. It can be prepared from the following starting materials:

- 3-methyl-3-buten-2-ol (methylbutenol)
- 3-methylpropene (isobutylene)

- Isoprene

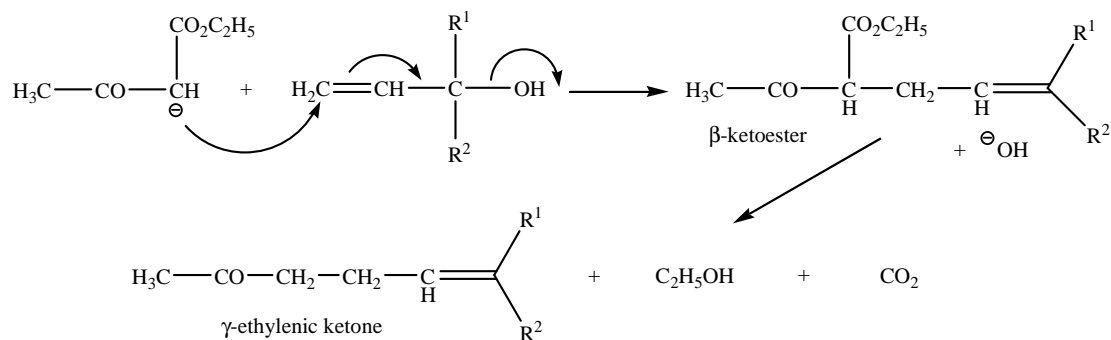
### 1.9.4.2.1 Synthesis from Methylbutenol

This synthesis was the subject of one of the first endeavours of the Research Center of Roure Bertand Dupont in Grasse. In 1940, Carroll published work on the action of  $\alpha$ -ethylinic alcohols on compounds with active methylene groups in the presence of alkaline ethylates or acetates. The first two publications were on the action of ethyl acetoacetate on linalool and or geraniol as well as cinnamic alcohol and phenylvinylcarbinol<sup>54,55</sup> in an attempt to obtain the corresponding acetates by using what could be considered as an inverse Claisen reaction (**Figure 1.65**).



**Figure 1.65: Inverse Claisen reaction**

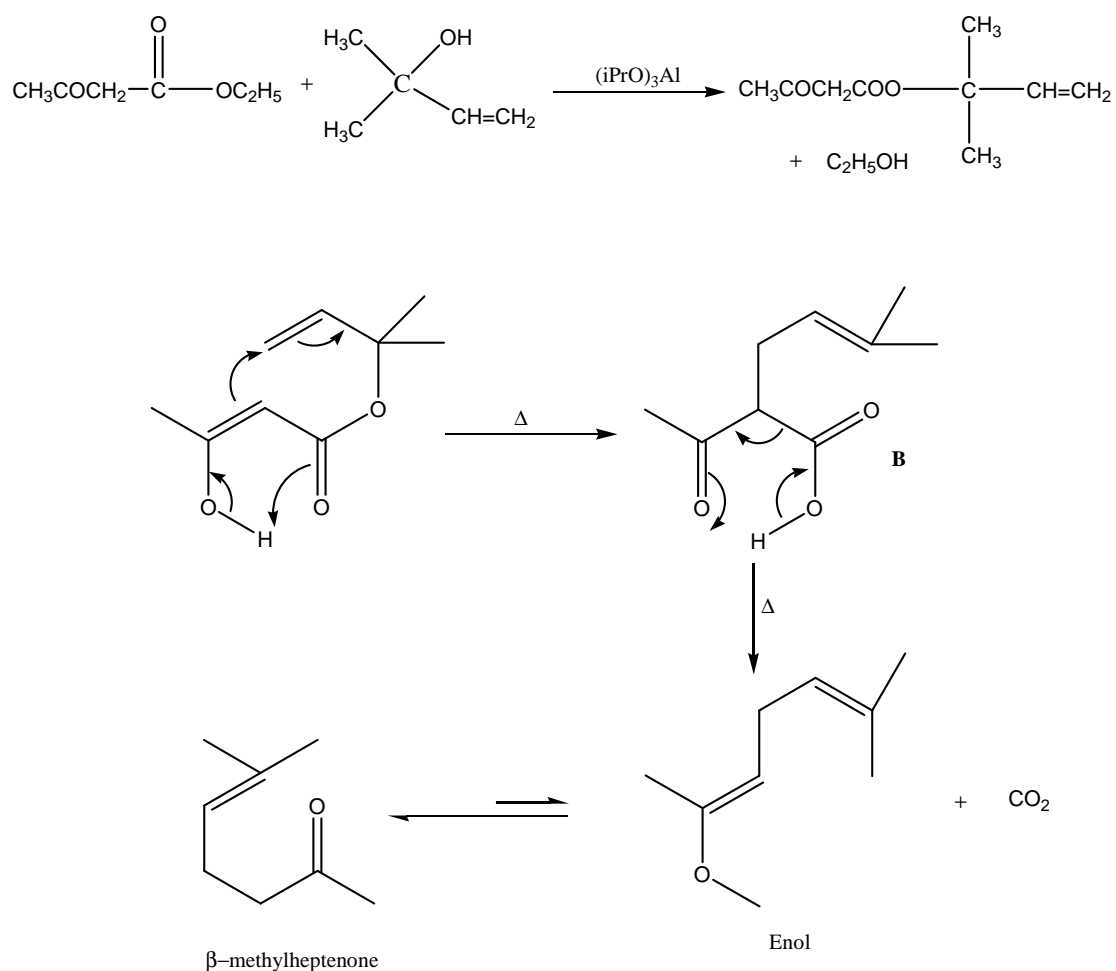
While Carroll did indeed observe the formation of these acetates in yields not exceeding 20%, the simultaneous formation of a ketone in yields in the range of 40% was also observed. The formation of this ketone was explained in terms of a Michael addition reaction followed by cleavage of the intermediate  $\beta$ -ketoester to give the observed  $\gamma$ -ethylenic ketone (**Figure 1.66**).



**Figure 1.66: Michael addition and cleavage of ketoester**

Kinetic studies of this reaction showed that ethanol and carbon dioxide gas were liberated at high temperature. The gas is carbon dioxide. These observations were explained in terms of an exchange reaction between the ethylenic alcohol present in the reaction mixture and the  $C_2H_5O-$  group of ethyl acetoacetate. This observation provided the impetus for the subsequent search for exchange catalysts which are more efficient than sodium ethylate (Such as magnesium and aluminium alcoholates). The use of catalysts such as these has made it possible to obtain yields as high as 80%, thereby permitting this reaction (now called the Carroll Reaction) to be used on an industrial scale.

The following mechanism has been proposed for the synthesis of  $\beta$ -methylheptenone from methylbutenol (**Figure 1.67**).

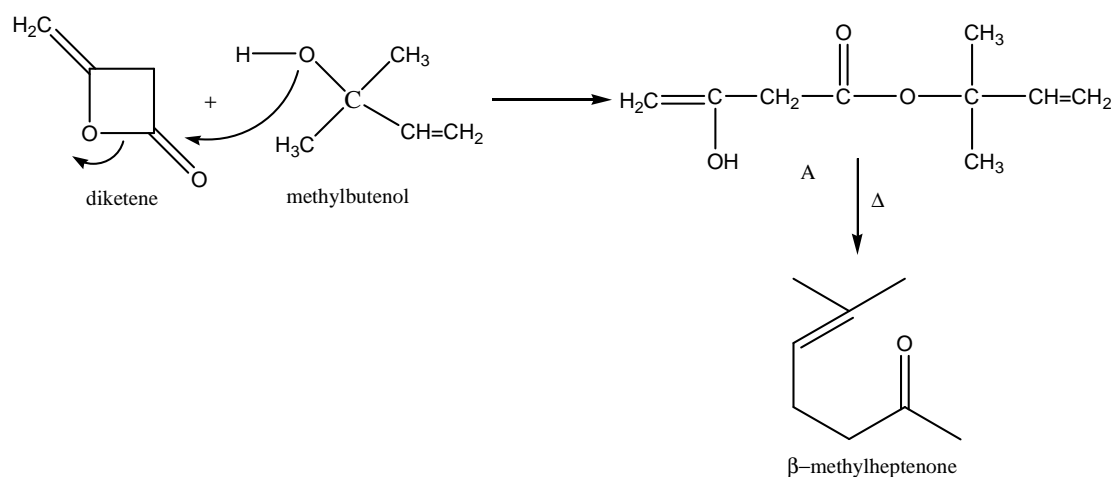


**Figure 1.67: Mechanism of Carroll reaction**



The exchange reaction, which constitutes the first step of this reaction, starts at temperatures of 110 -120°C. The second step which is a sigmatropic rearrangement involving 10 electrons ( $4n + 2$ ), requires a higher temperature and gives intermediate B, a  $\beta$ -keto acid. This intermediate finally decarboxylates to liberate  $\beta$ -methylheptenone.

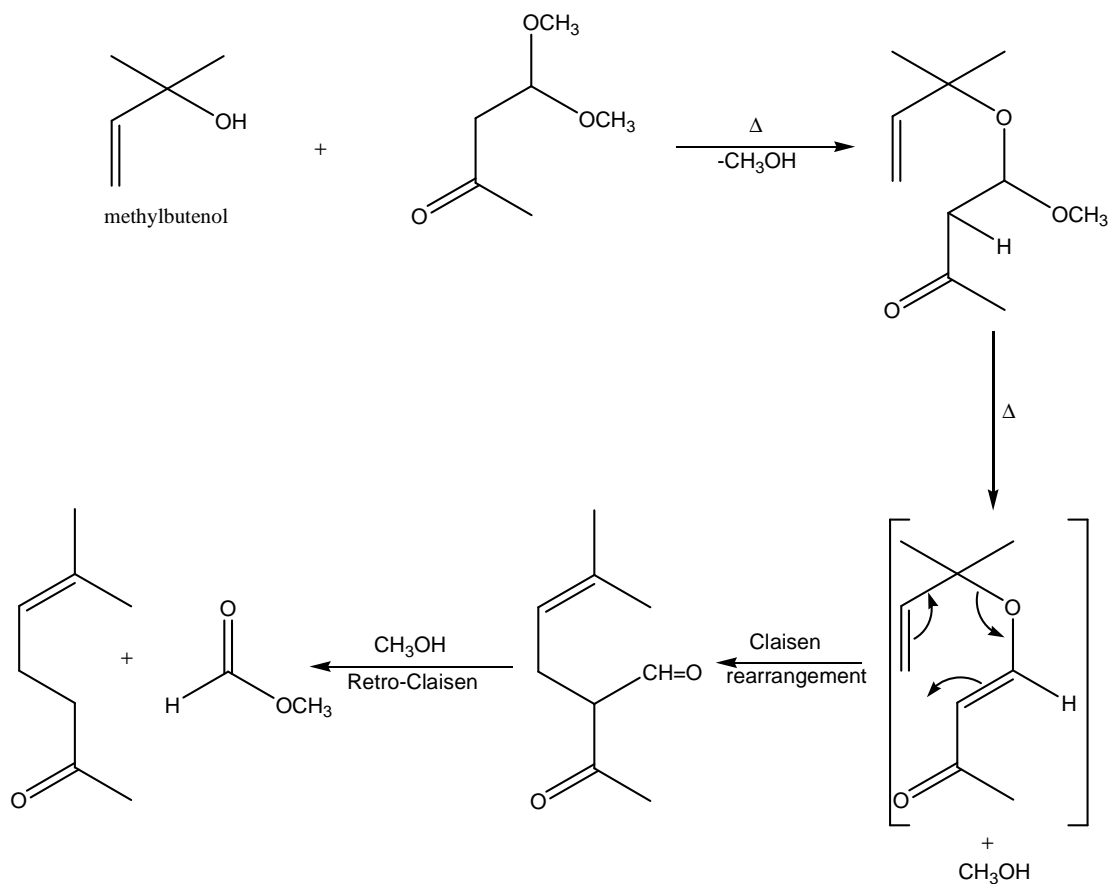
Researchers at Hoffman-La Roche have used a variant of this reaction which consists of preparing methylbutenyl acetoacetate, A, by the action of diketene on methylbutenol in the presence of catalysts (**Figure 1.68**)<sup>56</sup>.



**Figure 1.68: Action of diketene on methylbutenol**

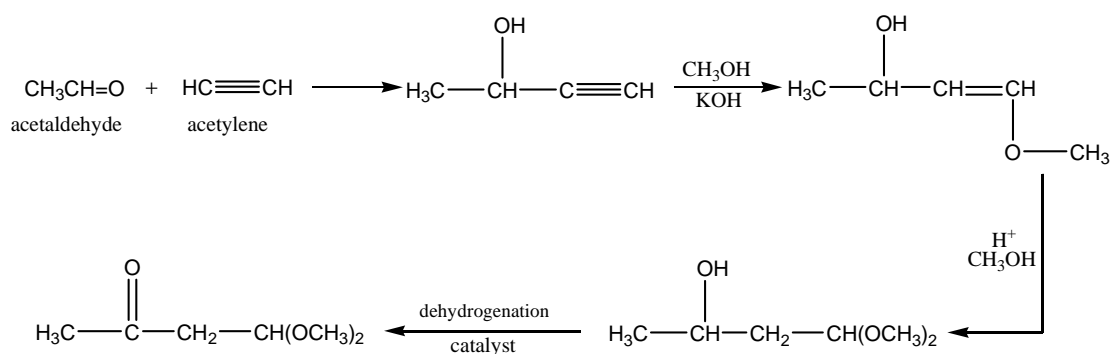
The acetoacetic acid ester thus formed is then pyrolysed to obtain  $\beta$ -methylheptenone. These results confirm the mechanism proposed by Carroll. The pyrolysis can also be catalysed by aluminium alcoholates.

Another variant, devised by workers at BASF, uses the following sequence (**Figure 1.69**)<sup>57</sup>.



**Figure 1.69: Pyrolysis of acetoacetic acid ester**

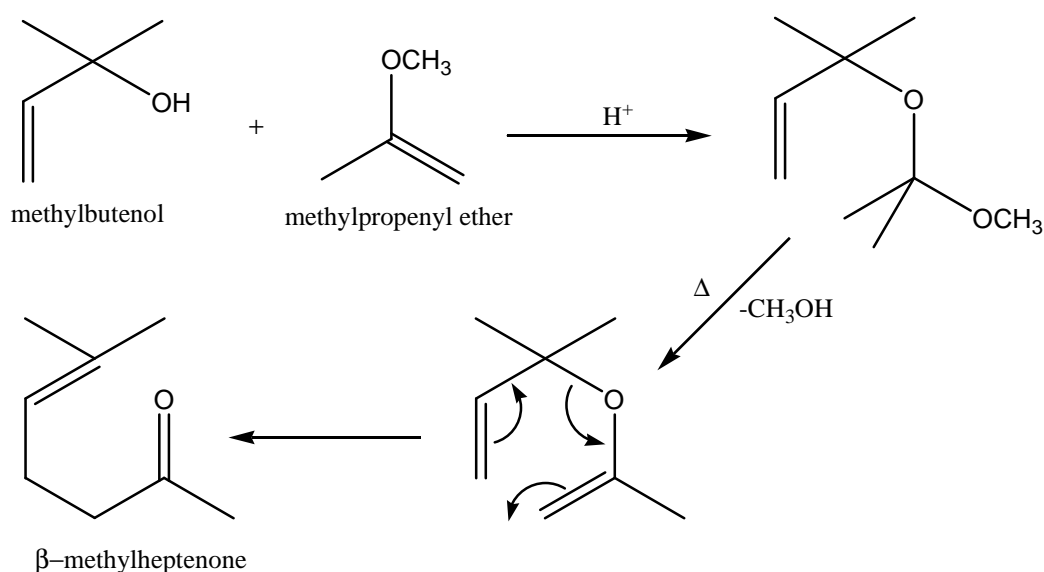
The dimethylacetal can be prepared from three rather inexpensive raw materials; acetylene, acetaldehyde, and methanol (**Figure 1.70**)<sup>58</sup>.



**Figure 1.70: Preparation of the dimethylacetal**

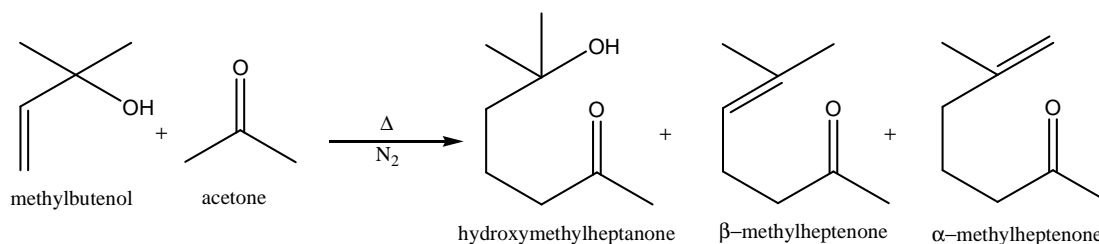
This compound also finds application in the industrial synthesis of Vitamin A by Eastman-Kodak.

A third synthesis of  $\beta$ -methylheptenone, also realized by workers at Hoffman-La Roche, is based on the chemistry of enol ethers (Hoffman USP 2,839,579). It consists of condensing methylbutenol with the methylpropenyl ether and pyrolysing the mixed acetal thus obtained. The vinylallylic ether formed as an intermediate in this reaction undergoes a Claisen rearrangement to give  $\beta$ -methylheptenone (**Figure 1.71**).



**Figure 1.71: Synthesis of methylheptenone based on enol ethers**

A fourth synthetic route has been elaborated by Japanese researchers<sup>33</sup>. It is based on the radical reaction of acetone with methylbutenol in the presence of peroxides – however, little information on this process is available (**Figure 1.72**).

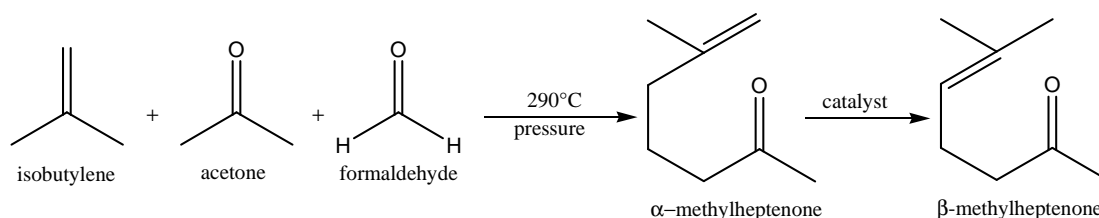


**Figure 1.72: Radical reaction of acetone with methylbutenol**

This reaction requires heating in an autoclave at 130°C for 24 hours under a nitrogen atmosphere. A mixture of  $\beta$ -methylheptenone,  $\alpha$ -methylheptenone and hydroxymethylheptanone is obtained. The last of this is dehydrated to  $\beta$ -methylheptenone.

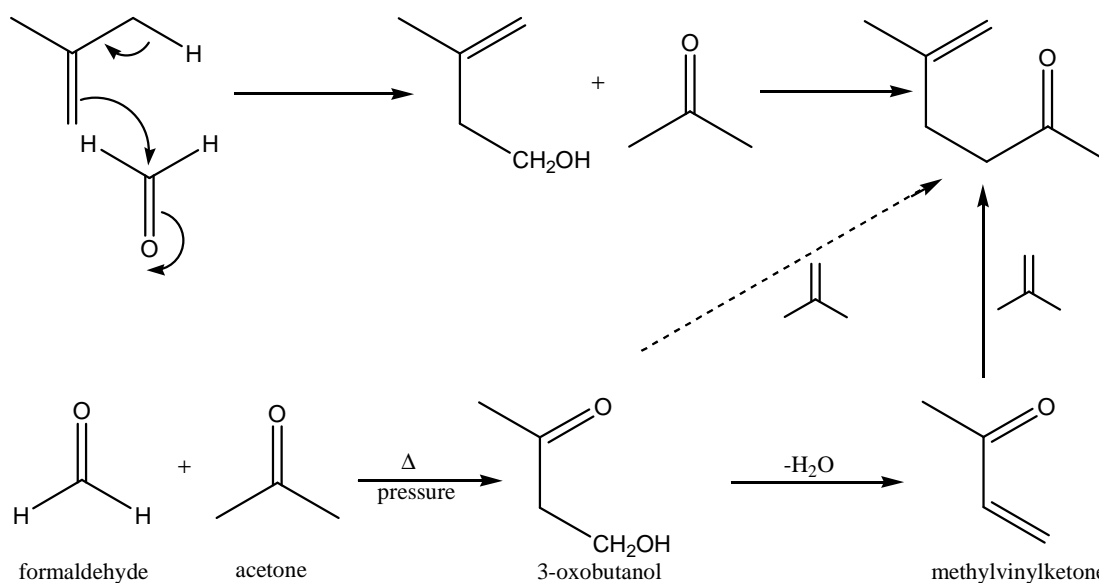
#### 1.9.4.2.2 Synthesis from Isobutylene<sup>33</sup>

In this industrial synthesis developed by BASF, acetone, isobutylene and formaldehyde are condensed at high temperatures and under high pressure to give principally  $\alpha$ -methylheptenone which is then isomerised to  $\beta$ -methylheptenone by treatment with special catalysts (**Figure 1.73**).



**Figure 1.73: Reaction of acetone, isobutylene, and formaldehyde**

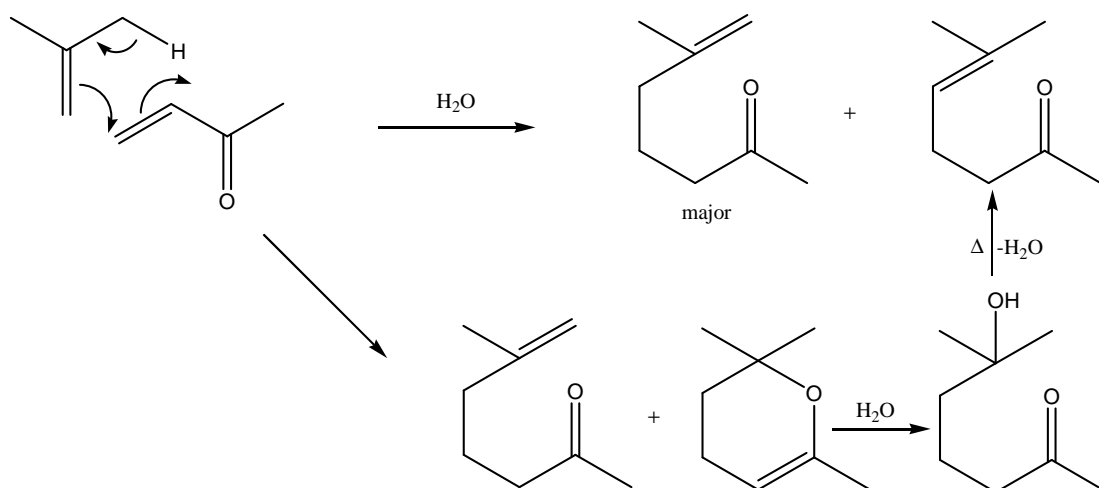
A mechanism involving two molecular steps can be envisaged along two different pathways (**Figure 1.74**).



**Figure 1.74: Mechanism of reaction**

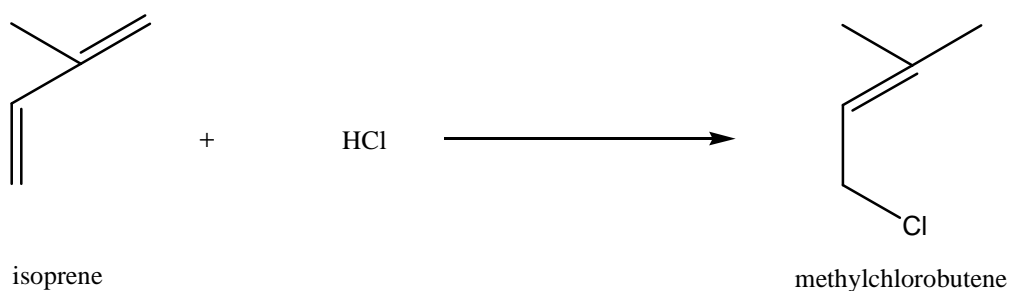
If 3-oxobutanol is prepared separately and then condensed with isobutylene at 270°C under high pressure, a mixture is obtained, although the  $\beta$ - isomer predominates.

Methylvinylketone also reacts with an excess of isobutylene at 270°C under pressure. The results vary depending on whether there is water in the reaction mixture (**Figure 1.75**).

**Figure 1.75: Reaction of methylvinylketone with isobutylene**

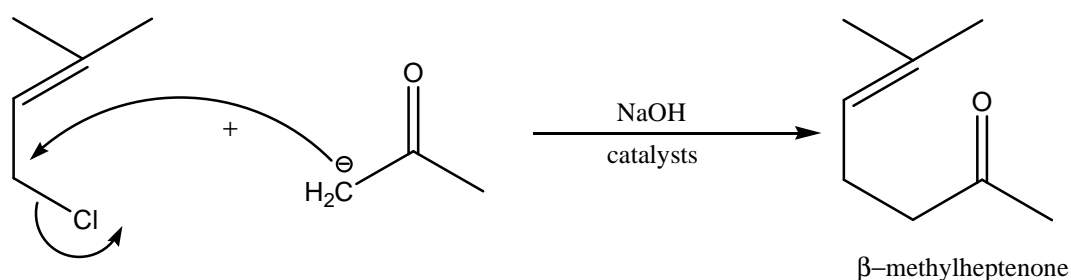
#### 1.9.4.2.3 Synthesis from Isoprene<sup>59</sup>

This route, developed by Rhone-Poulenc, involves the synthesis of methylchlorobutene (**Figure 1.76**).



**Figure 1.76: Synthesis of methylchlorobutene**

Methylchlorobutene is then condensed with acetone in the presence of sodium hydroxide and catalytic quantities of iodine or amines. An iodine-chlorine exchange takes place, thereby accelerating the reaction because the I<sup>-</sup> ion is a better leaving group than the Cl<sup>-</sup> ion (**Figure 1.77**).



**Figure 1.77: Condensation of methylchlorobutene with acetone**

This approach requires extremely pure isoprene, and is more relevant to the polymer and rubber industries than the perfumery industry.

#### 1.9.4.3 Linalool from Crude Sulphated Turpentine<sup>60</sup>

For thousands of years turpentine has been obtained from conifers by a process known as tapping. A cut is made in the bark which prompts the trees to exude oil which can be drained off into vessels attached to the tree. Turpentine thus obtained is referred to as gum turpentine. Nowadays, another form of turpentine is available in large quantities as a by-product of paper manufacture. When softwood (pine, fir, spruce) is converted into pulp in the Kraft paper process, the water insoluble liquids which were present in it are freed and can be removed by physical separation from the

process water. This material is known as crude sulphated turpentine (CST). Fractional distillation of CST gives a number of products as shown in **Table 1.10**.

**Table 1.10: Composition of distillate from CST**

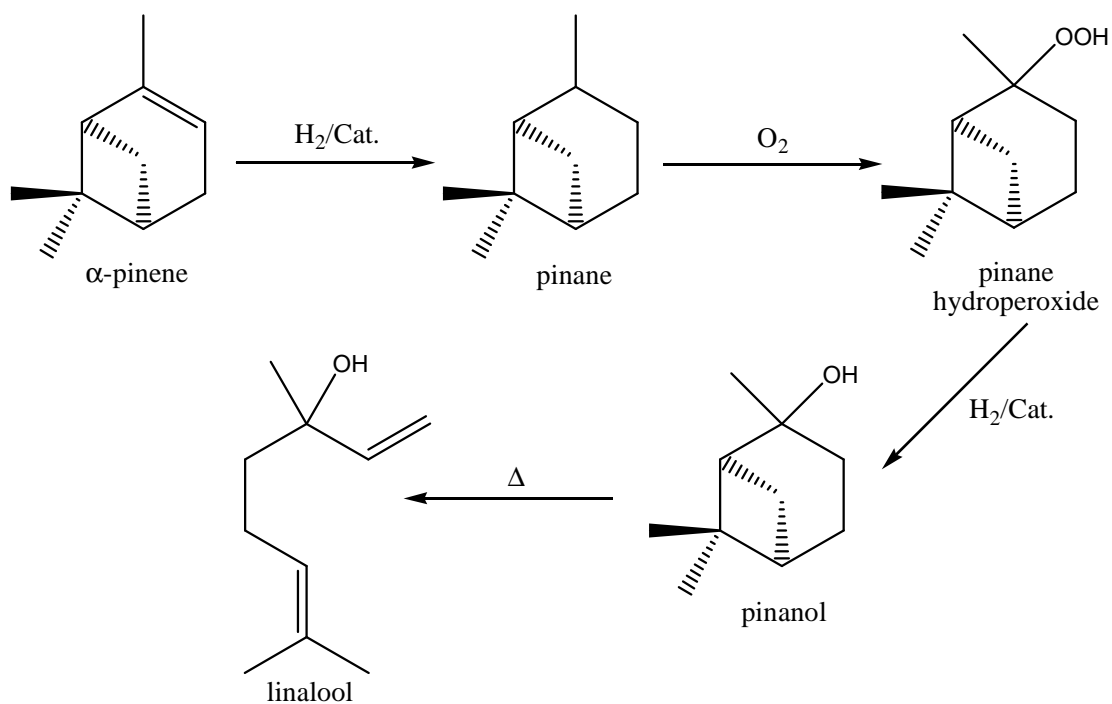
Product	Percentage
Lights	1-2
$\alpha$ -Pinene	60-70
$\beta$ -Pinene	20-25
Dipentene	3-10
Pine Oil	3-7
Estragole, anethole, caryophyllenes	1-2

Dipentene is the name given to racemic limonene. The residue from the distillation is known as tall oil and contains diterpenes such as abietic acid.

Thus, pure  $\alpha$ - and  $\beta$ -pinenes can be obtained by fractional distillation of turpentine. The two can be interconverted by catalytic isomerisation but this leads to an equilibrium mixture. The equilibrium could be driven in one direction by continuous removal of the lower boiling component through distillation. However,  $\alpha$ -pinene is the lower boiling of the two and is already more abundant. To increase the yield of  $\beta$ -pinene, it is necessary to use consecutive cycles of fractionation and isomerisation. This is obviously a costly process in terms of time and energy. As a result,  $\beta$ -pinene is about twice the price of  $\alpha$ -pinene and this affects the economics of other terpenoids prepared from them.

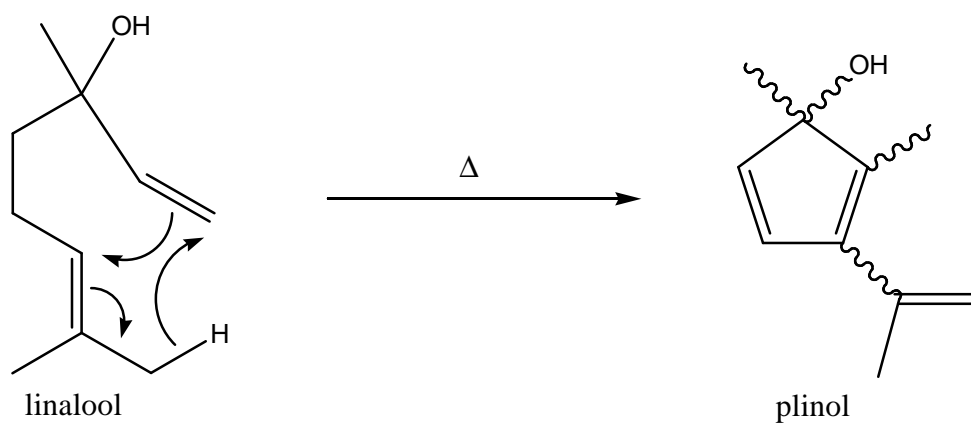
The preparation of linalool from  $\beta$ -pinene has been discussed in § 1.5.4.1.

Hydrogenation of  $\alpha$ -pinene gives pinane which can be oxidised by air under free radical conditions to give the hydroperoxide which can be reduced by hydrogenation to 2-pinanol<sup>61</sup>. Pyrolysis of the alcohol gives linalool (**Figure 1.78**).



**Figure 1.78: Synthesis of linalool from  $\alpha$ -pinene**

Previous investigations undertaken by AECI R & D and in the literature have resulted in poor selectivities to the desired product and hence poor yields<sup>62</sup>. The disadvantage of this process lies in a side reaction (**Figure 1.79**).



**Figure 1.79: Linalool decomposition**



Linalool is not stable under the pyrolysis conditions and some of it undergoes decomposition to give a mixture of isomeric alcohols known as plinol<sup>63</sup>. These have boiling points which are close to that of linalool making separation by distillation difficult. The pyrolysis is therefore run a below total conversion in order to minimise plinol formation. In order to separate the plinol from desired product, it is necessary to isomerise the linalool to geraniol and then fractionally distil since the boiling point of the plinol is sufficiently different from that of geraniol to allow separation. This, however, adds extra costs to the process.

#### **1.9.4.4 Other syntheses of Linalool**

There are numerous other examples of the synthesis of linalool by chemical<sup>28,44,64-66</sup> and biosynthetic<sup>31,67-70</sup> means but these are not of commercial value and fall outside the scope of this investigation.

### **1.10 Zeolites as Catalysts**

Since the mid 1960s when workers at the Union Carbide laboratories and workers at the Mobil laboratories announced dramatic examples of solid catalysis based on faujasitic zeolites, many different zeolitic solids have been used used for both laboratory based and industrial scale catalysis. Examples of chemical reactions catalysed by zeolites include cracking, hydrocracking, hydration, dehydration, alkylation, isomerization, oxidative addition, and dehydrocyclization<sup>71</sup>. Microporous aluminosilicate catalysts possessing the structures of well known minerals (such as faujasite, ferrierite, mordenite, and erionite) as well as many more that have no known naturally occurring analogues (ZSM-5, Theta-1, ZSM-23, zeolite Rho) are particularly well suited for the conversions of hydrocarbons, certain oxygenates and other species, into useful products<sup>72</sup>.

Zeolites are, in effect, solids possessing three-dimensional internal surfaces, replete with cages and channels, which may or may not intersect. Linking the pores, and distributed in a more or less spatially uniform fashion throughout their bulk, are the active sites which are bridging hydroxyl groups. Since 1992, when workers at the Mobil Research laboratories announced the discovery of a large family of mesoporous solids with aperture diameters ranging from 20 to 100 Angstroms), a further upsurge

in interest in new crystalline solid catalysts with open structures and vast, accessible internal areas ( $>600\text{m}^2/\text{g}$ ) has occurred<sup>73,74</sup>.

As zeolitic materials do not constitute a readily definable family of crystalline solids, use is often made of the simple notion of framework density (FD), which is the number of tetrahedral (T) atoms per 1000 Angstroms<sup>3</sup> in the structure. The well-known *Atlas of Zeolite Structure Types*<sup>75</sup> shows the distribution of these values for microporous and dense frameworks, the structures of which are well established.

In this investigation, three types of zeolites were evaluated, i.e. Na BEA (Zeolite Beta), NaY (Faujasite), and AB MOR (Mordenite). Zeolite Beta exists as an intergrowth of two closely related polymorphs, neither of which is obtainable in its pure form and which differ in the sequence in which the 12-ring pores stack. The composition is  $\text{Na}_n[\text{Al}_n\text{Si}_{64-n}\text{O}_{128}]$  with  $n < 7$ . Zeolite Beta has been found to be an active catalyst for a number of reactions, such as cracking of *n*-decane<sup>76</sup>.

Faujasite of formula  $(\text{Na}_2, \text{Ca}, \text{Mg})_{29}[\text{Al}_{58}\text{Si}_{134}\text{O}_{384}].240\text{H}_2\text{O}$  crystallizes with cubic symmetry. The secondary building units (SBUs) are double 6-rings, 6-2 (4- or 6-rings) and the framework density is 12.7T/1000 Angstroms<sup>3</sup>. Faujasites are of great practical value in the cracking of hydrocarbons<sup>77</sup>.

Mordenite of formula  $\text{Na}_8[\text{Al}_8\text{Si}_{40}\text{O}_{96}].24\text{H}_2\text{O}$  crystallizes with orthorhombic symmetry. The SBU is 5-1 and the FD is 17.2T/1000Angstroms<sup>3</sup>. The existence of side pockets off the main, large-pore channels in mordenite catalysts facilitates side-chain migration and isomerization to form branched hydrocarbons from linear alkanes. It is also a viable candidate for the selective Friedel-Crafts catalytic alkylation of naphthalene to 2,6-di-isopropylnaphthalene, an important starting material for speciality polyesters and liquid crystal polymers<sup>78</sup>.

## 1.11 Microreactors

The spatial and temporal control of chemical reactions in the chemically intensive environment of micro reactors, coupled with high surface interactions has been demonstrated to give faster reactions and improved product yields with greater product selectivity compared with conventional batch reactor methodology. These

advantages have been demonstrated for a wide range of chemical reactions and are of great interest to the pharmaceutical and fine chemicals industry, in the areas of high throughput drug discovery, reaction optimisation and process development<sup>79</sup>.

Microdevices in chemical processes represent a novel approach to production flexibility with the advantages of reduced reagent consumption, improved performance, interconnected channel networks with multifunctional possibilities, inherent mechanical stability and the possibility of parallelisation for inexpensive mass production<sup>80</sup>.

Recently developed microfabrication technologies can now be applied to many disciplines, which have all contributed to the rapidly growing miniaturization of chemical processes. Miniaturisation techniques developed in the electronics industry has been implemented in chemical and biochemical engineering, so that sample preparation, purification, mixing, reactions, separations and fraction collection can all be performed on an integrated monolith. This miniaturisation, combined with the integration of multiple functionalities can enable the construction of structures that exceed the performance of traditional macroscopic systems, can provide a multitude of new functionalities and offer the potential of low-cost mass production<sup>81</sup>. The introduction of photolithographic techniques for the fabrication of chemical and biochemical microdevices has led to an exponential increase in the number of applications<sup>82</sup>.

Reactions performed in microreactors invariably generate pure products in a high yield and in shorter periods of time than the equivalent batch reactions providing sufficient quantities to perform full characterisation. One of the obvious applications is in combinatorial chemistry and drug discovery, where the generation of compounds with either different reagents or under variable conditions is an essential factor<sup>83,84</sup>.

In order to ensure the effective and efficient scale-up of a chemical reaction step, a fundamental understanding of a particular process needs to be acquired in the early stage of the process development (laboratory scale, feasibility study). Therefore, an integrated approach using measurement and evaluation of reaction kinetics, thermodynamics, transport phenomena and basic scale-up/scale-down principles

needs to be applied. The most important part of this strategy is to develop a fundamental understanding of reaction kinetics and thermodynamics in multiphase systems and to develop suitable experimental tools for kinetic data measurement and kinetic parameter evaluation. The elimination or minimisation of the effect of transport phenomena (mass and heat transfer) in multiphase systems is critical for high substrate conversion and selectivity to desired product. A thorough understanding of reaction thermodynamics is critical in terms of the influence on the reaction equilibrium in the case of reversible reactions.

It has been shown that micro-fluidic devices can be used as very effective tools to rapidly find optimised reaction conditions without using large quantities of (often expensive) starting materials<sup>85</sup>. Scale up by parallelisation of microreactor units used in the development process reduces the cost of redesign and pilot plant experiments, and hence, allows the scale up process to be rapid. The laminar flow profile in the reduced dimensions of microdevices enables accurate heat and mass transfer characterisation and control, in addition to straightforward extraction of kinetic parameters from the available data<sup>86</sup>.

In this investigation it was recognized that microtechnology could offer unique possibilities to run the pyrolysis process at low residence times in a highly compact device. The improved heat and mass transfer would also result in more even heating (less 'hotspots' which are a source of product decomposition) and hence higher product selectivity. The testing microreactors (a generous gift from The Institut für Mikrotechnik, IMM) applied in this investigation have a sandwich design with two micro-structured platelets being attached face to face. The platelets carry 14 channels each, which are 25mm long, 500µm wide and 400µm deep. The channels together with the inlet and outlet regions were prepared by wet chemical etching. Operations in the microdevice can be performed up to 800°C at a pressure of 10bar.

## **1.12 Equipment Considerations**

### **1.12.1 Introduction**

In the development of the pyrolysis process due consideration had to be given to the design and operation of the equipment. The development process covers the whole

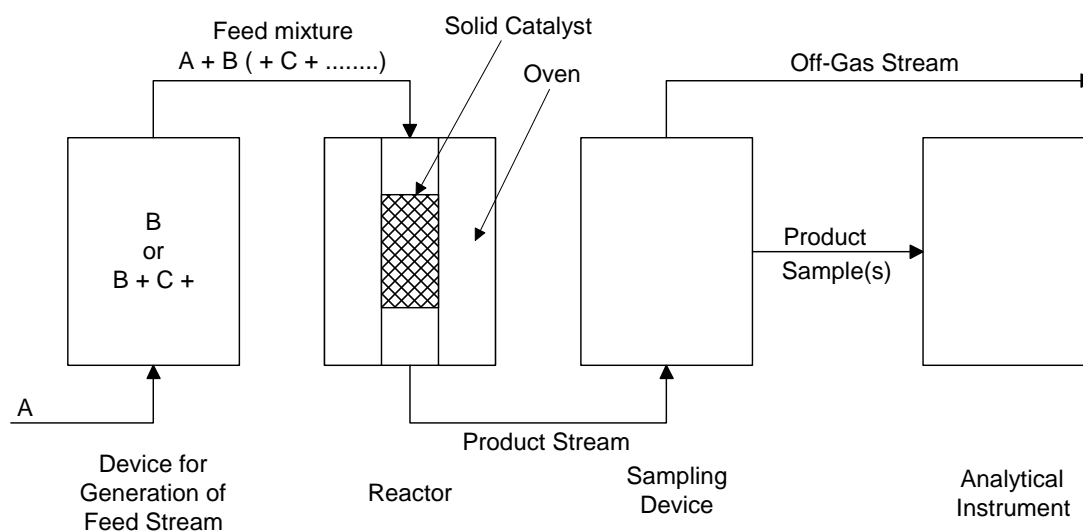
range from the new idea for a process or catalyst via the catalyst preparation, catalyst screening, establishing reaction networks, kinetic studies, and life tests to scale-up on pilot plant level. This demands an efficient and proper approach for laboratory scale experimentation. The objectives of the different development stages vary<sup>87</sup>:

- Screening must give the first data about the activity and selectivity of the various catalysts as a function of their composition and preparation history. As there are many variables, numerous catalysts should be screened at a high throughput rate. This yields the activity per unit of catalyst mass, active phase, or volume, depending on the specific goals. Often a first insight into the deactivation behaviour, i.e. the catalyst stability, is obtained simultaneously.
- Establishing the reaction network, using the wealth of techniques at the disposal of catalyst researchers, gives insight into how the catalyst works and provides the basis for the kinetic modelling studies.
- Time consuming kinetic studies are indispensable for the design, operation and process control. A description is needed for the catalytic rate as a function of the process variables, i.e. temperature, pressure, and composition of the reaction mixture.
- Lifetime studies are intended to test the catalysts during a longer time on stream, often on bench or pilot scale with real feeds and recycle streams. The latter allow investigation of the effect of trace impurities or accumulated components, not observed in laboratory-scale experiments.

### 1.12.2 Overall Equipment

To make sure that meaningful and reproducible results are obtained in laboratory-scale units, they must be properly designed and constructed, and parts which are prone to cause malfunctions should be avoided. The overall equipment used for catalytic studies is usually classified into (i) batch methods, (ii) semi-batch methods, (iii) transient methods (including the pulse reactor), and (iv) continuous flow methods. While all these methods have their specific advantages and disadvantages, continuously operated flow-type units are strongly preferred in practice<sup>88</sup>.

Such units are not only well suited for measuring the kinetics of the catalytic reaction, but they also enable the experimentalist to detect readily and quantitatively whether the catalyst preserves a constant activity, deactivates, or gets more active. A rough scheme for a continuously operated flow type unit for studying a gas phase reaction on a solid catalyst is depicted in **Figure 1.80**<sup>89</sup>.



**Figure 1.80: Fixed-bed reactor for studying gas phase reactions**

This is an example of a fixed-bed reactor which is most popular in heterogeneous catalysis, because they are easy to construct, relatively inexpensive, robust (since there are no moving parts) and a downscaled image of the most frequently employed reactor type in industrial catalysis. Ideally, the fixed-bed reactor behaves as a plug flow reactor (PFR) with no radial gradients of partial pressures or gas velocity and with a complete absence of axial mixing. In a PFR, the reactant and product partial pressures are thus only a function of the reactor length coordinate.

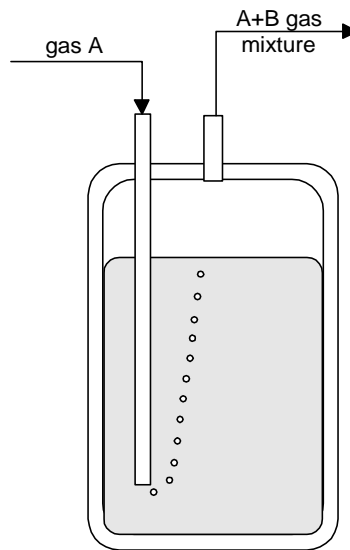
### 1.12.3 Generation of Feed Streams

The device for generating a gaseous feed stream consisting of vapours of one (B) or several components (B + C + ....) in a permanent gas A must meet a number of requirements<sup>90</sup>:

- The composition of the mixture must be strictly constant (stationarity requirement) during the whole experiment;

- The partial pressures of the higher molecular weight components in the gas mixture to be generated should be variable independent from each other, preferentially over a wide range; and
- The device should be reliable, durable (preferably without moving parts) and inexpensive.

The simplest and most frequently encountered case is that where the feed mixture consists of vapours of a single component B in the carrier gas A. The optimum device will then be a saturator which contains B in the liquid state (**Figure 1.81**).

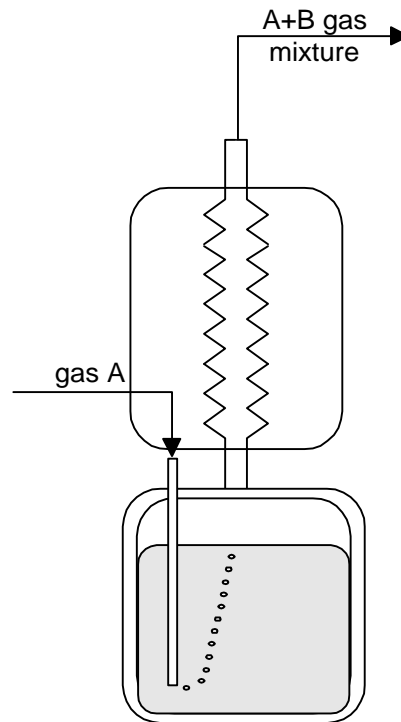


**Figure 1.81: Gas bubbling through liquid**

On its way through the saturator, the carrier gas A is loaded with vapours of B. Since its vapour pressure depends exponentially on the temperature, the saturator must be thoroughly thermostated. An externally thermostated water or oil bath circulating through a jacket around the saturator is often the best solution.

In practice, various saturator designs have been employed. If the carrier gas A is simply bubbled through the liquid B, as shown in **Figure 1.81**, it may happen that the gas/liquid mass and/or heat transfer are insufficient. On the way upwards, the gas bubbles will then be saturated incompletely with vapours of B, and the partial pressure of B in the gas mixture leaving the saturator will be ill-defined and irreproducible.

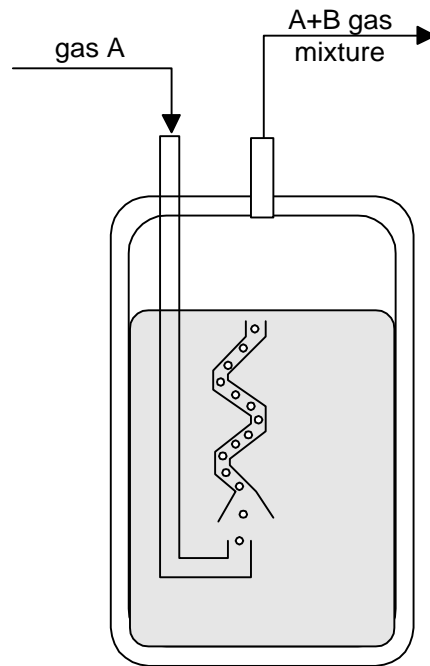
To avoid such problems, improved versions of saturators have been designed. In **Figure 1.82**, below, a too high saturator temperature  $T_1$  can deliberately be applied, whereupon a partial recondensation of B is enforced in a cooler held precisely at the appropriate saturation temperature  $T_2$ .



**Figure 1.82: Condensation after super-saturation**

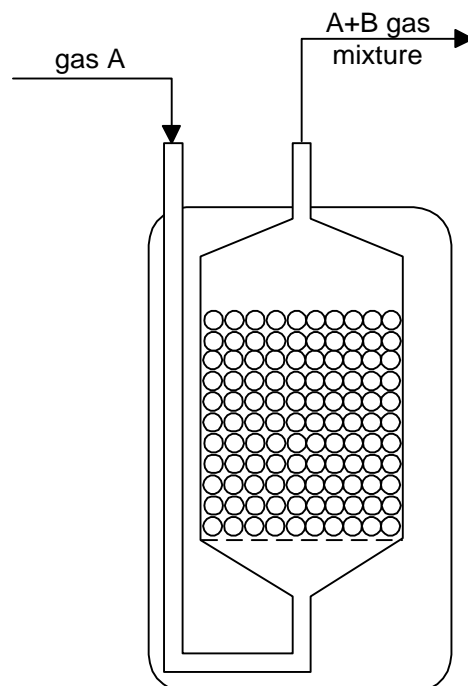
Another good method (**Figure 1.83**) is to prolong the way of the gas bubbles through the liquid and, hence, the contact time between both phases artificially. This can be achieved, for instance, by conducting the bubbles through a spiral-shaped chimney inside the saturator.





**Figure 1.83: Prolonged path of gas bubbles**

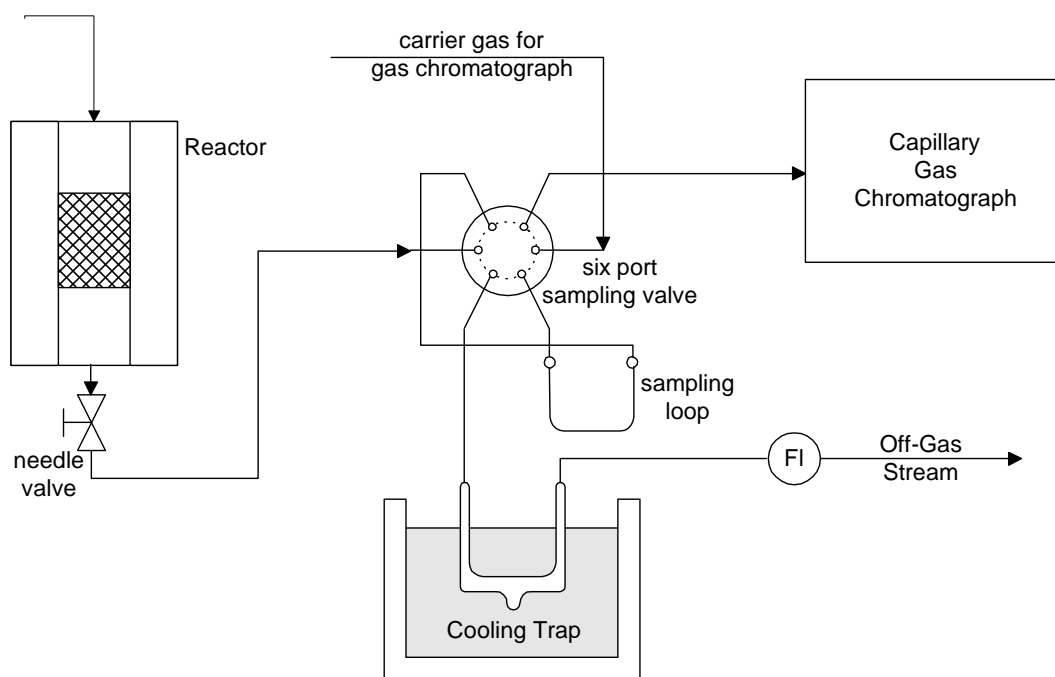
Perhaps the best technical solution (**Figure 1.84**) consists of adding to liquid B inside the saturator a chemically inert solid which may be porous e.g. glass beads. Normally, this brings about such a mass transfer enhancement that the vapour/liquid equilibrium is safely attained within a bed height of a few millimetres.



**Figure 1.84: Enhanced mass transfer through inert solid**

### 1.12.4 Product Condensation and Sampling

During the pyrolysis reaction, the reaction mixture may be exposed to temperatures in excess of  $500^{\circ}\text{C}$  and the reaction product has to be efficiently condensed and collected with minimal losses. Also, for reaction kinetic studies, the product may have to be collected while still in the vapour phase and analysed. In the vast majority of cases, the analytical instrument of choice will be a gas chromatograph equipped with a capillary column because such an instrument often allows a good separation of the products, and, if equipped with an appropriate detector, a reliable quantitative analysis of these products. The working principle of gas chromatography, however, is inherently discontinuous, requiring a fixed time for one analysis (between 10 minutes to an hour depending on the number of components and the desired resolution). To link the continuous flow-type reactor and the discontinuous analytical instrument, a kind of an interface is needed, viz. a multiport sampling valve<sup>90</sup>. An example of such a device is shown in **Fig 1.85**.

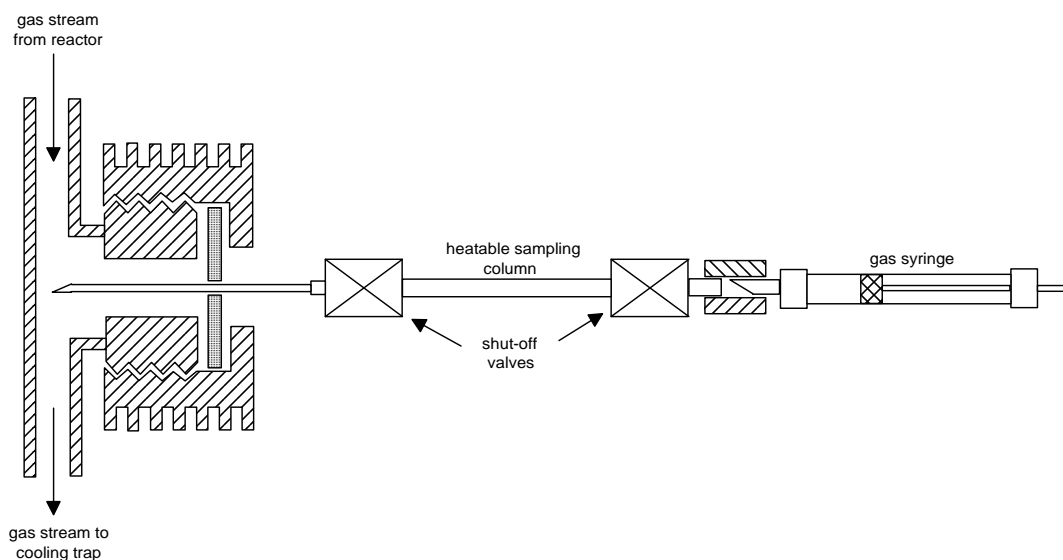


**Figure 1.85: Standard equipment for sampling gaseous products**

In its normal position, the multiport valve directs the reactor effluent through the sampling loop into the off-gas line, and upon actuating the valve, the content of the

loop is swept into the gas chromatograph. It is also recommended that an additional sample is collected in a cooling trap downstream of the six-port valve. This furnishes a time-averaged, integrated product sample which can be easily stored and analysed at a later date.

Various methods for instantaneous sampling have also been developed. In the simplest way, storable samples can be withdrawn from the product stream by gas syringes. It fails, in particular, if the samples contain higher molecular weight components which condense inside the syringe at ambient temperature. The gas syringe method has been significantly improved by placing a heatable sampling column between the syringe and the needle (**Figure 1.86**). The sampling column consists simply of a metal tube with a shut-off valve at each end.



**Figure 1.86: Instantaneous sampling with gas syringe**

## 1.13 Technology: Production of Terpene aroma chemicals

### 1.13.1 South African Market Analysis

South African international Flavour and Fragrance houses, the consumer goods companies, tobacco houses, and a number of traders active in importing flavour and fragrance chemicals were interviewed with respect to their purchases of terpene aroma chemicals. The import statistics for the previous two years were also obtained.

### 1.13.1.1 Import Statistics<sup>12</sup>

Import statistics for 2002 and 2003 were obtained as shown in **Table 1.11**. The trade statistics are however difficult to analyse. There is a loss of identity within a number of the categories, as the statistics are not disaggregated. For example, the category with the largest import value, \$ 2.2 million, includes terpene peroxides used in the rubber industry as well as the terpene esters used in the flavour and fragrance industry. Some general comments can however be made. South Africa imports in the region of \$1 – 1.1 million of synthetic pine oils, as well as \$0.8 – 0.9 million of the terpeneols. Another large terpene product import is camphor, \$0.3 – 0.5 million. The acyclic terpene alcohols i.e. linalool are imported at a value of roughly \$ 0.15 million.

**Table 1.11: South African Trade Statistics<sup>12</sup>**

Aroma Chemical	IMPORTS(US\$)		EXPORTS(US\$)	
	2002	2003	2002	2003
Pine Oil	1,146,754	1,093,242	15,545	62,537
Terpeneols	88,381	104,609	823	6
Camphor	331,860	594,516	26,821	27,418
Acyclic Terpene Alcohols	156,701	150,491	211	15
Gum, wood or sulphate turpentine	47,970	2,717	372,800	228,859
Ethers	240,537	20,868	34,344	30,498
Polycarboxylic acids, peroxides, anhydrides, halides and derivatives.	233,753	347,130		
Monocarboxylic acids, peroxides, anhydrides, halides and derivatives.	2,255,135	2,168,621		

### 1.13.1.2 Aroma Chemicals

Of the companies interviewed, only Symrise and Quest add value locally by blending and compounding. All the others import ready mixed compounds, the components of which they were reluctant to divulge. The two aroma chemicals used in the greatest volumes are menthol and anethole, which are used in toothpastes. Three Flavour and Fragrance houses, Firminech, Symrise and Quest, and a local Flavour House

Cranbrook Flavours, provided their usages of some of their individual terpene aroma chemicals purchased, however these are in trivial quantities (**Table 1.12**).

Symrise has a global buying strategy, although the local office sources the bulk of its aroma chemicals from its mother company in Germany. The company has a raw ingredient list of over 1,000 products, but the company is very small in South Africa and most ingredients are purchased only in kilogram or even gram volumes. Symrise will buy locally where appropriate.

Firmenich imports all of its raw materials from its parent company in France and only a limited amount of compounding is done locally. IFF supplies fragrances to the local market and markets about 350 tons of fragrance material in South Africa. These fragrances are all compounded in Europe and the blends are brought in as finished product. The parent company uses its global contacts to source worldwide at the best prices. Hence, even the local company can get favourable prices, even for very small volumes. IFF would purchase locally if the quality and price were acceptable.

Proctor & Gamble only imports finished products. Unilever now consists of three companies. The food division consists of Unilever, Best Foods, and Robertsons and is known as UBR. Lever Ponds, the personal care arm, makes laundry soap, personal products, deodorants and skincare products at the Durban factory and the Boksburg factory makes washing powder and liquid detergents. Levers is the chemical arm. Lever Ponds makes brands such as Omo, Sunlight, Domestos and Dove. All fragrances are imported as compounds which are mixed by the international flavour and fragrance houses. Unilever's Paris team purchases globally.

Quest International imports a number of terpene aroma chemicals. Some compounding is performed locally. These products are sourced from all over the world and the company is always looking for new supplies.

**Table 1.12: Terpene Aroma Chemical Usage in South Africa (kg)**

<b>Aroma Chemical</b>	<b>Firmenich</b>	<b>Cranbrook Flavours</b>	<b>Quest</b>	<b>Symrise Last 9 months</b>
Alpha -Terpineol			120	
Alpha Terpinene				97 grams
Anethole		15	600	3
Beta Pinene				1.4
Citral		20	600	
Citronellol	3	6	80	11
Geraniol	10 grams	5	200	4.5
Geranyl Butyrate				165 grams
Linalool		2	200	1,600
Linalyl Acetate	24 grams			
Nerol			20	
Methyl Ionone	5		10	
Menthol	1,500		1,200	7,827
Myrcene			6	5

### 1.13.1.3 Pine Oils and Terpeneols

Users of pine oils and terpeneols were also interviewed. Eniline Pharmaceuticals is a contract packer for Reckitt & Benckiser. Approximately 20 tons per month of pine oil is imported from IFF, Jacksonville USA, at a cost of about R 8/kg. Hence the total purchase of pine oil is around R 1.9 million per annum. The pine oil is used in Dettol a medicinal product, which is registered with the Medicine's Control Council and therefore has very strict quality specifications. Johnson & Johnson buys a blend of pine oils through IFF for use in the production of Savlon. IFF formulates according to Johnson and Johnson's in-house specification (which is confidential). Consumption is around 20 tons per annum. Adcock uses about 23 tons of pine oil per annum. The pine oil is also pharmaceutical grade and is all imported through an agent. The price is confidential but was reported to be much more than R 8/kg. It is therefore likely to be a higher-grade terpeneol product.

Sara Lee is an international company, which produces household cleaning products. The company uses a fatty acid derivative of pine oil imported from New Zealand. No other aroma chemicals are used but some formulated fragrances are bought from the

local fragrance houses. The parent company does any creative compounding required for Sara Lee and supplies the formulations directly.

#### **1.13.1.4 Camphor Market**

Camphor is used in South Africa in snuff products as well as in hand creams. Dingler Tobacco Products uses approximately 24 tons per annum of camphor in its snuff, which goes by the brand name of Taxi. The camphor is imported from China and sold by Crest Chemicals. Van Erkom's Tobacco in Potgietersrus produces the Singletons brand of snuff, but has not used any camphor in this product for two years. Adcock Ingram use in the region of 10 – 20 tons per annum of a pharmaceutical grade product.

#### **1.13.2 Conclusion**

The South African market for terpene aroma chemicals is extremely small. Due to the limited local market, there is unlikely to be substantial import substitution from a South African Terpene Aroma Chemicals business. Any business created will therefore have to export the majority of its products. Thus, in order to create an aroma chemicals business based on such limited quantities of feedstock, the production facility must be configured in order to optimise the number of products that can be produced for the minimal capital investment. At the same time, the production of synthetic pine oil or any aroma chemicals with a local demand should be maximised whilst not compromising the plant's overall profitability. This approach will maximise the investment return.

### **1.14 Feasibility of the Production of Terpene Aroma Chemicals<sup>14,16,91</sup>**

#### **1.14.1 Affordable Capital**

An evaluation model to assess the viability of the production of terpene aroma chemicals from the quantity of crude sulphated turpentine available in South Africa has been created. The model makes some assumptions regarding yields and recovery, but in so far as is possible takes into account known processes.

The basic objective of this model is to determine the affordable capital for the business. Comparison with an order of magnitude capital estimate will give an

indication as to the viability of the project. At this stage of technology definition, it is not possible to give any more than an order of magnitude estimate of the capital required.

The products selected for inclusion in the analysis have been based upon the results of the screening exercise above. This selection also takes into account those products for which some technical work has been performed in South Africa, for which a local market exists, and those with the potential for the highest value addition. The selection of the products also considers the possibility of creating a basket of products whilst at the same time attempting to minimise the amount of process steps needed, thereby reducing capital expenditure.

Based on this value chain two business cases can be identified:

1. Export Market

The production of linalool being maximised. Geraniol/nerol sells for the same price after one additional process step. Linalool also has a much higher selling price/kg than the pine oil and terpineol value chain.

2. Local Market

Production of pine oil, terpineol and terpineol acetate sufficient to satisfy the local market according to import statistics. Remaining crude sulphated turpentine is converted into linalool.

Both of these business cases have a number of sub-cases depending on the amount of crude sulphated turpentine available as feedstock. The sustainable level of crude sulphated turpentine has been determined to be 180 – 420 tons per annum.

Clearly, the business will not survive if dependent on the local market only, particularly if the feedstock availability drops to only 180 tons. A terpene aroma chemical business based on the amount of crude sulphated turpentine available in South Africa, must export as much linalool or other higher value added products as possible. The amount of linalool theoretically possible is in the range of only 46 - 153 tons.



### 1.14.2 Single Year Costing Model

The affordable capital can be determined based on a single year costing analysis. The single year costing essentially uses a year's trading accounts for the business that will result from the proposed investment, once it is at full output. The evaluation is done in constant money, with prices and costs on a consistent basis. Trading cash flow must fund sustenance capital expenditure and working capital increases, pay tax, reward the capital and working capital invested in the business. For a given set of assumptions about the fiscal environment, product construction duration, production phase up and project life, there is a fixed relationship between required reward, as a percentage of capital cost (including working capital) and the project IRR.

The single year costing method can therefore be used to estimate quickly the expected IRR if an estimate of capital is available, or conversely to estimate the affordable capital cost given a target IRR. A 20% return on investment was used in this determination, relating to a conservative real IRR in the order of 8%.

The results of this analysis are depicted below for the business case where exports of higher value added product such as linalool is maximised. Contribution margins of 35 – 45% were assumed. Insufficient process chemistry is available for a more accurate determination of the actual gross margins for the business (**Table 1.13**).

**Table 1.13: Affordable Capital for the Terpene Aroma Facility (Rands Millions)**

Gross Margin	Feedstock Availability (Tons)	
	420	180
35%	7.5	3.2
45%	9.7	4.2

The affordable capital is thus in the range of R 3.2 – 9.7 million. This capital assumes that the turnover of the business is maximised. Hence, as much of the higher-value products such as linalool, geraniol, citral etc. must be produced. The plant will

however be capable of producing other products for which a local market exists, such as pine oil, terpineol, terpeniol acetate, although coupled with a loss in value.

### 1.14.3 Capital Cost

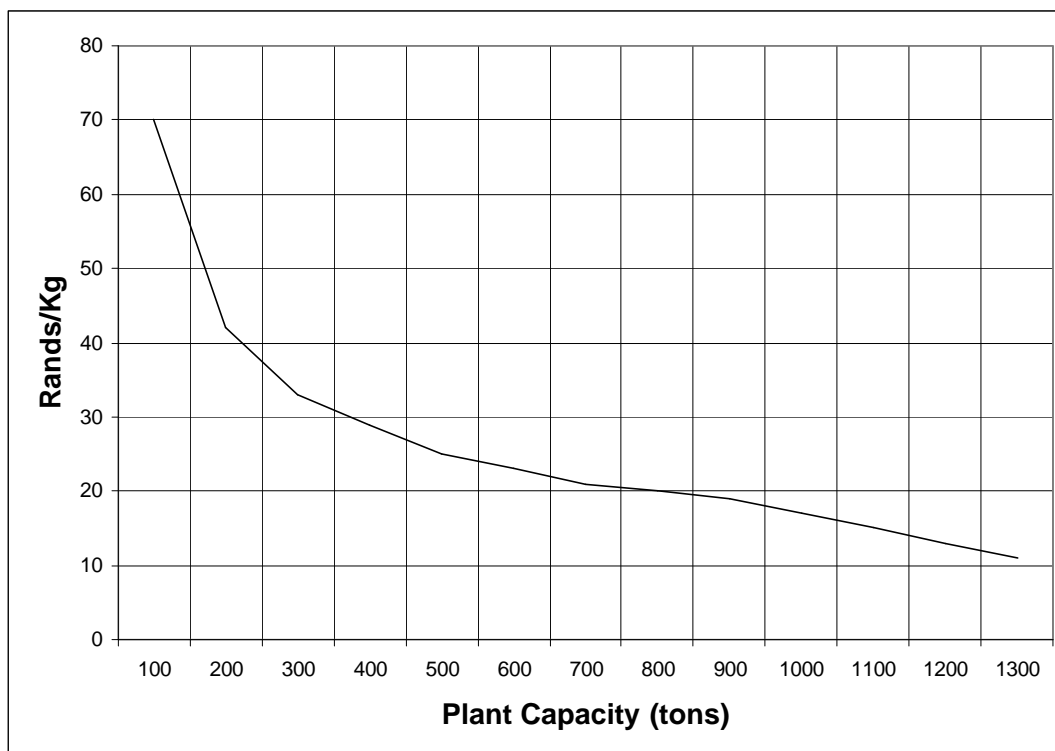
The capital costs estimate for a 420 tpa crude sulphated turpentine plant was performed. At this stage of technology definition, it is not possible to give any more than an order of magnitude estimate of the capital required. It should be emphasised that this estimate is based on the level of information available. There is very little technical data to define and size process equipment properly. The capital cost estimate is hence an order of magnitude costing. A more accurate costing would depend on more detailed process chemistry information being available. The capital estimate has therefore been based on the consultant's interpretation of the chemistry outlined in the literature and patents.

The estimate nevertheless provides a ballpark Inner Battery Limits plus Outer Battery Limits cost. No infrastructure has been costed. The capital estimates were based on the cost of the individual main plant items, to which an installation factor was applied in order to arrive at a total installed cost. Engineering and contingency costs were allowed for. Based on discussions with the CSIR, the capital estimate allows for only one oxidation reactor, such the CSIR's SAFOX™ reactor, and one Continuous Stirred Tank Reactor with reactor stills. It has been assumed that there is no requirement for crystallisation type process equipment. Based on the assumptions outlined above, the capital estimate is therefore in the order of R 11.57 million for a 420 ton plant. A summary of the capital estimate is provided below in **Table 1.14**.

**Table 1.14: Capital Estimate for 420 ton Crude Sulphated Turpentine plant**

<b>R Millions</b>	<b>420 Tons</b>
Reactors	3.46
Distillation	1.17
Heat Exchangers	0.25
Miscellaneous (pumps, filters, tanks, air compressors, etc)	2.11
<b>TOTAL EQUIPMENT</b>	<b>6.99</b>
Ancillary	1.40
Contingency	0.87
<b>TOTAL ERECTED PLANT</b>	<b>9.26</b>
Engineering	2.31
<b>TOTAL INSTALLED PLANT</b>	<b>11.57</b>
Affordable Capital (Table 16)	7.5 – 9.7

**Figure 1.87** shows the economy of scale for the terpene aroma chemical plant. The economy of scale of a production plant indicates how the capital investment per unit of production relates to the plant capacity and shows at what capacity the effectiveness of capital invested would reach a minimum. The chart shows that the capital cost per unit capacity plateaus to round about R 20/kg pAA at about 800 tpa. No substantial further capital cost benefit will be derived for a plant exceeding this capacity. Conversely, any plant built that has a smaller capacity will not benefit from the economy of scale and might not yield investment economics.



**Figure 1.87: Economy of Scale – Terpene Aroma Chemical Plant**

#### 1.14.4 Conclusion

At 420 ton per annum, the affordable capital of R 7.5 – 9.7 million must be compared to the estimate of R 11.6 million. However, there is no guarantee that the annual supply of crude sulphated turpentine at this level is sustainable. If the quantity of feedstock in South Africa is not maintained at the 420 tons per annum level, a business will not be able to afford the capital investment required. Given the fact that the feedstock supply at this point in time can only be guaranteed at the 180 tpa level, the risk in making this investment is considered too high.

However, should Sappi decide to keep both digesters committed to softwood, a minimum amount of 360 tons crude sulphated turpentine feedstock would be guaranteed annually. An investment in a plant to process 420 tpa crude sulphated turpentine then becomes potentially viable. However, more detailed process chemistry, requiring some technical development work will be required in order to

generate a more accurate techno-economic model upon which an investment decision can be made.

### 1.15 Research Hypothesis

How to design and construct a robust and reliable reactor system for the pyrolysis of *cis*-2-pinanol which would result in the economical production of linalool at reasonable conversion (20-30%) and high selectivity (~90%).

### 1.16 Specific Research Objectives

The main objective of this investigation was to develop a process for the selective isomerisation of *cis*-2-pinanol to linalool with minimum by-product formation and using process equipment that could be scaled to full-scale production. Since *cis*-2-pinanol could not be purchased in sufficient quantities for process development, a process had to be developed for the bench-scale preparation of kilogram quantities of *cis*-2-pinanol from  $\alpha$ -pinene obtained from the client. This process formed a minor part of this investigation.

Specific objectives related to the pinanol pyrolysis reaction were as follows:

- Designing and construction of a pyrolysis reactor system with peripherals which permitted the precise and accurate control of the reaction parameters;
- Benchmarking of a base case reaction and using this as a point of reference for further improvements to the process;
- Evaluation of various vaporizer designs;
- Evaluation of various condensation systems;
- Screening of various variables, factors, and materials to determine the effect on conversion and selectivity, e.g. inert packing, bases (ammonia, pyridine), materials of construction, zeolites;
- Determination of the most important variables required for optimum reaction performance;
- Preparation of a 1kg market sample of linalool with a specification of not less than 80% and to check the robustness of the system;
- Use of a microreactor as alternative to the tubular reactor and the effect on conversion and selectivity;

- Reaction kinetics of the tubular reactor system versus the microreactor and computational fluid dynamics (CFD) and mathematical modelling of both systems;
- Preliminary mass balances and process flow diagrams (PFDs); and
- Conceptual design of a full scale facility for the production of linalool.

## CHAPTER 2

### Experimental

#### 2.1 Materials

##### 2.1.1 Reagents for synthesis

All materials used for syntheses, the source(s) of procurement and the respective grade, are listed in **Table 2.1** and were used as received unless otherwise noted.

**Table 2.1: Reagents for synthesis**

Name	MW g/mol	CAS Number	Supplier	Purity
$\alpha$ -Pinene	136.24	[80-56-8]	Teubes Pty.Ltd	98%
Ni-55Ts	58.71	[7440-02-0]	Hoechst	60%
Carbon tetrachloride	153.8	[56-23-5]	Aldrich	99.5%
<i>cis</i> -Pinane	138.02	[6876-13-7]	Prepared	97.5%
Benzoyl peroxide	242.2	[94-36-0]	Aldrich	97%
Sodium hydroxide	40.02	[1310-73-2]	Aldrich	99%
Oxygen	32.00	[7782-44-7]	Air Products	99.9%
<i>cis</i> -Pinanol	154.06	[4948-29-2]	Prepared	88.9%
Nitrogen	28.01	[7727-37-9]	Air	99.9%

			Products	
Pyridine	79.10	[110-86-1]	Aldrich	99.8%
Methanol	32.04	[67-56-1]	Aldrich	99.8%
Ethanol	46.07	[64-17-5]	Aldrich	99.9%
Hexane	86.18	[110-54-3]	Aldrich	99%
Chloroform	119.38	[67-66-3]	Aldrich	99.9%
n-Propanol	60.01	[71-23-8]	Aldrich	99.5%
n-Butanol	74.12	[71-36-3]	Aldrich	99.8%
Mordenite	-	-	Sud-Chemie	99%
Faujasite	-	-	Sud-Chemie	99%
Beta Zeolite	-	-	Sud-Chemie	99%

### 2.1.2 Reagents for analysis

The reagents used as standard materials for gas chromatography are listed in **Table 2.2**.

**Table 2.2: Reagents for analysis**

Name	MW g/mol	CAS Number	Supplier	Purity
$\alpha$ -Pinene	136.24	[80-56-8]	Aldrich	98%
<i>cis</i> -Pinane	138.02	[6876-13-7]	Aldrich	99%
<i>cis</i> -Pinanol	154.06	[4948-29-2]	Prepared	95.8%
Linalool	154.06	[78-70-6]	Aldrich	97%



## 2.2 Equipment

The equipment used in the experimental study is listed in **Table 2.3**.

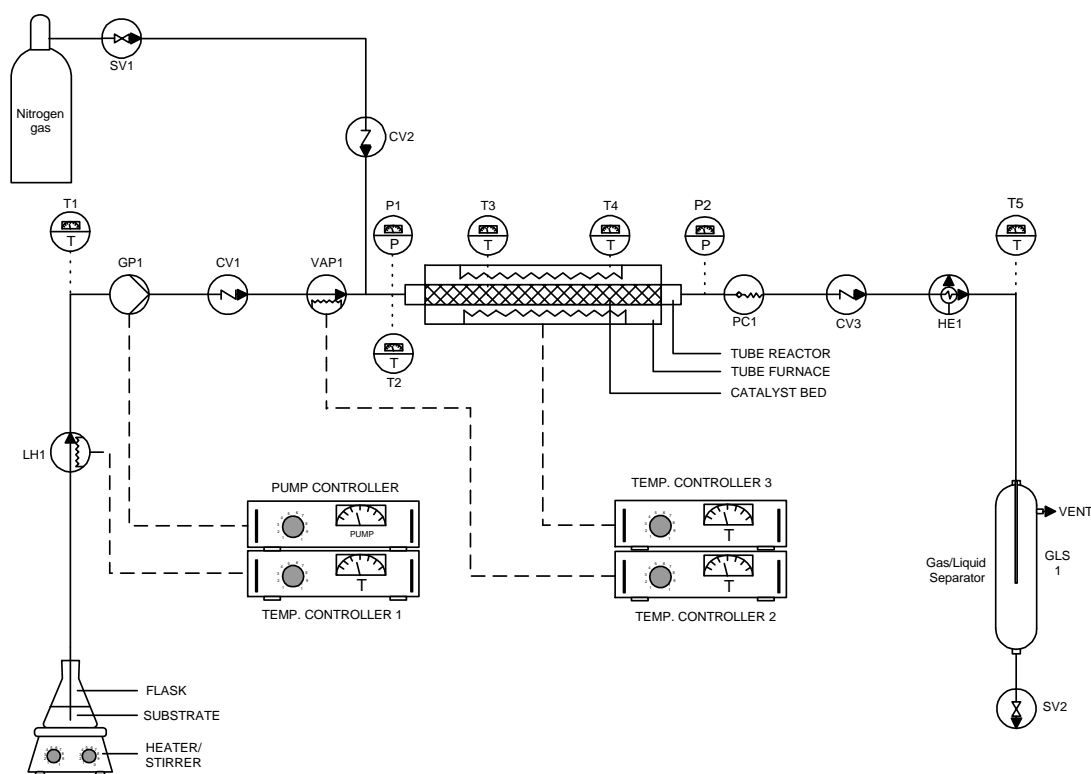
**Table 2.3: Equipment used for experimental study**

Name	Supplier
HPLC pump	Waters
Box Furnace (max. 1000°C)	Thermacraft
Temperature controller 1	Autoclave Engineers
Temperature controller 2 (Rex – c100)	RKC
Temperature controller 3 (uTC-52)	TCL
Chiller Unit (RTE-140)	Neslab
Microreactor (max. 800°C)	IMM
Counter-current micro heat exchanger	IMM

## 2.3 Design of pinanol pyrolysis rig

In the development of the pyrolysis process due consideration had to be given to the design and operation of the equipment. The pyrolysis rig would have to be used for all screening experiments, catalyst testing, reaction kinetics and for the preparation of a 1 kg market sample. The system was also required to be flexible enough to be able to accommodate different types of reactors and configurations. This demanded an efficient and proper approach for laboratory scale experimentation.

A schematic diagram of the pyrolysis rig is shown in **Figure 2.1**. The system in the diagram is a generalised version illustrating the essential components required for efficient vaporization of the starting material, reaction in the gaseous phase and condensation of the pyrolysis products. The system can be adapted to accommodate variations around each of these elements.



**Figure 2.1: Schematic diagram of pinanol pyrolysis rig**

The heart of the rig is the electrically heated reactor system. This consists of a split-box heating system with heating elements in each of the two halves. The heating elements are embedded in a high temperature, non-conductive insulating material. The effective heating area of the element is 150 mm long and 30 mm wide. The elements are capable of rapid heating and have a maximum temperature rating of 1000°C. The heating box can accommodate tubular stainless steel reactors of various sizes as well as microreactors. Thermocouples are situated close to the heating elements as well as next to the reactor wall for accurate temperature control and determination.

The supply of a consistent gaseous feed is critical for reproducible experimental results. This is achieved by the vaporizer, VAP1. The vaporizer has to meet three requirements for effective operation:

- The composition of the mixture must be strictly constant (stationarity requirement) during the whole experiment;

- The partial pressures of the components in the gas mixture to be generated should be variable independently from each other over a wide range; and
- The device should be reliable, durable (preferably without moving parts) and inexpensive.

A number of vaporizer designs were tried before settling on the current one (more details on vaporizer selection are given in § 2.4.1 (**Various vaporizer designs**)). This consists of a vertical brass tube (10 cm long x 2 cm internal diameter) which is filled with glass beads two-thirds of its length. The tube is electrically heated by a coiled element throughout its length. The inert gas is supplied from the bottom of the tube and the starting material is fed in from the top. There is a T-piece outlet to the reactor tube just below the liquid feed and above the glass beads. The liquid starting material is dripped onto the heated glass beads where it is vaporized. At the same time the hot inert gas coming through the beads mixes with the vapour and acts as a carrier gas to the tube reactor. The inert glass beads improve the mass transfer of vapour and inert gas and thus help to provide a consistent feed.

The hot, post-reaction vapours are condensed by the heat exchanger, HE1. The reaction is normally carried out at 500 to 600°C and the resultant vapours have to be efficiently condensed to avoid significant losses of the reaction mixture. The heat exchanger consists of coiled 3 mm internal diameter tubing enclosed in a thermally insulated flask through which is circulated cooling fluid (-10 °C). A Julabo cooling bath was used to circulate the cooling water through the heat exchanger.

The condensed reaction mixture is separated from the inert gas in the gas-liquid separator, GLS1. This consists of a stainless steel tube with a vent (for inert gas or vacuum fitting) and a sampling valve SV2. The liquid settles in the bottom of the tube and gases exit through the vent.

The inert gas supply was controlled by the use of a needle valve, SV1 and a one-way valve CV2. An in-line pressure regulator was installed (not shown in diagram) to provide gas at a constant pressure.

The substrate was delivered to the system via a positive displacement Waters HPLC pump capable of pulsation-free operation at low fluxes, GP1. Several pumps were tried before selecting this pump for the laboratory screening investigations. The line (LH1) to the pump was heated, since pinanol (mp. 60-65 °C) is a solid at room temperature and had to be melted before being used neat. However, if a solvent was used this was not necessary.

All tubing used in the system was stainless steel unless specified otherwise. Tubing from the pump to the vaporizer was 1 mm internal diameter whereas the rest of the tubing was 2 mm internal diameter. One-way valves and pressure control valves were also installed to prevent back-flow and to have precise control over process parameters. Thermocouples and pressure gauges were installed in strategic places to monitor conditions as well as for diagnostic purposes. Set temperatures were precisely controlled by digital temperature controllers supplied by Autoclave Engineers.

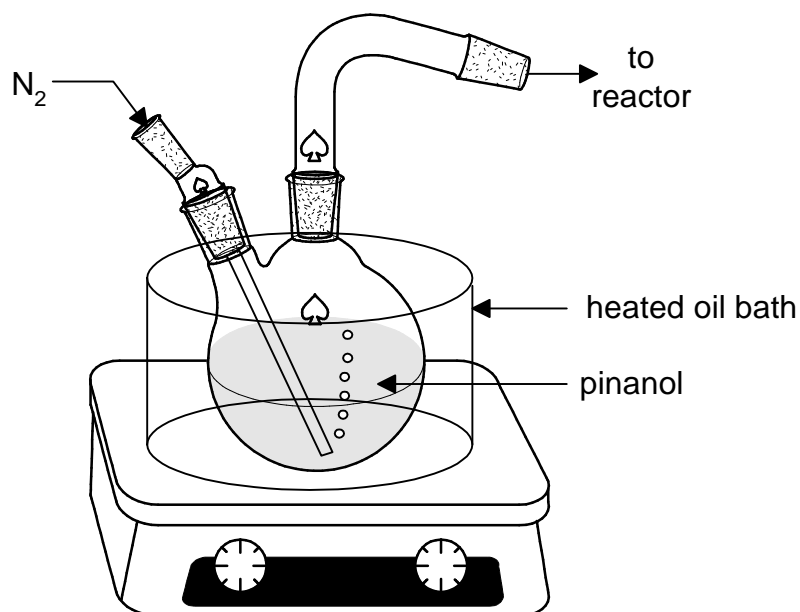
## 2.4 Procedures involving equipment evaluation

### 2.4.1 Various designs of vaporizer systems

As indicated earlier, the role of the vaporizer is very important if reproducible experimental results are to be obtained. *cis*-2-Pinanol has a boiling point of 220 °C and it is essential that it is efficiently vaporized to provide a consistent gaseous mixture to the pyrolysis reactor. As discussed in § 1.10.3 (**Generation of feed streams**) there are various designs of vaporizer systems. In this investigation, five types of vaporizer design were investigated:

1. **Vaporizer 1:** Nitrogen sparging through boiling liquid in round-bottomed-flask (**Figure 2.2**).

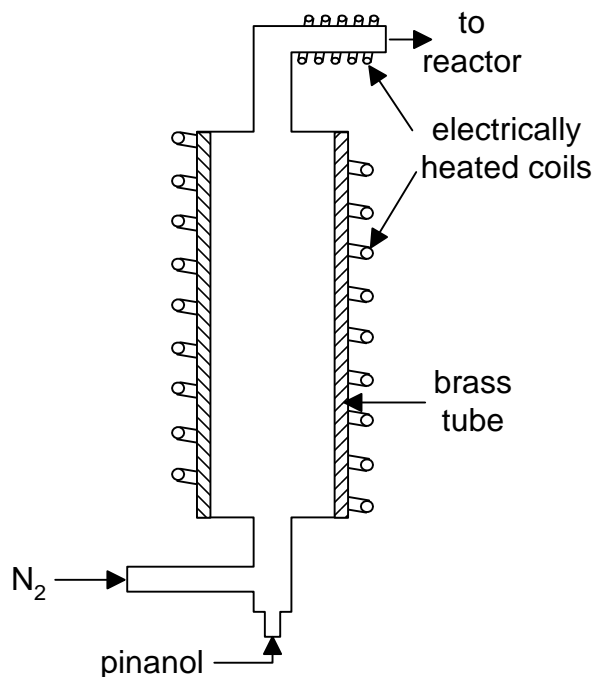
In this system, which was used in a previous investigation, nitrogen gas was sparged through the boiling pinanol liquid in a round-bottomed-flask and heated by an oil bath. The saturated vapour phase was then routed towards the pyrolysis reactor.



**Figure 2.2: Nitrogen sparging through boiling pinacol**

2. **Vaporizer 2:** Heated tube with pinacol and gas feeds from bottom (**Figure 2.3**).

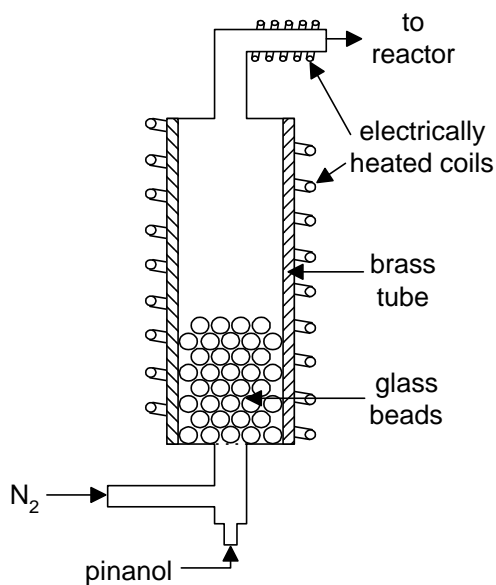
In this vaporizer design, pinacol is pumped into the bottom of an electrically heated brass tube. Nitrogen is also piped into the tube but from below the pinacol feed. The outlet from the vaporizer is also electrically heated before entry into the reactor to ensure that no condensation occurs and the feed is still in a gaseous phase.



**Figure 2.3: Cross-section of bottom fed vaporizer**

3. **Vaporizer 3:** Heated tube with pinanol and gas feeds from bottom with glass beads (**Figure 2.4**).

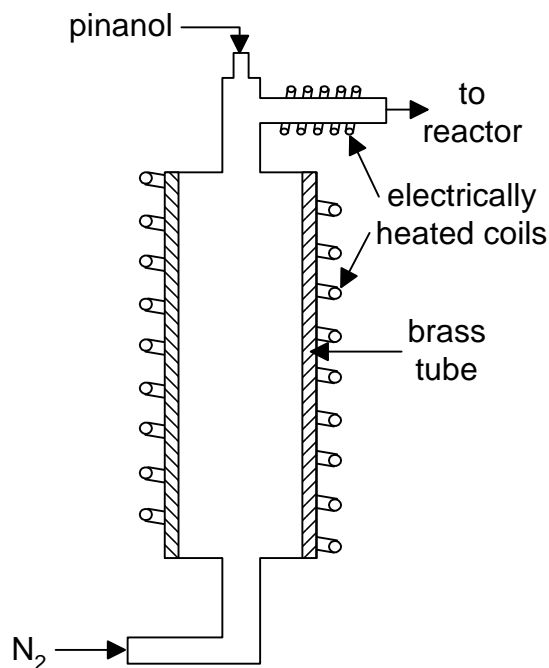
This vaporizer design is a variation on the one described above since glass beads are placed at the bottom of the heated brass tube to aid in dispersion of the vapours.



**Figure 2.4: Cross-section of bottom-fed vaporizer with glass beads**

4. **Vaporizer 4:** Heated tube with counter-current pinanol/nitrogen flow (**Figure 2.5**).

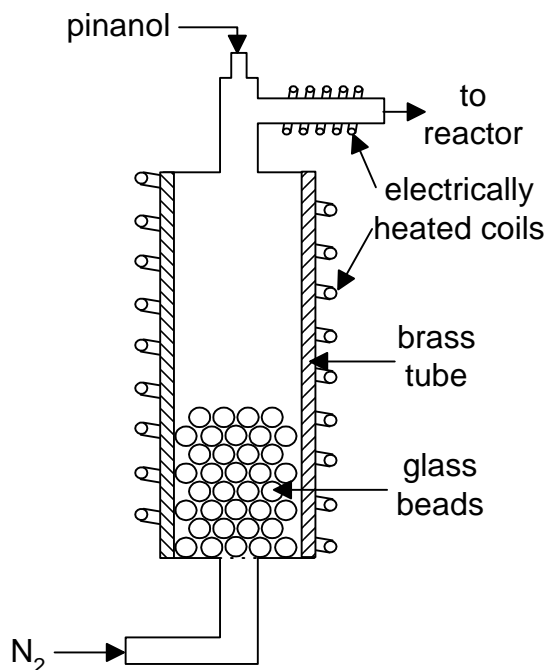
In this vaporizer design both the pinanol and nitrogen were fed into the heated brass tube in a counter-current configuration. The pinanol was pumped into the top of the brass tube while nitrogen was fed in from the bottom. The outlet tube to the reactor was also electrically heated.



**Figure 2.5: Cross-section of counter-current vaporizer**

5. **Vaporizer 5:** Heated tube with counter-current pinanol/nitrogen flow with glass beads (**Figure 2.6**).

This vaporizer design is a variation on the one described above since glass beads are placed at the bottom of the heated brass tube to aid in dispersion of the vapours.



**Figure 2.6: Cross-section of counter-current vaporizer with glass beads**

#### 2.4.1.1 Experimental procedure for evaluation of vaporizers

The equipment used for this evaluation was very similar to that described in § 2.3, except that the vaporizers were changed. The reactions were carried out in a tubular reactor and the experimental conditions are shown in **Table 2.4**.

**Table 2.4: Experimental conditions used for vaporizer evaluation**

<b>Reactor configuration</b>	Stainless steel, tubular, 4.6mm ID, 150 mm long, heated length 50 mm, wall thickness 1 mm
<b>Vaporizer heater temperature</b>	250 °C
<b>Post vaporizer temperature heater</b>	250 °C
<b>Reactor temperature</b>	550 °C
<b>Condenser</b>	PTFE coil (1m) in chilled bath at -10 °C
<b>Feed</b>	10% m/m pinacol in n-butanol



<b>Feed rate</b>	0.5 ml/min
<b>Inert gas</b>	nitrogen
<b>Inert gas flow rate</b>	10 ml/min.

In these experiments, a 10% m/m solution of *cis*-2-pinanol was prepared by dissolving pinanol (2g, 0.0130 moles, 90% purity) in n-butanol (18g). The solution was transferred to a specially modified HPLC pump containing a 20ml calibrated syringe. The nitrogen flow was turned on and the flow rate calibrated using a bubble flowmeter. The heaters of the pyrolysis rig were all set to the specified temperatures and the lines of the system were purged with 5 ml of the feed material. The reaction was initiated by starting the HPLC pump at the specified flow rate of 0.5 ml/min. Samples of 1 ml were collected and prepared for analysis by GC. Pinanol and linalool in the sample were quantified as % m/m by using calibration curves as discussed in § 2.6 (Analytical procedures). The conversions and selectivities were calculated based on these results.

The results were statistically analysed with Design Expert using a one factor statistical design to determine if there were significant differences between the various vaporizer designs. The design summary is shown in **Table 2.5**.

**Table 2.5: Design summary: Various vaporizer designs**

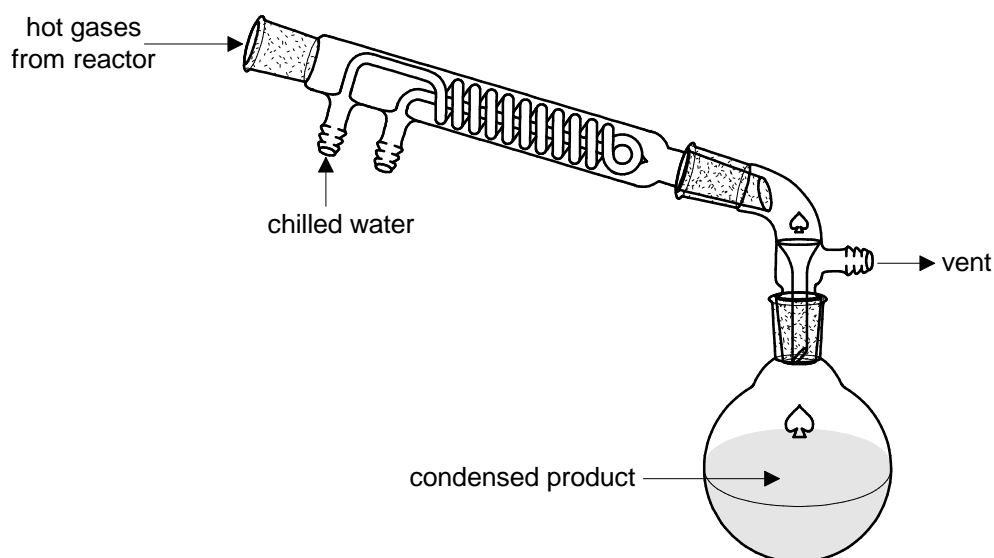
<b>Study Type</b>	Factorial		<b>Experiments 50</b>			
<b>Initial Design</b>	Full Factorial					
<b>Center Points</b>	0					
<b>Design Model</b>	Main effects					
<b>Response</b>	<b>Name</b>	<b>Units</b>	<b>Obs</b>	<b>Minimum</b>	<b>Maximum</b>	
Y1	Conversion	%	50	15.80	38.40	
Y2	Selectivity	%	50	50.20	74.70	
<b>Factor</b>	<b>Name</b>	<b>Units</b>	<b>Type</b>	<b>Low Actual</b>	<b>High Actual</b>	<b>Levels</b>
A	Vaporizer	Type	Categorical	Level 1 of A	Level 5 of A	5

### 2.4.2 Various designs of condenser systems

The condensation system is a vital part of the pyrolysis rig and has to be efficient to ensure that the results produced are reliable and reproducible. The pyrolysis reaction is carried out at a relatively high temperature (400-700 °C for screening experiments) and the hot gaseous product has to be condensed without substantial loss of material especially if solvents are used as diluents. In this investigation five types of condenser systems were considered:

1. Glass condenser system (**Figure 2.7**).

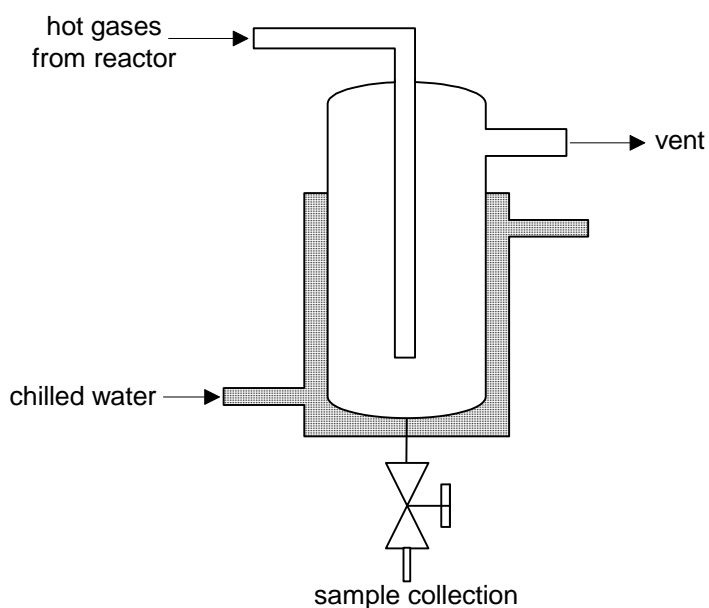
In this system the hot emission of gases from the reactor are passed through a glass condenser containing a coiled tube through which chilled water is passed. The vapours are condensed and collected in a round-bottomed-flask.



**Figure 2.7: Glass condenser system**

2. Gas cooling trap system (**Figure 2.8**).

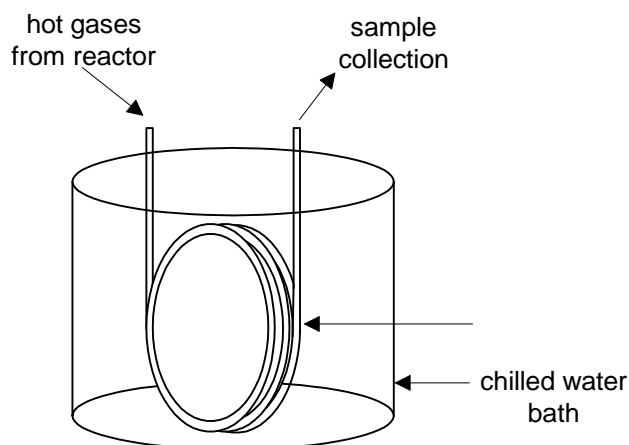
In this system the hot gaseous mixture is blown onto the cold surface of a jacketed glass bulb through which is passed chilled water at -10 °C. The condensed liquid is allowed to be kept in the vessel until ready for collection through an integrated sampling valve.



**Figure 2.8: Gas cooling trap system**

3. Coiled PTFE tubing/chilled bath system (**Figure 2.9**).

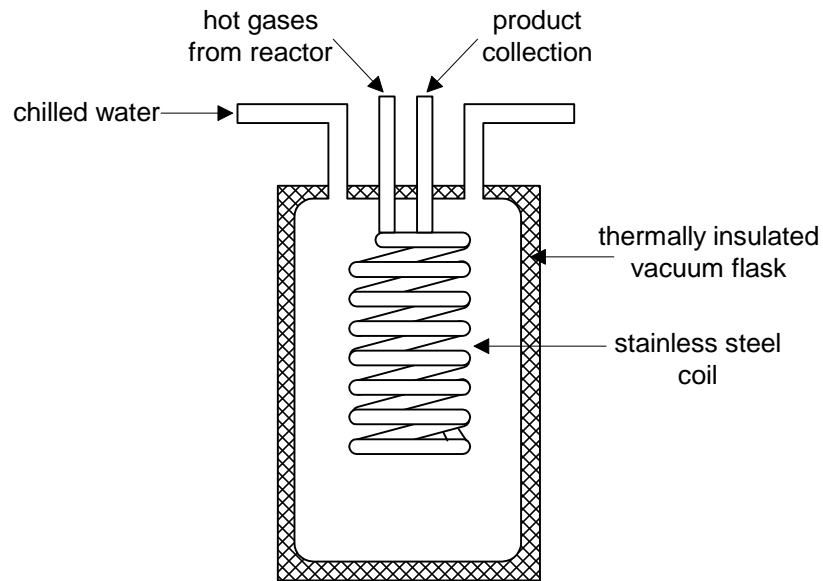
In this system the hot gaseous mixture is passed through coiled PTFE tubing which is situated in a chilled bath at  $-10^{\circ}\text{C}$ .



**Figure 2.9: Coiled PTFE tubing/chilled bath system**

4. Coiled tube/vacuum flask system (**Figure 2.10**).

In this system a stainless steel coiled tube has been integrated into a sealed thermally insulated vacuum flask system through which is circulated chilled water at  $-10^{\circ}\text{C}$ .



**Figure 2.10: Coiled tube/vacuum flask system**

5. Counter-flow Micro Heat Exchanger (COMH) (**Figure 2.11**)

This device comprises a stack of several micro structured plates (10 + 10 pieces) that are arranged for a counter-current flow pattern. Each plate consists of 34 parallel micro channels of 300 $\mu\text{m}$  width and 200 $\mu\text{m}$  depth. The plate stack is encompassed by two ceramic Macor plates, for thermal insulation against the environment, and two steel end caps. The specific heat transfer area was 18 000  $\text{m}^2/\text{m}^3$  and heat transfer coefficient of 2 300  $\text{W}/\text{m}^2\text{K}$ .



**Figure 2.11: Counter-flow Micro Heat Exchanger (COMH)**

#### 2.4.2.1 Experimental procedure for evaluation of condensation systems

The equipment used for this evaluation was very similar to that described in § 2.3, except that the condenser systems were changed. The reactions were carried out in a tubular reactor and the experimental conditions are shown in **Table 2.6**.

**Table 2.6: Experimental conditions used for condenser evaluation**

<b>Reactor configuration</b>	Stainless steel, tubular, 4.6mm ID, 150 mm long, heated length 50 mm, wall thickness 1 mm
<b>Vaporizer heater temperature</b>	250 °C
<b>Post vaporizer temperature heater</b>	250 °C
<b>Reactor temperature</b>	550 °C
<b>Condenser systems</b>	Various at -10 °C
<b>Feed</b>	10% m/m pinanol in n-butanol
<b>Feed rate</b>	0.5 ml/min
<b>Inert gas</b>	nitrogen
<b>Inert gas flow rate</b>	10 ml/min.

In these experiments, a 10% m/m solution of *cis*-2-pinanol was prepared by dissolving pinanol (2g, 0.0130 moles, 90% purity) in n-butanol (18g). The solution was transferred to a specially modified HPLC pump containing a 20ml calibrated syringe. The syringe was topped up with pinanol solutions after each run. The nitrogen flow was turned on and the flow rate calibrated using a bubble flowmeter. The heaters of the pyrolysis rig were all set to the specified temperatures and the lines of the system were purged with 5 ml of the feed material. The reaction was initiated by starting the HPLC pump at the specified flow rate of 0.5 ml/min and feeding in precisely 10 ml (8.1g) of the pinanol. Samples were collected and accurately weighed to two decimal places. The percentage mass balance was based on these results.

## 2.5 Synthesis procedures

### 2.5.1 *cis*-2-Pinanol preparation

*cis*-2-Pinanol can be prepared from  $\alpha$ -pinene via the following reactions:

1. The selective hydrogenation of  $\alpha$ -pinene using poisoned nickel catalyst to produce mainly *cis*-pinane;
2. The oxidation of *cis*-pinane in the presence of a radical initiator to form pinane-2-hydroperoxide; and
3. Reduction of pinane-2-hydroperoxide with sodium sulfite to form a mixture of *cis*- and *trans*-pinanol.

#### 2.5.1.1 General procedure for hydrogenation of $\alpha$ -pinene

$\alpha$ -Pinene (300 g, 2.174 mol); Ni 96B catalyst (30 g, 10% by mass to pinene) and carbon tetrachloride (CCl<sub>4</sub>) (0.2681 g, 1.763 mmol) were charged to a 600 ml Parr reactor. The contents were flushed with hydrogen gas three times before being heated to 80°C. At 80°C, the content was pressurized to 15 bars with hydrogen. The reaction was monitored by gas chromatography by sampling every hour until the reaction was complete. The reaction was deemed to be complete when 98% of  $\alpha$ -pinene was consumed. The catalyst was removed by filtration and the filtrate was distilled using a rotary evaporator at 80°C and 20 mbar.

In the 8L Parr reactor,  $\alpha$ -pinene (4.321 kg, 31.31 moles), Ni 96B (430 g, 10% by mass to  $\alpha$ -pinene) and carbon tetrachloride (3.63 g, 23.88 mmol) were used. The *cis*-pinane was also distilled using a rotary evaporator at 80°C and 20 mbar.

#### 2.5.1.2 General procedure for the oxidation of *cis*-pinane

In the 1L Labmax reactor, pinanes (543 g, 3.62 mol), NaOH (36 g, 0.91 mol), benzoyl peroxide (0.8712 g, 3.6 mmol) and water (36 g) were used. The NaOH was added to the reactor as a solution in water. The Labmax was sealed and evacuated and the contents heated to 110°C. The reactor was then pressurized to 3 bars with oxygen. The reaction was monitored by gas chromatography. Samples were taken hourly to check the progress. The reaction was stopped when ~25% of pinanes was converted. This was done to prevent the formation of by-products by further decomposition of

the product. After this, the reactor contents were cooled to room temperature and drained.

In the 8L Parr reactor, *cis*-pinane (3.6 kg, 26.09 moles), NaOH (261 g, 6.525 mol), AIBN (4.26 g, 26.0 mmoles) and water (261 g) were used.

#### 2.5.1.3 General procedure for the reduction of pinane-2-hydroperoxide

In 2L round bottom flask, sodium sulfite (350g) was dissolved in water (1400 ml) and then heated to 60°C. At 60°C, the post oxidation mixture (350 g) was added slowly with vigorous stirring. The reaction was run for 4 hrs at 60°C. After that, the contents were transferred to a separating funnel and phases separated. The organic phase was washed three times with 200 ml of warm (~60°C) water. The excess *cis*-pinane was distilled at 80°C and 20 mbar of vacuum using a rotary evaporator.

In the GR15 glass reactor, sodium sulfite (2kg), post-oxidized mixture (2kg) and water (8L) was used.

#### 2.5.1.4 Purification of *cis*-2-pinanol

After the pinane distillation, the crude mixture was placed in a round-bottom-flask fitted with a thermometer, magnetic stirrer and still head connected to a receiver flask via a condenser. The contents were heated to 60°C under 0.2 mbar vacuum pressure. *cis*-Pinane started distilling off at 35-50°C. After all the *cis*-pinane was removed, the temperature was increased to 85°C and *cis*-2-pinanol began distilling over at 60-75°C.

The *cis*-2-pinanol mixture still had the original level of *trans*-pinanol since it was not possible to remove by fractional distillation. A sublimation procedure was therefore developed to produce pure *cis*-2-pinanol as an analysis standard. In this procedure, a distilled mixture of *cis*- and *trans*-pinanol (~10g) was placed in a Buchii sublimation apparatus. Chilled water at -10°C was passed through the internal cold finger. The vessel was evacuated to a vacuum pressure of 0.1 mm Hg while being heated at a temperature of 30°C. The *cis*-2-pinanol selectively sublimed and collected as needle-like crystals on the cold finger. After about 5 hours of sublimation the vacuum was

slowly released and the cold finger was carefully removed from the vessel. The crystalline material was scraped off the cold finger and weighed. Approximately 1.5g of very pure *cis*-2-pinanol (>99%) was collected with just trace quantities of the *trans*-isomer.

## **2.5.2 Pinanol pyrolysis – Tubular reactor (AECI R&D)**

### **2.5.2.1 Equipment**

The pyrolysis reaction was performed in a laboratory tubular reactor consisting of a quartz tube with a diameter of 0.025m and a length of 0.5m. The tube was vertically positioned into an electric tubular furnace, so that the length subjected to constant heat flux was 0.15m. This length was considered to be the total length of the reactor, and used as such for the average residence time calculations.

A glass tube, wound with heating tape, connected the reactor to a boil-up flask, which in turn was submerged in an oil bath. An inlet dip tube submerged below the feed surface was used for the sparging of the inert gas, which in this case was a mixture of 5% ammonia in nitrogen. The carrier gas flow rate was controlled by means of a needle valve and monitored by means of a rotameter. The flow rate of the pinanol vapour fed to the system was controlled by the oil bath temperature. A condenser was placed at the outlet of the reactor to cool and condense the hot exit gases. A glass receiver flask was placed at the bottom of the condenser and glass wool was placed in the exhaust of the receiver.

### **2.5.2.2 Experimental procedures**

The boiling flask was charged with pinanol and submerged into an oil bath at 250 °C, the latter temperature being the optimum for a continuous and constant flow of pinanol through the reactor. The carrier gas (5% ammonia/nitrogen) was passed through the pinanol solution at a predetermined flow rate (considering the required residence time) and through the reactor set at a specific temperature. The variables considered in the procedure were as follows:

- Residence time (or flow rate through the reactor);
- Temperature registered in the reactor; and



- The influence of quartz Raschig rings (as packing) at a height of 0.1m as opposed to the unpacked reactor.

The rotameter calibration is given in **Table 2.7**.

**Table 2.7: Calibration points for nitrogen gas flowmeter**

Rotameter scale	Flow rate (L/min)	Empty tube residence time (s)	Packed bed residence time (s)
12	2.90	0.32	0.52
10	2.35	0.40	0.64
8	1.72	0.55	0.88
6	1.17	0.80	1.29
5	0.92	1.02	1.65

The residence time was calculated from the average velocity at the inlet (200 °C) and a heated length of tube of tube (0.15m). For each of these flow rates, the furnace temperature was varied between 500 °C and 600 °C in 20 °C intervals. The constant flow rate and temperature were maintained for around 5 minutes. Approximately 15g of crude reaction mixture was generated in this time period. This series of tests at the specified flow rate and temperature were completed for both the unpacked reactor, as well as the reactor packed with Raschig rings. The hot gases exiting the reactor were cooled and condensed, sampled and analysed by gas chromatography.

### 2.5.3 Pinanol pyrolysis – Screening experiments

All the pinanol pyrolysis screening experiments were carried out in a tubular reactor using the experimental conditions as shown in **Table 2.8**.

**Table 2.8: Experimental conditions used for screening experiments**

<b>Reactor configuration</b>	Stainless steel, tubular, 4.6mm ID, 150 mm long, heated length 50 mm, wall thickness 1 mm
------------------------------	---

<b>Vaporizer heater temperature</b>	250 °C
<b>Post vaporizer temperature heater</b>	250 °C
<b>Reactor temperature</b>	400 - 700 °C
<b>Condenser system</b>	PTFE coil (1m) in chilled bath at - 10 °C
<b>Feed</b>	10% pinanol/butanol unless specified otherwise
<b>Feed rate</b>	various
<b>Inert gas</b>	Nitrogen unless specified otherwise
<b>Inert gas flow rate</b>	various

The general procedure used was as follows:

In these experiments, a 10% m/m solution of *cis*-2-pinanol was prepared by dissolving pinanol (2g, 0.0130 moles, 90% purity) in n-butanol (18g), unless specified otherwise. The solution was transferred to a specially modified HPLC pump containing a 20ml calibrated syringe. The nitrogen flow was turned on and the flow rate calibrated using a bubble flowmeter. The heaters of the pyrolysis rig were all set to the specified temperatures and the lines of the system were purged with 5 ml of the feed material. The reaction was initiated by starting the HPLC pump at the specified flow rate. Samples of 1 ml were collected and prepared for analysis by GC. Pinanol and linalool in the sample were quantified as % m/m by using standard calibration curves. The conversions and selectivities were calculated based on these results.

#### **2.5.3.1 n-Butanol base case reaction**

This series of experiments (including the repeat) were carried out according to the general procedure described in § 2.5.3 and to the conditions specified in **Table 2.8**. The feed rate was 0.5ml/min and the inert gas (nitrogen) flow rate was 10ml/min.

### **2.5.3.2 Effect of solvent**

This series of experiments were carried out according to the general procedure described in § 2.5.3 and to the conditions specified in **Table 2.8**. The feed rate was 0.5ml/min and the inert gas (nitrogen) flow rate was 10ml/min. The feed material was prepared as a 10% m/m solution in various solvents, i.e. methanol, ethanol, n-propanol, n-butanol, hexane, and chloroform.

### **2.5.3.3 Effect of pinanol concentration**

This series of experiments were carried out according to the general procedure described in § 2.5.3 and to the conditions specified in **Table 2.8**. The feed rate was 0.5ml/min and the inert gas (nitrogen) flow rate was 10ml/min. Various concentrations of pinanol in ethanol was prepared, i.e. 10%, 20%, 40%, 60%, 80%, and 100%.

### **2.5.3.4 Vacuum pyrolysis**

These experiments were carried out according to the general procedure described in § 2.5.3 and to the conditions specified in **Table 2.8**. The equipment was slightly modified to be able to function under vacuum conditions. A cooling gas trap was installed in addition to the cooling coil condenser system to enable the system to be put under vacuum while still having the capability to obtain samples without having to break the vacuum and disturb the equilibrium. Ethanol was used as the diluent and reactions were carried out at -10 and -20kPa.

### **2.5.3.5 Effect of inert packing**

This series of experiments were carried out according to the general procedure described in § 2.5.3 and to the conditions specified in **Table 2.8**. The feed was 10% pinanol/ethanol with a feed rate of 0.5ml/min and the inert gas (nitrogen) flow rate was 10ml/min. Glass wool, glass beads and quartz pieces were inserted into the heated zone of the stainless steel tubular reactor. The ends of the reactor tube (in the case of the glass beads and quartz pieces) were stuffed with a wad of glass wool to prevent movement of the packing during the reaction.

### 2.5.3.6 Effect of various materials

This series of experiments were carried out according to the general procedure described in § 2.5.3 and to the conditions specified in **Table 2.8**. The feed was 10% pinanol/ethanol with a feed rate of 0.5ml/min and the inert gas (nitrogen) flow rate was 10ml/min. The reactors were changed for evaluation of the various materials. The standard stainless tubular reactor was used as the base case for this evaluation. Copper tubing with an internal diameter of 5mm was used for the copper material studies. Quartz and glass tubing with internal diameters of 5mm and 4.5mm, respectively, were used for the studies on quartz and glass. Gold, silver, and platinum were coated as nanoparticles on the glass reactor using the following procedures.

#### 2.5.3.6.1 Procedure for coating of gold nanoparticles on glass tube<sup>92</sup>

Gold chloride,  $\text{AuCl}_3$  (0.12g) was dissolved in 10ml of distilled water. A phase transfer catalyst, tetraoctylammonium bromide (TOAB) (0.96g) was dissolved in 9ml of chloroform. The resulting  $\text{AuCl}_3$  and TOAB solutions were added together and stirred for 1 hour at room temperature. This mixture was placed in a 25ml separating funnel and the chloroform layer collected. Dodecanethiol (86 $\mu\text{L}$ ) was then added to the stirring chloroform solution and stirred further for 5 minutes. Sodium borohydride (0.18g) was then dissolved in 11ml of distilled water. The aqueous solution was added to the organic solution, stirred overnight and then transferred to a 25ml separating funnel. The resulting chloroform phase was then collected and ethanol (10ml) added. The solution was then centrifuged at 4500rpm for 30 minutes. The resulting precipitate of dodecanethiol gold nanoparticles was reconstituted in chloroform.

The glass tube (15cm long, 5mm ID) was first etched by rinsing with 1M sodium hydroxide (1 hour) followed by deionised water (10 minutes) and then with 0.1M HCl (30 minutes). Upon rinsing with water again the glass tube was dried in an oven at 100 °C for 1 hour to remove all moisture. A (3-mercaptopropyl)trimethoxysilane (MPTES) solution was prepared by adding 2ml to 25ml of 2-propanol. This solution was then pumped into the glass tube using a plastic syringe for 1 hour and then allowed to stand overnight. The tube was then rinsed with 2-propanol and annealed at 110 °C in an oven for 10 minutes.

A solution of dodecanethiol gold nanoparticles in chloroform was pumped through the glass tube with a plastic syringe and allowed to stand for one hour. The excess gold solution was then removed from the capillary by pumping with a water filled syringe and then dried in an oven at 100 °C for 1 hour before use.

#### **2.5.3.6.2 Procedure for coating of silver nanoparticles on glass tube<sup>93</sup>**

The glass tube (15cm long, 5mm ID) was first etched by rinsing with 1M sodium hydroxide (1 hour) followed by deionised water (10 minutes) and then with 0.1M HCl (30 minutes). Upon rinsing with water again the glass tube was dried in an oven at 100 °C for 1 hour to remove all moisture. An ammoniacal silver nitrate solution was prepared as follows. Silver nitrate (3.397g, 0.02moles) was dissolved in 100ml of deionised water in a beaker. Aqueous ammonia (25%) was then added to this solution drop by drop until a clear colourless solution was obtained. The pH value of this solution was 9.3. The solution was syringed into the glass tube and the ends were sealed. The glass tube was placed in an oven at 70 °C for 3 hours, rinsed with deionised water and then oven dried for 1 hour at 100 °C.

#### **2.5.3.6.3 Procedure for coating of platinum nanoparticles on glass tube<sup>94</sup>**

The glass tube (15cm long, 5mm ID) was coated with gold nanoparticles as described in **Section 2.5.3.6.1**. A 0.05mM hydrogen hexachloroplatinate ( $\text{H}_2\text{PtCl}_6$ ) solution (20ml) was prepared and to this was added 5mM ascorbic acid (20ml). The solution was thoroughly stirred and then syringed into the glass tube. The ends were sealed and the tube was allowed to stand for 3 hours. The solution was then removed from the tube; the tube was rinsed with deionised water and then oven dried at 100 °C for 1 hour.

#### **2.5.3.7 Effect of zeolites**

This series of experiments were carried out according to the general procedure described in **Section 2.5.3** and to the conditions specified in **Table 2.8**. The feed was 10% pinanol/ethanol with a feed rate of 0.5ml/min and the inert gas (nitrogen) flow rate was 10ml/min. The heated zone of the stainless steel tubular reactor was packed with the sodium forms of three zeolites, i.e. faujasite, mordenite and beta zeolite. The

ends of the tube were packed with wads of glass wool to hold the zeolite plugs in place.

### 2.5.3.8 Effect of pyridine

This series of experiments were carried out according to the general procedure described in **Section 2.5.3** and to the conditions specified in **Table 2.8**. The feed was 10% pinanol/ethanol with a feed rate of 0.5ml/min and the inert gas (nitrogen) flow rate was 10ml/min. Pyridine was added to the pinanol solution as a mass percentage of the pinanol, i.e. 1%, 2%, 3%, 4% and 5%.

### 2.5.3.9 Effect of ammonia

This series of experiments were carried out according to the general procedure described in § 2.5.3 and to the conditions specified in **Table 2.8**. The feed was 10% pinanol/ethanol with a feed rate of 0.5ml/min and the inert gas flow rate was 10ml/min. The only difference in these experiments was that the nitrogen gas was replaced with a 5% ammonia/nitrogen mixture. As a comparison, ten experiments were conducted at 550 °C using the ammonia mixture and ten experiments were conducted using only nitrogen gas. The results were statistically analysed with Design Expert using a one factor statistical design to determine if there were significant differences between the two treatments. The design summary is shown in **Table 2.9**.

**Table 2.9: Design summary: nitrogen vs ammonia/nitrogen**

<b>Study Type</b>	Factorial		<b>Experiments</b>	20
<b>Initial Design</b>	Full Factorial		<b>Blocks</b>	No Blocks
<b>Center Points</b>	0			
<b>Design Model</b>	Main effects			
<b>Response</b>	<b>Name</b>	<b>Units</b>	<b>Obs</b>	<b>Minimum</b>
<b>Maximum</b>	<b>Trans</b>			
Y1	Conversion	%	20	40.10
52.80	None			
Y2	Selectivity	%	20	76.50
88.40	None			
<b>Factor</b>	<b>Name</b>	<b>Units</b>	<b>Type</b>	<b>Low Actual</b>
<b>High Actual</b>				
A	Gas Type	-	Categorical	Nitrogen
	Nitrogen/Ammonia			

#### 2.5.4 Determination of important reaction variables

The important variables in the pinanol pyrolysis reaction were determined by conducting a full factorial statistical design where the variables investigated were temperature, feed rate, inert gas flow rate, and pinanol concentration. A design summary is shown in **Table 2.10**.

**Table 2.10: Design summary of pinanol/ethanol pyrolysis statistical design**

<b>Study Type</b>	Factorial				
<b>Experiments</b>	19				
<b>Initial Design</b>	2 Level Factorial				
<b>Center Points</b>	3				
<b>Design Model</b>	4FI				
<b>Response</b>	<b>Name</b>	<b>Units</b>	<b>Obs</b>	<b>Minimum</b>	<b>Maximum</b>
Y1	Conversion	%	19	1.40	85.00
Y2	Selectivity	%	19	41.70	96.40
<b>Factor</b>	<b>Name</b>	<b>Units</b>	<b>Type</b>	<b>Low Actual</b>	<b>High</b>
<b>Actual</b>	<b>Low Coded</b>	<b>High Coded</b>			
A	Temperature	C	Numeric	500.00	650.00
B	Gas Flow	ml/min	Numeric	10.00	20.00
C	Pinanol Flow	ml/min	Numeric	0.20	1.00
D	Pinanol conc.	%m/m	Numeric	10.00	30.00

This series of experiments were carried out according to the general procedure described in § 2.5.3 and to the conditions specified in **Table 2.8**. Ethanol was used as diluent.

#### 2.5.5 Investigation of linalool decomposition

This series of experiments were carried out according to the general procedure described in § 2.5.3 and to the conditions specified in **Table 2.8**. The pinanol was replaced with pure linalool at a 10% m/m level and the solvents used as diluents were methanol, ethanol, n-propanol, n-butanol, hexane and chloroform. The samples produced were analysed by GC and GC-MS to determine the decomposition products and the extent of decomposition with temperature.

### 2.5.6 Preparation of 1kg market sample and robustness test

A 1kg sample of linalool with a purity specification of not less than 90% was required for market evaluation by the client. The sample was prepared using the experimental conditions as shown in **Table 2.11**. The pyrolysis rig was run on a semi-continuous basis for 15 days and was only stopped on the weekends, to replace the tubular reactor, and to clean out blocked pipes from carbonisation residues.

**Table 2.11: Experimental conditions used for preparation of 1kg market sample**

<b>Reactor configuration</b>	Stainless steel, tubular, 4.6mm ID, 150 mm long, heated length 50 mm, wall thickness 1 mm, volume 3.32cm <sup>3</sup>
<b>Vaporizer heater temperature</b>	250 °C
<b>Post vaporizer temperature heater</b>	250 °C
<b>Reactor temperature</b>	650 °C
<b>Condenser systems</b>	Coiled tube/vacuum flask (-10 °C)
<b>Feed</b>	30% m/m pinanol in ethanol
<b>Feed rate</b>	1 ml/min
<b>Inert gas</b>	nitrogen
<b>Inert gas flow rate</b>	10 ml/min.

### 2.5.7 Use of microreactor system for pyrolysis

A welded microreactor was used for the pyrolysis reactions. These reactors have a sandwich design with two micro-structured platelets being attached face to face. The platelets carry 14 channels each, which are 25 mm long, 500 µm wide and 400 µm deep. The channels together with the inlet and outlet region were prepared by wet chemical etching. Each couple of platelets was sealed by laser welding, which allowed for leak-tightness of the reactors at operation temperatures exceeding 750°C. Inlet and outlet tubes were attached to the reactors by laser welding.



The reactions conducted in the microreactor system were done under the conditions shown in **Table 2.12**.

**Table 2.12: Experimental conditions used for microreactor reactions**

<b>Reactor configuration</b>	14 channel microreactor, 25mm long, 500µm wide, 400µm deep
<b>Vaporizer heater temperature</b>	250 °C
<b>Post vaporizer temperature heater</b>	250 °C
<b>Reactor temperature</b>	400 - 700 °C
<b>Condenser system</b>	PTFE coil (1m) in chilled bath at -10 °C
<b>Feed</b>	10% pinanol/ethanol
<b>Feed rate</b>	0.5ml/min
<b>Inert gas</b>	Nitrogen
<b>Inert gas flow rate</b>	various

The reactions in the microreactor system were conducted at inert gas flow rates of 5, 10, 15, and 20ml/min.

## 2.6 Analytical procedures

### 2.6.1 Gas Chromatography

Samples of all the reaction mixtures were analysed by gas chromatography using the following conditions (**Table 2.13**).

**Table 2.13: GC Conditions for analysis of reaction mixture**

<b>Column</b>	Factor Four, VF-5ms, 30m x .25mm ID
<b>Detector Temperature (°C)</b>	300
<b>Injector Temperature (°C)</b>	250
<b>Initial Temperature (°C)</b>	50
<b>Initial Time (mins)</b>	5
<b>Rate (°C/min)</b>	30
<b>Final Temperature (°C)</b>	220
<b>Final Time (mins)</b>	2
<b>Column Head Pressure (psi)</b>	10
<b>Injection Volume (µL)</b>	1

## CHAPTER 3

### Results and Discussion

#### 3.1 Equipment

##### 3.1.1 Evaluation of vaporizer systems

As described in the **Experimental section**, five vaporizer designs were evaluated using a one factor design, as follows:

1. **Vaporizer 1:** Nitrogen sparging through boiling liquid in round-bottomed-flask
2. **Vaporizer 2:** Heated tube with pinanol and gas feeds from bottom
3. **Vaporizer 3:** Heated tube with pinanol and gas feeds from bottom with glass beads
4. **Vaporizer 4:** Heated tube with countercurrent pinanol/nitrogen flow
5. **Vaporizer 5:** Heated tube with countercurrent pinanol/nitrogen flow with glass beads

There were five different levels and ten replications for each of the responses giving a total of fifty observations for each of the responses. The responses used for the one factor statistical design was conversion of pinanol and selectivity to linalool. Each of the responses were analysed separately.

##### 3.1.1.1 Analysis of conversion response for various vaporizer designs

The conversion results are given in **Table 3.1**.

**Table 3.1: Conversion response for the various vaporizer designs**

Run No.	% Conversion				
	Vaporizer 1	Vaporizer 2	Vaporizer 3	Vaporizer 4	Vaporizer 5
1	17.3	31.8	30.8	20.9	25.6
2	20.0	34.2	17.3	31.0	27.7
3	34.5	15.8	17.1	30.5	25.4
4	16.6	26.4	21.0	27.1	22.8
5	37.6	32.1	24.5	23.1	26.5
6	33.6	20.6	18.0	23.7	23.3
7	38.4	24.6	25.7	21.8	23.6
8	38.4	25.7	21.6	28.1	21.3
9	16.4	20.2	24.2	28.9	28.0
10	18.6	17.7	26.0	27.5	21.9
<b>Average</b>	<b>27.1</b>	<b>24.9</b>	<b>22.6</b>	<b>26.3</b>	<b>24.6</b>

The ANOVA (Analysis of variance) results are shown in **Table 3.2**.

**Table 3.2: Conversion ANOVA**

Source	Sum of squares	DF	Mean square	F Value	Prob>F
<b>Model</b>	119.33	4	29.83	0.83	0.5129
<i>A</i>	<i>119.33</i>	<i>4</i>	<i>29.83</i>	<i>0.83</i>	<i>0.5129</i>
<b>Pure Error</b>	1616.58	45	35.92		
<b>Cor Total</b>	1735.92	49			

The "Model F-value" of 0.83 implies the model is not significant relative to the noise. There is a 51.29 % chance that a "Model F-value" this large could occur due to noise. Values of "Prob > F" less than 0.0500 indicate model terms are significant. In this case there are no significant model terms. Values greater than 0.1000 indicate the model terms are not significant. The negative "Pred R-Squared" implies that the overall mean is a better predictor of the responses than the current model.

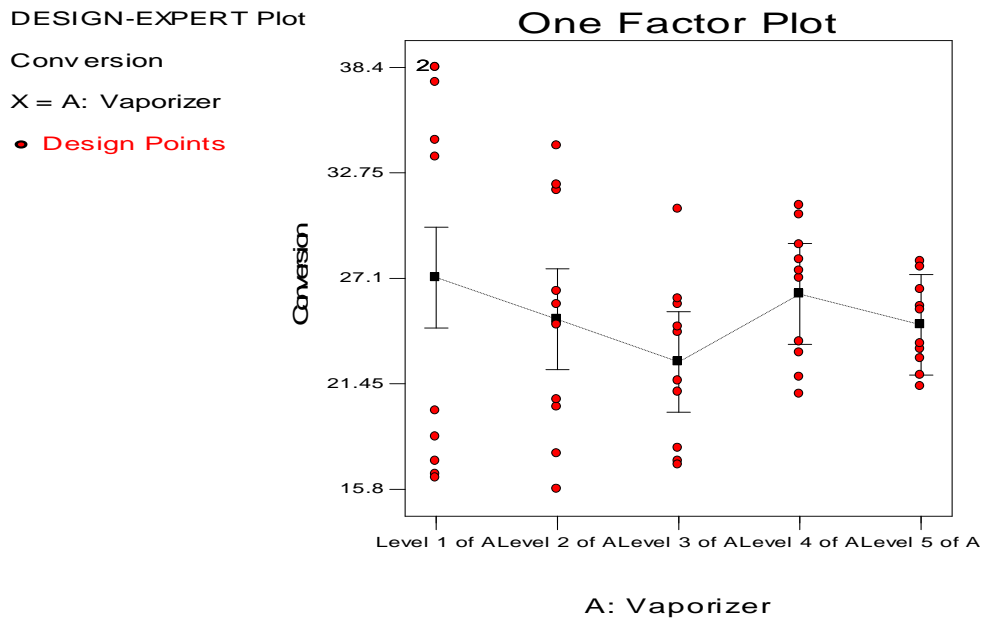
The analyses of the various treatments are shown in **Table 3.3**.

**Table 3.3: Conversion: Analysis of treatments**

<b>Treatment</b>	<b>Mean diff.</b>	<b>DF</b>	<b>Std. Error</b>	<b>T for H<sub>0</sub> Coeff=0</b>	<b>Prob &gt;  t </b>
1 vs 2	2.23	1	2.68	0.83	0.4098
1 vs 3	4.52	1	2.68	1.69	0.0987
1 vs 4	0.88	1	2.68	0.33	0.7442
1 vs 5	2.53	1	2.68	0.94	0.3503
2 vs 3	2.29	1	2.68	0.85	0.3974
2 vs 4	-1.35	1	2.68	-0.50	0.6170
2 vs 5	0.30	1	2.68	0.11	0.9114
3 vs 4	-3.64	1	2.68	-1.36	0.1812
3 vs 5	-1.99	1	2.68	-0.74	0.4617
4 vs 5	1.65	1	2.68	0.62	0.5413

In the analysis of treatments, values of “Prob>|t|” less than 0.05 indicate the difference in the treatment means is significant. In the case of conversion, none of the treatments were significantly different from each other in terms of the overall means.

A One factor plot for the various vaporizer designs is shown in **Figure 3.1**.



**Figure 3.1: Conversion: One Factor Plot of various vaporizer designs**

The one factor plot in **Figure 3.1** clearly indicates that although the overall means of the treatments are relatively similar, the spread of results for each vaporizer system is very different. Vaporizer 1 was the most inconsistent ranging from 38.4% to 16.4% (difference of 22.0%) for conversion. This clearly indicates that the composition of the feed material leaving the vaporizer system and entering the reactor was quite variable from experiment to experiment. This can be expected of this system which relies on the boiling of a bulk liquid system under reflux conditions. The energy requirements required to maintain the temperatures required for boiling would also be quite large. This was the system which was used for the initial investigation conducted by AECI R&D<sup>15</sup>.

Vaporizer 2 performed slightly better in terms of consistency ranging from 15.8 to 34.2% (18.4% difference). In this system the feed material was fed into the tubular vaporizer at a consistent flow rate from the bottom. However, because the bottom of the vaporizer was cooler than the other sections there tended to be an accumulation of liquid which resulted in “sputtering” and therefore inconsistent results. The addition of glass beads (Vaporizer 3) to improve the dispersion of liquid and gas did slightly improve the performance i.e. ranging from 17.2 to 30.8% (13.6% difference).

Vaporizer 4 displayed very consistent results ranging from 20.9 to 31.0% (10.1% difference) and this improved even further by the addition of glass beads ranging from 21.3 to 28.0% (difference of only 6.7%). In these systems the starting material was fed in from the top directly onto the heated tubular surface and counter-currently to the heated gas from the bottom. The liquid was therefore instantly vaporized, mixed and then fed into the reactor, resulting in a well dispersed, consistent gas/vapour mixture. The addition of glass beads (Vaporizer 5) increased the consistency of performance. This system was therefore selected for all subsequent experimental trials.

### 3.1.1.2 Analysis of selectivity response for various vaporizer designs

The selectivity results are given in **Table 3.4**.

**Table 3.4: Selectivity response for the various vaporizer designs**

Run No.	% Selectivity				
	Vaporizer 1	Vaporizer 2	Vaporizer 3	Vaporizer 4	Vaporizer 5
1	65.5	68.9	63.8	63.8	64.6
2	57.0	58.6	62.2	70.5	72.2
3	58.9	64.5	67.4	72.9	71.2
4	57.0	53.7	66.3	71.8	61.7
5	62.8	58.3	65.1	60.5	70.2
6	52.4	65.8	61.9	65.6	61.1
7	52.4	73.0	61.2	64.2	69.2
8	50.2	74.7	68.2	70.5	61.3
9	61.7	72.2	61.6	69.2	67.3
10	56.5	71.3	66.7	68.3	70.9
<b>Average</b>	<b>57.4</b>	<b>66.1</b>	<b>64.4</b>	<b>67.7</b>	<b>67.0</b>

The ANOVA (Analysis of variance) results are shown in **Table 3.5**.

**Table 3.5: Selectivity ANOVA**

Source	Sum of	DF	Mean	F Value	Prob>F
--------	--------	----	------	---------	--------

	<b>squares</b>		<b>square</b>		
Model	689.35	4	172.34	7.25	0.0001
A	689.35	4	172.34	7.25	0.0001
Pure Error	1070.01	45	23.78		
Cor Total	1759.36	49			

The Model F-value of 7.25 implies the model is significant. There is only a 0.01% chance that a "Model F-Value" this large could occur due to noise. Values of "Prob > F" less than 0.0500 indicate model terms are significant. In this case A is a significant model term. Values greater than 0.1000 indicate the model terms are not significant. The "Pred R-Squared" of 0.2492 is in reasonable agreement with the "Adj R-Squared" of 0.3378. The "Adeq Precision" values were 6.673 and this measures the signal to noise ratio. A ratio greater than 4 is desirable. The ratio of 6.673 indicates an adequate signal and therefore this model could be used to navigate the design space.

The analysis of the various treatments is shown in **Table 3.6**.

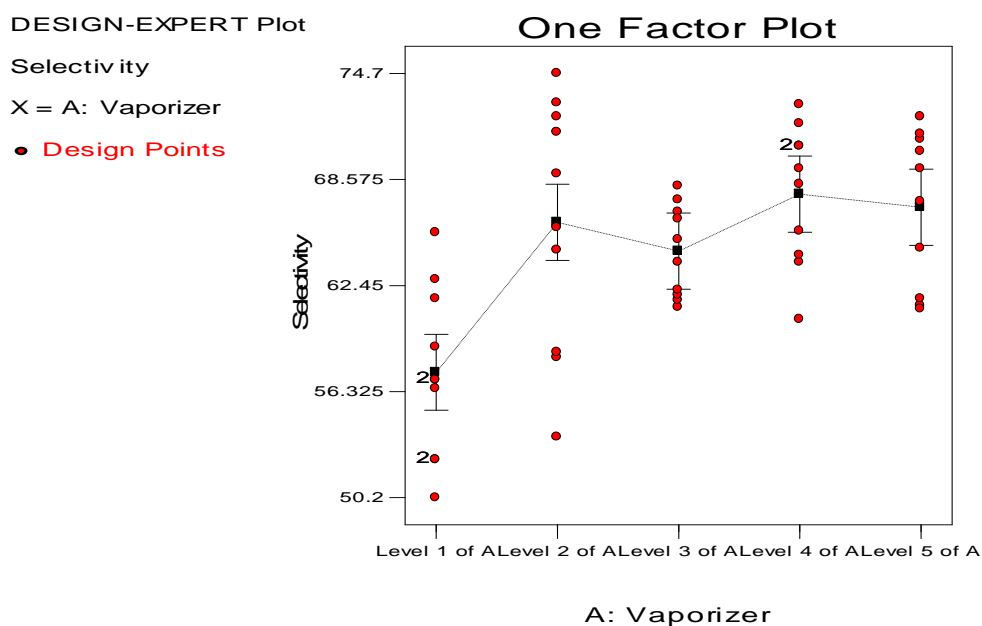
**Table 3.6: Selectivity: Analysis of treatments**

<b>Treatment</b>	<b>Mean diff.</b>	<b>DF</b>	<b>Std. Error</b>	<b>T for H<sub>0</sub> Coeff=0</b>	<b>Prob &gt;  t </b>
1 vs 2	-8.66	1	2.18	-3.97	0.0003
1 vs 3	-7.00	1	2.18	-3.21	0.0025
1 vs 4	-10.29	1	2.18	-4.72	< 0.0001
1 vs 5	-9.53	1	2.18	-4.37	< 0.0001
2 vs 3	1.66	1	2.18	0.76	0.4505
2 vs 4	-1.63	1	2.18	-0.75	0.4587
2 vs 5	-0.87	1	2.18	-0.40	0.6918
3 vs 4	-3.29	1	2.18	-1.51	0.1384
3 vs 5	-2.53	1	2.18	-1.16	0.2521
4 vs 5	0.76	1	2.18	0.35	0.7291

In the analysis of treatments, values of "Prob>|t|" less than 0.05 indicate the difference in the treatment means is significant. In the case of selectivity, there were significant differences between Vaporizer 1 and the others. The other vaporizers were not significantly different from each other.



A One factor plot for the various vaporizer designs is shown in **Figure 3.2**.



**Figure 3.2: Selectivity: One Factor Plot of various vaporizer designs**

**Figure 3.2** clearly indicates the differences between Vaporizer 1 and the other four designs. Not only was the average selectivity lower (57.4% vs 67.7%) but there was also inconsistency between experiments with results ranging from 50.2 to 65.5% (8.1% difference). The highest average selectivity was obtained for Vaporizer 4 (67.7%) while the most consistent was Vaporizer 3. The preferred vaporizer (based on conversion), Vaporizer 5, showed good average selectivity (67.0%) as well as good consistency.

### 3.1.2 Evaluation of condenser systems

As described in the Experimental section, five condenser designs were evaluated using a one factor design. The following condenser systems were evaluated:

1. **Condenser 1:** Glass condenser system
2. **Condenser 2:** Gas cooling trap system
3. **Condenser 3:** Coiled PTFE tubing/chilled bath system
4. **Condenser 4:** Coiled tube/vacuum flask system
5. **Condenser 5:** Counter-flow Micro Heat Exchanger (COMH)

There were five different levels and ten replications for the response giving a total of fifty observations. The responses used for the one factor statistical design was percentage mass recovery of the product mixture based on mass of starting material. The results for the experiments are given in **Table 3.7**.

**Table 3.7: Mass recovery response for the various condenser designs**

Run No.	% Mass recovery				
	Condenser 1	Condenser 2	Condenser 3	Condenser 4	Condenser 5
1	62.2	54.1	78.1	87.7	92.7
2	53.5	51.5	79.6	81.0	97.9
3	66.9	51.4	84.5	88.1	94.6
4	51.8	59.6	82.9	87.9	98.2
5	65.2	50.5	73.7	89.4	97.5
6	53.0	57.7	75.1	88.6	97.3
7	51.6	55.3	79.2	91.9	92.4
8	66.6	56.8	71.3	92.0	95.7
9	69.3	57.0	79.7	84.7	97.0
10	69.2	57.0	71.6	88.2	97.8
<b>Average</b>	<b>60.9</b>	<b>55.1</b>	<b>77.6</b>	<b>88.0</b>	<b>96.1</b>

The ANOVA (Analysis of variance) results are shown in **Table 3.8**.

**Table 3.8: ANOVA**

Source	Sum of squares	DF	Mean square	F Value	Prob>F
<b>Model</b>	12129.08	4	3032.27	148.23	< 0.0001
<i>A</i>	<i>12129.08</i>	<i>4</i>	<i>3032.27</i>	<i>148.23</i>	<i>&lt; 0.0001</i>
<b>Pure Error</b>	920.56	45	20.46		
<b>Cor Total</b>	13049.64	49			

The Model F-value of 148.23 implies the model is significant. There is only a 0.01% chance that a "Model F-Value" this large could occur due to noise. Values of "Prob > F" less than 0.0500 indicate model terms are significant. In this case A is a significant model term. Values greater than 0.1000 indicate the model terms are not significant.

The "Pred R-Squared" of 0.9129 is in reasonable agreement with the "Adj R-Squared" of 0.9232. "Adeq Precision" measures the signal to noise ratio. A ratio greater than 4

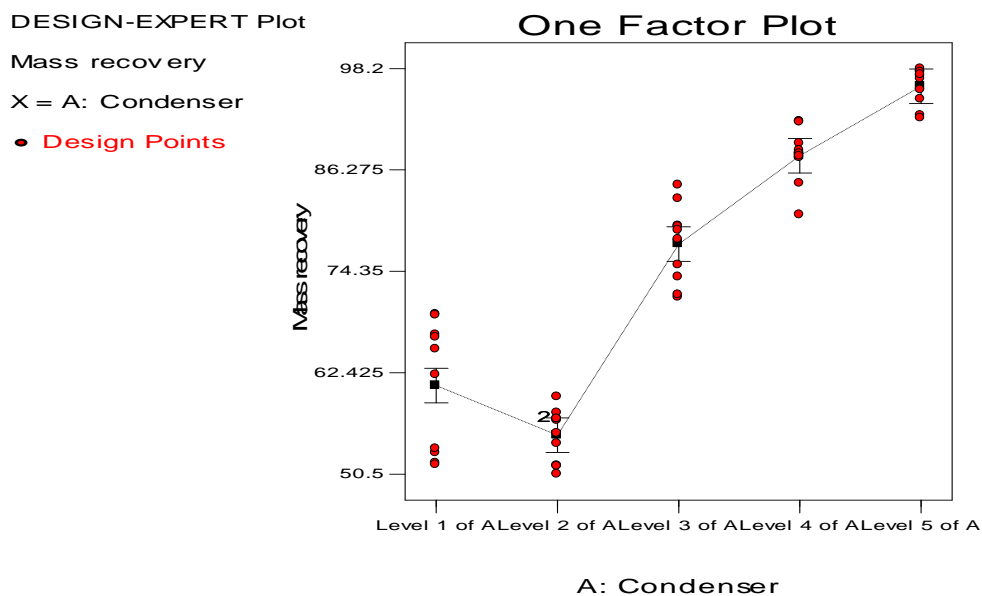
is desirable. The ratio of 28.680 for this model indicates an adequate signal. This model can be used to navigate the design space.

The analysis of the various treatments is shown in **Table 3.9**.

**Table 3.9: Analysis of treatments**

Treatment	Mean diff.	DF	Std. Error	T for H <sub>0</sub> Coeff=0	Prob >  t
1 vs 2	5.84	1	2.02	2.89	0.0060
1 vs 3	-16.64	1	2.02	-8.23	< 0.0001
1 vs 4	-27.02	1	2.02	-13.36	< 0.0001
1 vs 5	-35.18	1	2.02	-17.39	< 0.0001
2 vs 3	-22.48	1	2.02	-11.11	< 0.0001
2 vs 4	-32.86	1	2.02	-16.25	< 0.0001
2 vs 5	-41.02	1	2.02	-20.28	< 0.0001
3 vs 4	-10.38	1	2.02	-5.13	< 0.0001
3 vs 5	-18.54	1	2.02	-9.17	< 0.0001
4 vs 5	-8.16	1	2.02	-4.03	0.0002

Values of “Prob > |t|” of less than 0.05 indicates significant differences and in this design there were significant differences between all the various condenser designs. This is further illustrated in **Figure 3.3** where a one factor plot was done.



**Figure 3.3: One Factor Plot of various condenser designs**

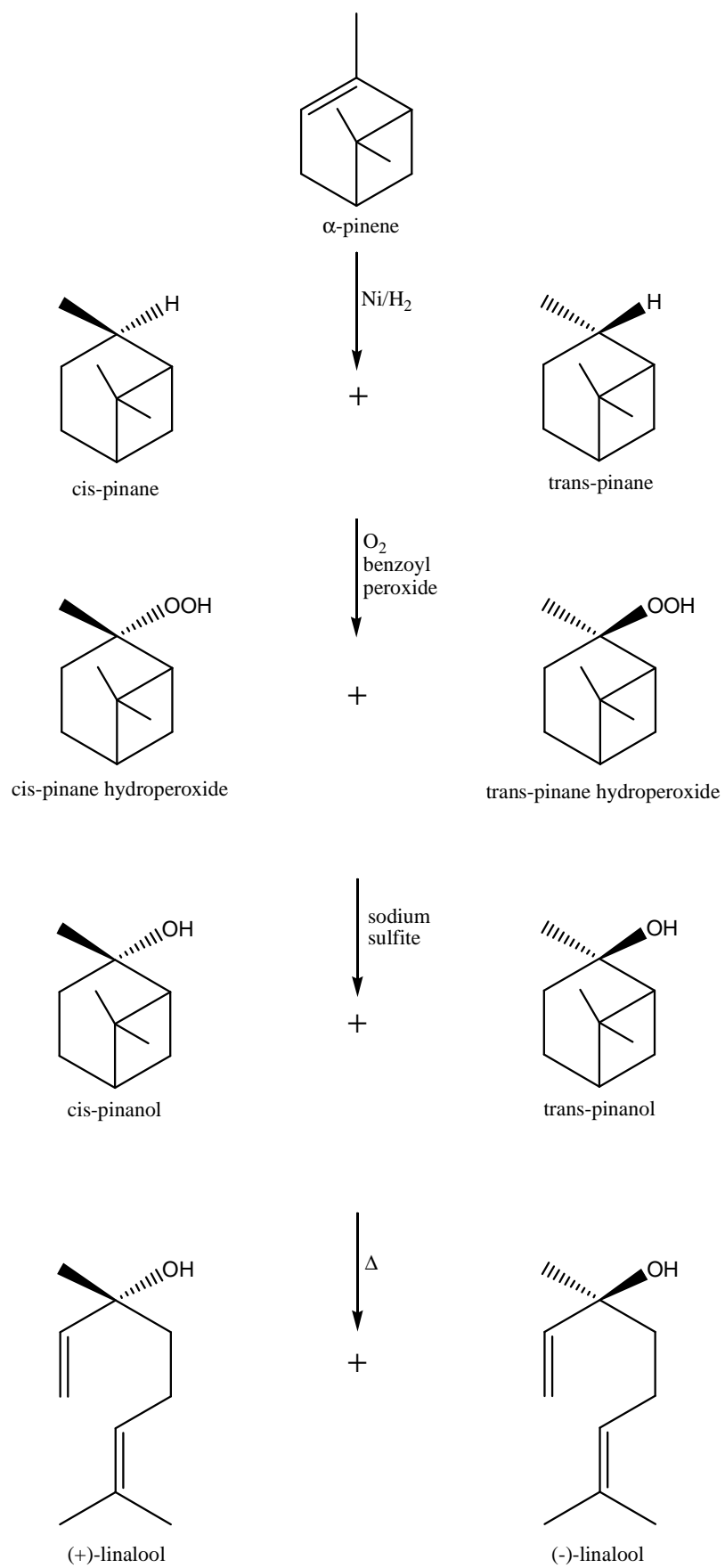
The worst average mass balance was obtained with condenser 2 (55.1%). The efficiency of condenser systems are closely related to the heat transfer area of the cooled surface and therefore one would expect that the larger the heat transfer area the more efficient the condensation process would be, and hence, the better the mass balance. Of the various designs, condenser 2 has the lowest heat transfer area and therefore performed poorly. Condenser system 1 was only slightly better with an average mass balance of (60.9%). This was the system that was used in the initial investigation<sup>15</sup>. The range of the mass balance (51.6 to 69.3%, 17.7% difference) also indicates an inconsistent performance with quite a lot of variation between runs.

In condensers 3 and 4, long lengths (~1m) of fine tubing was used (1/8" and 1/16" ID, respectively) and the surface to volume ratio was therefore significantly improved resulting in enhanced performances with average mass balances of 77.6% and 88.0%, respectively. There was also not much variation between runs, resulting in more consistent performances. Condenser 4 was significantly better because of the finer tubing and enclosure in a thermally insulated flask, thus resulting in better insulation and more efficient cooling.

The best performance was delivered by condenser 5, the counter-flow micro heat exchanger (COMH), with an average mass balance of 96.1%. This is hardly surprising because of the huge heat transfer area and the counter-flow design. The heat transfer characteristics are greatly improved resulting in highly efficient cooling and condensation of the hot, volatile vapours.

### **3.2 cis-2-Pinanol preparation**

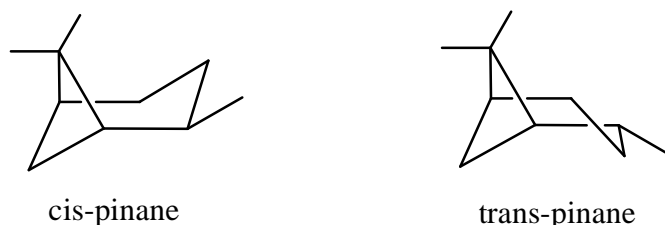
In this investigation, the preparation of *cis*-2-pinanol was done purely for the preparation of material for evaluation of the pyrolysis reaction and on a larger scale for generation of a 1kg market sample for the client. The synthesis that was used is shown in **Figure 3.4** where  $\alpha$ -pinene is used as the starting material.



**Figure 3.4: Reaction scheme for synthesis of *cis*-2-pinanol**

### 3.2.1 Preparation of cis-Pinane

The molecule of pinane exhibits a bicyclic structure and can exist as four spatial isomers of *cis*- and *trans*-pinane (**Figure 3.5**).



**Figure 3.5:** *Cis*- and *trans*-pinane

Either of these can occur as two optical isomers. This is due to the presence of three asymmetric carbon atoms. Moreover, a six-membered ring can occur as a chair or boat conformation. Depending on reaction conditions, hydrogen addition to the double bond can result in the formation of two *cis*- and *trans*-pinane isomers; in this case, the asymmetry of two carbon atoms is retained. In the in-situ reduction with hydrogen, the position of the double bond in a pinene molecule has no effect on the isomeric composition of the resulting pinane.

In initial experiments,  $\alpha$ -pinene was hydrogenated in the presence of sponge nickel catalyst in a 300ml Parr pressure vessel as shown in **Table 3.10**.

**Table 3.10: Results of  $\alpha$ -pinene hydrogenation in 300 ml Parr reactor**

Exp. Ref.	Temp °C	Pressure bars	Time hrs	%Conv.	%Selec.	<i>Cis:trans</i>
PH1	50	15	8	43.2	88.7	10:1
PH2	80	10	6	94.7	94.6	12:1
PH3	80	15	6	96.9	96.2	14:1
PH4	80	15	6	97.7	96.8	14:1

At a temperature of 50°C and hydrogen pressure of 15 bars (**PH1**) the conversion was only 43.2% and the selectivity 88.7% even after 8 hours of reaction. The *cis/trans* ratio was 10:1. In **PH2** the temperature was increased to 80°C and the pressure decreased to 10 bars. There was a significant improvement in the conversion (94.7%)

and the selectivity (94.6%). The *cis/trans* ratio also improved to 12:1. In subsequent experiments (**PH3** and **PH4**) the pressure was increased to 15 bars. There wasn't a significant improvement in conversion but a slight improvement in the *cis/trans* ratio and hence selectivity to the *cis*-isomer.

**Table 3.11** shows the results of experiments where the sponge nickel catalyst was partially poisoned with a chlorinated solvent, carbon tetrachloride.

**Table 3.11: Hydrogenation using partially poisoned Ni catalyst**

Exp. Ref.	Temp °C	Pressure bars	Time hrs	%Conv.	%Selec.	Cis:trans
PHP1	80	15	6	87.5	96.8	16:1
PHP2	80	15	6	31.3	96.2	16:1

There was a decrease in the conversion (87.5%), the selectivity was unchanged and there was a slight improvement in the *cis/trans* ratio. In **PHP2**, the catalyst was filtered and recycled. The conversion was significantly reduced to 31% after 6 hours of reaction. However, the selectivity and *cis/trans* ratio was unchanged.

The hydrogenation was scaled up to the 8L Parr to generate more material for the oxidation reaction step. Three reactions were conducted under identical conditions to the small scale reactions using poisoned nickel catalyst. The results of these experiments are shown in **Table 3.12**.

**Table 3.12: Results of 8L Parr hydrogenations using poisoned nickel catalyst**

Exp. Ref.	Temp °C	Pressure bars	Time hrs	%Conv.	%Selec.	Cis:trans
PHSU1	80	15	4	99.4	97.7	18:1
PHSU2	80	15	4	99.4	96.0	18:1
PHSU3	80	15	4	99.6	97.8	18:1

In all three reactions, excellent conversions and selectivities were obtained. The reaction was complete within four hours and there was even further improvement in the *cis/trans* ratio. This is definitely an indication of the superior mass transfer characteristics of the 8L Parr reactor as compared to the 300ml Parr reactors. The 8L

Parr reactor has more stirrer blades and is fitted with a special gassing stirrer which forces gas into the reaction mixture thus resulting in faster adsorption onto the catalyst surface and hence faster reaction rates.

The results obtained are in agreement with Ill'ina, et al<sup>95</sup>, who studied the kinetics of  $\alpha$ -pinene hydrogenation. Although the reactions were carried out with palladium catalyst, similar trends were observed in this investigation. They found that the cis/trans ratio increased with an increase in temperature and an increase in hydrogen pressure. They also concluded that the two factors which affected the selectivity the most was the interaction of the pinene with the catalyst surface and the concentration of surface hydride species. The two  $sp^2$ -hybrid carbon atoms at the C=C bond in the pinene molecule form a plane in which all four substituents are located (two carbon atoms of the pinene ring, the carbon atom of the methyl group, and a hydrogen atom). The  $\pi$  orbital of the double bond is oriented perpendicularly to this plane. The  $-CH_2$  unit is arranged on one side of the plane, whereas the much more bulky  $-C(CH_3)_2$  unit is arranged on the other side. The pinene molecule is activated upon adsorption because of the formation of a  $\pi$  complex with a surface nickel atom. The maximum overlapping of the  $\pi$  orbital and the d orbital of nickel is possible in the case when the steric effect of substituents arranged on the adsorption side of the pinene molecule is minimum. Thus, the most favourable form of adsorbed pinene is a structure in which the bulky methyl unit is directed oppositely to the surface of the catalyst. In the adsorbed complex, the methyl group is also deflected from the catalyst surface for steric reasons. Because of this, the  $-C(CH_3)_2$  unit and the methyl group occur on the side of the plane formed by the  $sp^2$ -hybrid carbon atoms of the C=C bond, and this structure is responsible for the formation of *cis*-pinane.

### 3.2.2 Preparation of pinane-2-hydroperoxide and reduction to *cis*-2-pinanol

The autoxidation of *cis*-pinane has been extensively studied<sup>1-7</sup>. The main products formed are *cis*- and *trans*-2-pinanol in a ratio of about 78% *cis*- to 22% *trans*-alcohol, formed as a result of the 2-pinanyloxy radical. The reaction is normally not taken to full conversion because of the formation of numerous by-products. The oxidates of the reaction were reduced with sodium sulfite to the corresponding alcohols. Initially, autoxidations were carried out at temperatures of 60, 80, 100, and 120°C as shown in



**Table 3.13.** The reactions were normally stopped at a conversion of ~15% to minimise by-product formation.

**Table 3.13: Autoxidation of *cis*-pinane**

Exp. Ref.	Press. bars	Temp. °C	Time Hrs	Conv %	Selec %	Cis:Trans
AO1	1	60	48	15.4	75.3	3.7:1
AO2	1	80	18	15.0	65.4	3.9:1
AO3	1	100	4	16.3	63.4	3.9:1
AO4	1	120	1	14.1	43.6	3.7:1

It is quite clear from these reactions that as the temperature is increased from 60 to 120°C the time taken to reach 15% conversion is greatly reduced. However, the selectivity to *cis*-2-pinanol simultaneously decreases with increasing temperature. The *cis/trans* ratio is relatively constant. Brose, et al<sup>96</sup>, have done extensive studies on the autoxidation reaction and have found that the *cis*- and *trans*-2-hydroperoxy pinanes, the main oxidation products, are decomposed more rapidly at temperatures higher than 100°C forming products resulting from the fragmentation of the 2-pinanyloxy radicals. Moreover, with increasing temperature more products with the *p*-menthane skeleton are obtained. This is evident from a GC-MS analysis of a typical autoxidation sample where the following compounds were identified: *iso*-pinocampone, *iso*-pinocampheol, *iso*-verbenone, *iso*-verbenol, 1-acetyl-2,2-dimethyl-3-ethyl-cyclobutane,  $\alpha$ -terpineol, 4,4,8-trimethyl-2,3-dioxabicyclo-[3,3,1]nonane-8-ol, and *trans*-pinane-2,9-diol. Using this method also produces a substantial amount of the *trans*-isomer which is much less reactive than the *cis*-isomer and therefore, difficult to convert to linalool in the pyrolysis reaction. A method was therefore required to selectively produce *cis*-2-pinanol with minimal by-product formation.

In a process described by Filliatre, et al<sup>97</sup>, the autoxidation was carried out in the presence of catalytic amounts of azoisobutyronitrile (AIBN) as radical initiator,

followed by a stoichiometric reduction with sodium sulfite. In addition the presence of an organic or inorganic base was claimed to reduce the formation of by-products. A similar process is described in a US patent by **Risco**, et al. Selectivities of up to 95% are claimed with a *cis*- and *trans*-pinanol ratio of 4:1. A similar process was carried out in our laboratories and the results for these experiments are shown in **Table 3.14**.

**Table 3.14: Oxidation of *cis*-pinane using AIBN as initiator in 300ml Parr reactor**

<b>Exp. Ref.</b>	<b>Press.</b> <b>bars</b>	<b>Temp.</b> <b>°C</b>	<b>Time</b> <b>Hrs</b>	<b>Conv</b> <b>%</b>	<b>Selec</b> <b>%</b>	<b>Cis:Trans</b>
AIBN1	Atm.	90	24	0	0	-
AIBN2	Atm.	110	24	0	0	-
AIBN3	3	90	4	20.0	43.81	4:1
AIBN4	3	110	4	36.7	77.46	4:1

There was no conversion of the pinane when the reaction was run at atmospheric pressure with oxygen bubbling through the mixture (**AIBN1**) even after 24 hours reaction at 90°C. Increasing the temperature to 110°C (**AIBN2**) also did not result in any conversion of the pinane. However, when the reaction was conducted in a Parr reactor at 3 bar oxygen pressure (**AIBN3**), a 20% conversion was observed after only 4 hours of reaction time at 90°C. The selectivity to the *cis*-pinanol under these conditions was only 43.81%. Increasing the temperature to 110°C (**AIBN4**) resulted in an increase in conversion to 36.7% and an increase in the selectivity to 77.46%. However, in both these cases the *cis/trans* ratio was still too low at 4:1.

At this stage although improvements were being made to the conversion and selectivity of the reaction, the results were still not suitable for an industrial process because of the high levels of the *trans*-isomer. In subsequent oxidation reactions benzoyl peroxide was investigated as the radical initiator. The results of these experiments are shown in **Table 3.15**.

**Table 3.15: Oxidation of *cis*-pinane using benzoyl peroxide as initiator**

<b>Exp. Ref.</b>	<b>Press.</b> <b>bars</b>	<b>Temp.</b> <b>°C</b>	<b>Time</b> <b>Hrs</b>	<b>Conv</b> <b>%</b>	<b>Selec</b> <b>%</b>	<b>Cis:Trans</b>
BP1	Atm.	90	24	0	0	-
BP2	3	90	8	17.3	84.5	7:1
BP3	3	110	4	28.7	96.2	9:1
BP4	3	110	4	31.1	95.6	9:1

As in the case of AIBN, no reaction was observed under atmospheric conditions by the bubbling of oxygen through the reaction mixture at 90°C (**BP1**) for 24 hours. When the reaction was conducted under a pressure of 3 bars at the same temperature (**BP2**), however, a conversion of 17.3% was observed and a relatively high selectivity (when compared to the equivalent **AIBN3** reaction) of 84.5%. The *cis*/*trans* ratio was also significantly higher at 7:1 compared to 4:1 for AIBN. Increasing the temperature to 110°C (**BP3**) resulted in higher conversion and a significant improvement in the *cis*-2-pinanol selectivity. There was also a corresponding improvement in the *cis*/*trans* ratio from 7:1 to 9:1. The reaction was repeated under identical conditions and the similarity of the results obtained confirms that this was not a spurious result. The benzoyl peroxide reaction was scaled up to the 8L Parr reactor and was run under identical conditions. The results of these experiments are shown in **Table 3.16**.

**Table 3.16: *cis*-Pinane oxidation in 8L Parr reactor using benzoyl peroxide**

<b>Exp. Ref.</b>	<b>Press.</b> <b>bars</b>	<b>Temp.</b> <b>°C</b>	<b>Time</b> <b>Hrs</b>	<b>Conv</b> <b>%</b>	<b>Selec</b> <b>%</b>	<b>Cis:Trans</b>
BPSU1	3	110	2	32.5	95.1	9:1
BPSU2	3	110	2	29.9	94.8	9:1

At the 8L Parr scale, the oxidation reaction was reproducible as similar results were obtained when compared to the smaller scale reactions in terms of conversion, selectivity, and *cis/trans* ratio. However, a similar conversion was achieved in about 2 hours, half the time of the small scale reaction. The use of a gas entrainment impellor results in much better dispersion of oxygen through the reaction mixture and hence improves interfacial contact between the liquid and gas. This significantly improves the mass transfer characteristics and results in higher reaction efficiencies and faster conversion.

### 3.2.3 Purification of *cis*-2-pinanol

Since the oxidation reaction is not taken to completion, the unreacted *cis*-pinane is fractionally distilled and recycled. This is a relatively simple distillation since the difference in boiling points between *cis*-2-pinanol and *cis*-pinane is approximately 52°C. The *cis/trans* ratio remained unchanged during the distillation process and a relatively pure *cis*-2-pinanol sample (88.9% *cis*-pinanol, 9.9% *trans*-pinanol) was obtained for evaluation of the pyrolysis reaction.

It was found that samples of pinanol which were stored in bottles had long needle-like crystals in the upper section of the bottle. Analysis of these needles by GC showed that they were almost exclusively *cis*-2-pinanol. The *cis*-2-pinanol was obviously selectively subliming on the walls of the storage bottle. A procedure was developed for the purification of the pinanol mixture by sublimation and this was used as a calibration standard for the quantification of pinanol. The *cis*-pinanol purity of this sample was 95.8% with a small amount of *trans*-pinanol (3.9%)

**Table 3.17** shows the composition of the pinanol mixture following one distillation step, two distillation steps and lastly after sublimation following the second distillation step.

**Table 3.17: Purification of pinanol mixture**

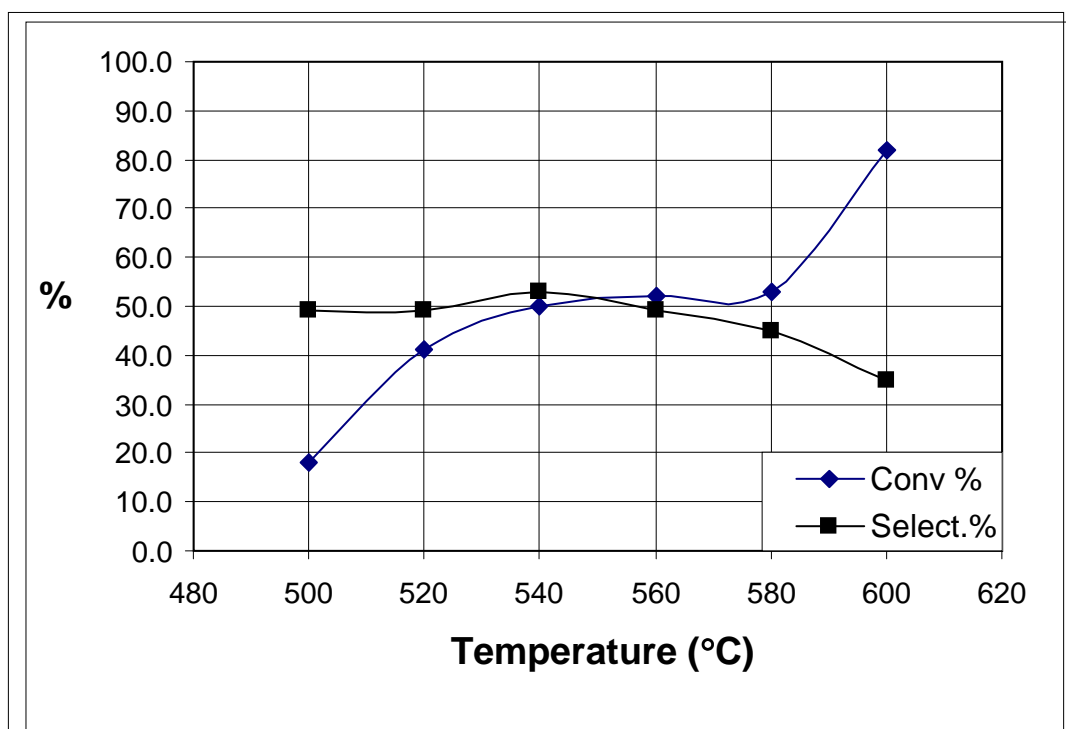
Purity after first distillation	85.6% <i>cis</i> -pinanol, 9.5% <i>trans</i> -pinanol, 4.9% <i>cis</i> -pinane
Purity after second distillation	88.9% <i>cis</i> -pinanol, 9.9% <i>trans</i> -pinanol, 1.2% <i>cis</i> -pinane
Purity after sublimation	95.8% <i>cis</i> -pinanol, 3.9% <i>trans</i> -pinanol

### 3.3 Pinanol pyrolysis – Initial investigation

In a previous study undertaken by AECL, Research and Development Department, the pyrolysis of *cis*-2-pinanol was investigated using a tubular, externally heated reactor system consisting of a quartz tube with diameter 0.025m and a length of 0.5m<sup>15</sup>. Pinanol was refluxed in a round bottom flask and nitrogen gas containing 5% ammonia was used as a carrier for the pinanol vapours to the tubular reactor. The experiments were carried out at various temperatures ranging from 500 to 600°C. Each set of experiments was performed in both an empty tube and in a packed bed. The results of these experiments are shown in **Tables 3.18** and **3.19** and graphically in **Figures 3.6** and **3.7**, respectively.

**Table 3.18: Pinanol pyrolysis in quartz tube without packing**

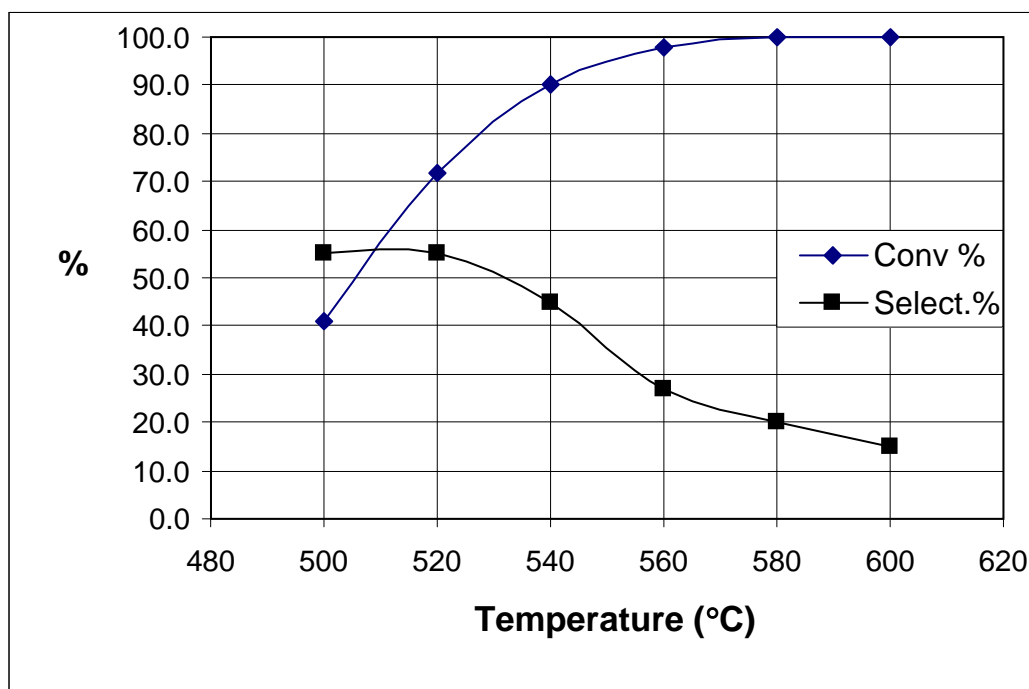
Exp.	Gas Flow	Temp	Conv	Select.
Ref.	L/min	C	%	%
QT-1	2.9	500	18.0	49.0
QT-2	2.9	520	41.0	49.0
QT-3	2.9	540	50.0	53.0
QT-4	2.9	560	52.0	49.0
QT-5	2.9	580	53.0	45.0
QT-6	2.9	600	82.0	35.0



**Figure 3.6: Pinanol pyrolysis in quartz tube without packing**

**Table 3.19: Pinanol pyrolysis in quartz tube with packing**

Exp.	Gas Flow	Temp	Conv	Select.
Ref.	L/min	C	%	%
QTP-1	2.9	500	41.0	55.0
QTP-1	2.9	520	72.0	55.0
QTP-1	2.9	540	90.0	45.0
QTP-1	2.9	560	98.0	27.0
QTP-1	2.9	580	100.0	20.0
QTP-1	2.9	600	100.0	15.0



**Figure 3.7: Pinanol pyrolysis in quartz tube with packing**

The highest conversion of pinanol in the unpacked reactor was 82% (Table 1, Figure 1). This occurred at a flow rate of the carrier gas of 2.9 L/min (or 0.52s residence time) and at a recorded temperature of approximately 600°C. The highest selectivity to linalool was only 53% and this was achieved at a conversion of 50% resulting in an overall yield of 26.5%. It was found that under these conditions, decomposition products totalled 35% of the total product. Higher flow rates were beneficial for the conversion of pinanol since the effect of heat transfer exceeds the effect of residence time. However, at these flows the selectivity of the pinanol conversion to linalool is the lowest (highest decomposition).

The effect of temperature on conversion and selectivity in the packed reactor is shown in Table 2, Figure 2. As opposed to the unpacked reactor, a conversion of more than 90% was observed at temperatures above 560°C. Over the operating range of 500 - 600°C no significant effect of residence time was observed, the highest selectivity to linalool in the reactor packed with quartz Raschig rings was 60%. The scatter of conversion and selectivity was attributed to the operation at different initial concentrations of pinanol and analytical inaccuracy.

In general, it was found that at all flow rates, the reactor packed with quartz Raschig rings performed better than the unpacked reactor. However, the rapid decrease of selectivity with increasing operating temperature was observed in the case of the packed reactor. The decomposition decreased as the flow rate through the reactor increased primarily as a result of reduced residence time. At higher temperatures, the unpacked reactor yielded more linalool than the packed reactor, but in both cases decomposition increased as temperature increased. Above 520°C, decomposition in the packed reactor increased dramatically, while in the unpacked reactor, substantial decomposition occurred at 580°C.

### 3.4 Pinanol pyrolysis – Screening experiments

During the pinanol pyrolysis investigation, the following variables were screened to determine their effect on *cis*-pinanol conversion and linalool selectivity:

- Solvent
- Pinanol concentration
- Vacuum pyrolysis
- Inert packing material
- Various materials of construction
- Zeolites
- Pyridine
- Nitrogen/ammonia mixture

#### 3.4.1 n-Butanol base case

In previous work conducted by Semikolenov and co-workers<sup>61</sup>, the pyrolysis of pinanol was conducted using n-butanol as diluent in an n-butanol/pinanol mass ratio of 9:1. The *cis/trans* pinanol ratio was 3:1 whereas in this investigation it was 9:1 at a *cis*-pinanol purity of 85%. The reaction in n-butanol was used as the benchmark or base case against which subsequent reactions were measured. All reactions were carried out in the 4.6mm ID stainless steel tubular reactor.

The results for the reactions carried out in n-butanol are given in **Tables 3.20** and **3.21** and illustrated graphically in **Figure 3.8**.

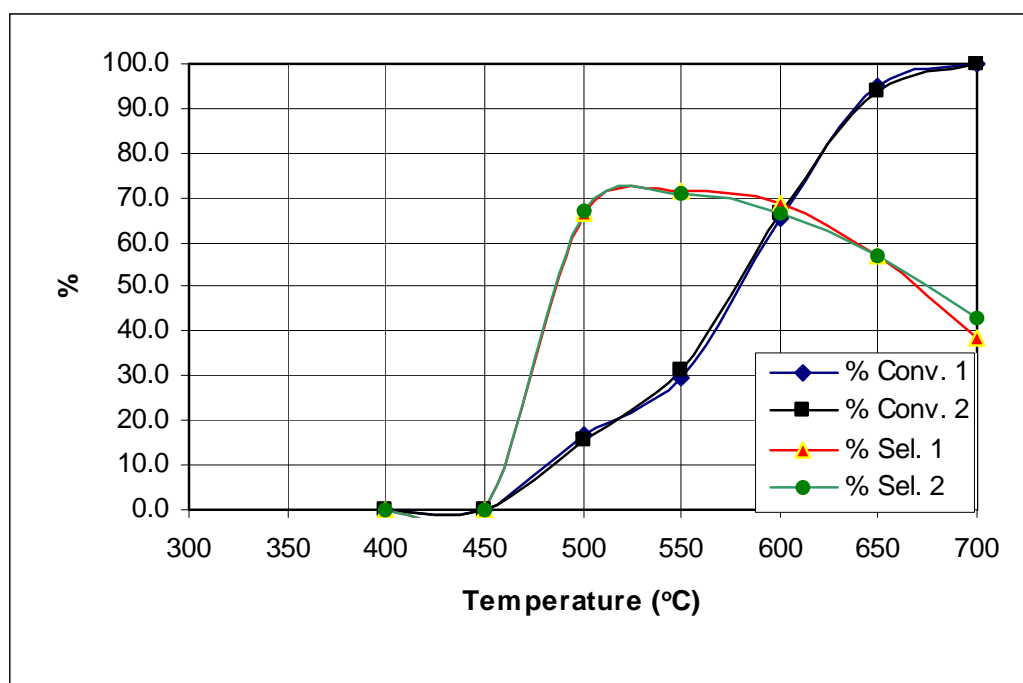


**Table 3.20: Pinanol pyrolysis using *n*-butanol as diluent**

Exp.	[Pinanol]	Solvent	SM Flow	Gas Flow	Temp	Conv	Select.
Ref.	%mm		ml/min	ml/min	°C	%	%
TR-But-1.1	10	<i>n</i> -butanol	0.5	10	400	0.0	0.0
TR-But-1.2	10	<i>n</i> -butanol	0.5	10	450	0.0	0.0
TR-But-1.3	10	<i>n</i> -butanol	0.5	10	500	16.7	66.4
TR-But-1.4	10	<i>n</i> -butanol	0.5	10	550	29.4	71.3
TR-But-1.5	10	<i>n</i> -butanol	0.5	10	600	65.3	68.6
TR-But-1.6	10	<i>n</i> -butanol	0.5	10	650	95.0	56.8
TR-But-1.7	10	<i>n</i> -butanol	0.5	10	700	100	38.5

**Table 3.21: Pinanol pyrolysis using *n*-butanol as diluent-repeat**

Exp.	[Pinanol]	Solvent	SM Flow	Gas Flow	Temp	Conv	Select.
Ref.	%mm		ml/min	ml/min	°C	%	%
TR-But-2.1	10	<i>n</i> -butanol	0.5	10	400	0.0	0.0
TR-But-2.2	10	<i>n</i> -butanol	0.5	10	450	0.0	0.0
TR-But-2.3	10	<i>n</i> -butanol	0.5	10	500	15.8	67.3
TR-But-2.4	10	<i>n</i> -butanol	0.5	10	550	31.4	71.2
TR-But-2.5	10	<i>n</i> -butanol	0.5	10	600	66.5	66.4
TR-But-2.6	10	<i>n</i> -butanol	0.5	10	650	94.1	57.0
TR-But-2.7	10	<i>n</i> -butanol	0.5	10	700	100	43.2

**Figure 3.8: Pinanol pyrolysis using *n*-butanol as diluent**

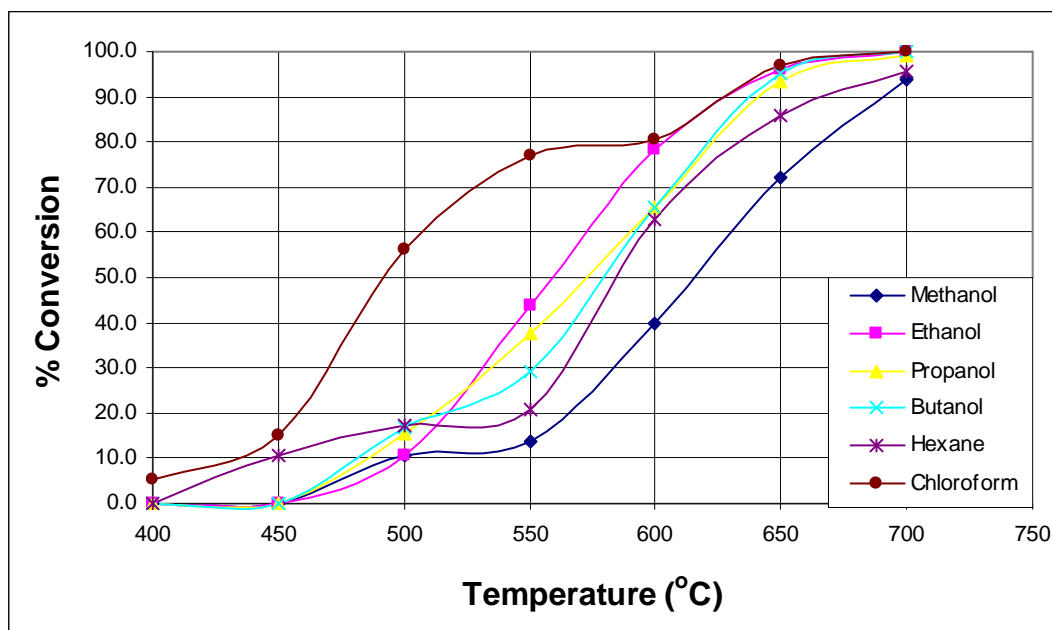
The graphs and figure clearly shows that initially there is no conversion at 400 and 450 °C. However, as the temperature was increased, there was a steady increase in the percentage conversion, with complete conversion being achieved at 700 °C. In the previous investigation complete conversion was achieved at 580 °C in the packed reactor and the maximum conversion in the unpacked reactor was 82% at 600 °C. The maximum selectivity (71.3%) was achieved at 550 °C and then dropped to ~40% as the temperature was increased. The reasons for the decrease in selectivity is discussed in greater detail in § 3.9 (Reaction Kinetics) and § 3.10 (General Discussion). The results show a significant improvement in selectivity when compared to the previous investigation where the highest selectivity achieved (both packed and unpacked reactor) was only 55%. There is obviously a trade-off between conversion and selectivity but from a downstream processing viewpoint, it makes more sense to obtain a high selectivity at a reasonably lower conversion (~30% to achieve an acceptable productivity rate) since it is more difficult to separate the by-products from the product (based on boiling point differences) than it is to separate pinanol from linalool. In addition, this also makes economic sense since the pinanol can always be recycled after vacuum distillation.

### 3.4.2 Effect of solvent

The results for these experiments are given in **Tables 3.22, 3.23** and **Figures 3.9, 3.10**.

**Table 3.22: Effect of solvent on pinanol conversion**

Temp.	% Conversion in solvent					
	Methanol	Ethanol	Propanol	Butanol	Hexane	Chloroform
400	0.0	0.0	0.0	0.0	0.0	5.2
450	0.0	0.0	0.0	0.0	10.7	15.0
500	10.5	10.8	15.6	16.7	17.4	56.4
550	13.5	43.6	37.8	29.4	21.0	76.9
600	39.8	78.5	65.7	65.3	63.0	80.5
650	72.2	96.2	93.5	95.0	85.9	97.1
700	93.7	100	99.2	100	95.7	100

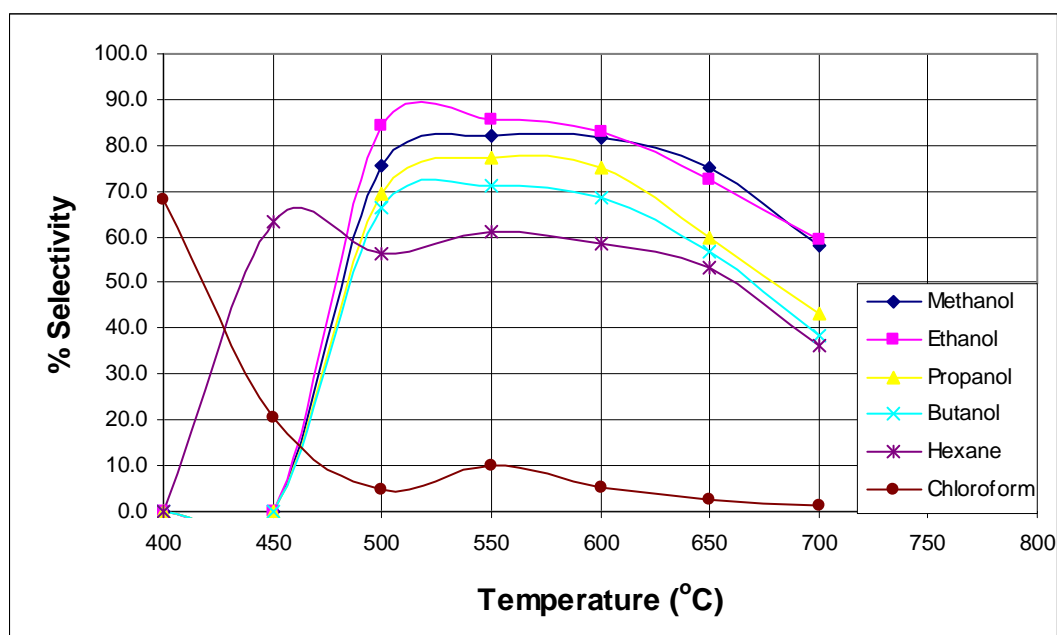


**Figure 3.9: Effect of solvent on pinanol conversion**

All the solvents seemed to have followed a similar trend as far as increasing conversion with temperature was concerned. At the lower temperatures conversion in chloroform was somewhat higher but was similar at the upper end of the temperature scale. The conversion in the alcohols generally increased with an increase in chain length with just ethanol showing a deviation from this trend. Hexane showed a similar trend to the alcohols. The increase in conversion with the increase in chain length is to be expected due to the higher heat transfer characteristics of the higher boiling solvents. In the case of chloroform, the solvent did not appear to be inert since the solvent became darker with increase in temperature. At 650 °C the solvent was completely black whereas the other mixtures were a straw yellow colour. This clearly indicated decomposition of both the solvent and the pinanol mixture. This observation is supported by the selectivity results.

**Table 3.23: Effect of solvent on linalool selectivity**

Temp.	% Selectivity in solvent					
	Methanol	Ethanol	Propanol	Butanol	Hexane	Chloroform
400	0.0	0.0	0.0	0.0	0.0	68.3
450	0.0	0.0	0.0	0.0	63.4	20.5
500	75.5	84.1	69.3	66.4	56.2	4.8
550	82.3	85.8	77.2	71.3	61.3	9.9
600	81.6	82.9	74.9	68.6	58.7	5.2
650	75.1	72.3	59.8	56.8	53.2	2.5
700	58.1	59.2	43.1	38.5	36.1	1.3

**Figure 3.10: Effect of solvent on linalool selectivity**

The selectivity results for chloroform clearly indicate that extensive decomposition had taken place during the reaction. The GC trace showed numerous peaks indicating that decomposition of the starting material/product had indeed taken place. This obviously excludes chloroform as a suitable solvent for the pyrolysis reaction. The selectivity in hexane was also lower than the butanol base case reaction.

The selectivity seemed to generally decrease with increasing chain length of the alcohols with ethanol and methanol showing very similar results. The highest selectivity (85.8%) was achieved in ethanol at 550°C. At this temperature the selectivity in methanol was 82.3%. Either of these solvents would then be suitable for

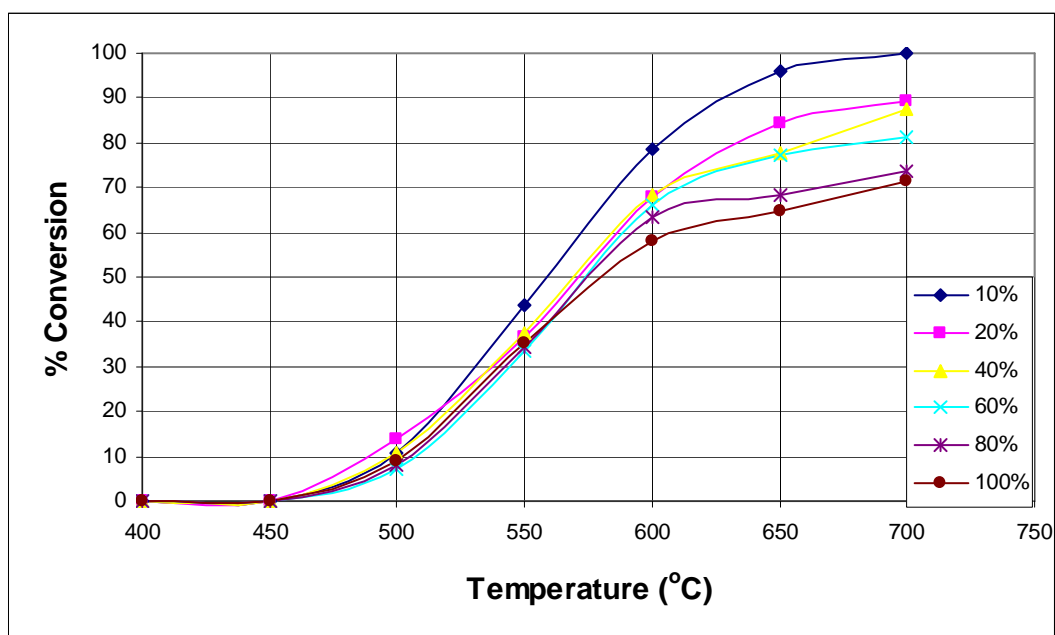
the pyrolysis reaction both from a processing (easier to distil) and from an economic (cheaper solvents) viewpoint.

### 3.4.3 Effect of pinanol concentration using ethanol as diluent

The effect of pinanol concentration on conversion and selectivity was determined at various temperatures using ethanol as the solvent of choice. The results for these experiments are given in **Tables 3.24, 3.25** and **Figures 3.11, 3.12**.

**Table 3.24: Effect of pinanol concentration on conversion**

Temp.	% Conversion at various pinanol concentrations					
	10%	20%	40%	60%	80%	100%
400	0.0	0.0	0.0	0.0	0.0	0.0
450	0.0	0.0	0.0	0.0	0.0	0.0
500	10.8	13.7	10.6	7.3	8.1	8.8
550	43.6	36.8	37.6	33.3	34.3	35.2
600	78.5	67.9	68.1	66.1	63.3	58.2
650	96.2	84.4	77.5	77.2	68.4	64.8
700	100	89.3	87.7	81.3	73.5	71.3



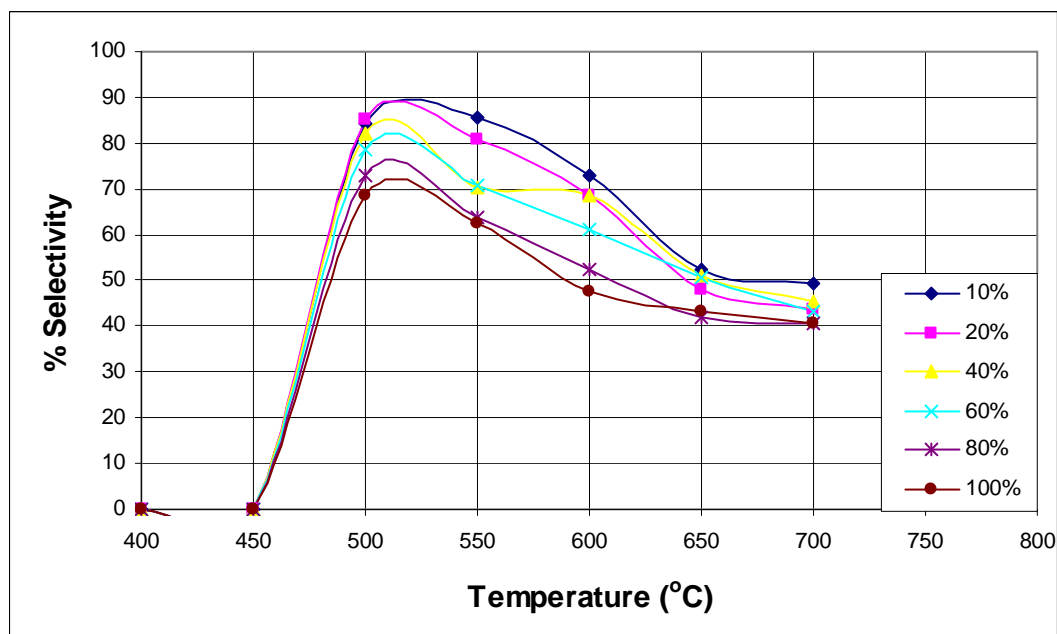
**Figure 3.11: Effect of pinanol concentration on conversion**

The results clearly indicate that conversion decreases with an increase in concentration of pinanol at the various temperatures and becomes more pronounced at

the upper end of the temperature scale. This result is expected as there is a limited surface area where the pinanol molecules can make contact in the tubular reactor. At the lower concentrations the pinanol molecules would be better dispersed in the gas phase and since there are fewer molecules per surface area we would expect more of them to make effective contact with the hot surface and thus be converted. On the other hand, while the percentage conversion may be reduced, the throughput would obviously be higher at higher concentrations and one would have to consider this when selecting conditions for scale-up.

**Table 3.25: Effect of pinanol concentration on linalool selectivity**

% Selectivity at various pinanol concentrations						
Temp.	10%	20%	40%	60%	80%	100%
400	0.0	0.0	0.0	0.0	0.0	0.0
450	0.0	0.0	0.0	0.0	0.0	0.0
500	84.1	85.2	82.3	78.4	72.8	68.7
550	85.8	80.8	70.5	70.6	63.9	62.5
600	72.9	68.5	68.4	61.2	52.2	47.6
650	52.3	47.9	51.0	50.7	41.9	43.3
700	49.2	43.6	45.2	43.2	40.4	40.4



**Figure 3.12: Effect of pinanol concentration on linalool selectivity**

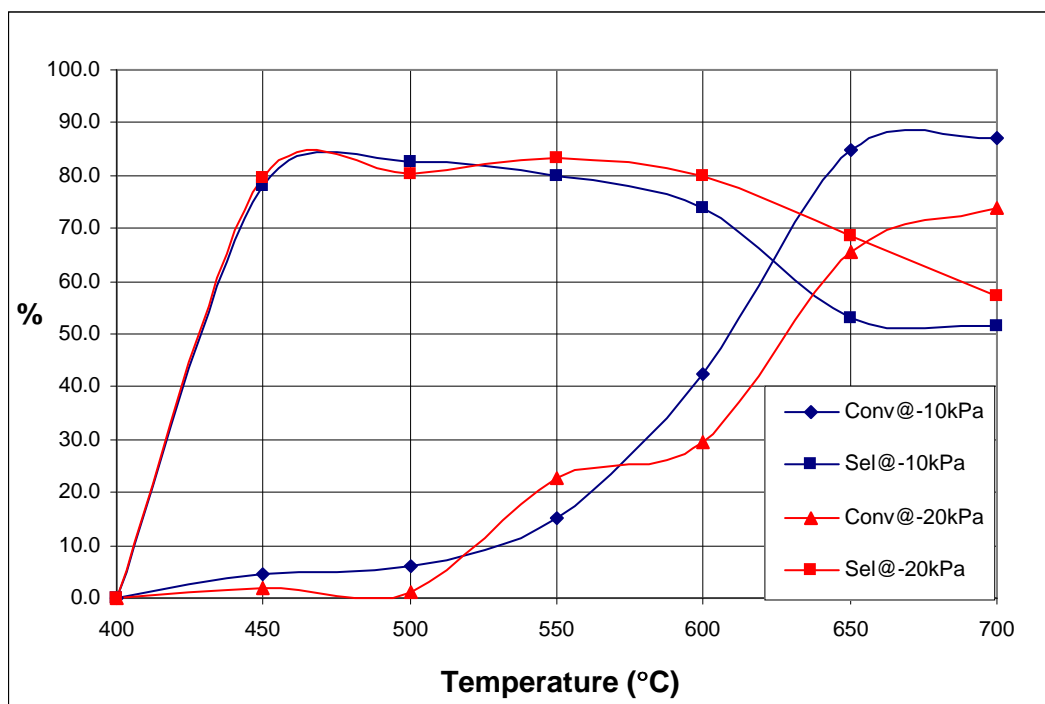
A similar effect to that observed for conversion, was also observed in the selectivity results. The highest selectivity (85.8%) was observed at 550 °C at a concentration of 10% with similar results (85.2%) also at 500°C and 20% concentration. The diluting effect of the solvent is negated at the higher concentrations which means that more linalool molecules are exposed per surface area and are therefore subject to further reaction thus producing larger amounts of by-products (**refer to § 3.9 and § 3.10**). Once again, the throughput of the production process needs to be considered and one should choose the conditions that would give the desired product purity at maximum throughput.

#### 3.4.4 Vacuum pyrolysis

The results for the pyrolysis reactions done under vacuum are given in **Table 3.26** and **Figure 3.13**. Ethanol was used as the diluent.

**Table 3.26: Pinanol pyrolysis under vacuum**

Temp.	Conversion and selectivity at -10 and -20 kPa			
	-10kPa		-20kPa	
	% Conv.	%Sel.	% Conv	% Sel.
400	0.0	0.0	0.0	0
450	4.5	78.2	1.8	79.7
500	6.0	82.5	1.3	80.2
550	15.1	80.0	22.7	83.4
600	42.3	73.9	29.5	80.1
650	84.7	53.2	65.6	68.5
700	87.3	51.5	73.9	57.2



**Figure 3.13: Pinacol pyrolysis under vacuum**

Reactions were done under vacuum conditions to prove that it would be possible to conduct the reaction in the absence of an inert gas. Both the conversion and selectivity were somewhat lower than for the base case in ethanol under similar conditions, so no real advantages are offered. It was also difficult to control the feed rate since the vacuum tended to suck the feed uncontrollably past the piston pump. While there would be a minor saving on nitrogen requirements this could be offset by higher capital and maintenance costs for a vacuum system. The post-reactor condensation system would also have to be more efficient since the liquids would boil at a reduced temperature and would require lower temperatures for efficient condensation.

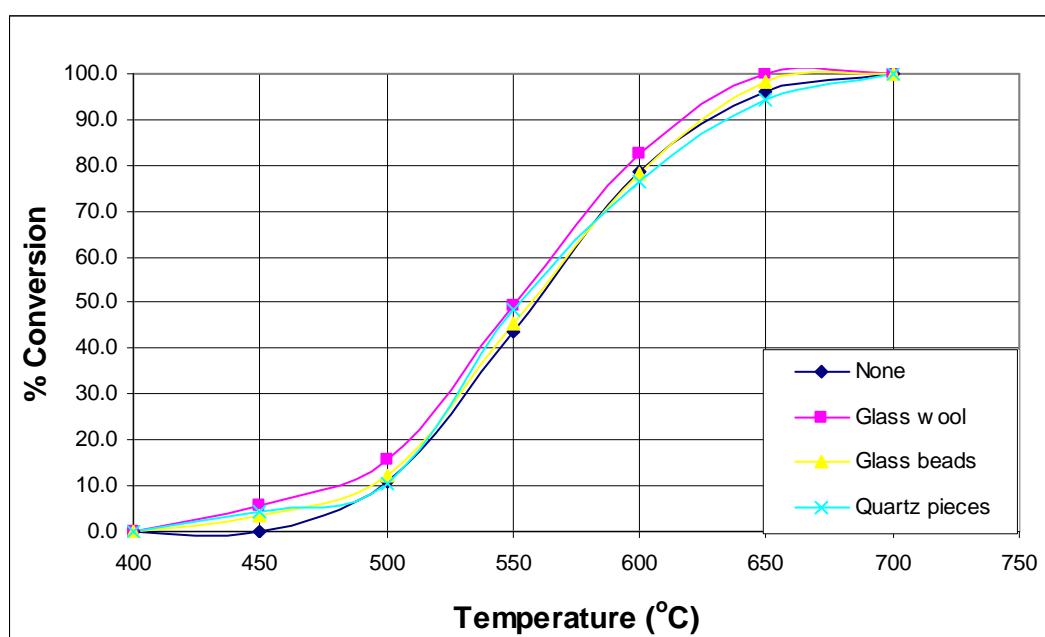
### 3.4.5 Effect of inert packing

In this series of experiments, the effect of inert packing material on conversion and selectivity was investigated. The results for these experiments are given in **Tables 3.27, 3.28** and **Figures 3.14 and 3.15**.



**Table 3.27: Effect of inert packing on pinanol conversion**

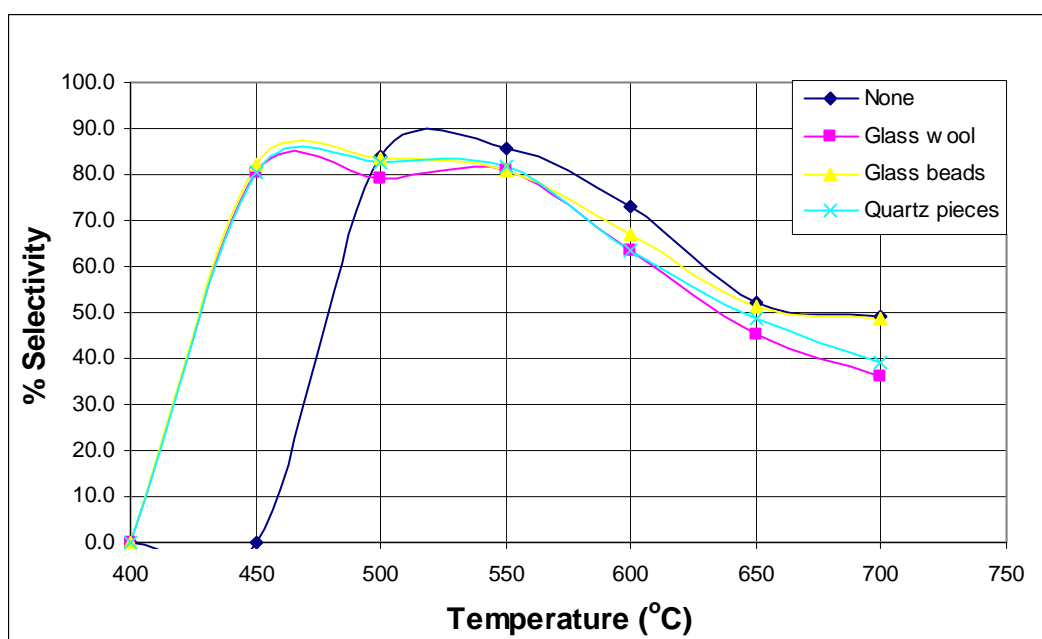
Temp.	Pinanol conversion (%)			
	None	Glass wool	Glass beads	Quartz pieces
400	0.0	0.0	0.0	0.0
450	0.0	5.6	3.6	4.2
500	10.8	15.7	12.3	10.5
550	43.6	49.3	45.2	48.6
600	78.5	82.5	78.3	76.5
650	96.2	100	98.4	94.3
700	100	100	100	100

**Figure 3.14: Effect of inert packing on pinanol pyrolysis**

In the initial investigation conducted by AECI R&D, inert packing material seemed to have a small effect on both conversion and selectivity. As far as conversion was concerned, a slight increase (49.3% @ 550 °C for glass wool) was observed when compared to the ethanol base case (43.6% @ 550 °C), where no packing was utilised. The highest conversions at the various temperatures were observed with glass wool. One would expect the gas hold up to be more pronounced with glass wool because of the finer, more compact needle-like glass fibres than the round glass beads with larger spaces in-between beads. This would result in a larger heated surface area for reaction to take place and which could explain the observed increase in conversion.

**Table 3.28: Effect of inert packing on linalool selectivity**

Temp.	Inert packing and Linalool selectivity (%)			
	None	Glass wool	Glass beads	Quartz pieces
400	0.0	0.0	0.0	0.0
450	0.0	80.5	82.1	80.3
500	84.1	79.2	83.4	82.5
550	85.8	81.0	80.9	81.6
600	72.9	63.5	66.8	63.4
650	52.3	45.1	51.3	48.7
700	49.2	36.3	48.5	39.2

**Figure 3.15: Effect of inert packing on linalool selectivity**

The results in Table 3.28 on the other hand showed a slight decrease in selectivity with packing at similar temperatures compared to when packing was absent e.g. 85.8% at 550 °C (no packing) and 81.0% at the same temperature for glass wool. These observations are probably the result of increased residence time of the reaction mixture in the heated zone in the packed reactor tubes. Increased residence time can have an effect both on conversion and selectivity. A longer residence time, while resulting in higher conversions of pinanol, also exposes the linalool molecule for a longer period to the higher surface temperatures and this may result in more by-products and hence lower selectivity. There is also the possibility that with prolonged usage of the reactor (as in a continuous process) there will be a build-up of coke deposits and a possibility

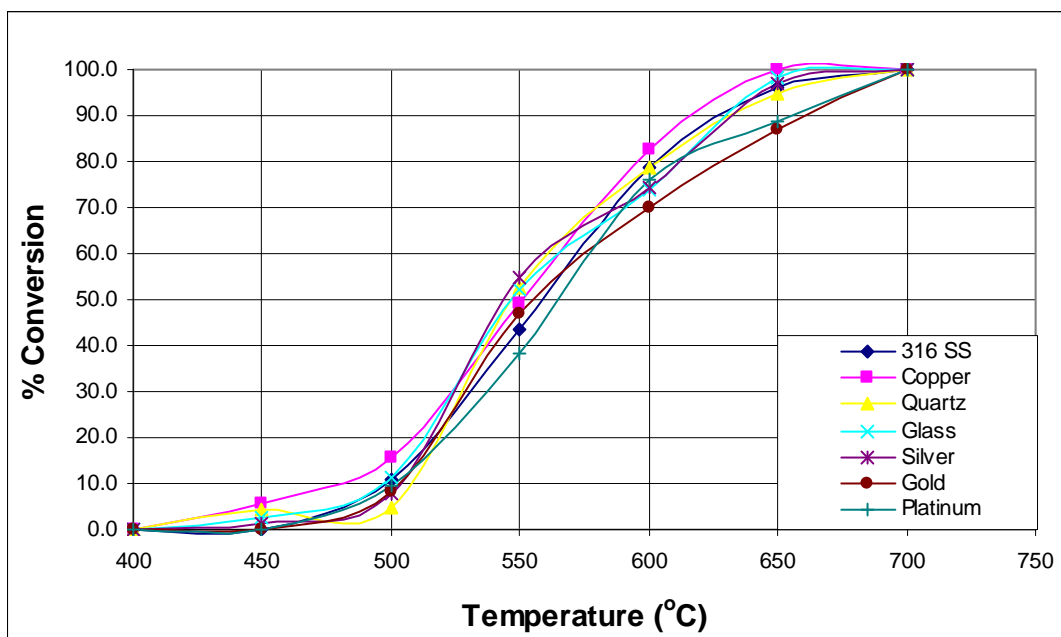
of blockages with a packed bed reactor. The inert packing material therefore offers no advantages as far as reaction and process performance is concerned.

#### 3.4.6 Effect of various reactor materials

In this type of pyrolysis reaction, the materials of construction used in the pyrolysis zone are critical from an operability as well as economic perspective. Firstly, very high temperatures are used which could affect the useful lifetime of the materials and obviously have an effect on cost of replacement. Secondly, the heat transfer characteristics of the material are important for efficient power usage and utilisation of electricity for heating. Thirdly, it is important to ensure that the material is inert and does not negatively affect the performance of the reaction in terms of conversion and more importantly, selectivity. From a reactivity point of view, it would also be interesting to determine if any of the materials had any catalytic effect. The investigation was conducted bearing all these factors in mind and the results for these experiments are shown in **Tables 3.29, 3.30** and **Figures 3.16, 3.17**.

**Table 3.29: Effect of various materials on pinanol conversion**

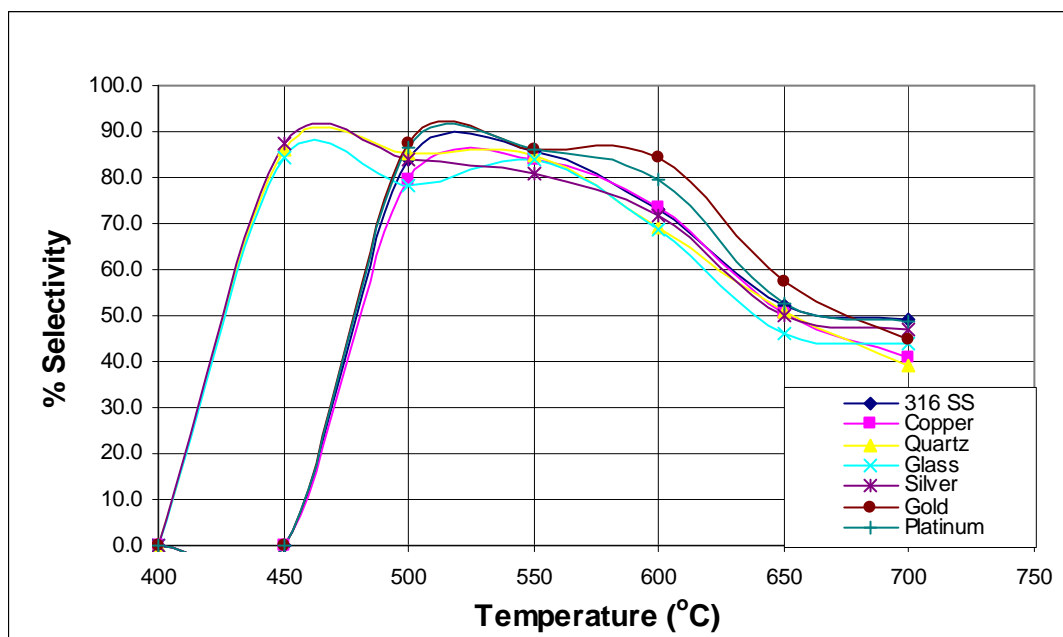
Effect of various materials on pinanol conversion (%)							
Temp.	316 SS	Copper	Quartz	Glass	Silver	Gold	Platinum
400	0.0	0.0	0.0	0.0	0.0	0.0	0.0
450	0.0	0.0	4.2	2.4	1.5	0.0	0.0
500	10.8	15.7	4.8	11.1	8.0	8.1	9.5
550	43.6	49.3	52.7	52.3	55.0	46.9	38.1
600	78.5	82.5	78.5	73.7	74.2	70.2	76.1
650	96.2	100.0	94.6	98.1	96.9	87.0	88.8
700	100	100	100.0	100.0	100.0	100.0	100.0



**Figure 3.16: Effect of various materials on pinacol conversion**

**Table 3.30: Effect of various materials on linalool selectivity**

Temp.	Linalool selectivity (%)						
	316 SS	Copper	Quartz	Glass	Silver	Gold	Platinum
400	0.0	0.0	0.0	0.0	0.0	0.0	0.0
450	0.0	0.0	86.0	84.5	87.3	0.0	0.0
500	84.1	79.4	85.3	78.4	83.7	87.3	86.6
550	85.8	83.9	84.6	84.0	81.0	86.2	85.9
600	72.9	73.3	69.1	68.6	71.9	84.5	79.6
650	52.3	50.4	50.9	45.9	49.8	57.4	52.6
700	49.2	40.9	39.2	44.1	46.9	44.7	48.7



**Figure 3.17: Effect of various materials on linalool selectivity**

In terms of both conversion and selectivity, there did not appear to be any significant differences between the use of various materials and no significant improvements over the 316SS base case are noticeable. In terms of conversion, copper displayed the highest conversion across the temperature range. Copper is a very good conductor of heat and the increase could be attributed to this fact. In terms of selectivity, the gold coated 316SS reactor had the highest selectivity across the temperature range. However, even coating of the reactor with gold nanoparticles would still be an expensive exercise and the improvement was only marginal which does not warrant its use from a capital cost perspective. Glass is also not a very robust material, especially on large scale, and the joining of glass tubing to steel components would not be a trivial exercise. None of the materials investigated, displayed any catalytic activity.

Although, the investigation showed that in terms of performance there wasn't much to choose between the various materials, from a scalability point of view, 316 stainless steel would be the best material to use. Stainless steel is robust, readily available, relatively inexpensive and very easy to machine and fit into existing plant structures. Over time there was also evidence of coke build-up which means that the tubular

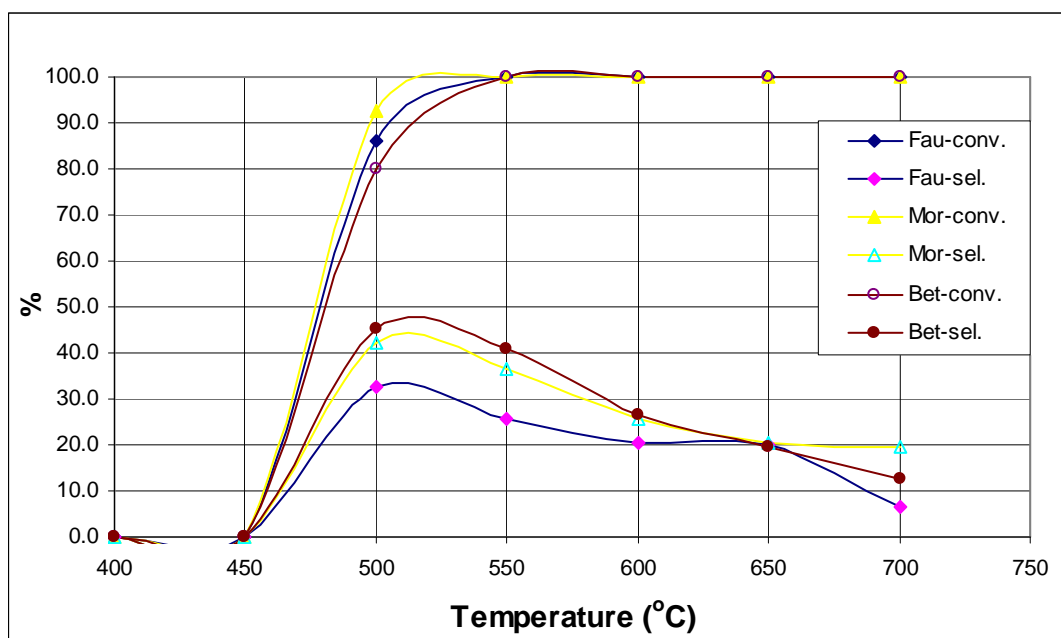
reactors would have to be occasionally removed and cleaned and this could be easily done with 316 SS.

### 3.4.7 Effect of zeolites

In this investigation three zeolites, viz. faujasite, mordenite, and beta zeolite, were tested for their catalytic activity in the pinanol pyrolysis reaction. The results for these experiments are shown in **Table 3.31** and **Figure 3.18**.

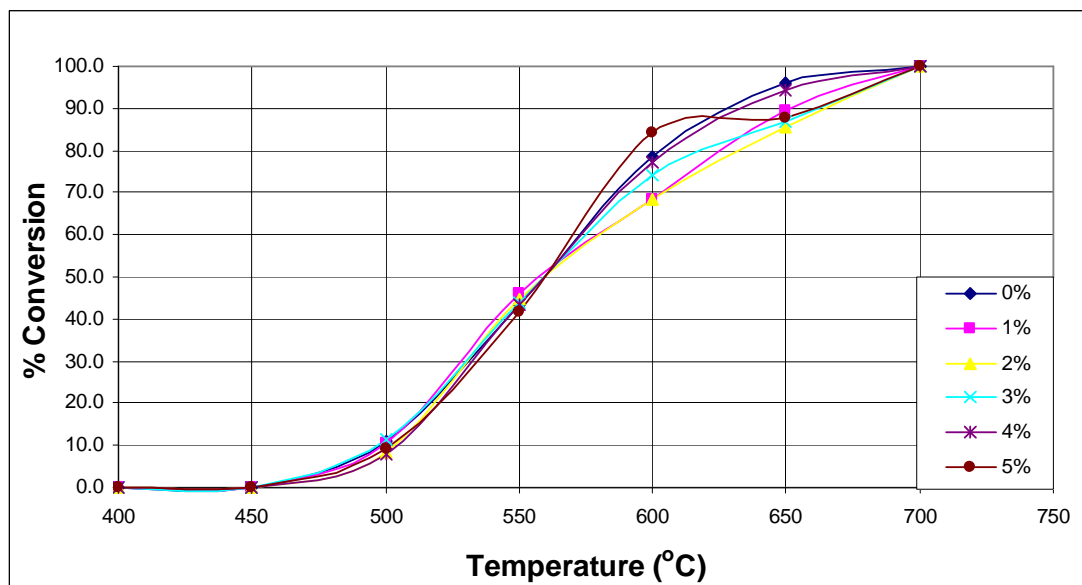
**Table 3.31: Effect of zeolite catalysts on conversion and selectivity**

Temp C	Effect of zeolites on % conversion and selectivity					
	faujasite		mordenite		beta	
	Conv %	Select. %	Conv %	Select. %	Conv %	Select. %
400	0.0	0.0	0.0	0.0	0.0	0.0
450	0.0	0.0	0.0	0.0	0.0	0.0
500	85.9	32.4	92.6	42.3	79.8	45.3
550	100.0	25.6	100.0	36.4	100.0	40.9
600	100.0	20.5	100.0	25.8	100.0	26.5
650	100.0	19.8	100.0	20.6	100.0	19.7
700	100.0	6.5	100.0	19.7	100.0	12.8



**Figure 3.18: Effect of zeolite catalysts on conversion and selectivity**





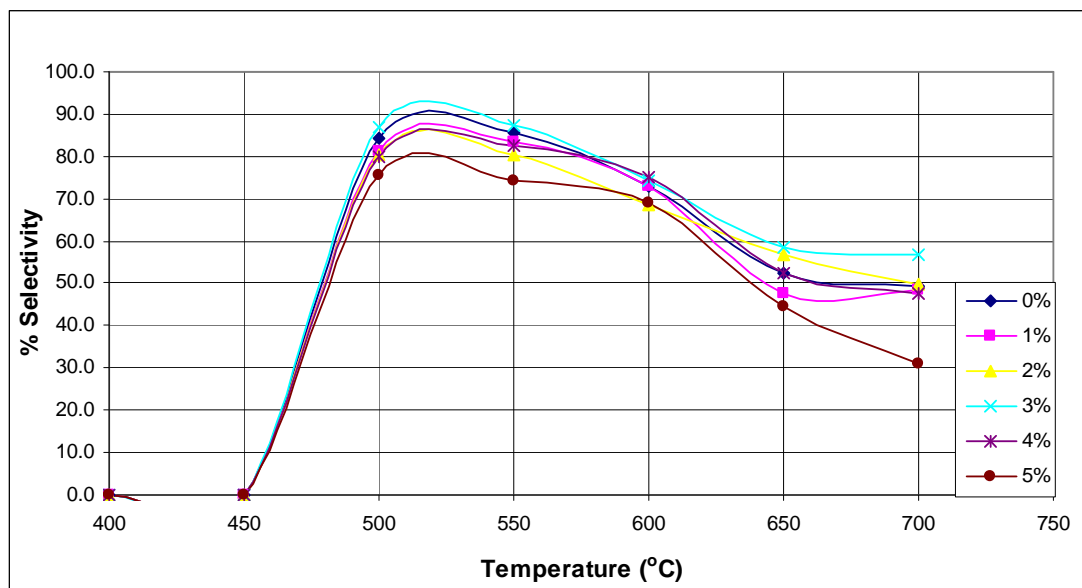
**Figure 3.19: Effect of pyridine concentration on pinanol conversion**

In terms of conversion, there did not appear to be significant differences between the base case and the experiments where pyridine was used, especially at the lower temperatures.

**Table 3.33: Effect of pyridine concentration on linalool selectivity**

Temp.	% Selectivity at various pyridine concentrations					
	0%	1%	2%	3%	4%	5%
400	0.0	0.0	0.0	0.0	0.0	0.0
450	0.0	0.0	0.0	0.0	0.0	0.0
500	84.1	81.3	80.4	87.0	80.0	75.5
550	85.8	83.2	80.2	87.2	82.5	74.2
600	72.9	73.0	68.4	74.2	74.9	69.0
650	52.3	47.6	56.7	58.6	52.6	44.5
700	49.2	48.4	49.6	56.9	47.8	31





**Figure 3.20: Effect of pyridine concentration on linalool selectivity**

It was found that there was no substantial improvement in the selectivity to linalool, e.g. at 550°C the selectivity for the base case was 85.8% and the highest selectivity (at 3% concentration) for pyridine was 87.2%. Although a slight improvement was achieved, the additional cost of pyridine coupled with complications in the downstream processing would not be warranted. However, a general trend was observed as the pyridine concentration was increased. The selectivity peaked at 3% pyridine (87.2% at 550°C) but generally decreased as the pyridine concentration was increased to 5% (75.5% at 550°C).

### 3.4.9 Effect of ammonia

Since it was observed that the addition of bases did have a positive effect on linalool selectivity (§ 3.4.8) it was decided to test the addition of ammonia. The effect of a 5% ammonia/nitrogen mixture on the conversion and selectivity response was measured and compared to the use of nitrogen only, which was the control. There were two different levels and ten replications giving a total of twenty observations for each of the responses. The responses used for the one factor statistical design was conversion of pinanol and selectivity to linalool. Each of the responses were analysed separately.

### 3.4.9.1 Analysis of conversion response

The conversion results for the ammonia/nitrogen mixture and pure nitrogen are given in **Table 3.34**.

**Table 3.34: Conversion response for ammonia vs nitrogen**

Run No.	% Conversion	
	N <sub>2</sub>	NH <sub>3</sub> /N <sub>2</sub>
1	46.1	47.3
2	44.7	50.1
3	48.7	44.5
4	40.2	52.2
5	48.3	52.8
6	44.9	50.4
7	45.1	42.4
8	41.3	49.4
9	43.3	40.1
10	43.6	45.3
<b>Ave.</b>	<b>44.6</b>	<b>47.5</b>

The ANOVA (Analysis of variance) results are shown in **Table 3.35**.

**Table 3.35: Conversion ANOVA**

Source	Sum of squares	DF	Mean square	F Value	Prob>F
<b>Model</b>	40.04	1	40.04	3.14	0.0934
<i>A</i>	<i>40.04</i>	<i>1</i>	<i>40.04</i>	<i>3.14</i>	<i>0.0934</i>
<b>Pure Error</b>	229.62	18	12.76		
<b>Cor Total</b>	269.67	19			
<b>Pred R-squared</b>	-0.0512				
<b>Adj R-squared</b>	0.1012				
<b>Adeq precision</b>	2.506				

The Model F-value of 3.14 implies there is a 9.34% chance that a "Model F-Value" this large could occur due to noise. Values of "Prob > F" less than 0.0500 indicate model terms are significant. In this case there are no significant model terms.

A negative "Pred R-Squared" (-0.0512) implies that the overall mean is a better predictor of the response than the current model. "Adeq Precision" measures the signal to noise ratio. A ratio of 2.51 indicates an inadequate signal (<4) and therefore this model should not be used to navigate the design space.

The analysis of the various treatments are shown in **Table 3.36**.

**Table 3.36: Conversion: Analysis of treatments**

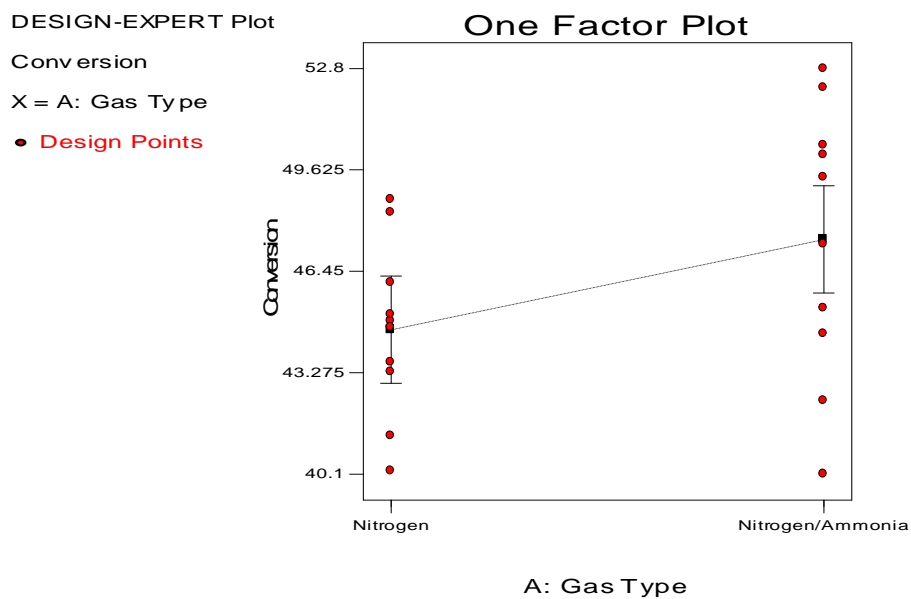
Standard	Estimated	
	Mean	Error
1-Nitrogen	44.62	1.13
2-Nitrogen/Ammonia	47.45	1.13

Treatment	Mean Difference	Standard DFEror	t for H <sub>0</sub> Coeff=0	Prob >  t
1 vs 2	-2.83	11.60	-1.77	0.0934

The "Prob>|t" value is greater than 0.05% which indicates that there are no significant differences between the two treatments as far as the conversion response is concerned, at the 95% significance level.

A One factor plot for the two treatments is shown in **Figure 3.21**.



**Figure 3.21: Conversion: One Factor Plot for two treatments**

The one factor plot shows that there is very little difference between the average conversions for the two treatments i.e. 2.83%. The addition of ammonia therefore had no significant effect as far as conversion was concerned.

### 3.4.9.2 Analysis of selectivity response

The selectivity results for the ammonia/nitrogen mixture and pure nitrogen are given in **Table 3.37**.

**Table 3.37: Selectivity response for ammonia vs nitrogen**

Run No.	% Selectivity	
	N <sub>2</sub>	NH <sub>3</sub> /N <sub>2</sub>
1	76.5	85.5
2	79.4	81.1
3	82.2	78.5
4	77.3	86.2
5	80.3	86.1
6	78.0	78.9
7	77.3	86.0
8	83.9	82.5
9	83.8	88.4
10	83.7	81.0
<b>Ave.</b>	<b>80.2</b>	<b>83.4</b>

The ANOVA (Analysis of variance) results are shown in **Table 3.38**.

**Table 3.38: Selectivity ANOVA**

Source	Sum of squares	DF	Mean square	F Value	Prob>F
<b>Model</b>	50.56	1	50.56	4.89	0.0403
<b>A</b>	50.56	1	50.56	4.89	0.0403
<b>Pure Error</b>	186.30	18	10.35		
<b>Cor Total</b>	236.86	19			
<b>Pred R-squared</b>	0.1900				
<b>Adj R-squared</b>	0.1698				
<b>Adeq precision</b>	4.126				

The Model F-value of 4.89 implies the model is significant. There is only a 4.03% chance that a "Model F-Value" this large could occur due to noise. Values of "Prob >

F" less than 0.0500 indicate model terms are significant. In this case A is asignificant model term.

The "Pred R-Squared" of 0.1900 is in reasonable agreement with the "Adj R-Squared" of 0.1698. "Adeq Precision" measures the signal to noise ratio. A ratio of 4.13 indicates an adequate signal and therefore this model could be used to navigate the design space.

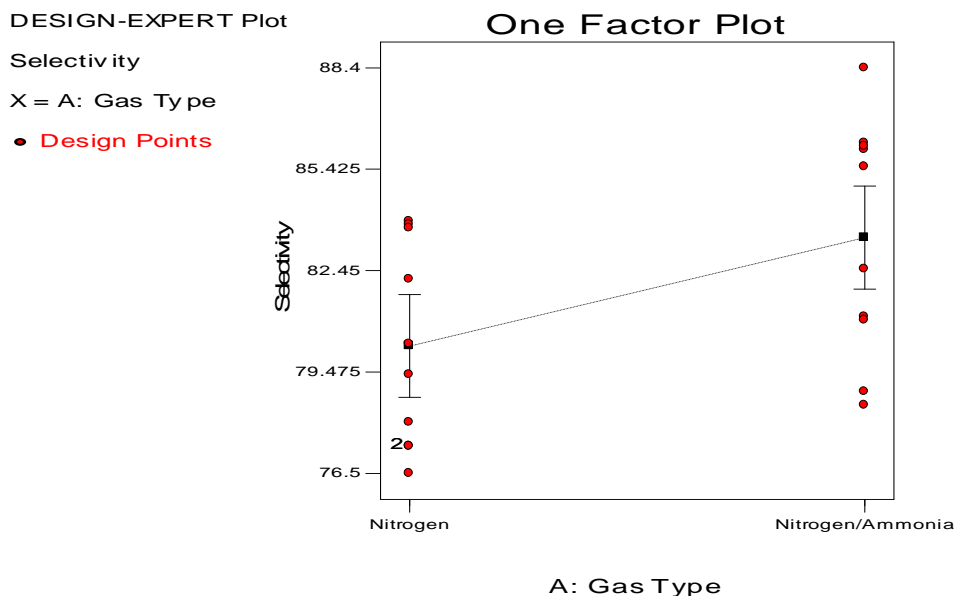
The analysis of the various treatments is shown in **Table 3.39**.

**Table 3.39: Selectivity: Analysis of treatments**

	<b>Estimated Mean</b>	<b>Standard Error</b>		
1-Nitrogen	80.24	1.02		
2-Nitrogen/Ammonia	83.42	1.02		
<b>Treatment</b>	<b>Mean Difference</b>	<b>Standard DF Error</b>	<b>t for H<sub>0</sub> Coeff=0</b>	<b>Prob &gt;  t </b>
1 vs 2	-3.18	11.44	-2.21	0.0403

The "Prob>|t|" value is greater than 0.05% which indicates that there is a significant difference between the two treatments as far as the selectivity response is concerned, at the 95% significance level.

A One factor plot for the two treatments is shown in **Figure 3.22**.



**Figure 3.22: Selectivity: One Factor Plot for two treatments**

The one factor plot gives a visual representation of the differences in selectivity between the two treatments as well as showing the spread of the design points. The mean difference between the two treatments was 3.18%. From a process point of view, this difference would have to be factored in to see if there is a significant difference between the additional cost and product quality. However, unlike in the case of pyridine, the addition of ammonia could be easily incorporated into the process for the following reasons:

- It is relatively inexpensive;
- It can easily be incorporated into the existing gas stream or bought as a mixture from commercial suppliers of nitrogen;
- Since it's used in small quantities and is volatile it shouldn't interfere with the product specifications; and
- Since it is a gas it should be easy to separate from the final product.

### 3.5 Determination of important reaction variables

The important variables were determined by conducting a two level factorial statistical design. The four variables investigated were as follows:

- A: Temperature (°C)

- B: Inert gas flow rate (ml/min)
- C: Pinanol/ethanol flow rate (ml/min)
- D: Pinanol concentration (% m/m)

The results for these experiments are shown in **Table 3.40**.

**Table 3.40: Results of statistical design for the pyrolysis of a pinanol/ethanol mixture**

		Factor 1	Factor 2	Factor 3	Factor 4	Response 1	Response 2
Std	Run	A:Temp.	B:Gas Flow	C:Pinanol Flow	D:Pinanol conc.	Conversion	Selectivity
		°C	ml/min	ml/min	%m/m	%	%
2	1	650.00	10.00	0.20	10.00	83.6	61.9
10	2	650.00	10.00	0.20	30.00	85.0	41.7
6	3	650.00	10.00	1.00	10.00	26.8	92.6
8	4	650.00	20.00	1.00	10.00	33.8	84.3
14	5	650.00	10.00	1.00	30.00	30.5	84.3
18	6	575.00	15.00	0.60	20.00	16.6	68.0
16	7	650.00	20.00	1.00	30.00	20.2	83.5
3	8	500.00	20.00	0.20	10.00	35.2	59.7
1	9	500.00	10.00	0.20	10.00	24.4	69.1
4	10	650.00	20.00	0.20	10.00	52.5	59.8
17	11	575.00	15.00	0.60	20.00	18.1	69.0
11	12	500.00	20.00	0.20	30.00	29.0	71.4
15	13	500.00	20.00	1.00	30.00	1.4	96.2
7	14	500.00	20.00	1.00	10.00	3.0	93.4
13	15	500.00	10.00	1.00	30.00	13.7	67.5
9	16	500.00	10.00	0.20	30.00	10.9	81.5
5	17	500.00	10.00	1.00	10.00	15.3	66.7
12	18	650.00	20.00	0.20	30.00	51.2	54.7
19	19	575.00	15.00	0.60	20.00	16.9	66.4

### 3.5.1 Analysis of conversion response

#### 3.5.1.1 Selection of main effects

The effects and contribution of the various terms are shown in **Table 3.41**.

Table 3.41: Conversion – Effects list

	Term	Effect	Sum of Squares	% Contribtn
M	A	31.3375	3928.16	37.6078
M	B	-7.9875	255.201	2.44327
M	C	-28.3875	3223.4	30.8606
E	D	-4.0875	66.8306	0.639831
M	AB	-9.0625	328.516	3.14518
M	AC	-11.8625	562.876	5.38893
E	AD	1.6375	10.7256	0.102686
E	BC	1.0125	4.10062	0.039259
E	BD	-1.5875	10.0806	0.0965111
E	CD	0.8125	2.64063	0.0252811
M	ABC	14.3875	828.001	7.92721
E	ABD	-3.4125	46.5806	0.445959
E	ACD	-3.3125	43.8906	0.420205
E	BCD	-2.7375	29.9756	0.286984
E	ABCD	-0.9125	3.33062	0.0318871
M	Curvature	-15.6941	985.213	9.43235
E	Lack Of Fit		0	0
E	Pure Error		115.527	1.10604
	Lenth's ME	10.2616		
	Lenth's SME	18.8156		

DESIGN-EXPERT Plot  
Conversion

A: Temperature  
B: Gas Flow  
C: Pinanol Flow  
D: Pinanol conc.

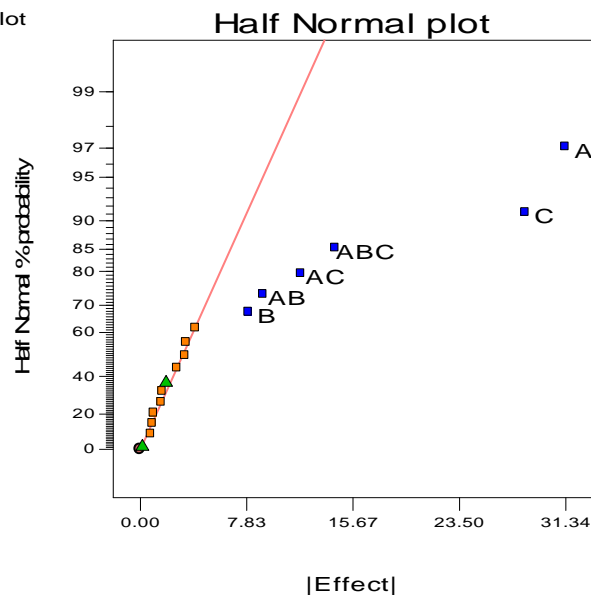


Figure 3.23: Conversion: Half-normal probability plot



The effects list shows the contribution of the most important factors in this design to the conversion response and this is also graphically illustrated in **Figure 3.23**. It is quite clear that the most important factors are A and C and there are also interactions between AB, AC, and ABC. While factor A (temperature, 37% contribution) has a positive effect, C (pinanol feed rate, 30% contribution) has a negative effect, meaning that as C is increased there is a corresponding decrease in the percentage conversion.

### 3.5.1.2 Conversion ANOVA

The analysis of variance (ANOVA) for the conversion response (after selection of most important terms) is shown in **Table 3.42**.

**Table 3.42: ANOVA for conversion response**

	<b>Sum of Squares</b>	<b>DF</b>	<b>Mean Square</b>	<b>F Value</b>	<b>Prob &gt; F</b>	
<b>Model</b>	9130.25	7	1304.32	39.58	< 0.0001	significant
<b>A</b>	3928.16	1	3928.16	119.19	< 0.0001	
<b>B</b>	255.20	1	255.20	7.74	0.0194	
<b>C</b>	3223.40	1	3223.40	97.80	< 0.0001	
<b>AB</b>	328.52	1	328.52	9.97	0.0102	
<b>AC</b>	562.88	1	562.88	17.08	0.0020	
<b>ABC</b>	828.00	1	828.00	25.12	0.0005	
<b>Curvature</b>	985.21	1	985.21	29.89	0.0003	significant
<b>Residual</b>	329.58	10	32.96			
<b>Lack of Fit</b>	214.06	8	26.76	0.46	0.8221	not significant
<b>Pure Error</b>	115.53	2	57.76			
<b>Cor Total</b>	10445.04	18				
<b>Pred R-squared</b>	0.9408					
<b>Adj R-squared</b>	0.8931					
<b>Adeq. Precision</b>	20.779					

The Model F-value of 39.58 implies the model is significant. There is only a 0.01% chance that a "Model F-Value" this large could occur due to noise. Values of "Prob > F" less than 0.0500 indicate model terms are significant. In this case A, B, C, AB, AC, ABC are significant model terms.

The "Curvature F-value" of 29.89 implies there is significant curvature (as measured by difference between the average of the center points and the average of the factorial points) in the design space. There is only a 0.03% chance that a "Curvature F-value" this large could occur due to noise.

The "Lack of Fit F-value" of 0.46 implies the Lack of Fit is not significant relative to the pure error. There is a 82.21% chance that a "Lack of Fit F-value" this large could occur due to noise. Non-significant lack of fit is good since we want the model to fit.

The "Pred R-Squared" of 0.8931 is in reasonable agreement with the "Adj R-Squared" of 0.9408. "Adeq Precision" measures the signal to noise ratio. A ratio greater than 4 is desirable. The ratio of 20.779 indicates an adequate signal. This model can therefore be used to navigate the design space.

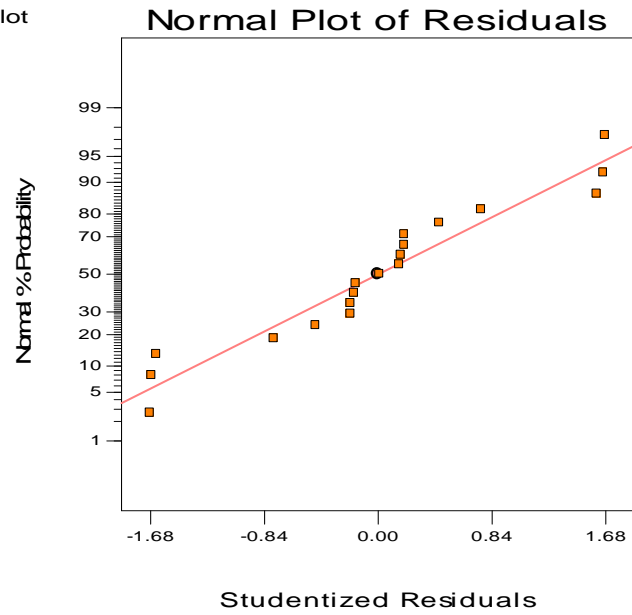
Based on the significant factors and contributions to the conversion response, the best model for this design appears to be as follows:

$$Y = \beta_0 + \beta_1 X_1 + \beta_2 X_2 + \beta_3 X_3 + \beta_{12} X_1 X_2 + \beta_{13} X_1 X_3 + \beta_{123} X_1 X_2 X_3$$

### 3.5.1.3 Validation of the model

A normal probability plot of the studentized residuals is shown in **Figure 3.24**. This indicates the number of standard deviations of the actual values from the respective predicted values. In this case, the plot is a straight line, indicating no abnormalities.

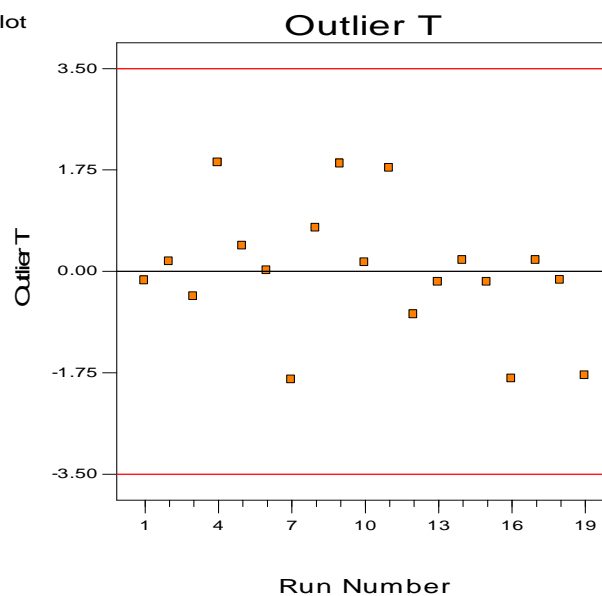
DESIGN-EXPERT Plot  
Conversion



**Figure 3.24: Conversion: Normal plot of studentized residuals**

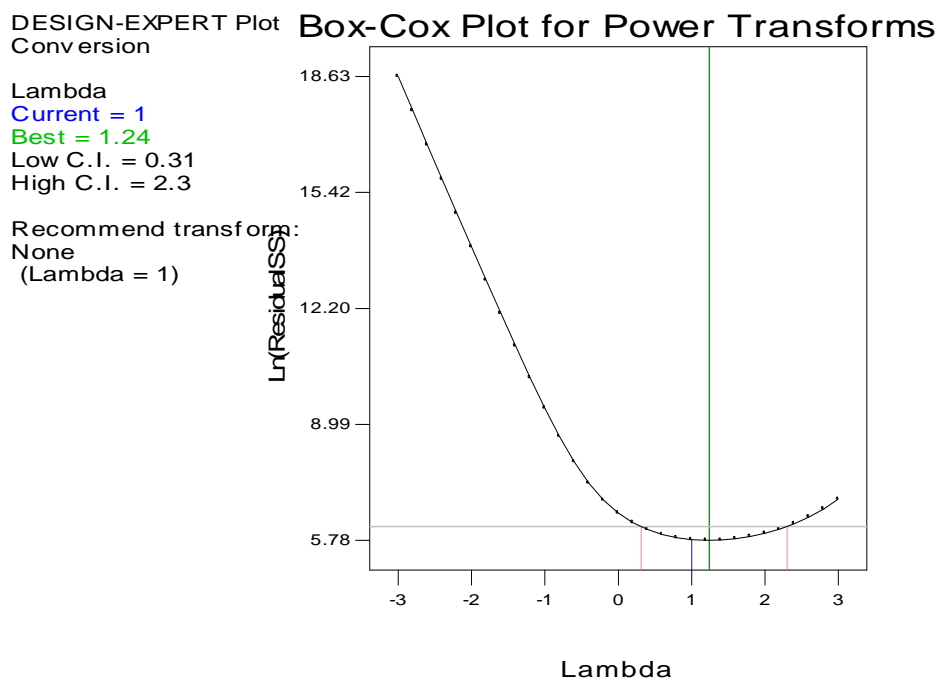
An Outlier T plot is shown in **Figure 3.25**. All the points fall well within the red lines set at  $\pm 3.5$  which indicate that there are no outliers amongst the individual experimental results.

DESIGN-EXPERT Plot  
Conversion



**Figure 3.25: Conversion: Plot of outlier T**

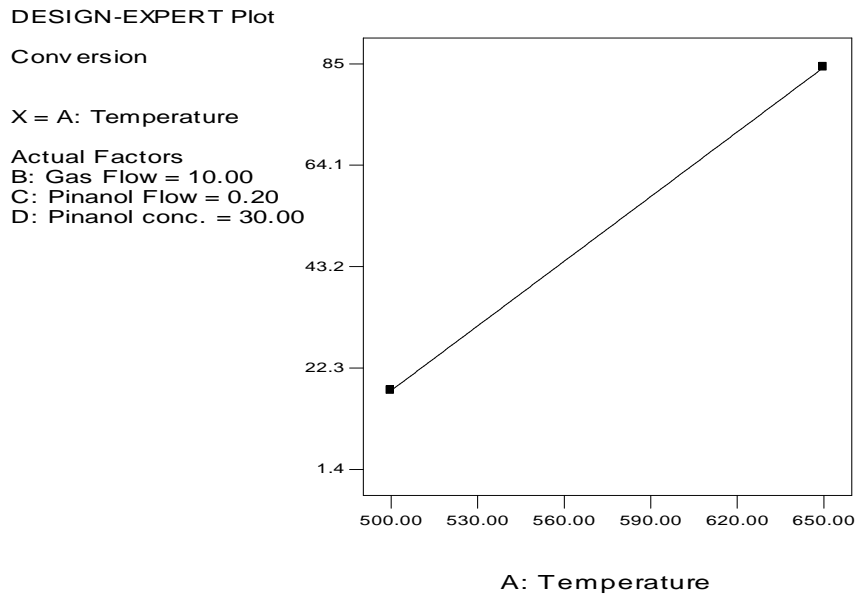
The Box-Cox diagnostic plot (**Figure 3.26**) was developed to analytically calculate the best power law transformation. The blue line shows the current transformation. In this case it points to a value of 1 for “Lambda” which symbolizes the power applied to the response values. A Lambda of 1 indicates no transformation. The green line indicates the best Lambda value, while the red lines indicate the 95% confidence interval surrounding it. Since this 95% confidence level includes 1, no transformation is recommended.



**Figure 3.26: Conversion: Box-Cox Plot**

#### 3.5.1.4 Examination of main effects and any interactions

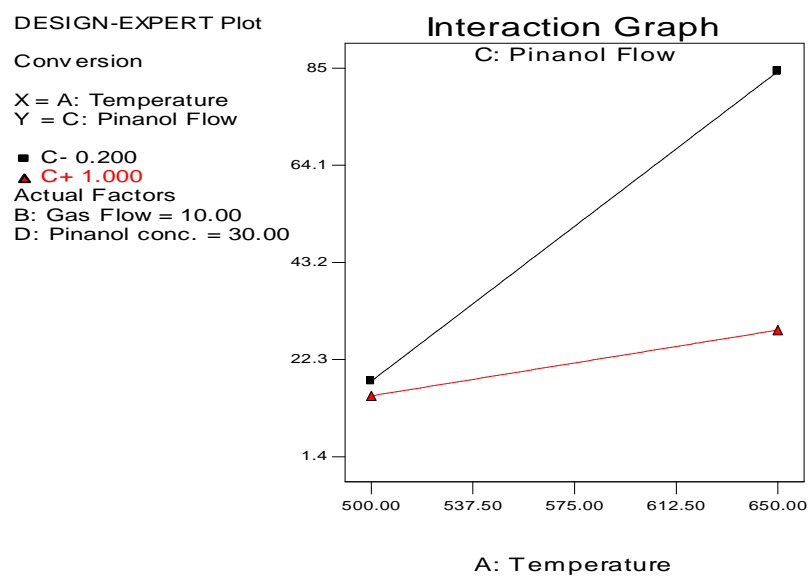
A one factor plot of the most significant factor (A, temperature) is shown in **Figure 3.27**.



**Figure 3.27: Conversion: One factor plot – Temperature**

The slope of the graph clearly shows the effect that temperature has on the conversion response. At the low level (500°C) the conversion was 17.65% and 84.3% at the higher level (650°C). In this plot B (low), C (low) and D (high) were the constants.

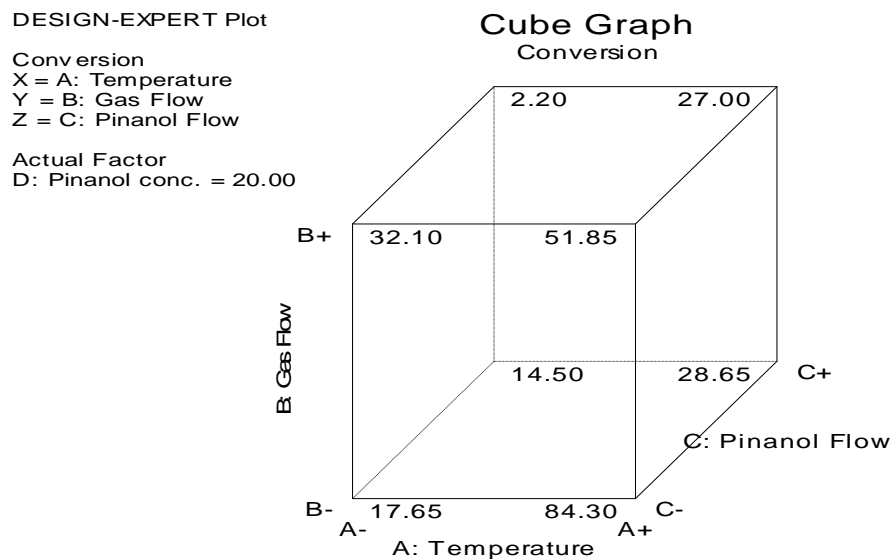
An interaction graph between the two most significant factors (A and C) is shown in **Figure 3.28**.



**Figure 3.28: Conversion: Interaction of temperature and gas flow rate**

The two lines shown in the graph are the low and high levels for factor C (pinanol flow rate). The difference in the slopes and hence the intersection of the lines for factor C gives an indication of the significance of the interaction. The graph indicates that at the higher level of C there is an increase in conversion from 14.5% to 30.5% as the temperature is increased from 500 to 650°C. This effect is accentuated at the low level of C where the conversion increases from 17.65% to 84.3% as temperature is increased.

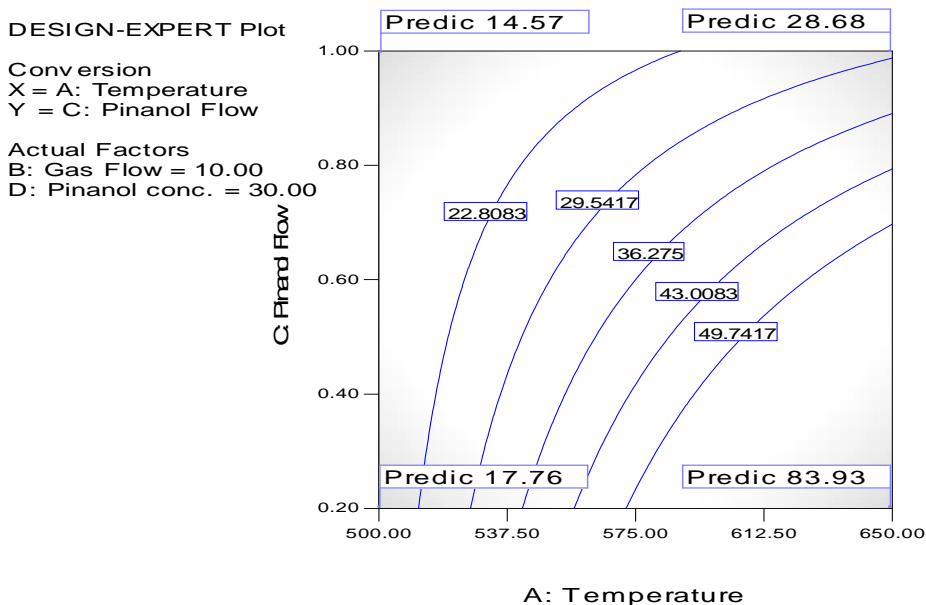
A cube plot of the three most significant single factors is shown in **Figure 3.29**.



**Figure 3.29: Conversion: Cube plot of A, B, C**

The cube plot shows how the three most significant factors combine to affect the conversion response. This cube plot once again emphasises the significance of A, temperature and C, pinanol flow rate on the conversion response. The highest conversion was achieved at high A, low C, and low B.

A contour plot for the conversion response is shown in **Figure 3.30**.



**Figure 3.30: Conversion: Contour surface plot**

Contour plots are useful for representing non-linear responses of second order and gives a fair idea of non-linearity. These plots are useful for predicting expected conversions anywhere on the design surface. In this case, the two most significant factors, A (temperature, °C) and C (pinacol flow, ml/min) were plotted and flags inserted at appropriate points on the design surface. The plot again emphasises that high A and low C are required for maximum conversion.

**3.5.2 Analysis of selectivity response**

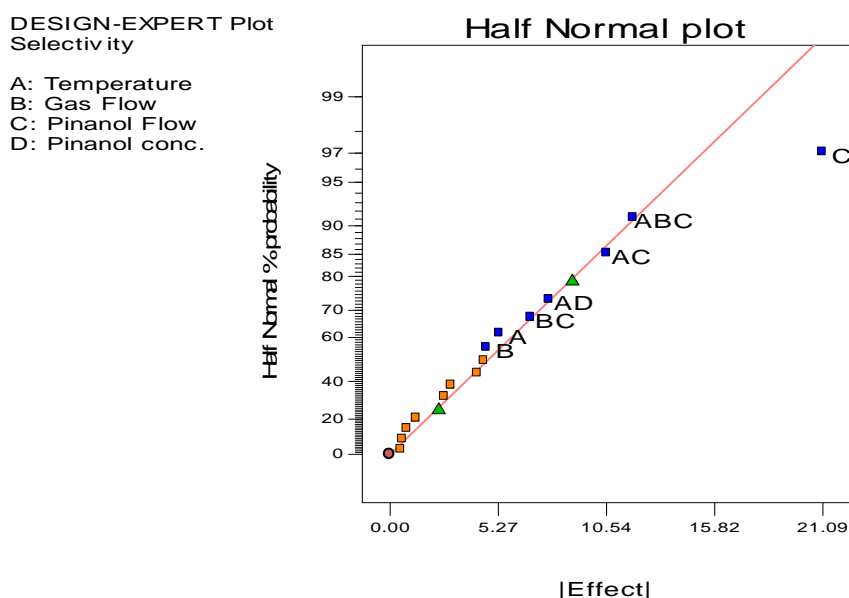
**3.5.2.1 Selection of main effects**

The effects and contribution of the various terms are shown in **Table 3.43**.

**Table 3.43: Selectivity – Effects list**

	<b>Term</b>	<b>Effect</b>	<b>Sum of Squares</b>	<b>% Contribtn</b>
M	A	-5.3375	113.956	3.05896
M	B	4.7125	88.8306	2.38452
M	C	21.0875	1778.73	47.7472
E	D	-0.8375	2.80562	0.0753125
E	AB	-4.2625	72.6756	1.95086
M	AC	10.5625	446.266	11.9793

M	AD	-7.7625	241.026	6.46995
M	BC	6.8625	188.376	5.05664
E	BD	2.9875	35.7006	0.958326
E	CD	-0.5375	1.15562	0.0310209
M	ABC	-11.8625	562.876	15.1095
E	ABD	2.6625	28.3556	0.761162
E	ACD	4.5875	84.1806	2.25969
E	BCD	-0.6125	1.50063	0.0402819
E	ABCD	-1.2875	6.63062	0.177989
M	Curvature	-4.14744	68.8051	1.84696
E	Lack Of Fit		0	0
E	Pure Error		3.44	0.0923413
	Lenth's ME	13.2907		
	Lenth's SME	24.3698		
	Lenth's SME	24.3698		



**Figure 3.31: Selectivity: Half-normal probability plot**

The effects list shows the contribution of the most important factors in this design to the conversion response and this is also graphically illustrated in **Figure 3.31**. By far the most important factor in this design is C, pinanol flow rate with a contribution of 47.75% to the model. The other individual factors do not make important contributions to the model. However, there appears to be a significant interaction between A and C (temperature and pinanol feed rate). There are also less important interactions between AD and BC.



### 3.5.2.2 Selectivity ANOVA

The analysis of variance (ANOVA) for the selectivity response (after selection of most important terms) is shown in **Table 3.44**.

**Table 3.44: ANOVA for selectivity response**

	<b>Sum of Squares</b>	<b>DF</b>	<b>Mean Square</b>	<b>F Value</b>	<b>Prob &gt; F</b>	
<b>Model</b>	3495.54	9	388.39	19.30	0.0002	significant
<i>A</i>	<i>113.96</i>	<i>1</i>	<i>113.96</i>	<i>5.66</i>	<i>0.0446</i>	
<i>B</i>	<i>88.83</i>	<i>1</i>	<i>88.83</i>	<i>4.41</i>	<i>0.0688</i>	
<i>C</i>	<i>1778.73</i>	<i>1</i>	<i>1778.73</i>	<i>88.40</i>	<i>&lt; 0.0001</i>	
<i>D</i>	<i>2.81</i>	<i>1</i>	<i>2.81</i>	<i>0.14</i>	<i>0.7185</i>	
<i>AB</i>	<i>72.68</i>	<i>1</i>	<i>72.68</i>	<i>3.61</i>	<i>0.0939</i>	
<i>AC</i>	<i>446.27</i>	<i>1</i>	<i>446.27</i>	<i>22.18</i>	<i>0.0015</i>	
<i>AD</i>	<i>241.03</i>	<i>1</i>	<i>241.03</i>	<i>11.98</i>	<i>0.0086</i>	
<i>BC</i>	<i>188.38</i>	<i>1</i>	<i>188.38</i>	<i>9.36</i>	<i>0.0156</i>	
<i>ABC</i>	<i>562.88</i>	<i>1</i>	<i>562.88</i>	<i>27.98</i>	<i>0.0007</i>	
<b>Curvature</b>	68.81	1	68.81	3.42	0.1016	not significant
<b>Residual</b>	160.96	8	20.12			
<i>Lack of Fit</i>	<i>157.52</i>	<i>6</i>	<i>26.25</i>	<i>15.26</i>	<i>0.0628</i>	<i>significant</i>
<i>Pure Error</i>	<i>3.44</i>	<i>2</i>	<i>1.72</i>			
<b>Cor Total</b>	3725.31	18				
<b>Pred R-squared</b>	0.9065					
<b>Adj R-squared</b>	0.6972					
<b>Adeq. Precision</b>	14.873					

The Model F-value of 19.30 implies the model is significant. There is only a 0.02% chance that a "Model F-Value" this large could occur due to noise. Values of "Prob > F" less than 0.0500 indicate model terms are significant. In this case A, C, AC, AD, BC, ABC are significant model terms.

The "Curvature F-value" of 3.42 implies the curvature (as measured by difference between the average of the center points and the average of the factorial points) in the

design space is not significant relative to the noise. There is a 10.16% chance that a "Curvature F-value" this large could occur due to noise.

The "Lack of Fit F-value" of 15.26 implies there is a 6.28% chance that a "Lack of Fit F-value" this large could occur due to noise. The lack of fit is significant since the "Prob>F" value, 0.0628, is less than 0.1 and hence this model cannot be used for predictions within the design space. This is also verified by the "Pred R-Squared". The "Pred R-Squared" of 0.6972 is not as close to the "Adj R-Squared" of 0.9065 as one might normally expect. This may indicate a large block effect or a possible problem with the model and/or data.

It seems that we are dealing with a very interesting phenomenon in the case of the selectivity model. The two response variables (conversion and selectivity) are not, strictly speaking, independent from each other. The results indicate that as the conversion is increased there is a simultaneous decrease in the selectivity. This makes it almost impossible to develop a model for selectivity.

### 3.5.3 Model Optimization

One of the tools used by the Design Expert® software package to predict optimum conditions for desired results is known as point prediction. The results of this are shown in **Tables 3.45** and **3.46**.

**Table 3.45: Point prediction model – low pinanol concentration**

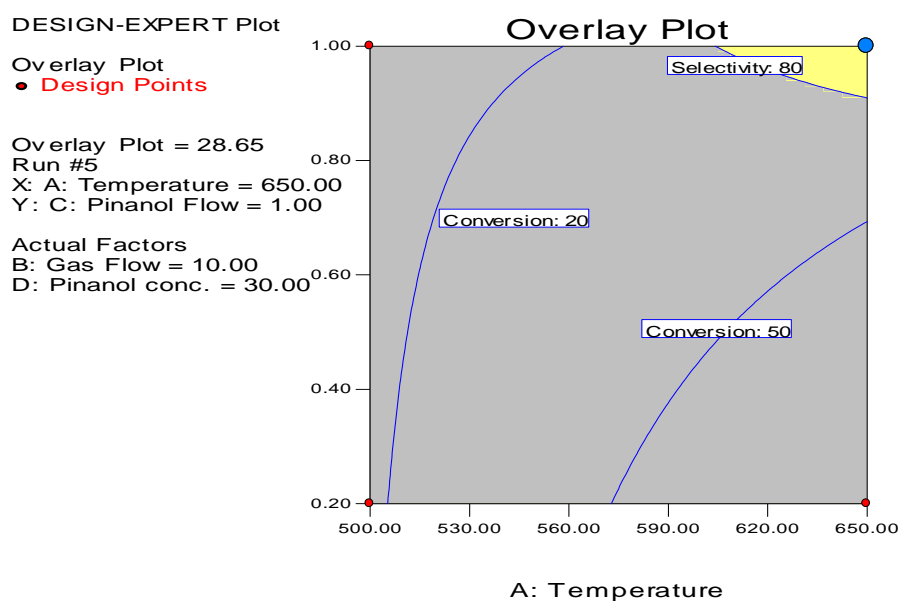
Factor	Name	Level	Low Level	High Level
<b>A</b>	<b>Temperature</b>	650	500.00	650.00
<b>B</b>	<b>Gas Flow</b>	10.00	10.00	20.00
<b>C</b>	<b>Pinanol Flow</b>	1.00	0.20	1.00
<b>D</b>	<b>Pinanol conc.</b>	10.00	10.00	30.00
<b>Prediction</b>				
<b>Conversion</b>	28.43%			
<b>Selectivity</b>	92.30%			

**Table 3.46: Point prediction model – high pinanol concentration**

Factor	Name	Level	Low Level	High Level
A	Temperature	650	500.00	650.00
B	Gas Flow	10.00	10.00	20.00
C	Pinanol Flow	1.00	0.20	1.00
D	Pinanol conc.	30.00	10.00	30.00
	<b>Prediction</b>			
	<b>Conversion</b>	28.43%		
	<b>Selectivity</b>	83.91%		

A desired outcome can be achieved by varying the values of the factors within the design space. In this case, a high selectivity with a reasonable conversion level (~30%) was selected and optimum conditions are shown in **Table 3.45**. By increasing the pinanol concentration (since we desire a high throughput as well) the same conversion can be achieved with a lower but still acceptable selectivity level (83.91%). This is shown in **Table 3.46**.

A more useful tool is the overlay plot as shown in **Figure 3.32**.

**Figure 3.32: Graphical optimisation: Overlay plot**

Overlay plots are especially useful in scaling up of processes and at plant scale where it is difficult to maintain the exact conditions. It provides an optimum “window” which is great for predicting results based on variations within this “window”. In this case the criteria selected for optimum conversion and selectivity was as follows:

- conversion: 25-30%
- selectivity: >80%

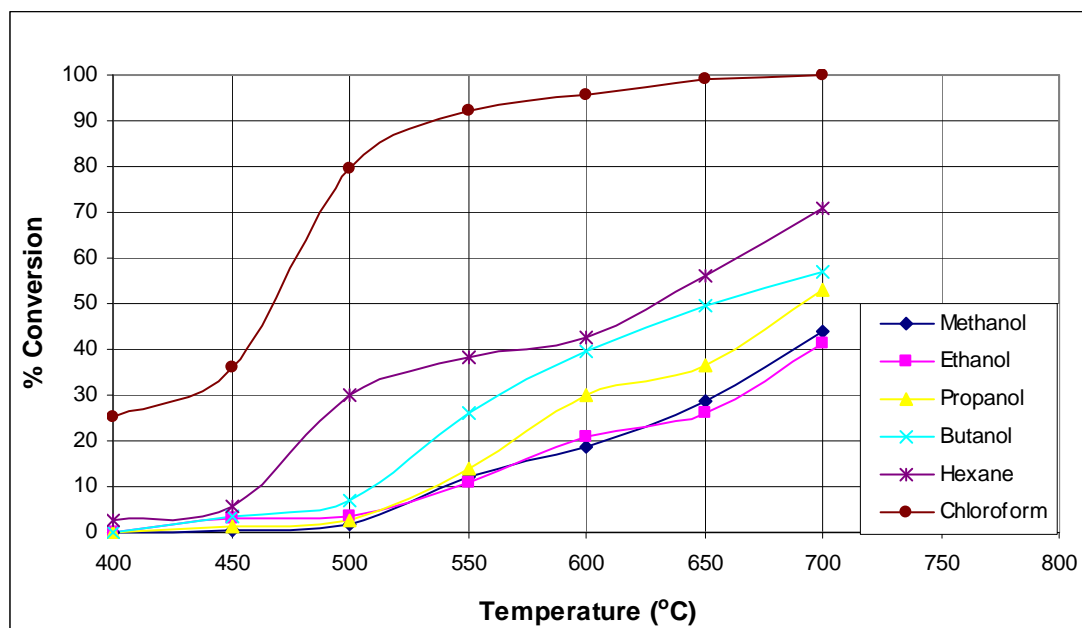
The “window” within which these results could be obtained falls in the upper right hand corner of the plot. The limits of this window vary between 605-650°C for temperature and 0.9 -1.0ml/min for pinanol feed rate. Run #5 is the closest in terms of conditions in this design. To maximise productivity, the pinanol concentration was kept constant at 30% m/m. Higher selectivities could be achieved at lower pinanol concentrations if so desired and if higher specifications of product are required. One would then have to sacrifice the productivity in order to achieve the higher product specifications.

### 3.6 Investigation of linalool decomposition

A pure linalool sample in various solvents was reacted under similar conditions to that used for the pinanol pyrolysis reaction. The results from this investigation are shown in **Table 3.47** and **Figure 3.33**.

**Table 3.47: Effect of temperature and solvent on linalool decomposition**

Temp.	Linalool conversion in various solvents					
	Methanol	Ethanol	Propanol	Butanol	Hexane	Chloroform
400	0	0.0	0.0	0.0	2.6	25.4
450	0.4	3.1	1.1	3.6	5.8	36.2
500	1.8	3.6	2.8	6.9	29.9	79.6
550	12.3	10.7	13.9	26.3	38.2	92.3
600	18.6	20.8	29.8	39.5	42.5	95.8
650	28.9	26.2	36.4	49.5	55.9	99.3
700	44.0	41.3	52.9	56.8	70.8	100



**Figure 3.33: Effect of temperature and solvent on linalool decomposition**

Several investigators<sup>60,61,99</sup> have pointed out that the decomposition of linalool under pyrolysis conditions is probably just as fast as its formation. This investigation was therefore undertaken to test this claim, to determine the extent of decomposition, as well as to characterise the by-products using GC-MS analysis.

The results show the linalool conversion generally increased as the temperature was increased. The trend was most pronounced when chloroform was used as solvent and linalool was almost fully decomposed at temperatures as low as 550°C. Hexane also showed significant decomposition but not as much as in chloroform. The alcohols showed a very similar trend to that observed for pinanol pyrolysis with greater decomposition taking place in the presence of the longer chain alcohols (§ 3.4.2). The lowest decomposition rates were obtained in the presence of methanol and ethanol. At 550°C (optimum temperature for pinanol pyrolysis), the conversions in the presence of methanol and ethanol was 12.3 and 10.7%, respectively. This corresponds very closely to the linalool selectivity in the pinanol pyrolysis under similar conditions (**Table 3.23**) e.g in the case of methanol the theoretical selectivity is 87.7% and the actual observed selectivity was 82.3%. This therefore indicates that the major source of by-products in pinanol pyrolysis is from the decomposition of linalool.

The major by-products (>1% of total peak area) produced from the decomposition of linalool are shown in **Table 3.49** and this can be compared to the by-products produced from a typical pinanol pyrolysis at 650°C (**Table 3.48**). The detailed GC-Mass spectra are shown in the **APPENDIX**.

**Table 3.48: GC-MS Data for a typical pinanol pyrolysis at 650 °C in ethanol**

Ret. Time	Name
11.043	2,6-dimethyl-2,4,6-octadiene
11.490	5,7-dimethyloct-6-en-2-one
12.520	3,7-dimethyl-1,6-octadien-3-ol (linalool)
12.800	1,2-dimethyl-3-(1-methylethenyl)-cyclopentanol (1 <i>R</i> , 2 <i>R</i> , 3 <i>S</i> )
12.943	1,2-dimethyl-3-(1-methylethenyl)-cyclopentanol (1 <i>R</i> , 2 <i>S</i> , 3 <i>S</i> )
12.949	1,2-dimethyl-3-(1-methylethenyl)-cyclopentanol (1 <i>R</i> , 2 <i>S</i> ,3 <i>R</i> )
12.995	<i>cis</i> -2-pinanol
13.115	<i>cis</i> -β-terpineol
14.259	<i>trans</i> -pinanol

**Table 3.49: GC-MS Data for linalool decomposition reaction at 650 °C in ethanol**

Ret. Time	Name
11.267	3,7-dimethyl-1,3,6-octatriene
12.520	3,7-dimethyl-1,6-octadien-3-ol (linalool)
12.800	1,2-dimethyl-3-(1-methylethenyl)-cyclopentanol (1 <i>R</i> , 2 <i>S</i> ,3 <i>R</i> )
12.943	1,2-dimethyl-3-(1-methylethenyl)-cyclopentanol (1 <i>R</i> , 2 <i>R</i> , 3 <i>S</i> )
12.949	1,2-dimethyl-3-(1-methylethenyl)-cyclopentanol (1 <i>R</i> , 2 <i>S</i> , 3 <i>S</i> )

The impurity profiles for both these samples are very similar with some additional by-products in the pinanol sample i.e. 5,7-dimethyloct-6-en-2-one and *cis*-β-terpineol.

These compounds are formed directly from cis-pinanol and the mechanism is discussed in § 3.11 (General Discussion).

### 3.7 Preparation of market sample/Robustness test

After distillation of the ethanol solvent, the crude linalool mixture produced (6.5 kg) had the following composition, **Table 3.50**:

**Table 3.50: Initial composition of crude market sample**

Component	% Peak Area
Linalool	22.8
Cis-Pinanol	61.8
Trans-Pinanol	11.1
By-products	4.3

This approximates a conversion of 30.5% at a selectivity of 84.2%, representing an overall yield of 25.7%.

The bulk of the linalool (1.33kg) was then distilled off and this had a composition as shown in **Table 3.51**:

**Table 3.51: Composition of market sample after first distillation**

Component	% Peak Area
Linalool	83.8
Cis-Pinanol	2.6
Trans-Pinanol	0.21
By-products	13.4

During this distillation 93.2% of the linalool was recovered and the procedure was quite effective for the removal of most of the cis- and trans-pinanol. However, the ratio of the impurities to linalool remained relatively unchanged. The impurities were mostly the four pinol isomers which have very similar boiling points to linalool. There was also an improvement in colour since the distillate that was produced was light yellow compared to the original brown colour. The distillation was also

problematic because of considerable foaming. This resulted in bumping and carry-over of material during the process.

The linalool was distilled a second time to try and achieve a purity specification of greater than 90%. The composition of the distilled mixture (1.07kg) is shown in **Table 3.52**.

**Table 3.52: Composition of final market sample**

<b>Component</b>	<b>% Peak Area</b>
Linalool	92.4
Cis-Pinanol	0.2
Trans-Pinanol	ND
By-products	7.4

After the second distillation the linalool purity increased to 92.4% and the recovery was 80.4% based on this distillation and 74.8% overall, based on the amount of linalool in the crude reaction mixture. The solution was clear and light yellow in colour. There were still significant amounts of the pinol by-products (7.4%) present as these are difficult to separate by distillation.

This process did demonstrate, however, that it was possible to produce a substantial amount of product in-specification even though we used a very small reactor system with an effective volume of only 3.32cm<sup>3</sup>. The scale-up of this process would be relatively easy since we would just multiply the number of reactors to give us the required throughput on a full scale plant.

The process also demonstrated the robustness of the reactor system and associated equipment since consistent results were produced over a prolonged period of time and no problems were experienced with the equipment. The only problem that was experienced was the slow build-up of coke on the hot reactor walls and the reactor had to be cleaned and replaced. The reactor itself held up well under the harsh conditions and there were no visible signs of damage or pitting. This is a good sign as far as materials of construction and scaling up of the process is concerned.



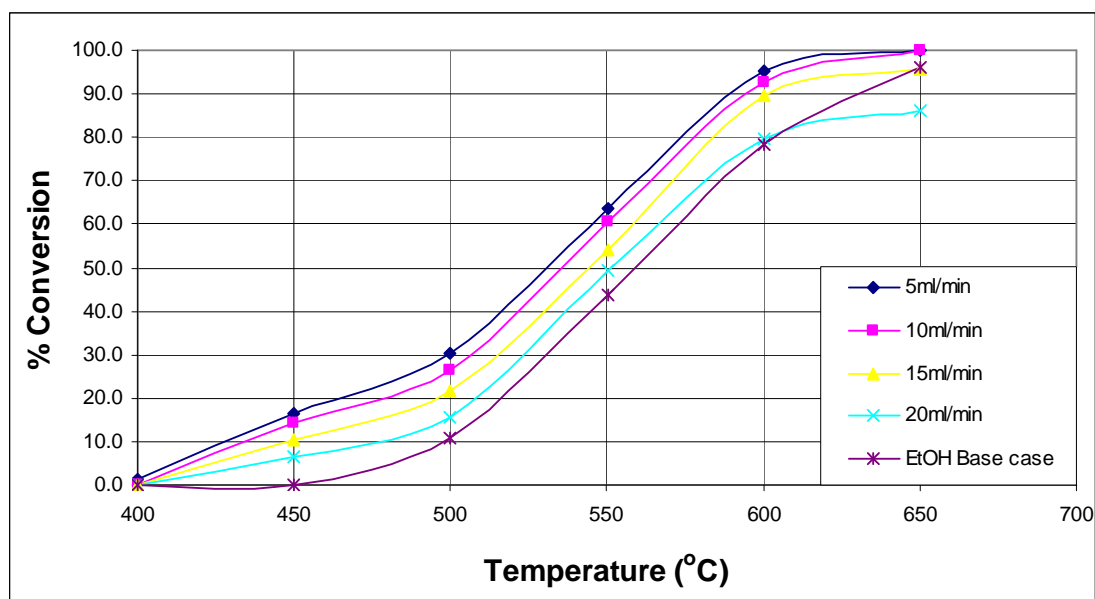
At this scale the proper equipment required for effective distillation was not available. It is therefore recommended that the distillation be further investigated on a larger scale with proper distillation equipment when more material becomes available.

### 3.8 Use of microreactor system for pinanol pyrolysis

The results for the reactions conducted in the microreactor are shown in **Tables 3.53, 3.54** and **Figures 3.34, 3.35**. The base case reaction conducted in ethanol was added for comparison purposes.

**Table 3.53: Conversion at various gas flow rates in microreactor**

Temp.	% conversion at various flow rates				EtOH Base case
	5ml/min	10ml/min	15ml/min	20ml/min	
400	1.2	0.0	0.0	0.0	0.0
450	16.3	14.3	10.5	6.3	0.0
500	30.5	26.5	21.8	15.6	10.8
550	63.8	60.7	54.2	49.3	43.6
600	95.3	92.6	89.5	79.8	78.5
650	100.0	99.8	95.6	86.2	96.2

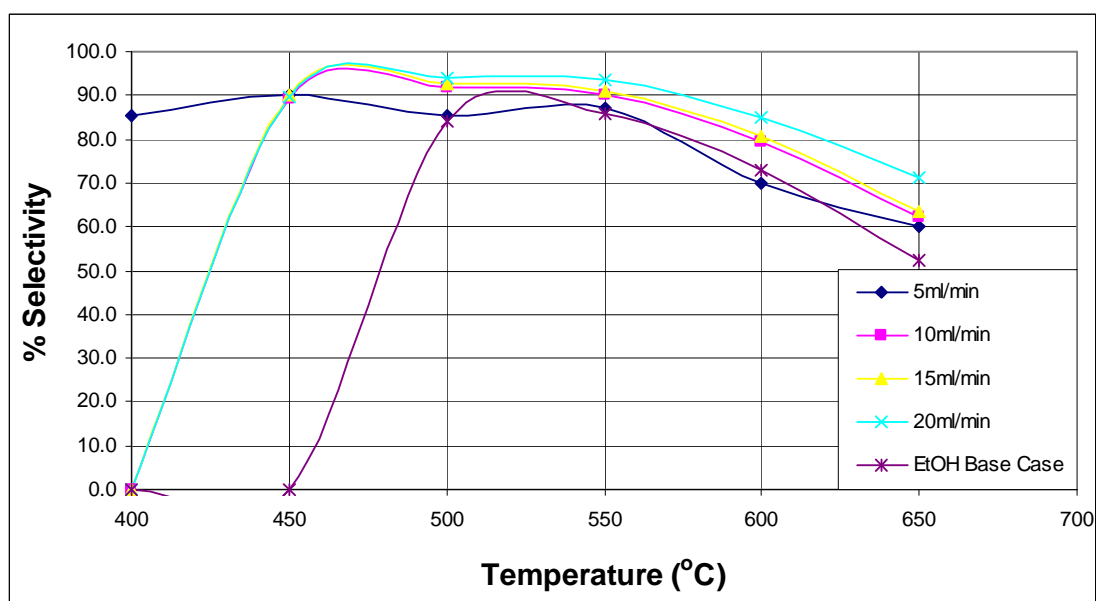


**Figure 3.34: Pinanol conversion at various flow rates in microreactor**

The results clearly indicate that pinanol conversion increased as the inert gas flow rate was decreased. This result was expected because the corresponding longer residence times will have allowed more pinanol molecules to react and be converted to linalool. When compared to the base case reaction (at 10ml/min) carried out in a tubular reactor, it is quite evident that the conversion was also significantly higher, e.g. at 550°C the conversion in the tubular reactor was 43.6% and that in the microreactor was 60.7%, a difference of 17.1%. The superior performance of the microreactor is probably due to the increased mass transfer and heat transfer characteristics due to the large surface area to volume ratio. This is discussed in more detail in § 3.9 where the reaction kinetics of both systems were compared and mathematical modelling studies were conducted.

**Table 3.54: Selectivity at various gas flow rates in microreactor**

Temp.	% selectivity at various flow rates				EtOH Base case
	5ml/min	10ml/min	15ml/min	20ml/min	
400	85.6	0.0	0.0	0.0	0.0
450	90.2	89.4	90.3	89.6	0.0
500	85.4	91.9	92.6	94.2	84.1
550	87.2	90.1	91.2	93.5	85.8
600	70.1	79.2	80.6	85.0	72.9
650	60.3	62.2	63.5	71.2	52.3



**Figure 3.35: Linalool selectivity at various gas flow rates in microreactor**

As far as selectivity was concerned there was an increase in linalool selectivity as the flow rate was increased. This was a result of the shorter residence times at the higher flow rates hence reducing the rate of linalool decomposition which is sensitive to time and temperature effects. However, it was also observed that the selectivity was higher when compared to the equivalent reaction in the tubular reactor over the temperature range, e.g. at 550°C the selectivity in the microreactor was 90.1% and 85.8% in the tubular reactor, a difference of 4.3%. This could also be attributed to the improved heat and mass transfer characteristics (**discussed in more detail in § 3.9**) normally associated with microreactor systems. The more even heating in the microreactor would result in fewer 'hotspot' and therefore less chance of linalool decomposition occurring.

Although the microreactor has demonstrated superior reaction performance in this investigation, careful consideration would have to be given to its use in a full scale production environment.

Firstly, the formation of coke is a real problem in high temperature reactions involving hydrocarbons and we have observed its formation in the pyrolysis reaction. In the preparation of the market sample, the tubular reactor was run for extended periods and blockages of the piping occurred due to the formation of coke. The reactions had to be occasionally stopped and the reactor cleaned out or replaced. This problem would be more severe in a microreactor since the channels are extremely small and we have indeed observed that the microreactors block up very quickly.

Secondly, since microtechnology is a relatively new technology, there are a limited number of manufacturers and suppliers in the market, and they are all from abroad. The technology required to produce microreactors is also new and costly. The cost of microreactors available from vendors is therefore very high and at this stage is not economically feasible for most industrial processes. Most processes would require multiple units running into the hundreds or even thousands (depending on the plant capacity) and this is simply not feasible at current prices. The CSIR is currently in the

process of developing a platform for the manufacture of microreactor systems and peripherals and if this is a success then manufacture in South Africa becomes a real possibility. The systems would then be available at reduced prices and one can reassess its use in industrial processes.

### 3.9 Reaction kinetics and mathematical modelling of the pyrolysis reaction in tubular and microreactor systems

#### 3.9.1 Theoretical

In this particular study, the reaction was carried out at temperatures ranging from 550°C to 750°C in a tubular reactor as well as in a multichannel microreactor. The goal was to elucidate the effects of geometry, temperature and residence time on the synthesis of linalool. Experimental work was followed up by modelling with CFD (Computational Fluid Dynamics) as well as the classical diffusion model with the chemical reactions solved using the MATLAB software system.

The pyrolysis and side reactions have been determined to be first order, which is typical of isomerisation reactions. The reaction proceeds according to the following scheme:



where  $k_{cis}$  and  $k_{lin}$  represent the rates of the forward and side reactions respectively. The reaction sequence has been simplified by lumping the side products as one product *HOL* (hydrocarbon olefins) and also by taking into account the reaction of only the *cis*- stereoisomer of 2-pinanol. These simplifications were consistent with our experimental findings under the reaction conditions since the conversion of the *trans* stereoisomer was found to be very insignificant in comparison with the *cis* stereoisomer and, as mentioned previously (§3.6), the main side product were the hydroxyolefins (*HOL*) or pinols.

### 3.9.2 Kinetics

According to the simplifications mentioned above, the kinetics of the isomerisation reaction can be described by the following rate equations:

$$\frac{dC_{cis}}{dt} = -k_{cis} C_{cis}, \quad (2)$$

$$\frac{dC_{lin}}{dt} = k_{cis} C_{cis} - k_{lin} C_{lin}, \quad (3)$$

$$\frac{dC_{hol}}{dt} = k_{lin} C_{lin}, \quad (4)$$

where  $C_{cis}$ ,  $C_{lin}$  and  $C_{hol}$  are the current concentrations of the *cis* 2-pinanol, linalool and hydroxyolefines respectively. The integral of Eq. (2) incorporating conversion of the *cis* stereoisomer is

$$\ln(1 - x_{cis}) = -k_{cis} \tau, \quad (5)$$

where  $\tau$  is the residence time in the reactor and  $x_{cis}$  is the conversion of the *cis* stereoisomer. A plot of  $\ln(1-x_{cis})$  against  $\tau$  results in a straight curve, whence  $k_{cis}$  can be determined from the gradient. The selectivity can be determined by combining Eq. (1) and Eq. (2) to give the equation<sup>100</sup>

$$\frac{C_{lin} - C_{lin0}}{C_{cis0} - C_{cis}} = \frac{C_{lin0}}{C_{cis0}} \frac{(1 - x_{cis})^{\frac{k_{lin}}{k_{cis}}} - 1}{x_{cis}} + \frac{1 - x_{cis}}{\frac{k_{lin}}{k_{cis}} - 1} \frac{1 - (1 - x_{cis})^{\frac{k_{lin}-1}{k_{cis}}}}{x_{cis}}, \quad (6)$$

where  $C_{cis0}$  and  $C_{lin0}$  are the initial concentrations of the *cis* 2-pinanol and linalool respectively. On account of the initial concentration of linalool being zero, Eq. (6) reduces to

$$\zeta_{lin} = \frac{C_{lin}}{C_{cis0} - C_{cis}} = \frac{1 - x_{cis}}{\frac{k_{lin}}{k_{cis}} - 1} \frac{1 - (1 - x_{cis})^{\frac{k_{lin}-1}{k_{cis}}}}{x_{cis}}. \quad (7)$$

After experimentally determining the value of  $k_{cis}$  from Eq. (5), and from experimental values of selectivity  $\zeta_{lin}$  and conversion  $x_{cis}$ , we could proceed to determine the value of  $k_{lin}$  from Eq. (7).

Having determined the values of  $k_{cis}$  and  $k_{lin}$ , we further performed an Arrhenius plot of  $\ln(k)$  against  $1/T$  according to the equation

$$k = k_0 e^{\left(\frac{-E_a}{RT}\right)} \quad \Rightarrow \quad \ln(k) = \ln(k_0) - \frac{E_a}{RT}, \quad (8)$$

where  $R$  is the universal gas constant. This plot enabled the determination of the frequency factor  $k_0$  and the activation energies  $E_a$  of both the forward and side reactions from the intercept and the gradient. This would in turn enable the determination of values of  $k$  at any given temperature within the applicable temperature range.

### 3.9.3 Mathematical modelling

The reaction was carried out in a tubular minichannel reactor as well as in a multichannel microreactor. The reaction in the tubular reactor has been modelled and simulated using the Computational Fluid Dynamics (CFD) software COMSOL Multiphysics and the mathematical software MATLAB.

#### 3.9.3.1 Diffusion Model

This model is a differential mass balance equation which is written in the non-conservative form as

$$\frac{\partial C_i}{\partial t} + \mathbf{u} \nabla C_i - \nabla \cdot (D_i \nabla C_i) - R_i = 0 \quad (9)$$

where  $\mathbf{u}$  is the fluid velocity vector,  $D_i$  is the diffusion coefficient of component  $i$  and  $R_i$  is the rate of reaction determined from Eq. (2) and Eq. (3). It is wholly sufficient to determine the composition of only these two components as the third component

(*HOL*) can be evaluated from a mass balance. This equation is denoted in its simplified one-dimensional form below.

$$\frac{\partial C_i}{\partial t} + u \frac{\partial C_i}{\partial x} - D_{iB} \frac{\partial^2 C_i}{\partial x^2} - R_i = 0 \quad i = cis, lin, \quad (10)$$

The initial conditions in this domain are

$$C_i(x,0) = 0, \quad (11)$$

and the boundary conditions

$$C_{cis}(t)|_{x=0-} = C_{cis0} \quad C_{lin}(t)|_{x=0-} = 0, \quad (12)$$

$$\left. \frac{\partial C_{cis}(t)}{\partial x} \right|_{x=L-} = 0 \quad \left. \frac{\partial C_{lin}(t)}{\partial x} \right|_{x=L-} = 0. \quad (13)$$

The diffusion coefficient is a function of temperature and can be reasonably estimated by the Wilke and Lee equation<sup>101</sup>

$$D_{iB} = \frac{(0.303 - 0.98/\sqrt{M_{iB}}) \cdot 10^{-7} \cdot T^{3/2}}{P \Omega_{iB}^2 \sigma^2 \sqrt{M_{iB}}} \quad [m^2/s] \quad (14)$$

where component *B* in this equation designates the carrier gas nitrogen, *T* is the absolute temperature, *P* is the pressure in [bar], *M<sub>iB</sub>* is the mean molar mass of the gas mixture, *Ω<sub>iB</sub>* is a dimensionless temperature-dependent diffusion collision integral and *σ* is a scale parameter with units of length. The system of equations (10)-(13) was solved in MATLAB using the partial differential equation solver “pdepe” which utilises the meshing method for spatial and time discretization of the system.

### 3.9.4 CFD Modelling

#### 3.9.4.1 Tubular reactor

In the COMSOL CFD package, Eq. (9) with insulation wall boundaries and a concentration inlet and convective flux outlet boundary is coupled with the simplified energy equation,

$$\rho C_p \left( \frac{\partial T}{\partial t} + \mathbf{u} \nabla T \right) + \nabla \cdot (\lambda_f \nabla T) - \sum_i (\Delta H_i) R_i = 0, \quad (15)$$

with heat conduction at the wall boundaries. In the equation,  $\rho$  is the fluid density,  $C_p$  the heat capacity of the mixture,  $\lambda_f$  is the thermal conductivity of the fluid and  $\Delta H_i$  is the enthalpy of reaction for the conversion of component  $i$ . The heat conduction at the wall boundary is designated by the equation

$$-\mathbf{n} \cdot (-\lambda_f \nabla T + \rho C_p T \mathbf{u}) = \frac{\lambda_w}{\delta} (\Delta T), \quad (16)$$

where  $\mathbf{n}$  is the normal vector to the boundary plane,  $\lambda_w$  is the thermal conductivity of the tube wall and  $\delta$  is the tube wall thickness. The inlet boundary is a heat flux boundary according to the equation

$$-\mathbf{n} \cdot (-\lambda_f \nabla T + \rho C_p T \mathbf{u}) = \rho C_p T_0 \mathbf{u}_0, \quad (17)$$

with the inlet temperature and velocity vector designated by  $T_0$  and  $\mathbf{u}_0$  respectively, whereas the outlet boundary is a convective flux boundary described by the equation

$$\mathbf{n} \cdot (-\lambda_f \nabla T) = 0 \quad (18)$$



The tube was appropriately meshed and the solution of Eq. (9) with its initial and boundary conditions corresponding to Eqs. (11) – (13) coupled with Eqs. (15) – (18) is solved by Finite Element Method (FEM) in COMSOL.

### 3.9.4.2 Microreactor

Due to the increased complexity in the geometry of the microreactor reaction chamber, the Navier-Stokes equations coupled with the continuity equation<sup>102</sup> for momentum and mass balances respectively were used in conjunction with Eqs (9) and (15). For the momentum balance, the no-slip boundary conditions were imposed for the chamber walls, with a velocity inlet boundary and a continuity outlet boundary, otherwise the convective flow and heat flow boundary conditions are the same as in the above sections.

## 3.9.5 Results and Discussion

### 3.9.5.1 Experimental results

The influence of temperature was studied by varying the heated section temperature from 550°C to 750°C in the tubular reactor and from 450°C to 650°C in the microreactor. The conversion of *cis* 2-pinanol was evaluated from gas chromatography (GC) plots and so was the selectivity for linalool. The GC plot also reveals the validity of our assumption that the *trans* 2-pinanol has a negligibly slow reaction rate, under the given conditions. The rate constant for the forward reaction  $k_{cis}$  at the set temperature is determined from Eq. (5) as alluded to in § 3.9.2 (**Kinetics**), in the paragraph just below Eq. (5). Since we also know the selectivity, the value of the rate constant for the side reaction  $k_{lin}$  was then determined from Eq. (7) as proposed in the paragraph immediately below Eq. (7). This was repeated for different temperatures.

The results of the pyrolysis from the tubular reactor and the microreactor are presented in **Table 3.55**.

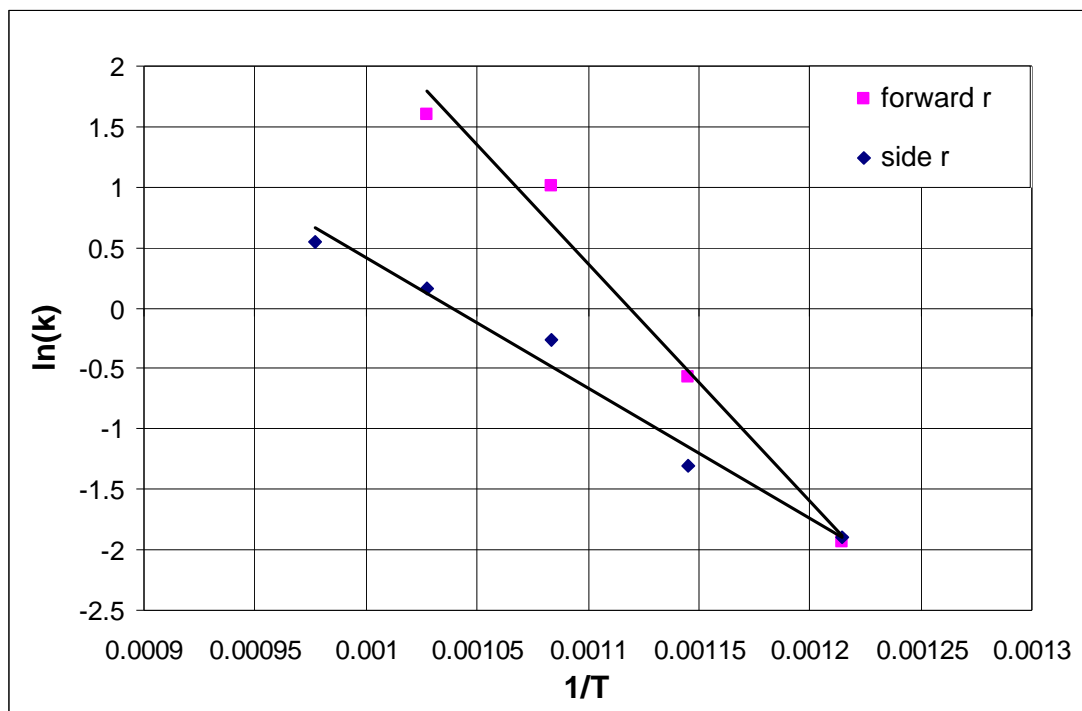
**Table 3.55: Comparative results of pinanol pyrolysis in the tubular and microreactor systems**

Temp °C	Tubular reactor			Microreactor		
	Res.time(s) F.r.(ml/min)	$x_{cis}$ (%) $\zeta_{lin}$ (%)	Yield (%)	Res.time(s) F.r.(ml/min)	$x_{cis}$ (%) $\zeta_{lin}$ (%)	Yield (%)

400	<b>0.25 s</b> <b>200ml/min</b>	-	-	<b>0.21 s</b> <b>20 ml/min</b>	0.00	0.00	0	
450		-	-		6.3	89.6	5.6	
500		5.1	89.7		4.5	15.6	94.2	14.7
550		9.6	83.2		8.0	49.3	93.5	46.1
600		19.8	83.3		16.5	79.8	85.0	67.8
650		53.9	81.1		43.7	86.2	71.2	61.4
700		81.7				-		-
750		71.2			58.2	-		-
		92.3						
		59.0						
400	<b>0.5 s</b> <b>100 ml/min</b>	-	-	<b>0.28</b> <b>15 ml/min</b>	0.00	0.00	0	
450		-	-		10.5	90.3	9.5	
500		4.4	88.4		3.9	21.8	92.6	20.2
550		9.8	91.8		9.0	54.2	91.2	49.4
600		29.3	86.8		25.4	89.5	80.6	72.1
650		73.3	70.6		51.7	95.6	63.5	60.7
700		89.7	60.3		54.1	-		-
750		94.0	52.7		49.6	-		-
400	<b>1 s</b> <b>50 ml/min</b>			<b>0.42</b> <b>10 ml/min</b>	0.00	0.00	0	
450					14.3	89.4	12.8	
500		7.3	90.5		6.6	26.5	91.9	24.4
550		9.8	91.6		9.0	60.7	90.1	54.7
600		40.3	83.1		33.5	92.6	79.2	73.3
650		74.0	70.4		52.1	99.8	62.2	62.1
700		81.5	56.6		46.2	-		-
750		94.3	47.1		44.4	-		-
400	<b>2 s</b> <b>25 ml/min</b>			<b>0.84</b> <b>5 ml/min</b>	1.2	85.6	1.0	
450		0.00				16.3	90.2	
		0.00			0			14.7
500		3.0	76.9		2.3	30.5	85.4	26.0
550		25.6	77.3		19.8	63.8	87.2	55.6
600		43.2	77.9		33.7	95.3	70.1	66.8
650		80.5	70.8		57.0	100	60.3	60.3
700		91.2	52.1		47.5	-		-

Use of the tubular minichannel reactor led to an improvement in the yield of linalool, when compared to the previously published work by Semikolenov et. al<sup>99</sup>. However, by comparing values of conversion and selectivity in **Table 3.55**, it is evident from first glance that the use of the microreactor configuration results in a further improvement in the yield of the linalool product – as much as 73.3% linalool yield could be realized with the microreactor compared to 58.2% maximum yield for the tubular reactor, albeit at lower flow rates for the microreactor.

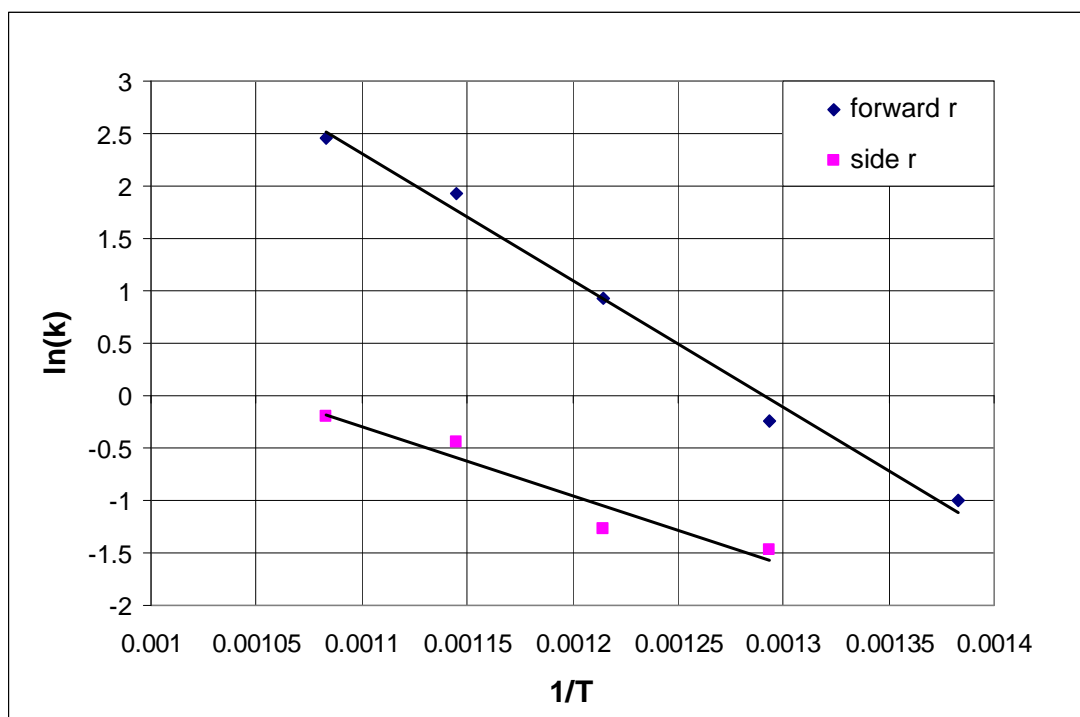
The values of the rate constants were plotted against temperature, resulting in Arrhenius plots for both reactions (**Figures 3.36, 3.37**).



Notes:  $E_{acis} = 154724 \text{ J/mol}$        $k_{0cis} = 1.170 \times 10^9 \text{ s}^{-1}$

$E_{alin} = 89533 \text{ J/mol}$        $k_{0lin} = 71969 \text{ s}^{-1}$

**Figure 3.36: Arrhenius plot for the tubular reactor system**



Notes:  $E_{acis} = 100724 \text{ J/mol}$        $k_{0cis} = 6.199 \times 10^6 \text{ s}^{-1}$

$E_{alin} = 54847 \text{ J/mol}$        $k_{0lin} = 1060 \text{ s}^{-1}$

**Figure 3.37: Arrhenius plot for the microreactor system**

The Arrhenius plot in **Figure 3.37** depicts a decrease in the activation energies of both the forward  $E_{acis}$  and side  $E_{alin}$  reaction in the case of the microreactor. This would imply that this configuration is more favourable from an energetic point of view. There is more enhanced heat transfer within the microreactor owing to the large surface-to-volume ratio, which is one of the outstanding properties of microreactors<sup>103</sup>. The side reaction, while always manifested, is more of an issue at higher temperatures, thus keeping the temperatures low somewhat suppresses its influence, leading to higher selectivities in microreactors.

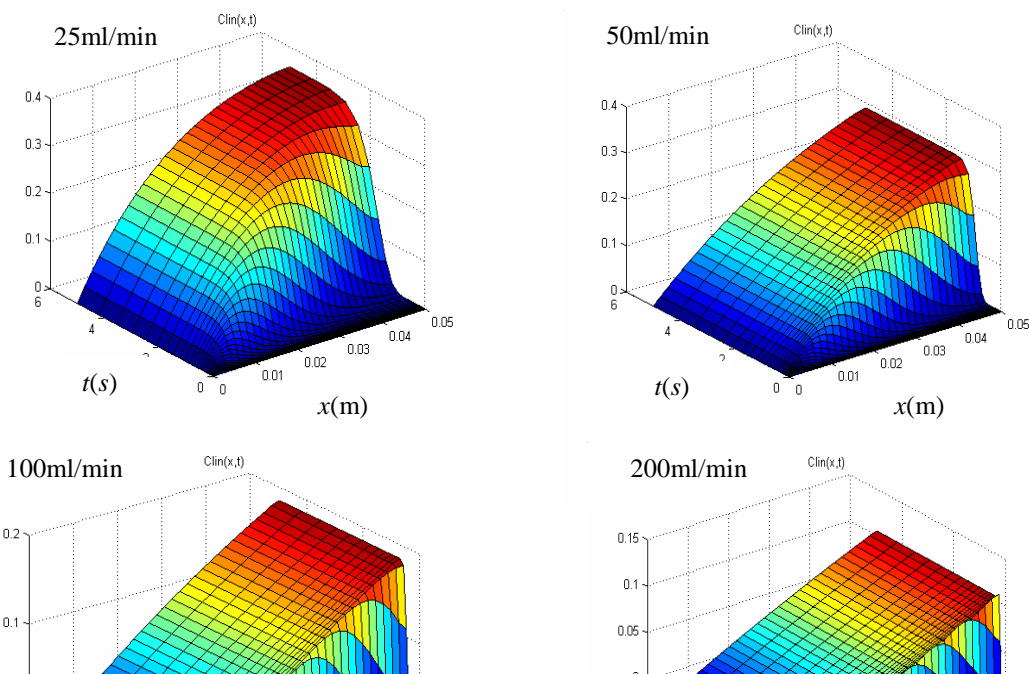
With the microreactor configuration, it is obviously expected that use of a catalyst would lead to further improvement in conversion and selectivity over conventional macrosystems owing to the enhancement of mass transfer in the microreactor which is due again to the large surface-to-volume ratio and the very minimal diffusion pathway in the microchannel. For a more comprehensive optimization study, the Arrhenius plot enables the prediction of rate constants at temperatures not measured within this

range and predicting the temperature and flow rates appertaining to the maximum yield value from a modelling or simulation study.

### 3.9.5.2 Modelling results

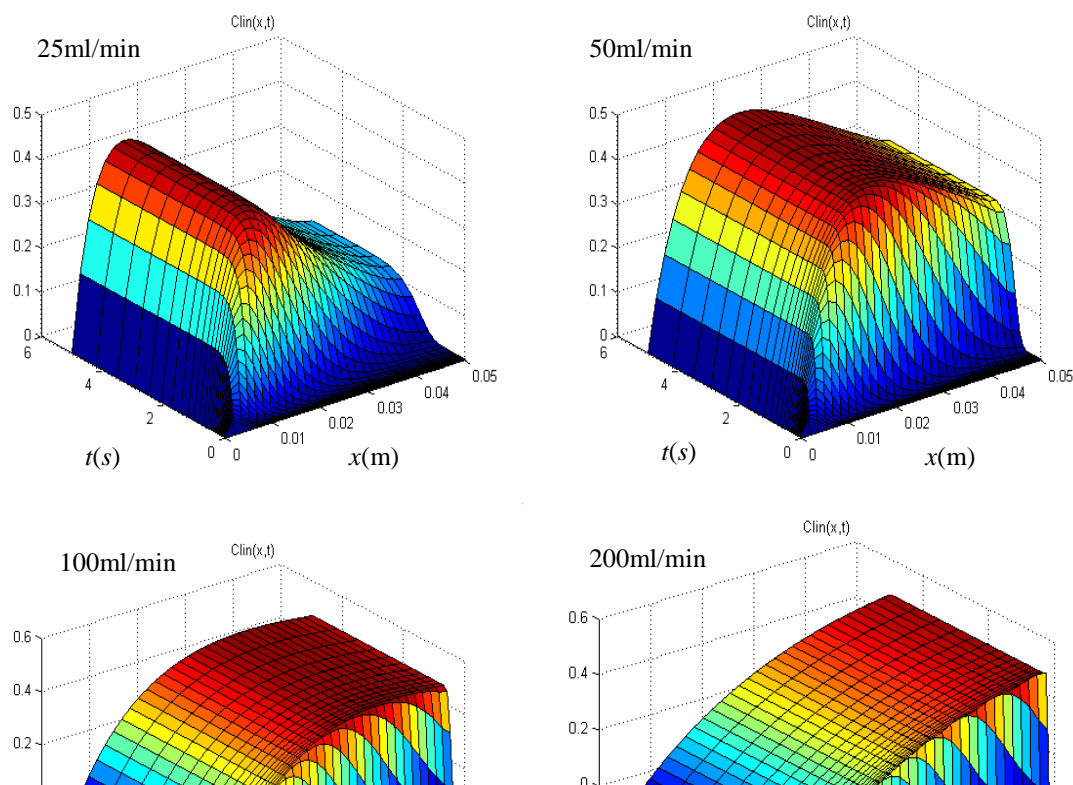
#### 3.9.5.2.1 Diffusion Model (MATLAB)

The system of Eqs. (10) – (13) was solved in MATLAB to provide an insight into the process along the length  $x$  of the tubular reactor. It is a one-dimensional model, which is easy to solve by using the “pdepe” solver and can be used as a first approximation of the modelling work. For the  $R$  term, the rate constants were evaluated from the Arrhenius plot in **Figure 3.36**, using Eq. (8), while the  $D_{iB}$  was evaluated from Eq. (14). The value of  $C_{cis0}$  was taken as  $0.73 \text{ mol/m}^3$ , for easier comparison with the starting material, which contained 0.73 mass fraction of the *cis*-2-pinanol. Only the heated section was evaluated and the temperature is assumed to be uniform along the cross-sectional area, thus heat flux was not taken into account. The conversion and selectivities follow largely the same pattern as the experimental results (**Table 3.56**). The effect of increasing flow rate from 25 – 200 ml/min on the concentration of linalool at two different temperatures  $600^\circ\text{C}$  and  $700^\circ$  is evident from **Figure 3.38** and **Figure 3.39**, respectively. Transient computations were done up to a time of 5 seconds, during which time steady state is reliably reached, as can be seen from all the plots. For the temperature  $600^\circ\text{C}$ , the increase in flow rate has the expected effect of decreasing the linalool concentration from about 0.34 to about 0.11 by virtue of pushing the reaction zone further towards the outlet of the heated zone. This is essentially due to the fact that the concentration of the linalool is still on the ascendance along the reactor length.



**Figure 3.38: Effect of flow rate of gas on the concentration of linalool at 600°C**

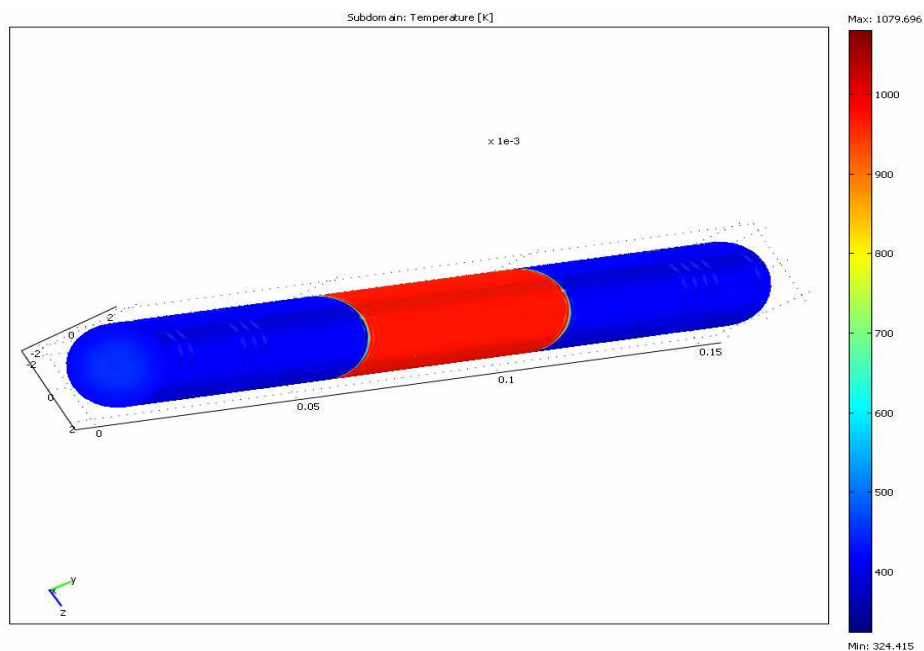
The situation is somewhat different at the higher temperature of 700°C, as depicted in **Figure 3.39**. At 25 ml/min and 50 ml/min a maximum concentration of linalool inside the reactor is clearly discernible. This is obviously due to the faster rate of the side reaction, which consumes the linalool product as soon as it is formed. Increasing the flow rate in this case results in an increase in the outlet concentration of linalool. This effect can be seen in **Table 3.55** as well, where we get a better selectivity for the linalool product with increasing flow rates again by virtue of the reaction zone being pushed towards the outlet, thereby pushing the maximum of the linalool towards the outlet. Indeed, it is observed from experiment that for the tubular reactor, the maximum yield of linalool is achieved at 200 ml/min and 700°C. The tabulated results for this model are depicted in **Table 3.56**.



**Figure 3.39: The effect of flow rate of gas on the concentration of linalool at 700°C**

#### **3.9.5.2.2 CFD modelling (COMSOL Multiphysics) – tubular reactor**

Three-dimensional simulations were performed by CFD using the COMSOL package and the results are tabulated alongside the results from Matlab for comparison's sake. Values from **Table 3.56** can also be compared with the experimental results from **Table 3.55** to ascertain the deviation of modelling from experimental results. Both modelling approaches predict a higher yield of linalool from higher flow rates and higher temperatures, which is consistent with experiment. CFD incorporates the length of the tubular reactor plus the heated section designated as red in **Figure 3.40**. The concentration profile of the linalool inside the tubular can be visualised by CFD methods as in **Figure 3.41**. As with the results from the Matlab, a maximum yield of linalool is observed inside the reactor at higher temperatures. Thus the need to optimize the linalool yield with respect to temperature and flow rate or residence time is evident. Both the forward and side reactions are considerably fast at higher temperatures and a high flow rate tends to dampen the influence of the side reaction.



**Figure 3.40: CFD model of tubular reactor with inlet and heated middle section**

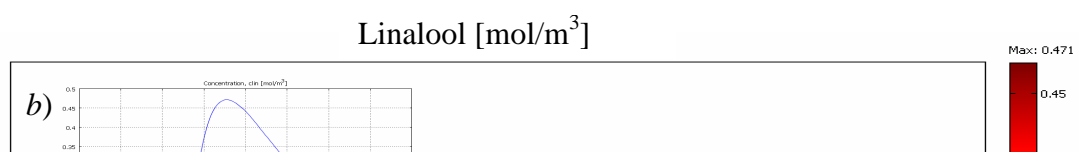
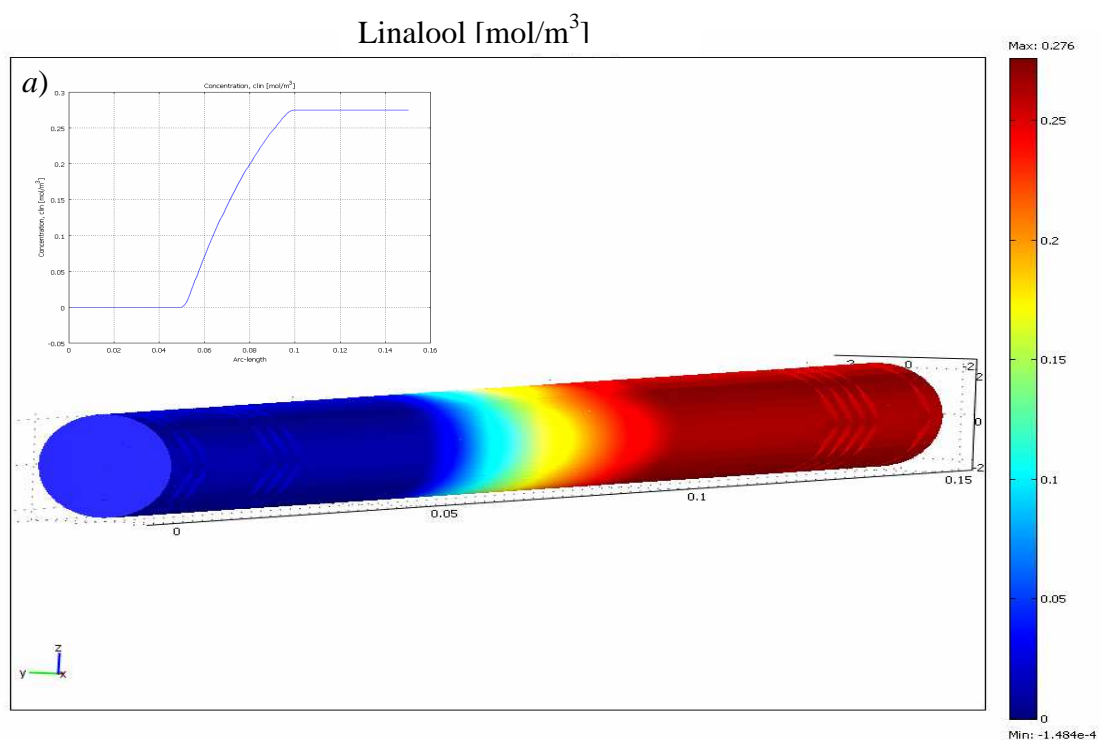
**Table 3.56: Modelling results from Matlab and CFD – Tubular reactor**

		Tubular reactor (Matlab)			Tubular reactor (CFD)		
Res.time(s)	Temp °C	$x_{cis}(\%)$		Yield (%)	$x_{cis}(\%)$		Yield (%)
		$\zeta_{lin}(\%)$			$\zeta_{lin}(\%)$		
<b>0.25 s</b> <b>200 ml/min</b>	550	4.5	98.9	4.5	3.3	98.7	3.3
	600	14.8	96.0	14.2	11.2	96.9	10.9
	650	40.0	92.0	36.8	30.4	94.1	28.6
	700	76.0	84.4	64.1	61.7	88.8	54.8
	750	97.2	70.1	68.1	90.2	79.4	71.6
<b>0.5 s</b> <b>100 ml/min</b>	550	8.7	97.8	8.5	7.3	96.7	7.1
	600	25.3	95.4	24.1	23.1	93.2	21.5
	650	63.3	83.6	52.9	55.0	86.8	47.7
	700	93.8	67.4	63.2	88.2	74.2	65.4
	750	99.8	47.7	44.6	97.2	56.8	53.4
<b>1 s</b> <b>50 ml/min</b>	550	15.9	92.6	14.7	14.4	96.2	13.9
	600	43.6	84.2	39.2	43.0	85.9	35.8
	650	79.5	68.8	53.9	74.5	72.8	61.1
	700	97.8	62.8	61.4	96.1	67.7	65.1
	750	99.9	40.3	40.3	99.9	46.0	46.0
<b>2 s</b>	550	28.8	85.4	24.6	26.71	92.0	24.6



<b>25 ml/min</b>	600	66.7	81.1	54.1	65.7	80.2	52.7
	650	94.5	62.2	58.8	95.7	64.2	61.4
	700	99.8	36.9	36.8	99.9	38.3	38.3

Authors Semikolenov, et. al<sup>99</sup> have reported a reduction in the rate of the side reaction by virtue of adding a butanol as a solvent to the mixture and addition of pyridine, which, due to its basicity neutralizes the acid centres in the reactor and thus inhibits its dehydration into side products. However, these effects were not observed to the same extent in our experimental runs.

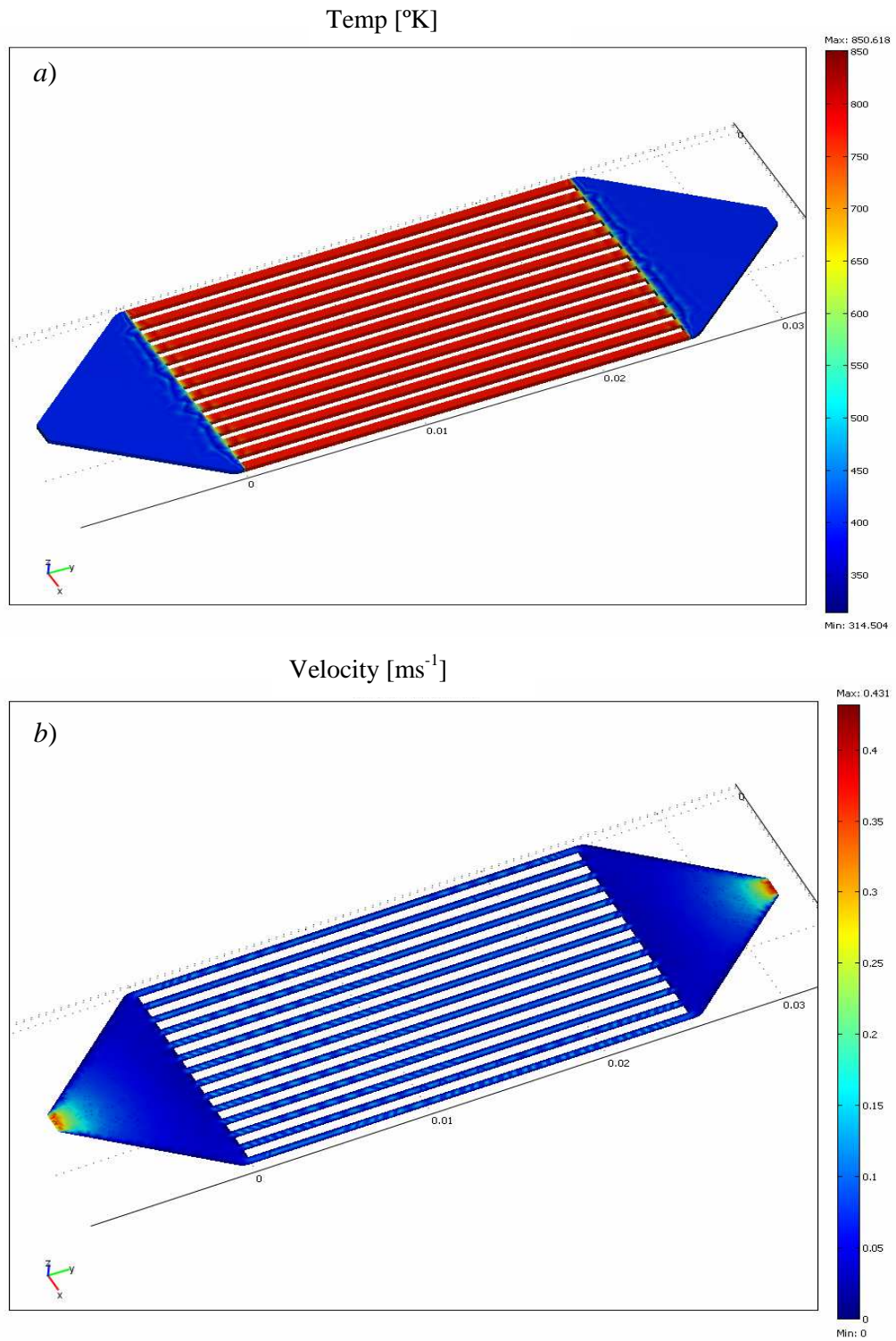


**Figure 3.41: Concentration profiles of linalool along the profile of the tubular reactor from CFD simulation at the flow rate 50ml/min at *a*) 600°C and at *b*) 700°C**

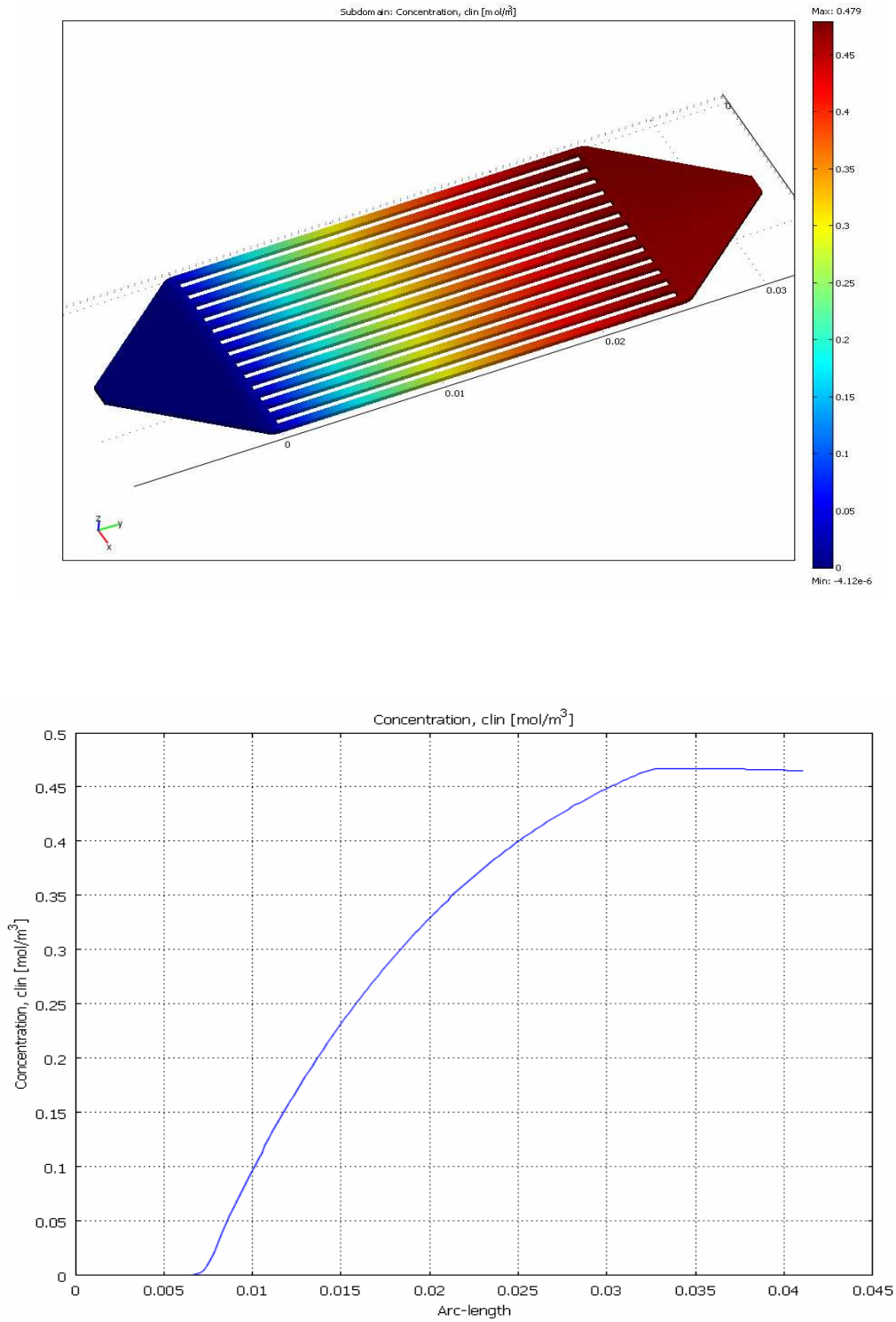
### 3.9.5.2.3 CFD modelling (COMSOL Multiphysics) – microreactor

A significant improvement in the linalool yield was recorded for the microreactor configuration, as reported in the experimental section; thus it was also modelled in COMSOL in order to be able to predict its behaviour within the range of experimental conditions. The geometry was modelled as depicted in **Figure 3.42**. The microchannels encompass the heated section in the middle as shown in **Figure 3.42 a)** and the velocity profile computed from the Navier-Stokes Equations is shown in **Figure 3.42 b)**.

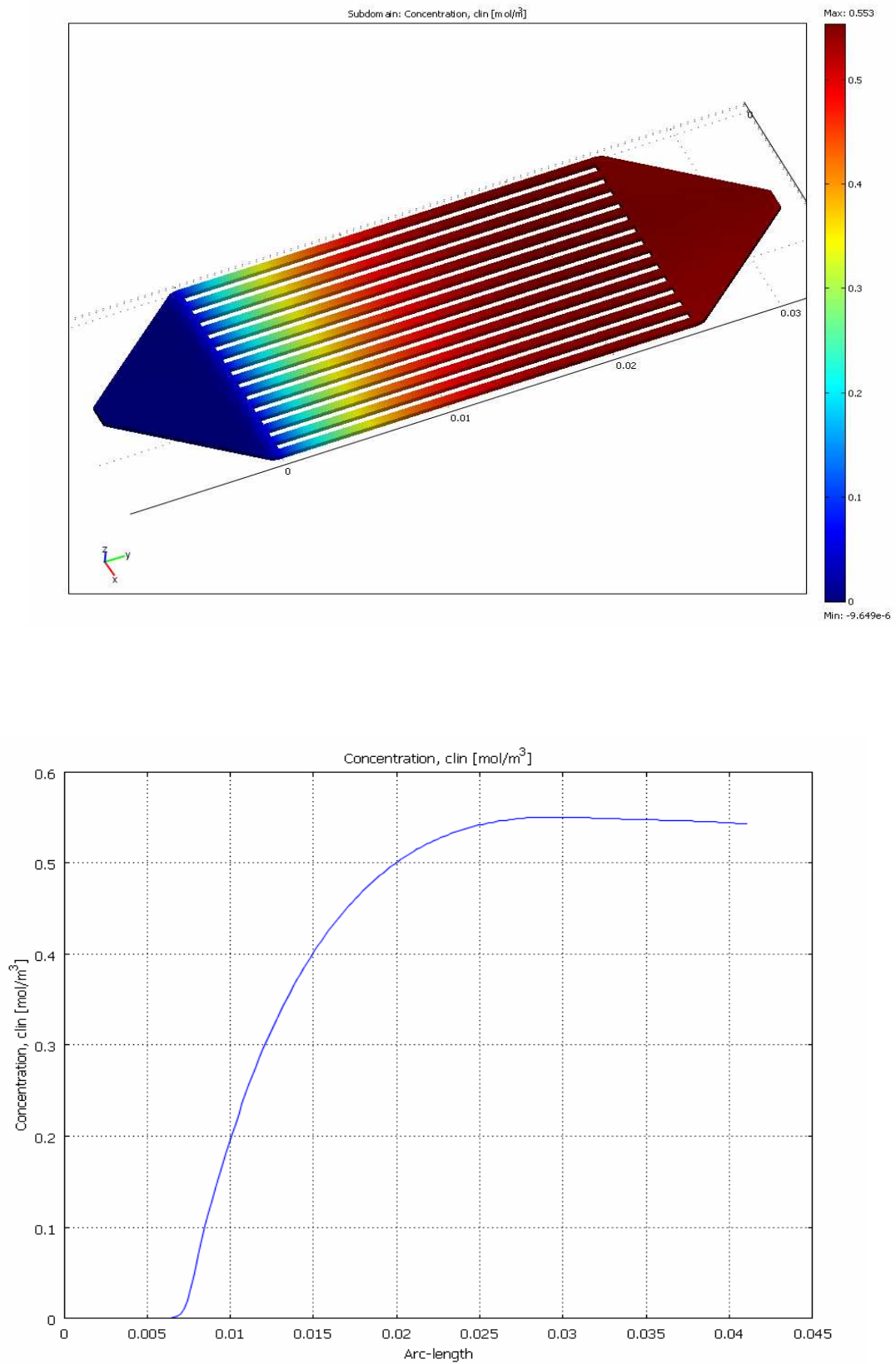
Practically the same behavioural trend with temperature is observed with the microreactor as was observed with the tubular reactor. This is depicted in **Figures 3.43-3.45** which show the concentration profile of linalool within the microreactor at three different temperatures at the same flow rate of 10 ml/min.



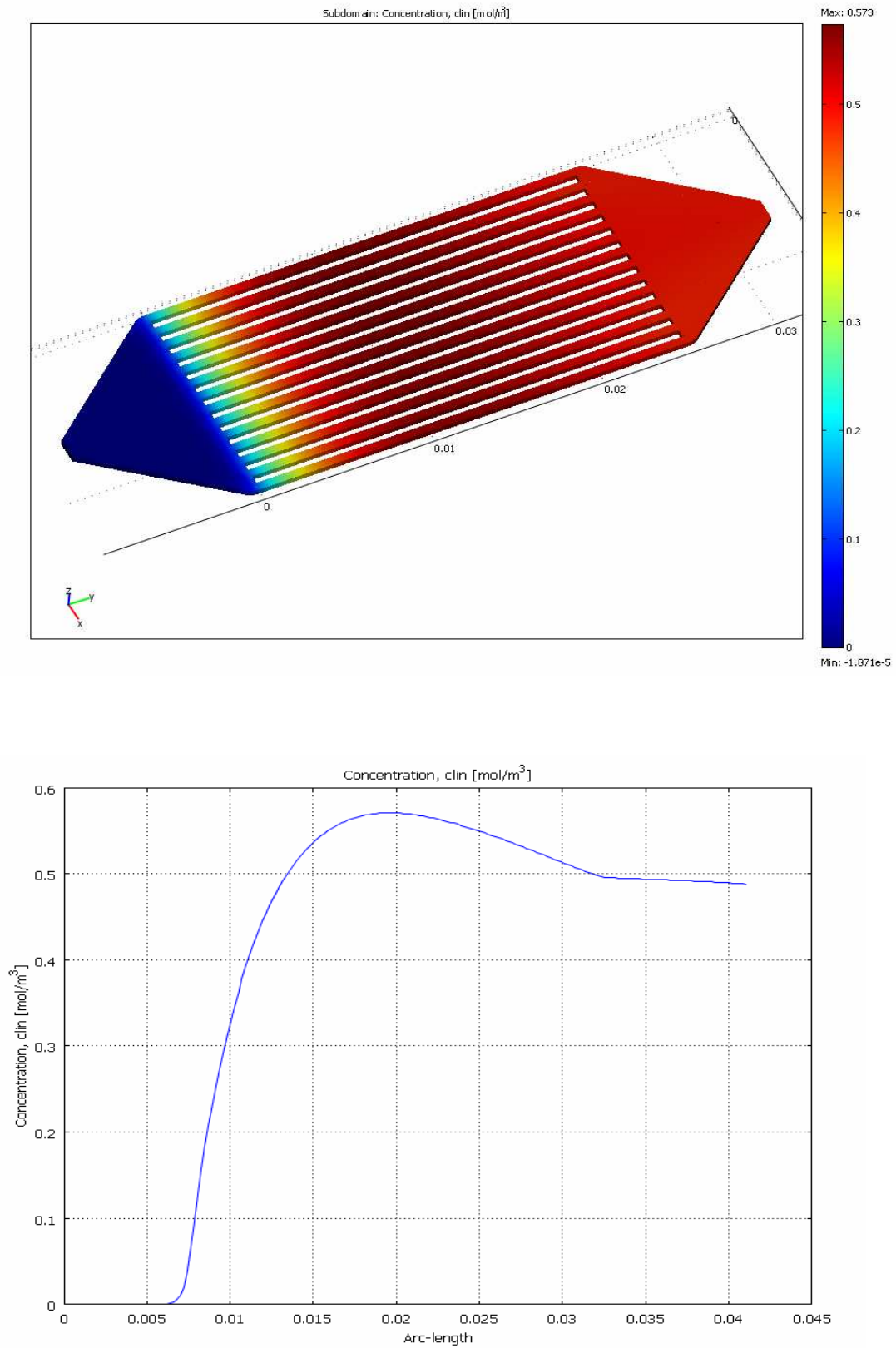
**Figure 3.42: a) temperature profile b) velocity profile along the microreactor**



**Figure 3.43: Concentration profile for linalool inside microreactor at 10 ml/min and 550°C**



**Figure 3.44: Concentration profile for linalool inside microreactor at 10ml/min and 600°C**



**Figure 3.45: Concentration profile for linalool inside microreactor at 10 ml/min and 650°C**

The effect of temperature is discernible from **Table 3.55**, which shows an increase in the yield of linalool with increase in temperature till about 600°C followed by a subsequent drop, again due to the increase in the rate of the side reaction. This behaviour is demonstrated in **Figures 3.43-3.45**, where a maximum linalool yield is predicted inside the reaction zone before receding to its final, lower value at the outlet. This information should be useful in any optimization study where we can safely assume that the global maximum for linalool yield lies between 550°C and 650°C. Some tabulated results of CFD simulations for the microreactor conditions are highlighted in **Table 3.57**.

**Table 3.57: CFD results for microreactor simulation**

		<b>microreactor (CFD)</b>		
<b>Res.time(s)</b> <b>F.r.(ml/min)</b>	<b>Temp °C</b>	$x_{cis}(\%)$	$\zeta_{lin}(\%)$	<b>Yield (%)</b>
<b>0.42 s</b> <b>10 ml/min</b>	500	41.5	93.7	38.9
	550	73.6	88.7	65.3
	600	94.6	80.2	75.9
	650	99.6	68.3	68.0
<b>0.28 s</b> <b>15 ml/min</b>	500	30.8	95.7	29.5
	550	60.0	92.7	55.6
	600	87.1	87.3	76.0
	650	98.3	73.8	72.5
<b>0.21 s</b> <b>20 ml/min</b>	500	24.7	97.0	24.0

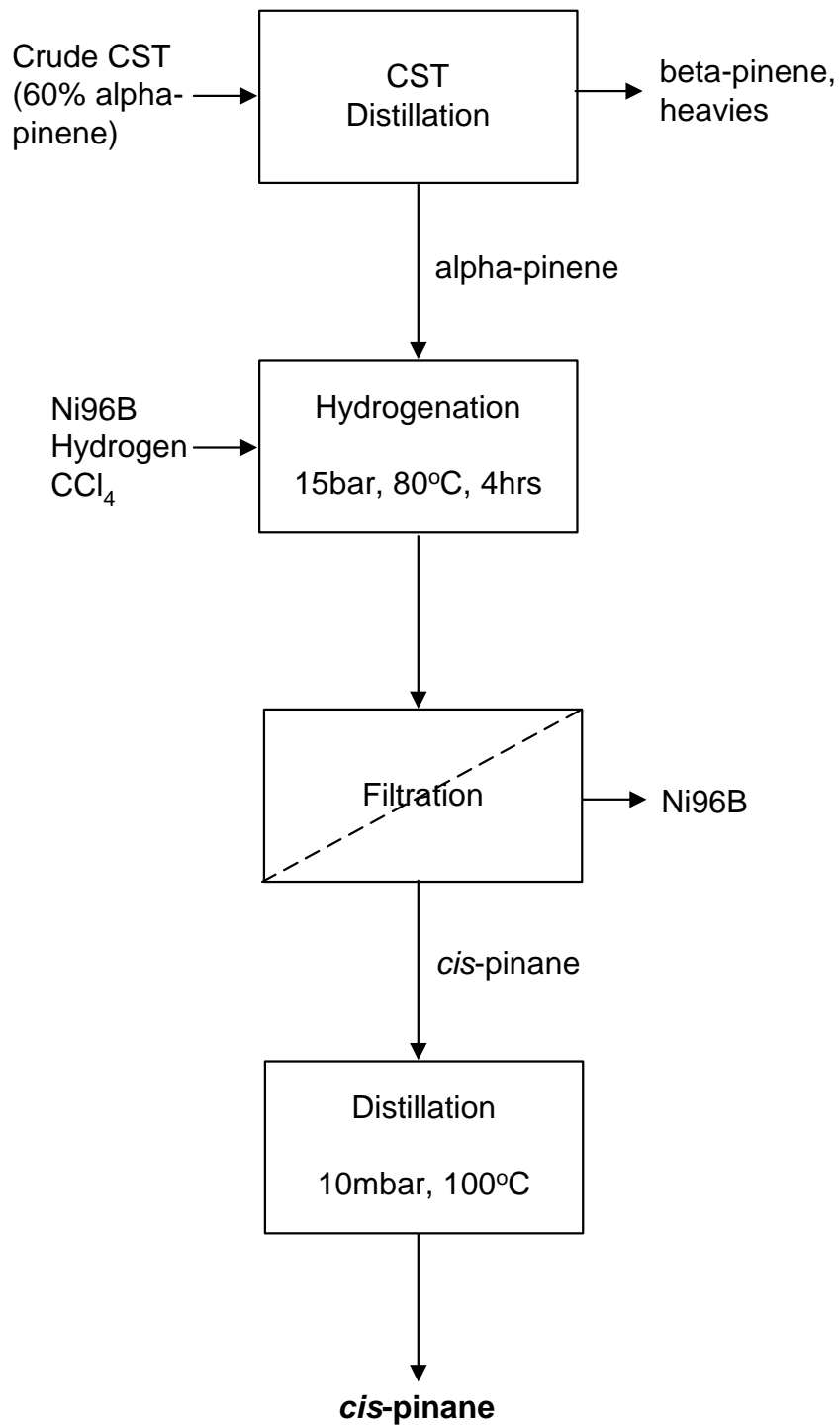
The optimum yield predicted by CFD simulation is at the temperature 600°C at the flow rate of either 10 ml/min or 15 ml/min. This is consistent with the experimentally obtained results. Overall, it is evident that the microreactor configuration presents an improvement in the yield, and on the whole, the modelling is considerably more precise owing to the accuracy of the data collection method.

### 3.10 Scale-up Issues

#### 3.10.1 Process Block and Flow Diagrams

The process block diagrams for the preparation of linalool from crude sulphated turpentine (CST) are shown in **Figures 3.46 to 3.48**.





**Figure 3.46: Process block diagram of *cis*-pinane preparation**

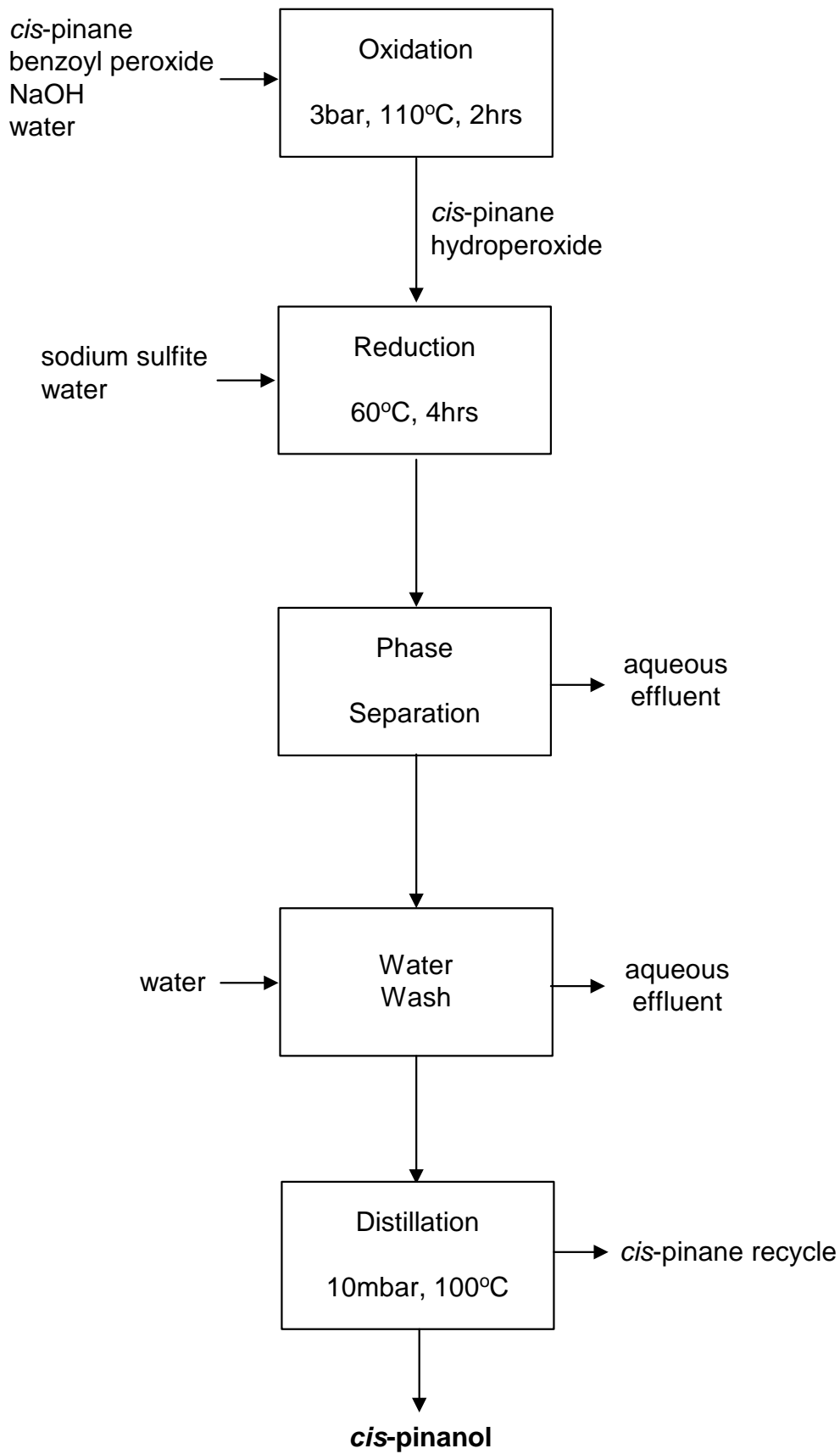
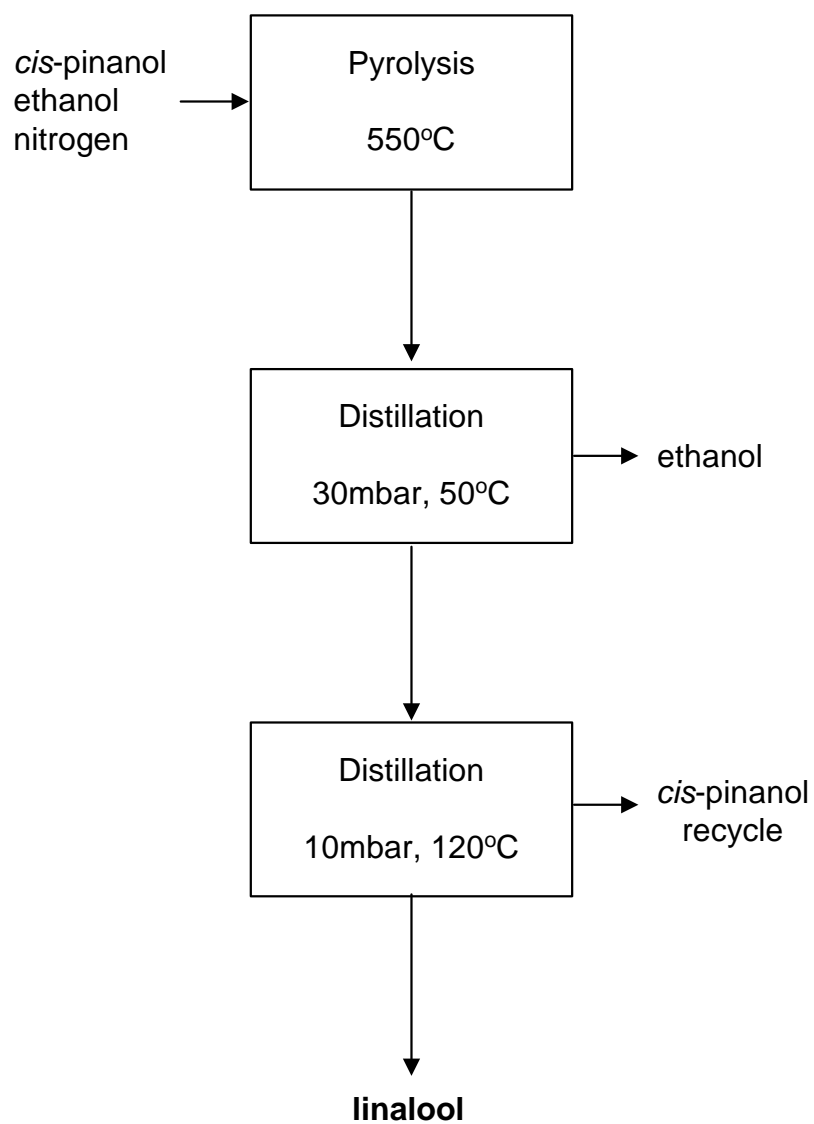
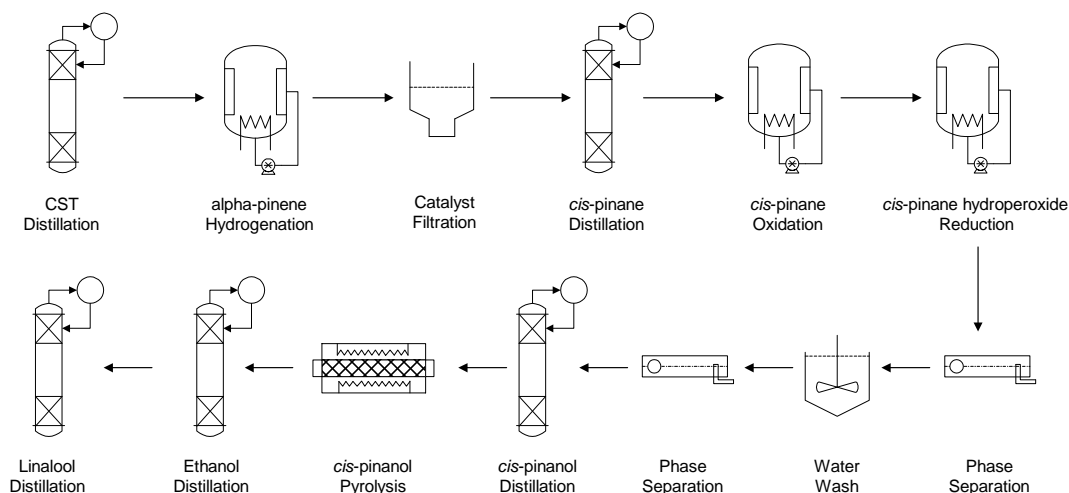


Figure 3.47: Process block diagram of *cis*-pinanol preparation



**Figure 3.48: Block flow diagram of linalool preparation**

A process flow diagram is shown in **Figure 3.49** outlining the unit operations and equipment requirements for the process.

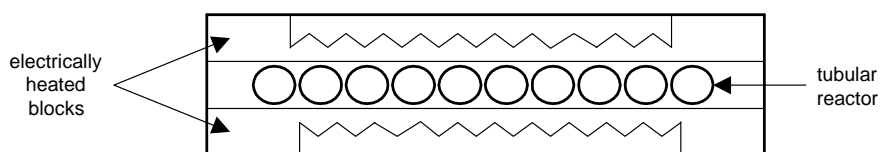


**Figure 3.49: Process flow diagram of linalool preparation**

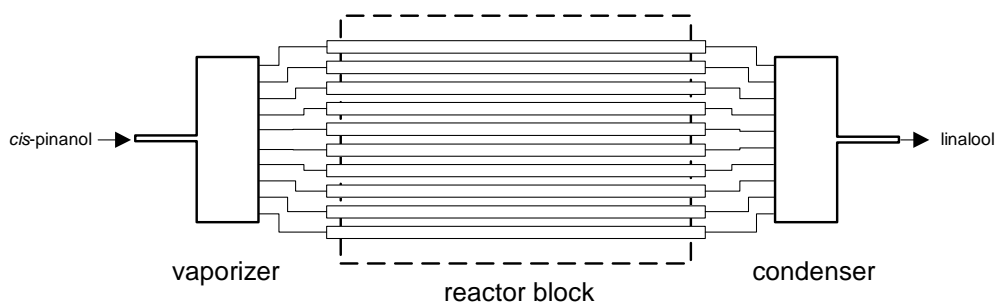
To summarise, the production of linalool from CST consists of four reaction steps and twelve process steps. All of these process steps have been conducted on a pilot scale where kilogram quantities of the various key intermediates have been produced. Pressure reactors would be required for the hydrogenation and oxidation reactions and vacuum distillation units for the distillation of CST, *cis*-pinane, *cis*-pinanol, and linalool. Other unit operations can be carried out in standard stirred tank vessels.

### 3.10.2 Large scale reactor design

Specialised equipment would have to be custom manufactured for the pyrolysis reaction. It has been demonstrated that the reaction can be carried out in a tubular reactor or a microreactor and the limitations of both systems have been discussed. It is proposed that in order to obtain the reaction performance required on a production scale, the configuration of the current tubular reactor system should be used. Production scale throughput could be obtained merely by multiplying the number of reactors to obtain the desired productivity. Various designs are feasible and one such example is shown in Figures 3.50 and 3.51.



**Figure 3.50: Cross-section through multi-reactor pyrolysis unit**



**Figure 3.51: Overhead view of multi-reactor pyrolysis unit**

In this design, each multi-reactor block would consist of ten tubular reactors in parallel. The required temperature would be provided by electrically heated elements or the use of flue gas could be considered since it is more energy efficient and cheaper. Several of these units could be incorporated in a rack-type system for easy maintenance and accessibility.

### **3.10.3 Raw material costing**

At this stage of the project, a basic raw material costing was conducted to give an idea of the techno-economic feasibility of the project (**Table 3.58**).

**Table 3.58: Raw material costing of Linalool process using CST as starting material****1. Distillation of crude sulphated turpentine**

Raw material name	m/m	MW	mol eq.	mol/part	kg/kg	at eff.	\$/kg	\$/part	% contr.
<b>CST</b>		136.24	1.00	7.34	1.00	1.67	0.07	0.12	
<b><math>\alpha</math>-pinene</b>		<b>136.24</b>	<b>1.00</b>	<b>7.34</b>	<b>1.00</b>			<b>0.12</b>	
Yield	60%								

**2. Preparation of cis-pinane from  $\alpha$ -pinene**

Raw material name	m/m	MW	mol eq.	mol/part	kg/kg	at eff.	\$/kg	\$/part	% contr.
<b><math>\alpha</math>-pinene</b>	94.54	136.24	1.00	7.23	0.99	1.05	0.12	0.12	58.8%
hydrogen	1.47	2.00	1.00	7.23	0.01	0.02	0.23	0.00	1.7%
nickel catalyst (Ni96B)	4.31	58.71	0.10	0.72	0.04	0.05	1.82	0.08	39.5%
<b>cis-pinane</b>		<b>138.24</b>	<b>1.00</b>	<b>7.23</b>	<b>1.00</b>			<b>0.21</b>	100.0%
Yield	94%				1.04				

**3. Preparation of cis-pinane hydroperoxide from cis-pinane**

Raw material name	m/m	MW	mol eq.	mol/part	kg/kg	at eff.	\$/kg	\$/part	% contr.
<b>cis-pinane</b>	80.06	138.24	1.00	5.87	0.81	0.84	0.21	0.18	33.2%
benzoyl peroxide	1.40	242.23	0.01	0.06	0.01	0.04	1.20	0.05	10.1%
Oxygen	18.53	32.00	1.00	5.87	0.19	0.59	0.51	0.30	56.7%
<b>cis-pinane hydroperoxide</b>		<b>170.23</b>	<b>1.00</b>	<b>5.87</b>	<b>1.00</b>			<b>0.53</b>	100%
Yield	32%				1.01				
cis-pinane recycle	95%		0.26	0.55	0.58	0.84			

**4. Preparation of cis-2-pinanol from cis-pinane hydroperoxide**

Raw material name	m/m	MW	mol eq.	mol/part	kg/kg	at eff.	\$/kg	\$/part	% contr.
<b>cis-pinane hydroperoxide</b>	81.82	170.23	1.00	6.48	1.10	1.16	0.53	0.61	81.5%
sodium sulfite	18.18	126.04	0.30	1.94	0.25	0.26	0.54	0.14	18.5%
<b>cis-2-pinanol</b>		<b>154.25</b>	<b>1.00</b>	<b>6.48</b>	<b>1.00</b>			<b>0.75</b>	100%
Yield	95%				1.35				

**5. Preparation of linalool from cis-2-pinanol**

Raw material name	m/m	MW	mol eq.	mol/part	kg/kg	at eff.	\$/kg	\$/part	% contr.
<b>cis-2-pinanol</b>	9.82	154.25	1.00	6.48	1.00	1.04	0.75	0.78	55.7%
ethanol	88.40	46.07	30.15	195.46	9.00	30.02	0.52	0.31	22.3%
nitrogen	1.78	28.02	1.00	6.48	0.18	0.61	0.51	0.31	22.0%
<b>linalool</b>		<b>154.25</b>	<b>1.00</b>	<b>6.48</b>	<b>1.00</b>			<b>1.40</b>	100%
Yield	30%				10.19				
cis-2-pinanol recycle	95%		0.30	0.70	0.74	1.04			
ethanol recycle	98%		29.42	0.60					

During the process development phase of any project, it is advisable to conduct a raw material costing since this would determine the feasibility of proceeding with the project. Obviously, if the raw material cost is greater than the selling price of the final product there would be no point in proceeding with the project since there would be no profit to be made. A general rule of thumb is that the raw material cost should be about 50% of the selling price for the project to be feasible. Cost of utilities, labour,

packaging, marketing, etc. still have to be added on. There is also the capital cost component for which there is a payback period before the plant starts making a profit on investment.

At the start of the project it is more difficult to do a costing since there would be no experimental data on material usage, yields, recycles, etc. At best, these can be estimated from the current literature including journal articles, patents, etc. However, this data would still have to be verified in the laboratory. In this costing, the data is based on actual experiments carried out on a pilot plant scale where kilograms of intermediates were produced. The source of information is also important especially with respect to the raw material and product prices. In the fragrance market this information is closely guarded since bulk prices are difficult to obtain and is very much open to negotiation. Fortunately, the CSIR has a close working relationship with Teubes Pty. Ltd., an experienced player in the flavours and fragrance market with international connections and as a result were able to obtain reliable data and prices.

CST is a waste product and as a result the only cost incurred (~R0.5/kg) is the transport of the material from the paper mills to Teubes Pty. Ltd. in Randburg, Gauteng where it is distilled. The  $\alpha$ -pinene content of CST is 60-65% and most of this is recovered during the distillation process. In the hydrogenation step of  $\alpha$ -pinene excellent yields were obtained (94%) and the distillation is relatively straightforward, resulting in high recovery of *cis*-pinane. The catalyst does make a sizeable contribution to the cost (39.5%) but could be recycled several times which would make the process more economical.

The oxidation step to produce pinane hydroperoxide is a little trickier since the conversion has to be kept at ~30% to obtain good selectivities. The model has included a recycle of *cis*-pinane which is then re-used in the process. During the oxidation process most of the hydroperoxide does get converted to *cis*-2-pinanol, but the remaining amount (<10%) is reduced with an excess of sodium sulfite.

The pyrolysis reaction has to also be kept at a conversion of ~30% to prevent the further decomposition of linalool to other by-products. The presence of these by-

products in linalool would make the purification a lot more difficult because of the close boiling points. The *cis*-2-pinanol can be separated by distillation and recycled. Ethanol, which is used as a diluent, is also distilled and recycled.

The raw material cost to produce a kilogram of linalool is \$1.40. There is a significant margin of 60.8% between the raw material cost of linalool and the current selling price (\$3.57/kg). This clearly indicates that the project is potentially feasible from an economic point of view and we can now proceed with confidence to the next stage which is the engineering design, building and commissioning of the large scale pyrolysis rig. The rest of the process steps will be conducted on existing equipment currently present at the CSIR's large scale facility (Imbiza in Isando, Gauteng).

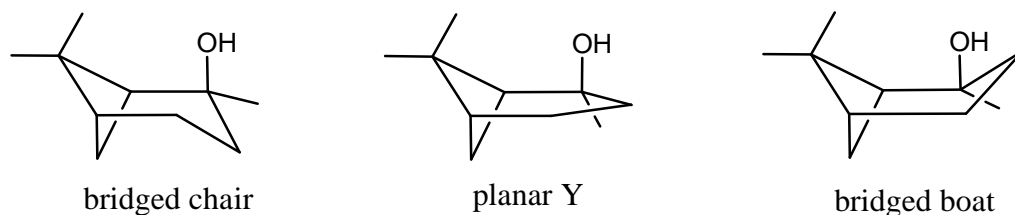
### 3.11 General Discussion

The ring opening of cyclic monoterpenes is a promising way to synthesize fragrance compounds and vitamins. Numerous studies have been conducted on the cleavage of the C-C bond either through catalysis<sup>104-109</sup> or through thermal isomerization<sup>40,62,63,110</sup>.

Numerous important fragrance compounds have been generated by thermal isomerization e.g.  $\beta$ -citronellene from pinane, myrcene from  $\beta$ -pinene, allocimene from  $\alpha$ -pinene and, of particular interest to this investigation, linalool from *cis*-2-pinanol.

In order to understand the possible products that could be formed and the mechanisms of the reactions involved, it is important to understand the structure and conformation of the pinanols. This also affects the relative reactivity of the various isomers. The bicyclo[3.1.1] skeleton of the pinanols has a great deal of flexibility and can adopt the bridged chair, the planar Y or the bridged boat conformations as shown in **Figure 3.52**<sup>111,112</sup>.



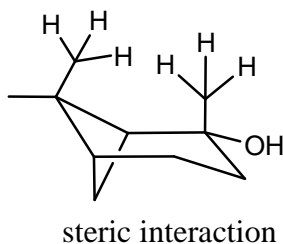


**Figure 3.52: Possible pinanol conformations**

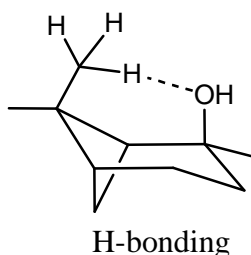
While the pinanols can be readily distinguished by their  $^1\text{H}$  NMR spectra due to the shielding of the  $\text{C}_{10}$  methyl by the ring in *cis*-pinanol, the conformations are more difficult to determine<sup>62</sup>. Whittaker<sup>113,114</sup> has applied  $^{13}\text{C}$  NMR analysis to determine the conformation of a variety of pinane derivatives. The analysis of *trans*-pinanol suggested that it existed in the Y conformation. This is surprising in that it is the only pinane not possessing a double bond (which locks the molecule in a Y conformation) to have this conformation. However, Kane<sup>111</sup> has done extensive  $^{13}\text{C}$  NMR studies and have reassigned the chemical shifts of  $\text{C}_7$ ,  $\text{C}_8$ , and  $\text{C}_{10}$ . The change of the chemical shifts have resulted in the reassignment of the chair conformation to *trans*-pinanol due to the upfield shift of  $\text{C}_7$ , resulting from steric interaction between  $\text{C}_3$  and  $\text{C}_7$ . The chair conformation would also be preferred by *cis*-pinanol. However, Stevens has calculated that the skewed boat is the preferred conformation for *cis*-pinanol<sup>115</sup>.

The relative reactivities of the *cis*- and *trans*-pinanol are explained by these conformations. Reactions carried out on the pyrolysis of mixtures containing *cis*- and *trans*-pinanol have shown that the pyrolysis of the *trans* isomer is negligible under conditions favourable for the isomerization of the *cis*-pinanol. The higher reactivity of *cis*-pinanol can be explained by two reasons:

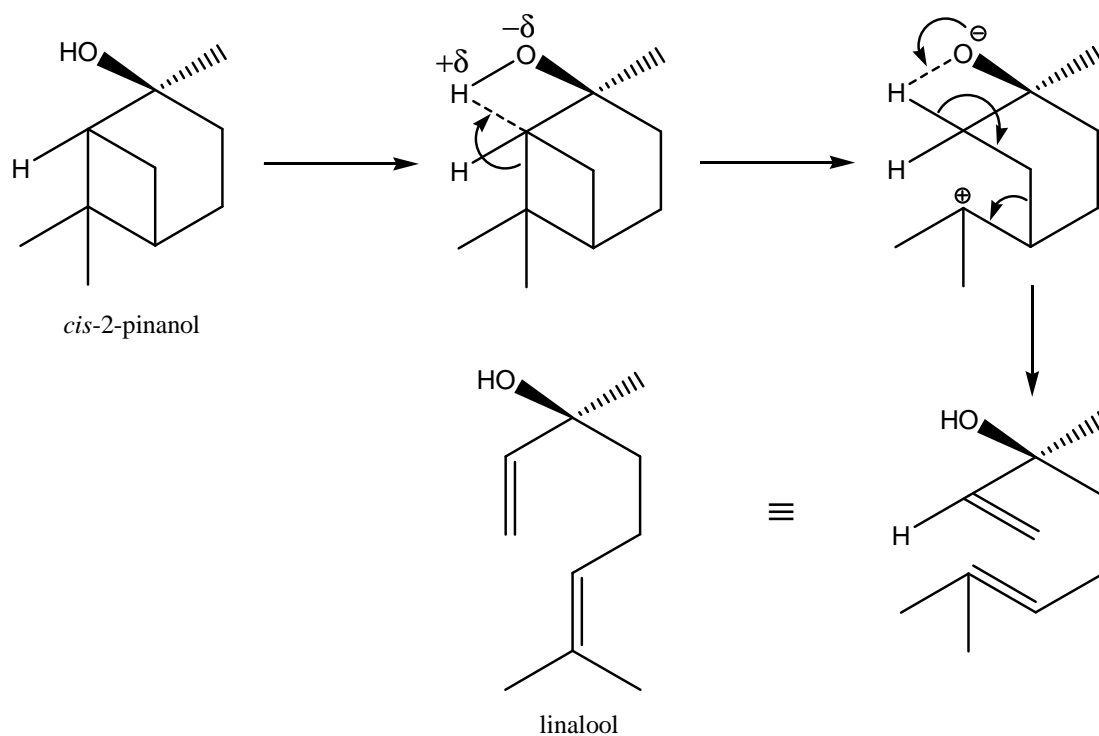
1. Weakening of the C-C bond of the pinane ring due to steric repulsion of  $-\text{CH}_3$  groups oriented in the same direction in *cis*-pinanol; and



2. Stabilization of the *trans*-pinanol molecule due to hydrogen bond formation between the H atom of the  $-CH_3$  group and the oxygen atom of the  $-OH$  group.



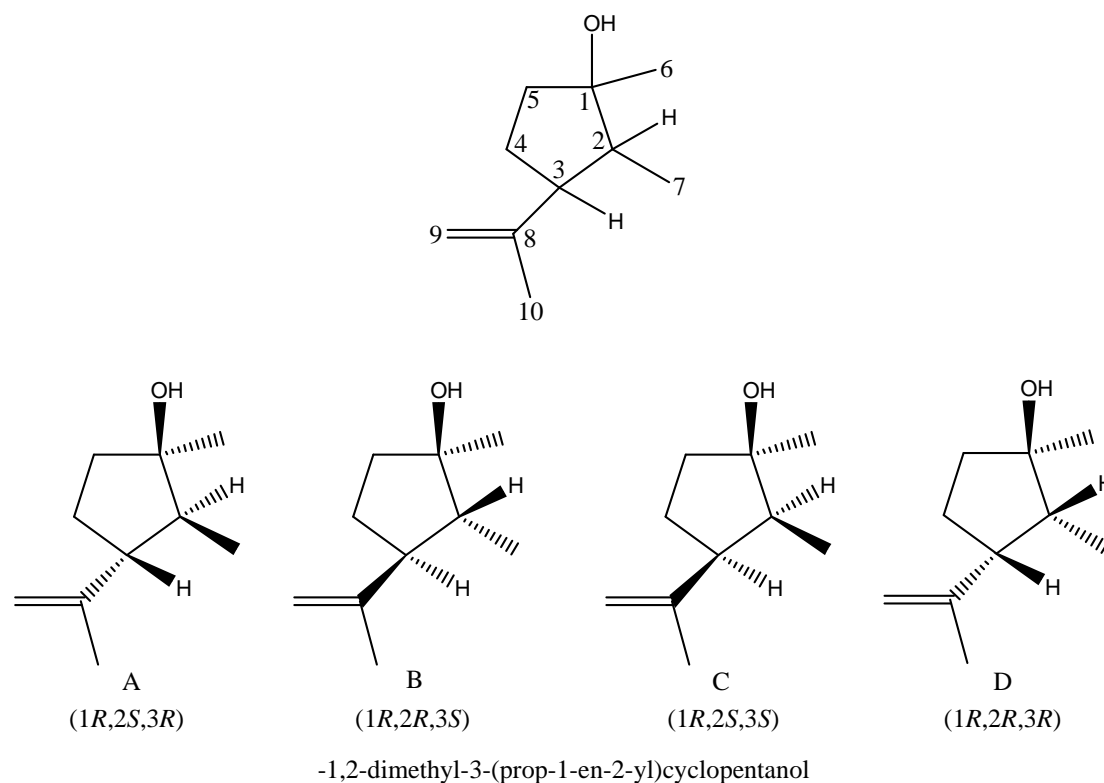
The mechanism involved in thermal isomerization has been the subject of several papers. In general, thermal isomerisation follows first order kinetics and this was verified by experimental work carried out on the reaction kinetics of the pyrolysis reaction of pinanol (§ 3.9). Investigations carried out by Semikolenov<sup>60,61,99</sup>, et al, have shown that *cis*-pinanol has 81 degrees of freedom. When the first vibrational level is completely populated, 2-pinanol can accumulate vibrational energy equal to  $81RT$ . In the temperature range used for the pyrolysis reaction, this energy amounts to 506.8-587.6 kJ/mol. The *cis*-pinanol molecule can be excited to accumulate the vibrational energy that is sufficient for the homolytic cleavage of the C-C bond (~420 kJ/mol) due to the absorption of infra-red radiation emitted by heated surface of the reactor tube. Another source of energy can be collision with any gas-phase molecule. The thermal excitation of the vibrational level of the O-H bond should favour proton abstraction. Thus, intramolecular protonation and OH-group proton-assisted deprotonation are possible at high temperature. The mechanism of this process is shown in **Figure 3.53**.



**Figure 3.53: Mechanism of linalool formation involving intramolecular protonation**

The intramolecular attack of the OH-group proton results in cleavage of the C-C bond in the four-membered ring. The further redistribution of the electron density results in a cleavage of the C-C bond in the six-membered ring, the formation of olefin bonds and the restoration of the O-H bond.

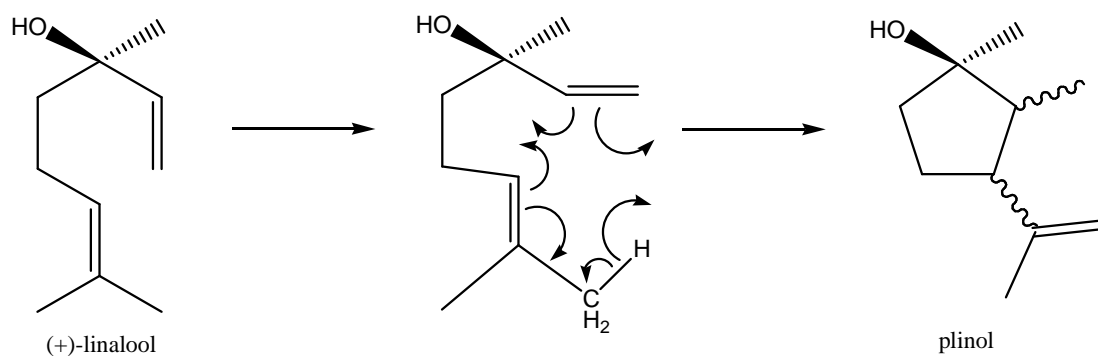
The major by-products formed during the pinanol pyrolysis are plinols. GC-MS analyses of the reaction products of pinanol pyrolysis as well decomposition studies of linalool confirm this (**Tables 3.48 and 3.49**). Reaction kinetic studies (§3.9) also revealed that these hydroxyolefins form at a significant rate and increases with increase in temperature and a decrease in residence time of the reaction mixture. In this study three plinols A, B, C (1,2-dimethyl-3-(propen-1-en-2-yl)cyclopentanol) were identified as shown in **Figure 3.54**.



**Figure 3.54: Plinols derived from linalool**

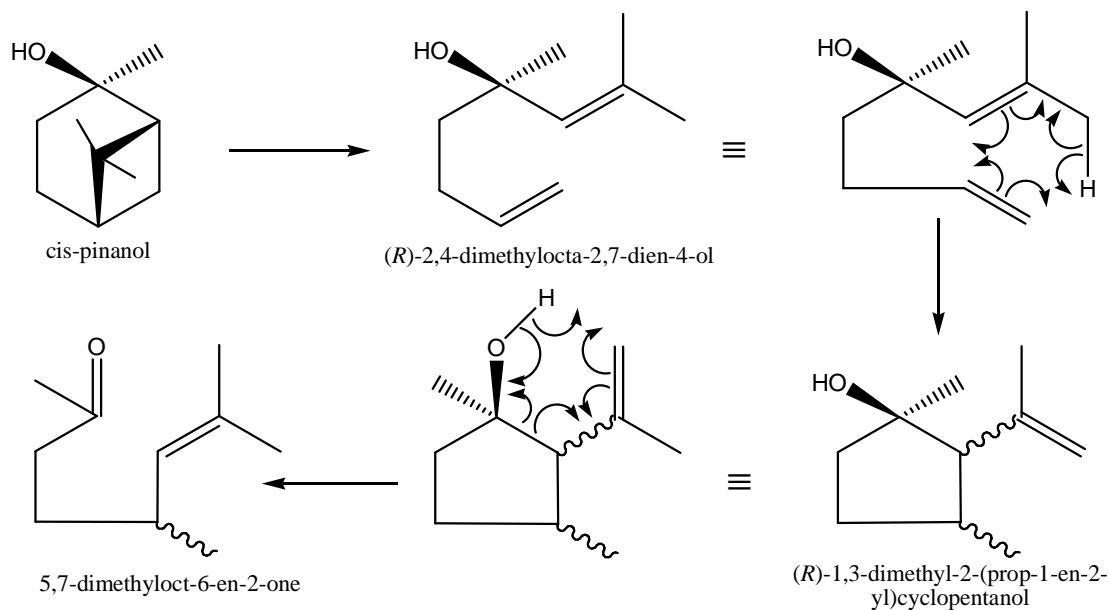
An investigation carried out by Strickler and co-workers<sup>116</sup> identified four configurations of these plinols derived from the pyrolysis of linalool, the fourth one being D (**Figure 3.54**). It is suspected that one of the plinols is co-eluting with *trans*-pinanol since the peak of this compound increases with an increase in temperature.

A possible mechanism for plinol formation is shown in **Figure 3.55**.



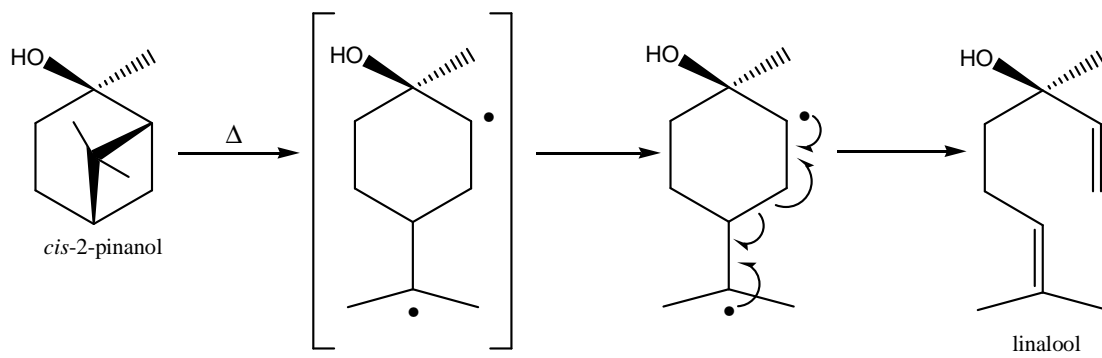
**Figure 3.55: Mechanism of plinol formation**

During this investigation, significant amounts of a methyl ketone (5,7-dimethyloct-6-en-2-one) and *cis*-2-terpineol were found by GC-MS analysis (Table 3.48). *cis*-2-Terpineol could be formed directly from *cis*-2-pinanol if the four-membered ring is cleaved before the six-membered ring and this appears to be the case here. A possible mechanism for the formation of the methyl ketone is shown in Figure 3.56.



**Figure 3.56: Mechanism of methyl ketone formation**

Another possible mechanism which explains linalool formation could proceed via a biradical intermediate. There is evidence for this mechanism in pinane type molecules and kinetic data for transformations of bicyclic compounds to the corresponding acyclic isomers have been reported in literature<sup>117-119</sup>. In the case of *cis*-pinanol, the biradical is thermally generated. This is followed by homolytic bond cleavage followed by intramolecular radical recombination to form linalool, as shown in Figure 3.57.



**Figure 3.57: Biradical mechanism of linalool formation**

## CHAPTER 4

### Conclusions

A successful bench-scale process was developed for the preparation of kilogram quantities of *cis*-2-pinanol involving the following reaction steps:

- $\alpha$ -pinene was hydrogenated at 80°C and 15bar for 4 hours to produce *cis*-pinane at a conversion of 99.6% and a selectivity of 97.8% (total pinanes). The *cis*- to *trans*-pinane ratio was 18:1;
- *cis*-pinane was oxidized with benzoyl peroxide at 110°C and 3bar for 2 hours to produce *cis*-2-pinanol (after reduction of pinane hydroperoxide) at a conversion of 32.5% and selectivity of 95.1% (total pinanols). The *cis*- to *trans*-pinanol ratio was 9:1

Purification of the crude reaction mixture by distillation resulted in a mixture with the following composition, i.e. 88.9% *cis*-pinanol, 9.9% *trans*-pinanol, and 1.2% *cis*-pinane. This was used as the feed material in this investigation.

A pinanol pyrolysis rig was also successfully designed and constructed for the evaluation of various process parameters. The best vaporizer design was a heated brass tube with a counter-current flow of nitrogen gas and pinanol feed material. The inclusion of glass beads aided in the mixing of the pinanol/solvent vapours with the inert gas and resulted in better and more consistent results. The best condenser design was found to be a counter-current flow micro heat exchanger (COMH). The massive surface area to volume ratio provided very efficient cooling and hence excellent mass balance closure from feed material to product stream. The initial reactor system used for all trials was a 316 stainless steel tubular reactor which was robust and provided consistent experimental results.

In the synthesis of linalool, the first part of the investigation involved a screening of various solvents, materials of construction, catalysts, additives, etc. The criteria used for a good reaction was to achieve the required selectivity of linalool (>80%) at a

conversion rate (>25%) that would be practical for scale up purposes and provide product within specification (>90%). In a previous investigation, the highest selectivity ever achieved was only 55% at a conversion of 41%. This result was used as a yardstick against which our results were measured. Investigations by other workers had used n-butanol as a diluent and this was used as our base case or benchmark to evaluate improvements in reaction performance. A selectivity of 71.3% was achieved at a conversion of 29.4%. When it was later discovered that there was significant improvement in performance when the reaction was carried out in ethanol, this then became the solvent of choice for subsequent investigations. A selectivity of 85.8% was achieved at a conversion of 43.6% at 550°C, nitrogen flow rate of 10ml/min and pinanol feed rate of 0.5ml/min using a 10% m/m pinanol concentration in ethanol.

In terms of the use of inert packing, this had no significant impact on reaction performance. There was a slight increase in conversion but the selectivity was also lower. The materials of construction also did not have significant impact on reaction performance and it was decided that the 316 stainless steel tubular reactor would be best suited for scale up in terms of reaction performance, cost, ease of handling and robustness.

The inclusion of pyridine in the feed mixture did not significantly improve the conversion or selectivity. The addition of ammonia to nitrogen did significantly improve reaction performance and would definitely be considered in scale up studies of the process since it is inexpensive and easily removed from the product.

The statistical design showed that the two most important variables were temperature and pinanol feed rate and that there was significant interaction between these two factors as far as selectivity was concerned. The optimum conditions were graphically predicted using an overlay plot as well as by doing a point prediction. Both these methods pointed towards a similar solution after setting criteria for conversion (>25%) and selectivity (>80%). The optimum conditions were selected as follows:

- Temperature of 650°
- Nitrogen flow rate of 10ml/min



- Pinanol feed rate of 1.0ml/min
- Pinanol concentration of 30% m/m in ethanol

The advantage of using these conditions is that linalool could be produced at a higher throughput than anything achieved thus far in the investigation. Using these conditions the predicted conversion was 30.5% at a selectivity of 84.3%.

The above conditions were used for the preparation of the 1kg market sample. After work-up the sample had 92.4% linalool, 0.2% cis-2-pinanol, and 7.4% of other by-products (mainly pinols).

The pinanol pyrolysis reaction was also carried out in a 14 channel microreactor system to determine the effect on reaction performance. There was a significant improvement in both conversion (60.7%) and selectivity (90.1%). Kinetic studies showed that the rate of reaction is faster in the microreactor when compared to the tubular reaction. The formation of by-products was also suppressed because of the reduced residence time and superior heat transfer characteristics. There are still limitations associated with the implementation of microreactors in full scale production units, e.g. availability, cost, and rapid blockages of the channels due to the build-up of coke. However, if these factors can be addressed then the use of microreactors for a reaction such as this should be considered on the industrial scale.

Computer modelling studies were also done using the MATLAB and COMSOL software packages. For the tubular reactor, it was observed from experiment that higher flow rates and higher temperatures tend to favour a higher yield of linalool, which was confirmed by CFD simulations in COMSOL and mathematical modelling in MATLAB. Use of the microreactor resulted in a considerable improvement in linalool yields in comparison with the tubular minichannel reactor, a lower activation energy for the microreactor also meant that the reaction 'took off' at lower temperatures, which consequentially means that the microreactor configuration is more energetically favourable.

Simulations of pinanol and linalool concentrations along the length of the reactor tubes definitely indicate that shorter tubes are preferable for optimum conversion and selectivity. Longer tubes result in longer residence times and further decomposition of linalool thus resulting in lower selectivities. Therefore, for scale-up, multiple tubes with similar dimensions to the ones currently being used are recommended. Narrower internal diameters would certainly be advantageous in terms of conversion and selectivity. However, this must be weighed against practical factors such as disassembly and cleaning to remove coke deposits after extended periods of operation.

The raw material cost to produce a kilogram of linalool is \$1.40. There is a significant margin of 60.8% between the raw material cost of linalool and the current selling price (\$3.57/kg). This clearly indicates that the project is potentially feasible from an economic point of view and we can now proceed with confidence to the next stage which is the engineering design, building and commissioning of the large scale pyrolysis rig. The rest of the process steps will be conducted on existing equipment currently present at the CSIR's large scale facility (Imbiza in Isando, Gauteng).

## BIBLIOGRAPHY

- (1) Teisseire, P. J. *Chemistry of fragrance substances*; VCH Publishers: New York, **1994**.
- (2) Wallach, O. *Liebigs Ann. Chem.* **1887**, 239.
- (3) Robinson, R. *Ann. Rept. Progr. Chem.* **1923**, 20, 100.
- (4) Muller, P. M. a. L., D. *Perfumes, art, science and technology*; Elsevier: Amsterdam, **1991**.
- (5) Curtis, T. a. W., D.G. *Introduction to perfumery*; 2nd. ed.; Ellis Horwood, **2001**.
- (6) Lawrence, B. M. *Essential oils*; Allured Publishing Corp.: Wheaton, **1976**.
- (7) Bedoukina, P. Z. *Perfumery and Flavouring Synthetics*; 3rd ed.; Allured Publishing Corp.: Wheaton, **1980**.
- (8) "An Overview of the Global Flavours and Fragrances Market," IAL Consultants, **2000**.
- (9) In *Chemical and Engineering News* July 14, **2003**.
- (10) Leffingwell and Associates, Independent Fragrance Market Report, July, **2005**.
- (11) "Flavour and Fragrance News Release," Freedonia Group, **2003**.
- (12) "Aroma Chemicals and the Flavour and Fragrance Industry," SRI Chemical Economic Handbook Report, August **2003**.
- (13) Chemicals SA 2004, South Africa's Chemical Industry Overview.
- (14) Hendricks, F., Personal Communication, November, **2006**.
- (15) De Vincentiis, D.G.P., and Mitchell, M.J., Report on Crude Sulphated Turpentine, AECI Research and Development Department, AERD 1304/C, **1996**.
- (16) Farnworth, S. "SPII Proposal: The manufacture of aroma, flavour and fragrance chemicals from locally available raw materials and industrial waste streams: Beneficiation of crude sulphated turpentine," CSIR/Bio-Chemtek/SFCPP/PP/05/1433/B, **2005**.

- (17) Thompson, K. "Converting papermaking and citrus by-products to performance chemicals," Arizona Chemical, **1980**.
- (18) Food and Agricultural Organization, Chapter 8: Turpentine from Pine Resin, Wiley, New York, **2002**.
- (19) Calkin, R. R., and Jellinek, J.S. *Perfumery, practice and principles*; John Wiley: New York, **1994**.
- (20) Trost, B. M. *Science* **2001**, 254.
- (21) Sheldon, R. A. *Chemical Industry* **1992**, 903.
- (22) Sheldon, R. A. *Chemical Industry* **1997**, 12.
- (23) Little, P. *Nature* **2004**, 427, 101-102.
- (24) Bauer, K., Garbe, D., Surburg, H. In *Ullmann's Encyclopedia of Industrial Chemistry*; Gerhartz, W., Yamamoto, Y.S., Elvers, B., Rounsaville, J.F., Schulz, G., Ed.; VCH Publishers: New York, **1998**; Vol. A11, p 156-157.
- (25) Pybus, D. H., and Sell, C.S. *The chemistry of fragrances*; RSC: Cambridge, 1999.
- (26) Banthorpe, D. V. *Terpenes*; Longmann's Scientific and Technical: New York, **1994**.
- (27) Ruzicka, L., et al *Experientia* **1953**, 3, 357.
- (28) Ruzicka, L. *Proc. Chem. Soc. (London)* **1959**, 341.
- (29) Hall, J. A. *Chem. Rev.* **1937**, 20, 305.
- (30) Eschenmoser, A., and Arigoni, B. *Helv. Chim. Acta* **2005**, 88, 3011-3050.
- (31) Banthorpe, D. V., Charlwood, B.V., and Francis, J.O. *Chemical Review* **1972**, 72, 115-155.
- (32) Williams, D. G. *The chemistry of essential oils*; Micelle Press: Dorset, **1996**.
- (33) Charles, S. *A fragrant introduction to terpenoid chemistry*; Royal Society of Chemistry: Cambridge, **2003**.
- (34) Newmann, A. A. *Chemistry of terpenes and terpenoids*; Academic Press: London, **1972**.
- (35) Cowley, K. J. *J. Org. Chem.* **1968**, 33, 3679.
- (36) Cowley, K. J., and Traynor, S.G. *Tetrahedron* **1978**, 34, 2783.
- (37) Ansari, H. R. *Tetrahedron* **1973**, 29, 1559.

- (38) Goldblatt, L. A., and Palkin, S., US Patent 2,420,131, **1947**.
- (39) Kogami, K., and Kumanotani, T. *Bull. Chem. Soc., Japan* **1968**, *41*, 2508.
- (40) Ohloff, G. *Tet. Letters* **1960**, *11*, 10.
- (41) Gradeff, P. S., and Formica, G. *Tet. Letters* **1976**, 4681.
- (42) Clark, G. S. *Perfumer Flav.* **1988**, *13*, 49-54.
- (43) Letizia, C. S., Cocchiara, J., Lalko, J., and API, A.M. *Food and Chemical Toxicology* **2003**, *41*, 943-964.
- (44) Lewinsohn, A. *Rivista Italiana delle Essenze e Profumi* **1924**, *5*, 45.
- (45) Prelog, V., and Watanabe *Liebigs Ann. Chem.* **1957**, *603*, 1-8.
- (46) Vergese, J., *Terpene Chemistry*, McGraw Hill, New Dehli, **1969**.
- (47) Derfer, J. M. *Perfumer Flav.* **1978**, *3*, 45.
- (48) Cori, O., Chayet, L., and Perez, L.M. *J.Org.Chem.* **1986**, *51*, 1310-1316.
- (49) Howell, A. R., and Pattenden, G. *J. Chem. Soc., Chemical Communications* **1990**, *2*, 103-104.
- (50) Howell, A. R., and Pattenden, G. *J. Org. Chem., Perkin Transactions 1: Organic and Bio-organic Chemistry* **1991**, *10*, 2715-2720.
- (51) De Doldan, G. V., Cardfell, D., and De Schiliuk, I.G. *Essenze Derivati Agrumari* **1992**, *60*, 350-357.
- (52) Karavanov, A. N., Gryaznov, V.M., Lebedeva, V.I., Litvinov, I.A., Vasilkov, A.Y., and Olenin, A.Y. *Catalysis Today* **1995**, *25*, 447-450.
- (53) Semigina, N. V., et al *Journal of Molecular Catalysis A: Chemical* **2004**, *208*, 273-284.
- (54) Carroll, D. *J. Chem. Soc. (London)* **1940**, 704-706.
- (55) Carroll, D. *J.Chem.Soc. (London)* **1941**, 507-511.
- (56) Roche, H.-L.; John-Wiley: New York, **1960**; Vol. II.
- (57) BASF, US Patent 6,534,109, **1957**.
- (58) Kimel, W., et al *J.Org.Chem.* **1958**, *23*, 153.
- (59) Takabe, K., Katagiri, T., and Tanaka, J. *Tetrahedron Letters* **1975**, *34*, 3005-3006.
- (60) Illyna, I. I., Simakova, I.L., and Semikolenov, V.A. *Kinet. Katal* **2001**, *42*, 686-692.

- (61) Semikolenov, V. A., Ilyna, I.I., and Simakova, I.L. *Applied Catalysis, A* **2001**, *211*, 91-107.
- (62) Coxon, J. M., Dansted, E., Hartshorn, M.P., and Richards, K.E. *Tet. Letters* **1969**, 1149.
- (63) Coxon, J. M., Garland, R.P., and Hartshorn, M.P. *Aust. J. Chem* **1972**, *25*, 353.
- (64) Ohwa, M., Kogure, T., and Eliel, E.L. *J. Org. Chem.* **1986**, *51*, 2599-2601.
- (65) Govindan, V., and Pandit, G.D. *Tetrahedron Letters* **1966**, *7*, 5097-5100.
- (66) Nair, G. V., and Pandit, G.D. *Tet. Letters* **1966**, *7*, 5097-5100.
- (67) Machado, A., Garcia-Poregrin, E., and Mayor, F. *Plant Science Letters* **1974**, *2*, 83-87.
- (68) Rao, P. G., Zutshi, U., Pushpangadan, P., Sobti, S.N., and Atal, C.K. *Indian Journal of Experimental Biology* **1979**, *17*, 530-532.
- (69) Suga, K., Watanabe, S. and Okoshi, I. *Bull. Chem. Soc., Japan* **1966**, *39*, 1335-1336.
- (70) Suga, T., Shishibori, T., and Bukeo, M. *Phytochemistry* **1971**, *10*, 2725-2727.
- (71) Thomas, J. M. *Angew. Chem.* **1988**, *27*, 1673.
- (72) Mortier, W. J., and Schoonheydt, R.A. *Prog. Solid State Chem.* **1985**, *16*, 1.
- (73) Kresge, C. T., et al *Nature* **1992**, *359*, 710.
- (74) Beck, J. S., et al *Journal of American Chemical Society* **1992**, *114*, 10934.
- (75) Meier, W. M., and Olson, D.H. *Atlas of zeolite structure types*; Butterworths: London, **1992**.
- (76) Lok, B. M., et al *Journal of American Chemical Society* **1984**, *106*, 6092.
- (77) Huo, Q., et al *J.Chem.Soc., Chem. Comm.* **1992**, 875.
- (78) Cusumano, J. A. *Chem. Tech.* **1992**, *22*, 482.
- (79) Fletcher, P. D. I., et al *Analyst* **1999**, *124*, 1273.
- (80) Chovan, T., and Guttman, A. *Trends in Biotechnology* **2002**, *20*, 116-122.

- (81) Jensen, K. F. *Chemical Engineering Science* **2000**, 56, 293-303.
- (82) Manz, A., et al *Journal of Chromatography* **1992**, 1992, 253-258.
- (83) Watts, P., and Haswell, S.J. *Drug Discovery Today* **2003**, 8, 586-593.
- (84) Thayer, A. M. *Chemical and Engineering News* **2005**, 83, 54-61.
- (85) Freemantle, M. *Chemical and Engineering News* **2005**, 83, 11.
- (86) Fletcher, P. D. I., et al *Tetrahedron* **2002**, 58, 4735-4757.
- (87) Kapteijn, F., and Moulijn, J.A. In *Handbook of heterogeneous catalysis*; Ertl, G., Knozinger, J., and Weitkamp, J., Ed.; VCH Publishers: Weinheim, Germany, **1997**; Vol. 3, p 1360-1365.
- (88) Anderson, J. R., and Pratt, K.C. *Introduction to characterisation and testing of catalysts*; Academic Press: New York, **1985**.
- (89) Eigenberger, G. In *Handbook of heterogeneous catalysis*; Ertl, G., Knozinger, J., and Weitkamp, J., Ed.; VCH Publishers: Weinham, Germany, **1997**; Vol. 3, p 1400-1403.
- (90) Weitkamp, J. In *Handbook of heterogeneous catalysis*; Ertl, G., Knozinger, J., and Weitkamp, J., Ed.; VCH Publishers: Weinheim, Germany, **1997**; Vol. 3, p 1377-1386.
- (91) Teubes (Pty) Ltd., Personal Communication, October, **2007**.
- (92) O' Mahoney, T., et al *Journal of Chromatography A* **2003**, 1004, 181-193.
- (93) Hozumi, A., Inagaki, M., and Shirihata, N. *Surface Science* **2006**, 600, 4044-4047.
- (94) Yang, M. H., et al *Talanta* **2007**, Article in Press, 1-5.
- (95) Illyna, I. I., Simakova, I.L., and Semikolenov, V.A. *Kinetics and Catalysis* **2002**, 43, 652-656.
- (96) Brose, T., Pritzkow, W., and Thomas, G. *J. Prakt. Chem.* **1992**, 334, 403-409.
- (97) Filliatre, C., and Lalande, P. *Bull. De La Soc. Chim. De France* **1968**, 10, 4141-4145.
- (98) Semikolenov, V. A., and Ilyna, I.I. In *Sym. on Heterogeneous Catalysis and Fine Chemicals* Lyon, **1999**, p 62.
- (99) Semikolenov, V. A. a. I., I.I., and Simakova, I.L. *Journal of Molecular Catalysis A: Chemical* **2002**, 182, 383-393.

- (100) Froment, G. F., and Bischoff, K.B. *Chemical reactor analysis and design*; John Wiley and sons: New York, **1979**.
- (101) Reid, R. C., Prausnitz, J.M., and Poling, B.E. *The properties of gases and liquids*; 4th ed.; McGraw Hill: New York, **1987**.
- (102) Berthier, J., and Silberzan, P. *Microfluidics for biotechnology*; Artech House: Norwood, USA, **2006**.
- (103) Ehrfeld, W., Golbig, K., Hessel, V., Lowe, H., and Richter, T. *Ind. Eng. Chem. Res.* **1999**, 38.
- (104) McVicker, G. B., et al *Journal of Catalysis* **2002**, 210, 137-148.
- (105) Teschner, D., DuPrez, D., and Paal, Z. *J. Mol. Catalysis A: Chemical* **2002**, 179, 201-212.
- (106) Lefebvre, F., Cazat, J.T., Dufaud, V., Niccolai, G.P., and Basset, J.M. *Applied Catalysis A: General* **1999**, 182, 1-8.
- (107) Akhmedov, V. M., et al *Applied Catalysis A: General* **1999**, 181, 51-61.
- (108) Lai, W. C., and Song, C. *Fuel Processing Technology* **1996**, 48, 1-27.
- (109) Vaarkamp, M., et al *Journal of Catalysis* **1995**, 151, 330-337.
- (110) Ohloff, G., et al *Helv. Chim. Acta* **1967**, 50, 759.
- (111) Kane, B. J., Marcelin, G., and Traynor, S.G. *J.Org.Chem.* **1980**, 45, 895-900.
- (112) Traynor, S. G., Kane, B.J., Jacquelyn, B.C., and Cardenas, C.G. *J.Org.Chem.* **1980**, 45, 900-906.
- (113) Holden, C. M., and Whittaker, D. *Org. Magn. Reson.* **1975**, 7, 125.
- (114) Banthorpe, D. V., and Whittaker, D. *Quart. Rev.* **1966**, 20, 373.
- (115) Texter, J., and Stevens, E.S. *J.Org.Chem.* **1979**, 44, 3222-3225.
- (116) Strickler, H., Ohloff, G., and Kovats, E. S. *Helv. Chim. Acta* **1967**, 50, 759.
- (117) Gajewski, J.J., et al, *Tetrahedron*, **2002**, 58, 6943-6950.
- (118) Hunt, H.G., and Hawkins, J.E., *J.Am.Chem.Soc.*, **1950**, 72, 5618-5620.
- (119) Hawkins, J.E., and Vogh, J.W., *J.Phys.Chem.*, **1953**, 57, 902-905



## LIST OF TABLES

Table 1.1: Value of the Flavour and Fragrance Industry 2002 .....	13
Table 1.2: Estimated Sales Volume Flavour and Fragrance Companies 2002.....	15
Table 1.3: Market for Fragrance in Sub-Saharan Africa: 2001-2004 <sup>8</sup> .....	17
Table 1.4: South African pulp mill capacities 2001 .....	22
Table 1.5: Specification of Tugela Turpentine .....	23
Table 1.6: Future CST Feedstock Supply in South Africa .....	24
Table 1.7: Classification of Terpenoids .....	37
Table 1.8: The 4-3-2-1 Rule.....	60
Table 1.9: Some of the more important terpenoid fragrance materials <sup>47</sup> .....	78
Table 1.10: Composition of distillate from CST .....	95
Table 1.11: South African Trade Statistics <sup>12</sup> .....	108
Table 1.12: Terpene Aroma Chemical Usage in South Africa (kg) .....	110
Table 1.13: Affordable Capital for the Terpene Aroma Facility (Rands Millions) ..	113
Table 1.14: Capital Estimate for 420 ton Crude Sulphated Turpentine plant.....	115
Table 2.1: Reagents for synthesis .....	119
Table 2.2: Reagents for analysis .....	120
Table 2.3: Equipment used for experimental study .....	121
Table 2.4: Experimental conditions used for vaporizer evaluation .....	128
Table 2.5: Design summary: Various vaporizer designs .....	129
Table 2.6: Experimental conditions used for condenser evaluation .....	133
Table 2.7: Calibration points for nitrogen gas flowmeter.....	137
Table 2.8: Experimental conditions used for screening experiments .....	137
Table 2.9: Design summary: nitrogen vs ammonia/nitrogen.....	142
Table 2.10: Design summary of pinanol/ethanol pyrolysis statistical design.....	143
Table 2.11: Experimental conditions used for preparation of 1kg market sample ..	144
Table 2.12: Experimental conditions used for microreactor reactions .....	145
Table 2.13: GC Conditions for analysis of reaction mixture .....	146
Table 3.1: Conversion response for the various vaporizer designs .....	148
Table 3.2: Conversion ANOVA .....	148
Table 3.3: Conversion: Analysis of treatments.....	149
Table 3.4: Selectivity response for the various vaporizer designs.....	151
Table 3.5: Selectivity ANOVA.....	151
Table 3.6: Selectivity: Analysis of treatments .....	152
Table 3.7: Mass recovery response for the various condenser designs .....	154
Table 3.8: ANOVA .....	154
Table 3.9: Analysis of treatments .....	155
Table 3.10: Results of $\alpha$ -pinene hydrogenation in 300 ml Parr reactor.....	158
Table 3.11: Hydrogenation using partially poisoned Ni catalyst.....	159
Table 3.12: Results of 8L Parr hydrogenations using poisoned nickel catalyst .....	159
Table 3.13: Autoxidation of <i>cis</i> -pinane .....	161
Table 3.14: Oxidation of <i>cis</i> -pinane using AIBN as initiator in 300ml Parr reactor .	162
Table 3.15: Oxidation of <i>cis</i> -pinane using benzoyl peroxide as initiator .....	163
Table 3.16: <i>cis</i> -Pinane oxidation in 8L Parr reactor using benzoyl peroxide.....	163
Table 3.17: Purification of pinanol mixture.....	165
Table 3.18: Pinanol pyrolysis in quartz tube without packing.....	165
Table 3.19: Pinanol pyrolysis in quartz tube with packing.....	166

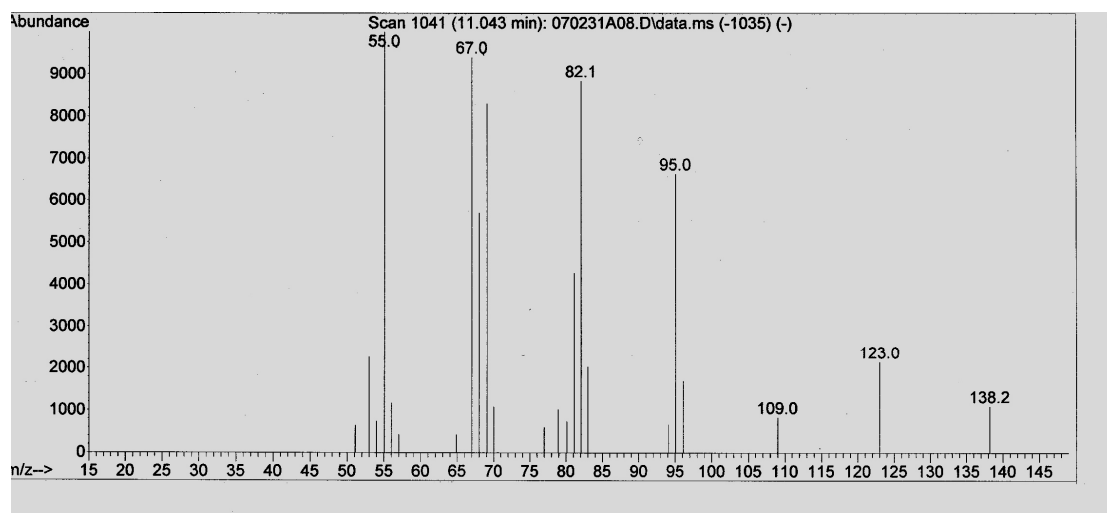
Table 3.20: Pinanol pyrolysis using <i>n</i> -butanol as diluent .....	169
Table 3.21: Pinanol pyrolysis using <i>n</i> -butanol as diluent-repeat .....	169
Table 3.22: Effect of solvent on pinanol conversion .....	170
Table 3.23: Effect of solvent on linalool selectivity .....	172
Table 3.24: Effect of pinanol concentration on conversion .....	173
Table 3.25: Effect of pinanol concentration on linalool selectivity .....	174
Table 3.26: Pinanol pyrolysis under vacuum .....	175
Table 3.27: Effect of inert packing on pinanol conversion .....	177
Table 3.28: Effect of inert packing on linalool selectivity .....	178
Table 3.29: Effect of various materials on pinanol conversion .....	179
Table 3.30: Effect of various materials on linalool selectivity .....	180
Table 3.31: Effect of zeolite catalysts on conversion and selectivity .....	182
Table 3.32: Effect of pyridine concentration on pinanol conversion .....	183
Table 3.33: Effect of pyridine concentration on linalool selectivity .....	184
Table 3.34: Conversion response for ammonia vs nitrogen .....	186
Table 3.35: Conversion ANOVA .....	186
Table 3.36: Conversion: Analysis of treatments .....	187
Table 3.37: Selectivity response for ammonia vs nitrogen .....	188
Table 3.38: Selectivity ANOVA .....	188
Table 3.39: Selectivity: Analysis of treatments .....	189
Table 3.40: Results of statistical design for the pyrolysis of a pinanol/ethanol mixture .....	191
Table 3.41: Conversion – Effects list .....	192
Table 3.42: ANOVA for conversion response .....	193
Table 3.43: Selectivity – Effects list .....	199
Table 3.44: ANOVA for selectivity response .....	201
Table 3.45: Point prediction model – low pinanol concentration .....	202
Table 3.46: Point prediction model – high pinanol concentration .....	203
Table 3.47: Effect of temperature and solvent on linalool decomposition .....	204
Table 3.48: GC-MS Data for a typical pinanol pyrolysis at 650 °C in ethanol .....	206
Table 3.49: GC-MS Data for linalool decomposition reaction at 650 °C in ethanol .....	206
Table 3.50: Initial composition of crude market sample .....	207
Table 3.51: Composition of market sample after first distillation .....	207
Table 3.52: Composition of final market sample .....	208
Table 3.53: Conversion at various gas flow rates in microreactor .....	209
Table 3.54: Selectivity at various gas flow rates in microreactor .....	210
Table 3.55: Comparative results of pinanol pyrolysis in the tubular and microreactor systems .....	217
Table 3.56: Modelling results from Matlab and CFD – Tubular reactor .....	224
Table 3.57: CFD results for microreactor simulation .....	232

## LIST OF FIGURES

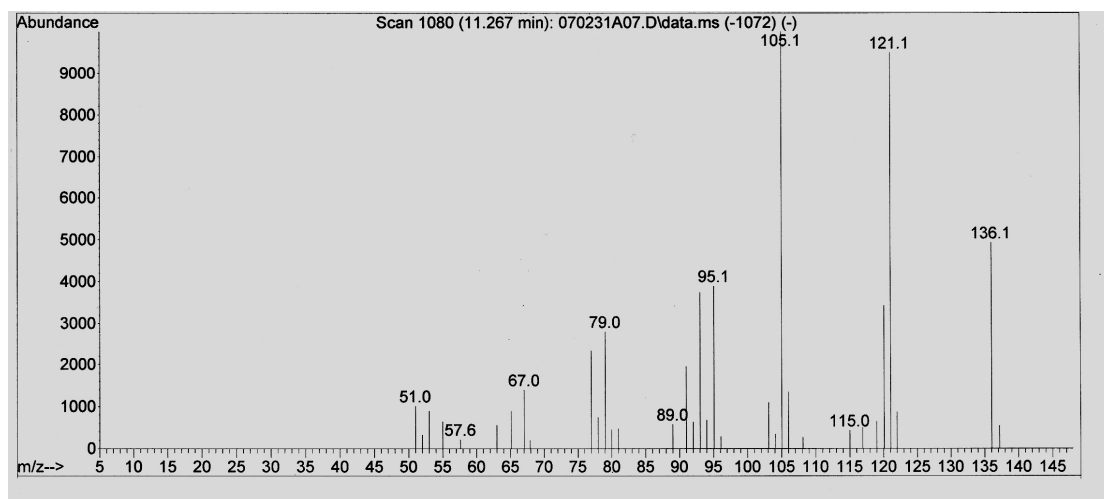
Figure 1.1: Fragrances End-Use Market .....	12
Figure 1.2: Fragrance Industry Value Chain.....	13
Figure 1.3: Conversion of Turpentine Oil to Aroma Chemicals .....	21
Figure 1.4: Atom utilisation .....	28
Figure 1.5: Thalidomide enantiomers .....	30
Figure 1.6: Head-to-tail fusion of isoprene units .....	36
Figure 1.7: “Isoprene Rule” .....	38
Figure 1.8: Typical monoterpenoids showing isoprene units .....	39
Figure 1.9: Head-to-tail coupling of isoprene units .....	39
Figure 1.10: “Regular” structure of geraniol .....	40
Figure 1.11: Squalene showing isoprene units .....	40
Figure 1.12: Conjugated chain of $\beta$ -carotene.....	40
Figure 1.13: Numbering system.....	41
Figure 1.14: Use of Greek letters .....	42
Figure 1.15: Principal hydrocarbons.....	43
Figure 1.16: Isopropylidene and Isoprene forms .....	43
Figure 1.17: Highly unsaturated hydrocarbons.....	44
Figure 1.18: Reactions of myrcene .....	44
Figure 1.19: Myrcene dimerization.....	45
Figure 1.20: Sigmatropic rearrangement – 1,5 H-migration.....	45
Figure 1.21: Transition states I and II.....	46
Figure 1.22: Effect of base on $\beta$ -ocimene .....	47
Figure 1.23: Photochemical reaction of $\beta$ -myrcene .....	48
Figure 1.24: Important derivatives of $\beta$ -myrcene .....	49
Figure 1.25: Rearrangement of geraniol to $\alpha$ -terpineol .....	49
Figure 1.26: Cyclisation of geranyl acetate .....	50
Figure 1.27: Condensation of citral with acetone .....	51
Figure 1.28: Result of citral reaction with methylethylketone .....	51
Figure 1.29: Effect of high temperature on linalool .....	51
Figure 1.30: Asymmetrical induction of linalool.....	52
Figure 1.31: Linalool esterification.....	53
Figure 1.32: Protonation of alcohols.....	54
Figure 1.33: Generation of isomeric allylic cation .....	55
Figure 1.34: Reaction of l-linalool with acetic anhydride .....	56
Figure 1.35: Expected reaction of linalool with acetic anhydride .....	57
Figure 1.36: Working of trans-anti-periplanar rule in Prelog’s reaction .....	58
Figure 1.38: Deprotonation of carbocation .....	61
Figure 1.39: Solvolysis of carbocation .....	61
Figure 1.40: H-Shift of carbocation .....	62
Figure 1.41: 1,2-carbon shift reaction.....	63
Figure 1.42: 1,2 carbon shift in pinane ring system.....	63
Figure 1.43: 1,2 Carbon shift in bornane system.....	64
Figure 1.44: Carbon shift of more heavily substituted carbon.....	65
Figure 1.45: Examples of methyl shift.....	66
Figure 1.46: Canonical forms at either extreme of hyperconjugation .....	67
Figure 1.47: Increasing stability .....	67
Figure 1.48: Canonical form of stabilised carbocation.....	67
Figure 1.49: 1,2 Hydrogen -shift.....	68

Figure 1.50: Canonical forms of the carbocation.....	68
Figure 1.51: Internal angles of regular polygons .....	69
Figure 1.52: Chair and boat conformations of cyclohexane ring.....	70
Figure 1.53: Newman projections.....	71
Figure 1.54: Steric interaction.....	71
Figure 1.55: Attack of ozone on electron-rich olefins .....	72
Figure 1.56: Polarisation of methylene bond.....	73
Figure 1.57: Selectivity through polarisability .....	74
<b>Figure 1.58: The Prins reaction .....</b>	<b>75</b>
Figure 1.59: Elimination of water from protonated alcohol .....	76
Figure 1.60: $\alpha$ -Bonds between geminal carbon atoms.....	77
Figure 1.61: Interconversion of key terpenoids .....	80
Figure 1.62: Pyrolysis products of $\alpha$ - and $\beta$ -pinene.....	84
Figure 1.63: Action of HCl on myrcene .....	85
Figure 1.64: Conversion of chlorides into acetates.....	86
Figure 1.65: Inverse Claisen reaction .....	87
Figure 1.66: Michael addition and cleavage of ketoester .....	87
Figure 1.67: Mechanism of Carroll reaction.....	88
Figure 1.68: Action of diketene on methylbutenol .....	89
Figure 1.69: Pyrolysis of acetoacetic acid ester.....	90
Figure 1.70: Preparation of the dimethylacetal.....	90
Figure 1.71: Synthesis of methylheptenone based on enol ethers .....	91
Figure 1.72: Radical reaction of acetone with methylbutenol .....	91
Figure 1.73: Reaction of acetone, isobutylene, and formaldehyde.....	92
Figure 1.74: Mechanism of reaction .....	93
Figure 1.75: Reaction of methylvinylketone with isobutylene.....	93
Figure 1.76: Synthesis of methylchlorobutene .....	94
Figure 1.77: Condensation of methylchlorobutene with acetone .....	94
Figure 1.78: Synthesis of linalool from $\alpha$ -pinene .....	96
Figure 1.79: Linalool decomposition.....	96
Figure 1.80: Fixed-bed reactor for studying gas phase reactions .....	102
Figure 1.81: Gas bubbling through liquid.....	103
Figure 1.82: Condensation after super-saturation.....	104
Figure 1.83: Prolonged path of gas bubbles.....	105
Figure 1.84: Enhanced mass transfer through inert solid .....	105
Figure 1.85: Standard equipment for sampling gaseous products .....	106
Figure 1.86: Instantaneous sampling with gas syringe .....	107
Figure 1.87: Economy of Scale – Terpene Aroma Chemical Plant.....	116
Figure 2.1: Schematic diagram of pinanol pyrolysis rig.....	122
Figure 2.2: Nitrogen sparging through boiling pinanol .....	125
Figure 2.3: Cross-section of bottom fed vaporizer .....	126
Figure 2.4: Cross-section of bottom-fed vaporizer with glass beads.....	126
Figure 2.5: Cross-section of counter-current vaporizer .....	127
Figure 2.6: Cross-section of counter-current vaporizer with glass beads.....	128
Figure 2.7: Glass condenser system.....	130
Figure 2.8: Gas cooling trap system .....	131
Figure 2.9: Coiled PTFE tubing/chilled bath system.....	131
Figure 2.10: Coiled tube/vacuum flask system.....	132
Figure 2.11: Counter-flow Micro Heat Exchanger (COMH) .....	132
Figure 3.1: Conversion: One Factor Plot of various vaporizer designs.....	150

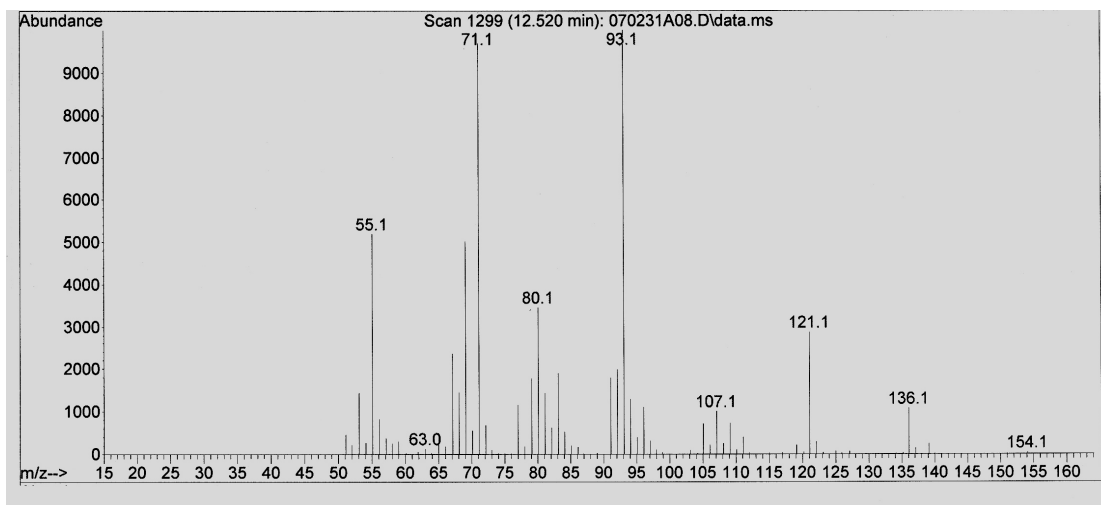
Figure 3.2: Selectivity: One Factor Plot of various vaporizer designs .....	153
Figure 3.3: One Factor Plot of various condenser designs .....	155
Figure 3.4: Reaction scheme for synthesis of <i>cis</i> -2-pinanol .....	157
Figure 3.5: <i>Cis</i> - and <i>trans</i> -pinane .....	158
Figure 3.6: Pinanol pyrolysis in quartz tube without packing .....	166
Figure 3.7: Pinanol pyrolysis in quartz tube with packing .....	167
Figure 3.8: Pinanol pyrolysis using <i>n</i> -butanol as diluent.....	169
Figure 3.9: Effect of solvent on pinanol conversion.....	171
Figure 3.10: Effect of solvent on linalool selectivity.....	172
Figure 3.11: Effect of pinanol concentration on conversion.....	173
Figure 3.12: Effect of pinanol concentration on linalool selectivity .....	174
Figure 3.13: Pinanol pyrolysis under vacuum .....	176
Figure 3.14: Effect of inert packing on pinanol pyrolysis .....	177
Figure 3.15: Effect of inert packing on linalool selectivity .....	178
Figure 3.16: Effect of various materials on pinanol conversion.....	180
Figure 3.17: Effect of various materials on linalool selectivity.....	181
Figure 3.18: Effect of zeolite catalysts on conversion and selectivity.....	182
Figure 3.19: Effect of pyridine concentration on pinanol conversion .....	184
Figure 3.20: Effect of pyridine concentration on linalool selectivity .....	185
Figure 3.21: Conversion: One Factor Plot for two treatments.....	187
Figure 3.22: Selectivity: One Factor Plot for two treatments .....	190
Figure 3.23: Conversion: Half-normal probability plot.....	192
Figure 3.24: Conversion: Normal plot of studentized residuals .....	195
Figure 3.25: Conversion: Plot of outlier T.....	195
Figure 3.26: Conversion: Box-Cox Plot .....	196
Figure 3.27: Conversion: One factor plot – Temperature.....	197
Figure 3.28: Conversion: Interaction of temperature and gas flow rate .....	197
Figure 3.29: Conversion: Cube plot of A, B, C .....	198
Figure 3.30: Conversion: Contour surface plot.....	199
Figure 3.31: Selectivity: Half-normal probability plot .....	200
Figure 3.32: Graphical optimisation: Overlay plot.....	203
Figure 3.33: Effect of temperature and solvent on linalool decomposition.....	205
Figure 3.34: Pinanol conversion at various flow rates in microreactor .....	209
Figure 3.35: Linalool selectivity at various gas flow rates in microreactor.....	211
Figure 3.36: Arrhenius plot for the tubular reactor system.....	219
Figure 3.37: Arrhenius plot for the microreactor system.....	220
Figure 3.38: Effect of flow rate of gas on the concentration of linalool at 600°C....	222
Figure 3.39: The effect of flow rate of gas on the concentration of linalool at 700°C .....	223
Figure 3.40: CFD model of tubular reactor with inlet and heated middle section....	224
Figure 3.41: Concentration profiles of linalool along the profile of the tubular reactor from CFD simulation at the flow rate 50ml/min at <i>a</i> ) 600°C and at <i>b</i> ).....	225

**APPENDIX**

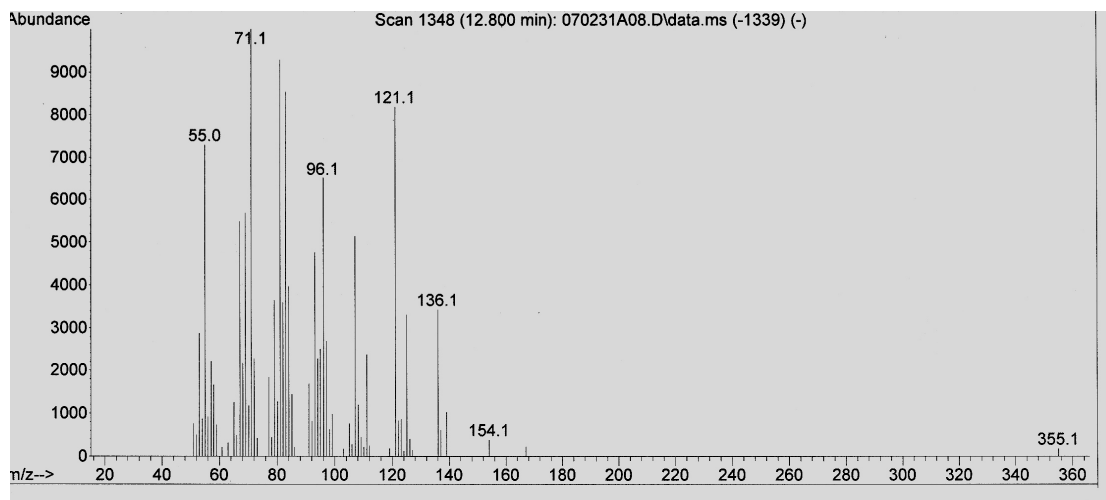
GC-Mass Spectrum of 2,6-dimethyl-2,4,6-octadiene (11.043min)



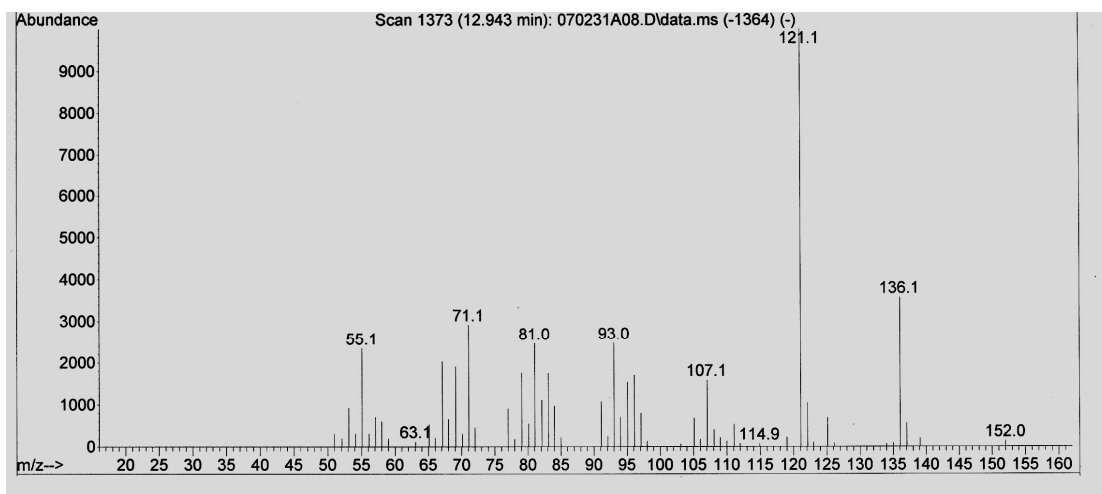
GC-Mass Spectrum of 3,7-dimethyl-1,3,6-octatriene (11.267min)



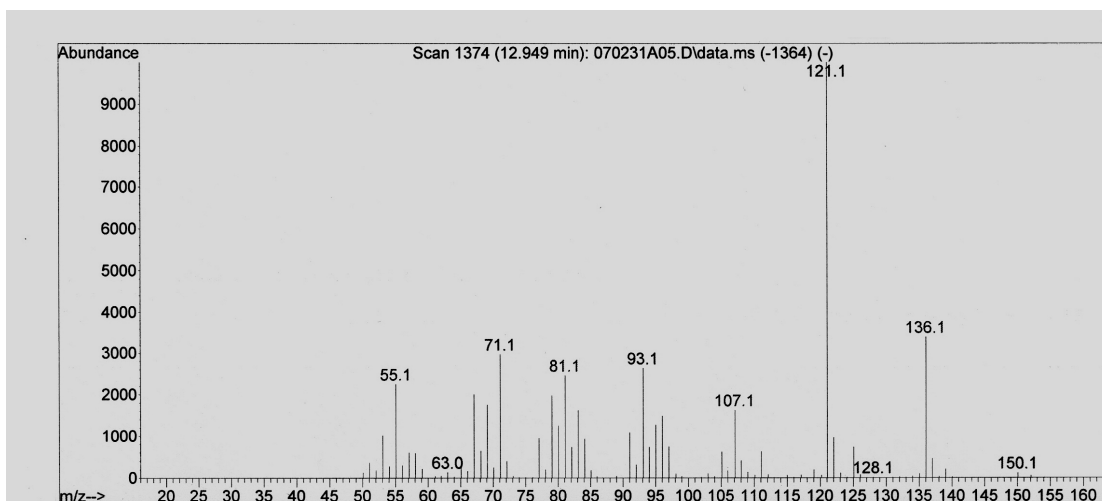
GC-Mass Spectrum of 3,7-dimethyl-1,6-octadien-3-ol (12.520min)



GC-Mass Spectrum of 1,2-dimethyl-3-(1-methylethenyl)-cyclopentanol  
(1*R*, 2*R*, 3*S*) (12.800min)

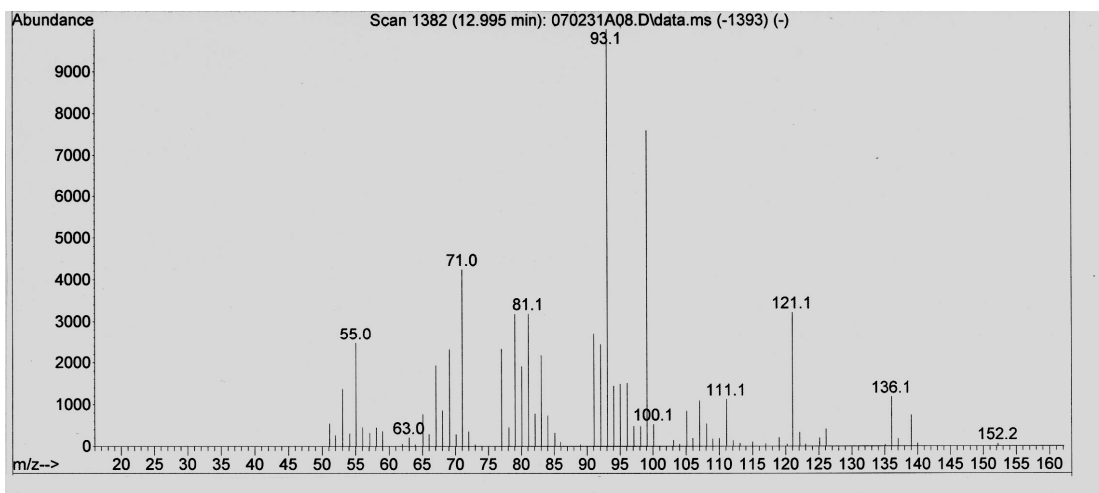
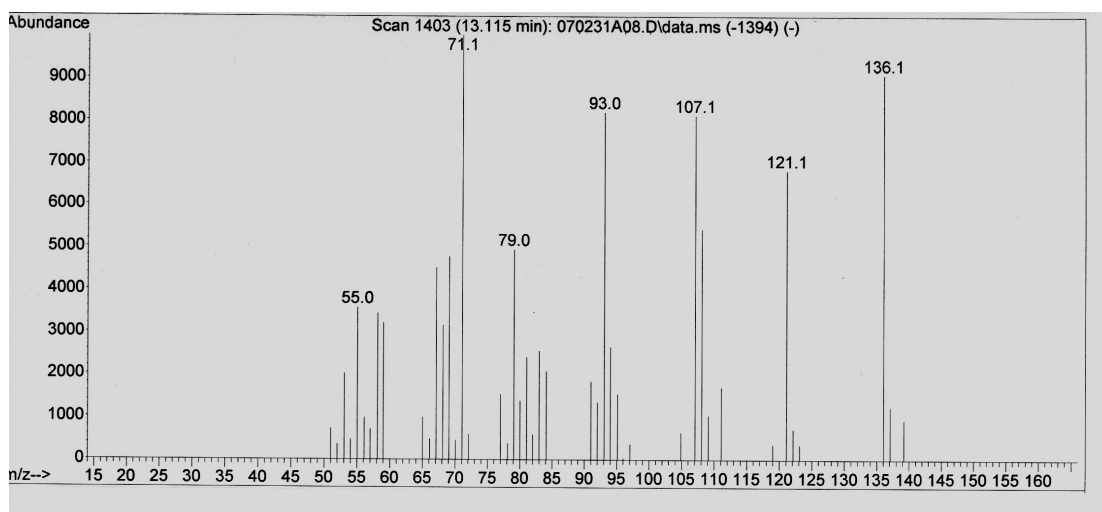


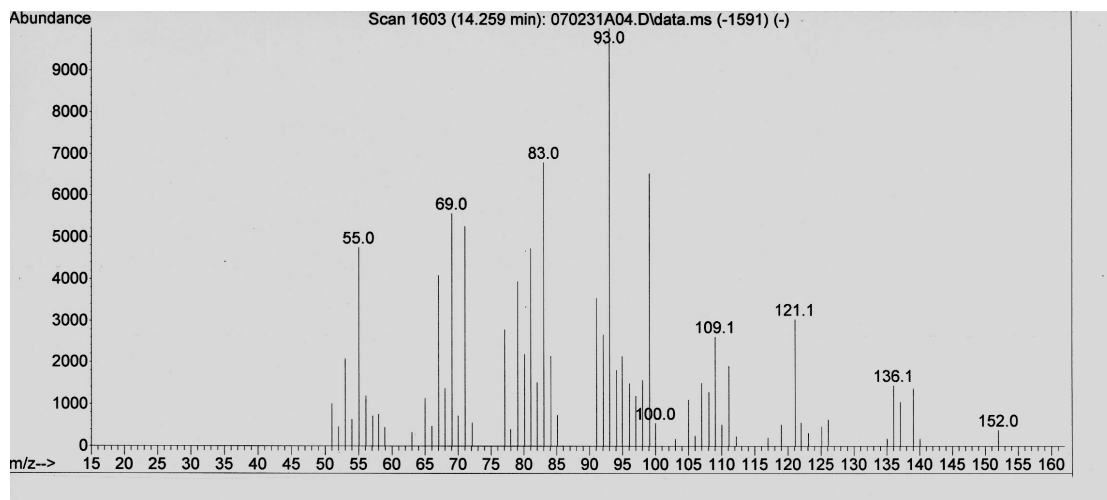
GC-Mass Spectrum of 1,2-dimethyl-3-(1-methylethenyl)-cyclopentanol  
(1*R*, 2*S*, 3*S*) (12.943min)



GC-Mass Spectrum of 1,2-dimethyl-3-(1-methylethenyl)-cyclopentanol  
(1*R*, 2*S*, 3*R*) (12.949min)



GC-Mass Spectrum of *cis*-2-pinanol (12.995min)GC-Mass Spectrum of *cis*- $\beta$ -terpineol (13.115min)



GC-Mass Spectrum of *trans*-pinanol (14.259min)